Optimising non-invasive magnetic resonance measurements of skeletal muscle volume and lipids content to evaluate the effect of Ramadan month fasting on metabolic health

Submitted by Ashwag Abdullah Alarfaj to the University of Exeter as a thesis for the degree of

Doctor of Philosophy in Sport and Health Sciences

30 November 2022

I certify that all material in this thesis which is not my own work has been identified and that no material has previously been submitted and approved for the award of a degree by this or any other University.

Signature: ……

Abstract

Metabolic diseases have reached pandemic levels, raising concerns about metabolic health. Their prevalence is expected to rise in the future. Ramadan fasting (RF), a yearly Islamic practice, involves abstaining from eating and drinking from sunrise until sunset. The effects of RF vary due to multiple factors, including the duration of fasting per day, variations in diet quality and quantity, and the level of physical activity observed during Ramadan, leading to heterogeneity in reported outcomes.

The main aim of the thesis was to test the hypothesis that 18 hrs/day RF causes systemic metabolic changes, which could be detected non-invasively by MRI and basic blood samples. The secondary aims were to study these changes on healthy female and male groups. Als, as part of this assessment, the validation of automated muscle and fat volumes measurements method and the optimisation of MR image acquisitions had to be undertaken to improve the automated measurements.

Methods: The validation of automated muscle volume measurements involved comparing them with the gold standard manual method in a population undergoing temporal changes in muscle volume. Subsequently, various MR sequences were assessed to identify the ones that produced images with the highest contrast-to-noise ratio and were most compatible with the automated threshold method.

To evaluate the effect of RF on the body mass index (BMI), muscle and subcutaneous adipose tissue volumes, liver and muscle ectopic lipids, abdominal visceral and subcutaneous fat (AVF and ASF), fasting blood glucose and insulin (FBG and FBI), and blood lipid profiles were monitored before, during, and a month after Ramadan.

Additionally, the dietary intake and physical activity habits were assessed during and one month after the end of RF.

Results: The automated and manual measurements of muscle volume exhibited strong agreement. Optimal results were obtained using fat-only and water-only images for automated measurements of muscle and fat volumes.

After RF, significant reductions were observed in BMI and skeletal muscle volume, while FBG, LDL, and ectopic muscle lipid increased in both males and females. AVF significantly decreased in males, and there was a tendency towards a decrease in ASF in both sexes. Although protein intake did not fall below the recommended guideline level, it was significantly lower during RF compared to the non-RF period.

Discussion: The study findings indicate that automated volume measurements demonstrate comparability to the gold standard method while saving time. The declines in BMI and abdominal adipose fats are factors in improving cardiometabolic health. The adverse increases in FBG, LDL, and ectopic muscle lipid could be attributed to circadian rhythm disruption, which impacts hormonal levels, lipolysis and hepatic gluconeogenesis. The decrease in muscle volume may be associated with the limited eating window during fasting.

Conclusion: An 18-hour RF regimen can lead to reductions in BMI and adipose fat tissues, although caution is warranted regarding the effects on muscle volume, FBG, and LDL. To counteract these effects, aligning with the wider literature, it is recommended to enhance protein intake and include resistance exercise. Furthermore, the study underscores the reliability of automated volume measurements as a time-efficient substitute for manual methods.

Abbreviations

Abbreviation	Meaning
MetS	Metabolic syndrome
FFA	Free fatty acids
TAG	Triacylglycerides
VAT	Visceral adipose tissue
SAT	Subcutaneous adipose tissue
IHCL	Intrahepatocellular lipids
ICCL	Intracardiomyocellular lipids
IMCL	Intramyocellular lipids
EMCL	Extramyocellular lipid
MSK	Musculoskeletal
IMAT	Intermuscular adipose tissue
IMF	Intramuscular fat
LDs	Lipid droplets
DAG	Diacylglycerol
T2DM	Type 2 diabetes
IR	Insulin resistance
CVD	Cardiovascular diseases
NAFLD	Non-alcoholic fatty liver disease
BMI	Body mass index
WC	waist circumference
T1-WI	T1-weighted image
TE	Echo Time
TR	Repetition Time
CHESS	Chemical shift selective
SNR	Signal-to-noise ratio
rf	radiofrequency
3D T1-WATS	3 Dimension T1-weighted water excitation Spatial-spectral pulses
PDFF	Proton density fat fraction
B0	Static magnetic field
CT	Computer tomography
MRI	Magnetic resonance imaging
MRS	Magnetic resonance spectroscopy
DXA	Dual-energy X-ray absorptiometry
T1-TSE	T1-weighted spin-echo
TSE	Turbo or fast spin echo
IF	Intermittent fasting
IER	intermittent energy restriction
eTRE	Early time restricted eating
dTRE	Delay time restricted eating
ROI	Region of interest
ASF	Abdominal subcutaneous fat
AVF	Abdominal visceral fat
SFAs	saturated fatty acids
PUFA	poly-unsaturated fatty acids
CGM	Continuous glucose monitoring
TIR	Time in range

List of tables

List of Figures

Chapter 1

Chapter 2

Chapter 3

Figure 3.3.1.2. MRI T1TSE image showing (A) signal intensity degradation in the edge of the peripheral slice resulting in the dark area on the right thigh (left side of the image), and (B) the impact of this degradation on automated thresholding segmentation of the muscle.

Figure 3.3.1.3. Example of 3D segmentation of the thigh muscle.

Figure 3.3.2.1. A comparison between images obtained and analysed with A) a T1-TSE sequence (slice thickness 5 mm, slice gap 10 mm) and (B) a T1-WATS sequence (slice thickness=10mm, slice gap= 5mm). Due to the differences in slice thickness and slice gap, the number of slices covering relatively similar but not exact areas differed between the two sequences. 14 slices were used for the T1-TSE sequence to cover 140mm, and 29 slices of the T1-WATS sequence to cover 145mm were used for the segmentation analysis. Images were taken from the same thigh. (C) example of a raw T1-WATS image, (D) example of a raw T1-TSE image.

Figure 3.3.2.2. (A)T1-FATS image segmentation, 5 central slices were used. (B) T1-FATS image, (C) T1-TSE, the tissues contrast in T1-FATS is higher than in T1-TSE.

Figure 3.4.1.1. An average muscle volume difference between two segmentation methods (automated vs manual). An MRI T1-TSE imaging sequence was post-processed to estimate muscle volume using the two segmentation methods. A direct comparison of thigh muscle volume measurements of the control leg at baseline. Statistical analysis was performed with Bland-Altman, (n=13).

Figure 3.4.1.2. Average muscle volume %change was calculated from automated and manual methods. Percentage change of thigh muscle volume after 2-days of leg immobilisation. Data are represented as % differences with error bars (standard error). Statistical analysis was performed with the Bland-Altman test (n=13).

Figure 3.4.1.3. Average muscle volume %change was calculated from automated and manual methods. Percentage change of thigh muscle volume after 7-days of leg immobilisation Data are represented as % differences with error bars (standard error). Statistical analysis was performed with the Bland-Altman test (n=13).

Figure 3.4.1.4. Average muscle volume determinations from two different methods (Automated Vs manual). MRI was done three times; pre-immobilisation, 2-day, and 7-day immobilisation. Data are presented as means with error bars representing standard error. Statistical analysis was performed with Two-way ANOVA. (*) represent the significant difference between pre-and post-2 and 7 days immobilisation (main effect). Two symbols $P<0.01$, four symbols $P<0.0001$, ($n=13$).

Figure 3.4.2.1. Average muscle volume difference between two MR-sequences (T1-WATS vs T1-TSE). A comparison of thigh muscle volume of control legs at baseline. WATS images (29 slices, covered 145 mm length), T1-TSE image (14 slices, covered 140mm length). Measurements were conducted by 3D slicer software (automatic thresholding technique). Data are presented as mean with error bars representing standard error (SEM) ($n=7$). Statistical analysis was performed with Bland-Altman analysis.

Figure 3.4.2.2. Average muscle volume %change after 2-day of thigh muscle damage and immobilisation. Measurements were calculated from T1-WATS and T1-TSE image sequences. A comparison between the two MRI sequences; T1-WATS (29 slices covered 145 mm length) and T1-TSE (14 slices covered 140mm length). Data are presented as mean with error bars representing standard error (SEM) ($n=7$). Statistical analysis was performed with Bland-Altman analysis.

Figure 3.4.2.3. Average muscle volume %change after 7-day of thigh muscle damage and immobilisation. Measurements were calculated from T1-WATS and T1-TSE image sequences. A comparison between the two MRI sequences. T1-WATS image (29 slices, covered 145 mm length), T1-TSE image (14 slices, covered 140mm length). Data are presented as mean with error bars representing standard error (SEM) (n=7). Statistical analysis was performed with Bland-Altman analysis.

Figure 3.4.2.4. (A) Damaged. Immobilised leg, (B) Damaged. Non-immobilised leg. Thigh muscle volume change at three-time intervals, baseline, 2-day and 7-day. A comparison between the two MRI sequences (T1-WATS and T1-TSE). T1-WATS images (29 slices, covered 145 mm length), T1-TSE images (14 slices, covered 140mm length). Statistical analysis was performed with Mixed-effect analysis. Data are presented as mean with error bars representing standard error (SEM) (n=7). (*) represents the significant difference between time points (main effect) and one symbol (P<0.05).

Figure 3.4.2.5. A comparison of total thigh fat volume change of damaged immobilised thigh. Images were taken at baseline (pre-immobilisation), after 2 and 7 days of immobilisation, 5 central slices were used. Data are presented as means with error bars representing standard error (SEM) (n=6). Statistical analysis was performed with mixed effect models.

Figure 3.5 Automated segmentation of thigh muscle using the thresholding technique. The area inside the red circle is an example of the vessels included in total muscle estimation.

Chapter 4

Figure 4.3.2. Study Design represents study tasks for each Phase. Phase 1 (Pre-Ramadan), Phase 2 (one week after commencing Ramadan fasting), Phase 3 (3.5 weeks after commencing Ramadan fasting), and Phase 4 (one month after end of Ramadan fasting). Participants' visits were within four days in non-fasting stages (Phase 1) and (Phase 4) and within two days in the fasting stage. Abbreviations: W&H: Height and Weight, W: weight, MRI: Magnetic resonances imaging FBS: Fasting blood samples, ND: Nutritional Diary, GENE.ACTIV: Activity watch.

Figure 4.4.1. Comparisons of Body mass index (BMI). Phase1(Pre-Ramadan) compared to Phase2 (one week after commencing Ramadan fasting) and Phase3 (3.5 weeks after commencing Ramadan fasting) to show Ramadan fasting effect (A). Phase1 (Pre-Ramadan) and Phase4 (one month after end of Ramadan fasting) (B) to explore if the impact of Ramadan fasting is continuous one month later. Data are presented as means with error bars representing standard error (SEM) (n=18 females, n=19 males). Statistical analysis was performed with measurements Two-way ANOVA (A) and Mixed-effects model (B). (*) represent the significant difference between time points, one symbol (P<0.05), two symbols P<0.01, and three symbols (P<0.001).

Figure 4.4.2. Comparisons of right thigh muscle volume (Th.M). Phase1 (Pre-Ramadan) compared to Phase2 (one week after commencing Ramadan fasting) and Phase3 (3.5 weeks after commencing Ramadan fasting) shows the effect of Ramadan fasting (A). A comparison between (pre-Ramadan) and (one month after end of Ramadan fasting) to elicit if the significant impact of Ramadan month fasting persists one month later (B). MR T1-WATS and Dixon-fat images of thigh muscle volume were measured automatically via thresholding technique using 3D slicer software. Data are presented as means with error bars representing standard error (SEM) (n=18 females, n=19 males). Statistical analysis was performed with mixed effect models. (*) represent the significant difference between time points (main effect), one symbol (P<0.05), two symbols P<0.01, and three symbols (P<0.001).

Figure 4.4.3. Abdominal visceral fat volume (AVF) comparison of three phases; Phase1 (pre-Ramadan), Phase2 (one week after commencing Ramadan fasting) and Phase3 (3.5 weeks after commencing Ramadan fasting), illustrate the effect of Ramadan fasting (A). Two phases comparison Phase1 (pre-Ramadan) and Phase4 (one month after end of Ramadan fasting) illustrate if the impact of Ramadan month fasting persists one month later (B). MR T1-FATS image (3-slices) or Dixon-Fat images (10-slices) of mid-abdomen measured automatically via thresholding technique using 3D slicer software. Data are presented as means with error bars representing standard error (SEM) (n=18 females, n=19 males). Statistical analysis was performed with mixed effect models. (*) represents the significant difference between time points (main effect), one symbol (P<0.05), two symbols P<0.01, and three symbols (P<0.001).

Figure 4.4.4 Abdominal subcutaneous fat volume (ASF) comparison of three phases; baseline (pre-Ramadan fasting), (one week after commencing Ramadan fasting) and (3.5 weeks after commencing

Ramadan fasting), shows the effect of Ramadan fasting (A). A comparison of two phases (pre-Ramadan) and (one month after the end of Ramadan fasting) to elicit if the significant impact of Ramadan fasting persists one month later (B). MR T1-FATS image (3-slices) or Dixon-Fat images (10-slices) of mid-abdomen measured automatically via thresholding technique using 3D slicer software. Data are presented as means with error bars representing standard error (SEM) (n=18 females, n=19 males). Statistical analysis was performed with mixed effect models. (*) represents the significant difference between time points (main effect), one symbol (P<0.05), two symbols P<0.01, and three symbols (P<0.001).

Figure 4.4.5. Fasting blood glucose concentration (mmol/l). Three phases comparison; Phase1 (pre-Ramadan), Phase2 (one week after commencing Ramadan fasting) and Phase3 (3.5 weeks after commencing Ramadan fasting), illustrate the effect of Ramadan month fasting (A). Two phases comparison, Phase1 (pre-Ramadan) and Phase4 (one month after end of Ramadan fasting) illustrate if the impact of Ramadan month fasting persists one month later (B). Data are presented as means with error bars representing standard error (SEM) (n=37, 18 females and 19 males). Statistical analysis was performed with mixed effect models. (*) represents the significant difference between time points (main effect), one symbol (P<0.05), two symbols P<0.01, and three symbols (P<0.001).

Figure 4.4.6 Fasting blood insulin concentration (mmol/l). Three Phases comparison; Phase 1 (pre-Ramadan), Phase2 (one week after commencing Ramadan fasting) and Phase3 (3.5 weeks after commencing Ramadan fasting), illustrate the effect of Ramadan month fasting (A). two phases comparison Phase1 (pre-Ramadan) and Phase4 (one month after end of Ramadan fasting) illustrate if the impact of Ramadan month fasting persists one month later (B). Data are presented as means with error bars representing standard error (SEM) (n=37, 18 females and 19 males). Statistical analysis was performed with mixed effect models.

Figure 4.4.7. HOMA-IR, three Phases comparison; Phase 1 (pre-Ramadan), Phase2 (one week after commencing Ramadan fasting) and Phase3 (3.5 weeks after commencing Ramadan fasting), illustrate the effect of Ramadan month fasting (A). two phases comparison Phase1 (pre-Ramadan) and Phase4 (one month after end of Ramadan fasting) illustrate if the impact of Ramadan month fasting persists one month later (B). Data are presented as means with error bars representing standard error (SEM) (n=37, 18 females and 19 males). Statistical analysis was performed with mixed effect models.

Figure 4.4.8. Low-density lipoprotein concentration (mmol/L). Three phases comparison; Phase1 (pre-Ramadan), Phase2 (one week after commencing Ramadan fasting) and Phase3 (3.5 weeks after commencing Ramadan fasting), shows the effect of Ramadan fasting (A). Two phases comparison; Phase1 (pre-Ramadan) and Phase4 (one month after the end of Ramadan fasting) to elicit if the significant effect of Ramadan fasting persists one month later (B). Data are presented as means with error bars representing standard error (SEM)(n=18 females, n=19 males). Statistical analysis was performed with mixed effect models. (*) represents the significant difference between time points (main effect), one symbol (P<0.05).

Figure 4.4.9. Total blood cholesterol (A), Total Triglycerides (B) concentrations changes. Three phases comparison; Phase1 (pre-Ramadan), Phase2 (one week after commencing Ramadan fasting) and Phase3 (3.5 weeks after commencing Ramadan fasting), shows the effect of Ramadan fasting. Two phases comparison; Phase1 (pre-Ramadan) and Phase4 (one month after the end of Ramadan fasting) to elicit if the significant effect of Ramadan fasting persists one month later (C), (D). Data are presented as means with error bars representing standard error (SEM)(n=18 females, n=19 males). Statistical analysis was performed with mixed effect models.

Figure 4.4.10. High density lipoprotein (A), and Albumin (B) concentrations changes. Three phases comparison; Phase1 (pre-Ramadan), Phase2 (one week after commencing Ramadan fasting) and Phase3 (3.5 weeks after commencing Ramadan fasting), shows the effect of Ramadan fasting. Two phases comparison; Phase1 (pre-Ramadan) and Phase4 (one month after the end of Ramadan fasting) to elicit if the significant effect of Ramadan fasting persists one month later (C), (D). Data are

presented as means with error bars representing standard error (SEM)(n=18 females, n=19 males). Statistical analysis was performed with mixed effect models.

Figure 4.4.11. Acetoacetate (A &B), and β-hydroxybutyrate (C&D) concentrations change. Three phases of comparison; Phase1 (pre-Ramadan), Phase2 (one week after commencing Ramadan fasting) and Phase3 (3.5 weeks after commencing Ramadan fasting), show the effect of Ramadan fasting. Two phases of comparison; Phase1 (pre-Ramadan) and Phase4 (one month after the end of Ramadan fasting) to elicit if the significant effect of Ramadan fasting persists one month later (C), (D). Data are presented as means with error bars representing standard error (SEM) (n=8 females, n=8 males). Statistical analysis was performed with mixed effect models.

Figure 4.4.12. Comparisons of habitual energy consumption (kcals) and macronutrients intake (grams) between Ramadan fasting period (started after Phase 2) and non-fasting period (started after Phase 4). Energy consumption (A), carbohydrate intake (B), fat intake (C), and protein intake(D). Data are presented as mean with error bars representing the standard error of mean (SEM)(*n*=18 females, *n*=17 males). Statistical analysis was performed with measures two-way ANOVA. (*) represents the significant difference between time points (main effect), one symbol ($P<0.05$).

Figure 4.4.13. Metabolic equivalent of tasks for the following activities: sedentary (A), light (B), moderate (C), vigorous (D) and total of all the above(E). Comparison between Ramadan fasting period (started on Phase 2) and non-fasting period (started on Phase 4). Data are presented as mean with error bars representing the standard error of mean (SEM) (females=18, males=18). Statistical analysis was performed with measurements Two-way ANOVA.

Chapter 5

Figure 5.3.1. Illustration of the experimental protocol. The study involved four phases, and in all of them, body mass, MRI scan and FBG were taken for the participants. Height was only taken in the first phase, and CGM devices were placed on the participants' upper arms during the last two weeks of Ramadan and one month after the end of Ramadan. Subjects wore the devices for one week in each period. FBS: fasting blood sample, CGM: continuous glucose monitor.

Figure 5.3.2. MRS single voxel positioning on m.vastus medialis, this region of interest was chose for MRS and Dixon FF% analysis (A). Quantification of (1) IMCL at 1.3 ppm, (2) EMCL at 1.5 ppm, and (11) water, although water signal was suppressed, there was a residual content of water at 4.7 ppm(B). A sample of 1H-MRS water unsaturated spectrum was markedly large compared to other spectra(C).

Figure 5.3.3. MRS-HISTO liver ROI for measuring IHCL. Area was carefully selected to avoid any large vessels.

Figure 5.3.4. Total thigh fat volume measurement (IMAT and SAT), from MR- Dixon fat-only image. Image post-processed using 3D-slicer software.

Figure 5.4.1. Comparisons of Body mass index (BMI). Phase1(Pre-Ramadan) compared to Phase2(one week after commencing Ramadan fasting) and Phase3 (3.5 weeks after commencing Ramadan fasting) to show Ramadan fasting effect (A). Phase1 (Pre-Ramadan) and Phase4 (one month after end of Ramadan fasting) (B) to explore if the impact of Ramadan fasting is continuous one month later. Data are presented as means with error bars representing standard error (SEM) (n=10 females, n=11 males). Statistical analysis was performed with measurements Two-way ANOVA (A) and Mixed-effects model (B). (*) represent the significant difference between time points, one symbol ($P<0.05$), two symbols $P<0.01$, and three symbols ($P<0.001$).

Figure 5.4.2.1. Comparisons of IMCL / Water ratio. Phase1 (pre-Ramadan) compared to Phase2 (one week after commencing Ramadan fasting) and Phase3 (3.5 weeks after commencing Ramadan fasting) shows the effect of Ramadan fasting (A). A comparison between Phase1 (pre-Ramadan) and Phase4 (one month after the end of Ramadan fasting) to elicit if the significant impact of Ramadan month fasting persists one month later (B). Data are presented as means with error bars representing standard error (SEM) (n=10 females, n=11 males). Statistical analysis was performed with measurements, Two-way ANOVA (A) and Mixed-effects model (B). (*) represent the significant difference between time points, one symbol (P<0.05), two symbols P<0.01, and three symbols (P<0.001).

Figure 5.4.3. Phase1 (pre-Ramadan) compared to Phase2 (one week after commencing Ramadan fasting) and Phase3 (3.5 weeks after commencing Ramadan fasting) shows the effect of Ramadan fasting (A). A comparison between Phase1 (pre-Ramadan) and Phase4 (one month after end of Ramadan fasting) to elicit if the significant impact of Ramadan month fasting persists one month later (B). Data are presented as means with error bars representing standard error (SEM) (n=10 females, n=11 males). Statistical analysis was performed with measurements Two-way ANOVA (A) and Mixed-effects model (B). (*) represent the significant difference between time points, one symbol (P<0.05), two symbols P<0.01, and three symbols (P<0.001).

Figure 5.4.4. Comparisons of right thigh fat volume (Th. F). Phase1 (pre-Ramadan) compared to Phase2 (one week after commencing Ramadan fasting) and Phase3 (3.5 weeks after commencing Ramadan fasting) shows the effect of Ramadan fasting (A). A comparison between Phase1 (pre-Ramadan) and Phase4 (one month after end of Ramadan fasting) to elicit if the significant impact of Ramadan month fasting persists one month later (B). MR Dixon-fat images of right thigh fat volume measured automatically via thresholding technique using 3D slicer software. Data are presented as means with error bars representing standard error (SEM) (n=10 females, n=11 males). Statistical analysis was performed with mixed effect models.

Figure 5.4.5 Estimation of liver fat deposition. (A&B) Dixon- PDFF sequences quantify %FF. (C, D) HISTO-MRS-STEAM quantify IHCL. (A&C) comparisons between; Phase1 (pre-Ramadan), Phase2 (one week after commencing Ramadan fasting) and Phase3 (3.5 weeks after commencing Ramadan fasting) show the temporal effect of Ramadan fasting. (B&D) Comparisons between Phase1 (pre-Ramadan) and Phase4 (one month after end of Ramadan fasting) to elicit if there are any significant changes one month after the end of Ramadan fasting. Data are presented as means with error bars representing standard error (SEM) (n=10 females, n=11 males). Statistical analysis was performed with mixed effect models.

Figure 5.4.6. serum calcium concentrations. A comparison between baseline (Pre-Ramadan) and Phase2 (one week after commencing Ramadan fasting) and Phase3 (3.5 weeks after commencing Ramadan fasting) to show Ramadan fasting effects (A). A comparison between Phase1 (Pre-Ramadan) and Phase4(one month after end of Ramadan fasting) shows no significant difference (B). Data are presented as means with error bars representing standard error (SEM) (n=10 females, n=11 males). Statistical analysis was performed with mixed effect models.

Figure 5.4.7. A comparison of the mean of 3-days water consumption during Ramadan fasting and one month after the end of Ramadan. Data are presented as means with error bars representing standard error (SEM) (n=10 females, n=11 males). Statistical analysis was performed with mixed effect models. Water amount recorded by participants in food diaries.

Figure 5.4.7. Continuous interstitial fluid glucose concentration. A comparison between Ramadan fasting and one month after the end of Ramadan fasting periods. (A) average glucose concentrations. (B) the average percentage of glucose concentration readings in the normal range. Data are presented as means with error bars representing standard error (SEM) (*n*=10 females, *n*=8 males). Statistical analysis was performed with measurements Two-way ANOVA.

Figure 5.4.8.1. Relationship between the changes in changes fasting blood glucose (FBG) and intrahepatocellular lipid (IHCL), (Phase 3) - (Phase 1). Left females (n=10) and right males (n=11). Statistical analysis was performed with Pearson's correlation test.

Figure 5.4.8.2. Relationship between the changes in changes fasting blood glucose (FBG) and intramyocellular lipid (IMCL), (Phase 3) - (Phase 1). Left females (n=10) and right males(n=11). Statistical analysis was performed with Pearson's correlation test.

Contents

Declaration

All the data collected, and procedures described in this thesis, including images analysis, venepunctures, blood samples preparation, dietary nutrition and physical activities analysis, continuous glucose monitoring, and statistical analysis, have been performed by myself, with the following exceptions.

Dr Sean Kilroe and Dr Tom Jameson collected the data in Chapter 3. Also, I used the result of Sean's manual measurements to compare it with my automated measurements. Gráinne Whelehan, Dr Marlou Dirks, Amy Booth and Kiera Wilkinson helped me in venepunctures and blood sample preparation in Chapters 4 and 5. Serum and plasma analysis carried out at the Clinical Chemistry department of the Royal Devon & Exeter NHS Foundation Trust. Some plasma lipids analyses in Chapter 4 were performed at the MRC Integrative Epidemiology Unit at the University of Bristol.

Hereby declare that the present thesis has been composed by myself and that it is a record of my work, except when help has been acknowledged. No part of this thesis has been submitted in any other application for a higher degree, and all sources of information have been referenced.

Ashwag Abdullah Alarfaj, November 2022.

Acknowledgements

For all 5 years (including the COVID-19 Pandemic year, which suspended the data collection), I had the opportunity to challenge myself from many perspectives as an overseas foreign postgraduate researcher, a mother to two lovely children, and a wife to a loving, kind and patient husband. Although PhD work was challenging, I have enjoyed undertaking the work described in this thesis within the Nutrition Physiology Group in the Department of Sport and health. During these years, I have worked with a very friendly, helpful, supportive group, all of whom did not hesitate to provide any support. I gratefully appreciate this experience. I want to express my sincere gratitude to the following people:

Professor Francis Stephens, for his supervision, his time spent educating me, listening to my thoughts, answering my questions, opening his door, fulfilling my demands, and kindly understanding my situation, assuring me and being very patient and gentle when I was stressed.

Dr Jonathan Fulford, also for his supervision, spent his time in the MRI department working hard to complete all the data needed in the research. Also, I appreciate his kindness, cooperation, and guidance. The work was so smooth and comfortable with you.

I appreciate you, doctors, and thank God I was lucky for your supervision.

To Dr Benjamin, many thanks for your support, smile and super useful seminars you arranged. From there, many ideas have lightened my mind, and I could not bring the Ramadan study idea without attending such valuable seminars.

Gráinne Whelehan, special thanks for offering your help, generous cooperation, beautiful friendship, coffee time chat, listening and guidance. You definitely added a special mark to my PhD journey. For Sean Kilroe, Marianna Coelho, Tom Jameson, George Pavis, Marlou Dirks, Amy Booth, Kiera Wilkinson, Alistair Monteyne, Sam West, Sam Bailey, Chris Koscien and all Nutritional Physiology Group and all the colleagues I have met in mezzanine office or the Department of Sport and Health Sciences of the University of Exeter. Many thanks for the nice attitude and welcoming behaviour. Many thanks to all my participants who did not hesitate to participate in the research and worked hard to complete all the study tasks with patience and understanding, especially in the holy month of Ramadan, when they committed to the religious obedience and the study tasks.

My husband Basim Bin shahween, I cannot succeed in my graduation degree without your persistent help, constant love, patience and calm, hard work and the high responsibility you have dedicated to our children and me. To my mum, my sunshine and source of tranquility, and my dad, my childhood hero, who always encouraged me, I hope you get well. Many thanks to my two sisters and four brothers, my extended family and friends for all the joy and support I had from you. To my pleasant children Abdullah, Leen and the one in my tummy now, this work for you and your generation to be the best than your older ones. Please work to the best for your world with morality and honesty.

Chapter 1

General introduction

1.1 Overview

Concerns have been raised in the last decade around metabolic health, including the increasing prevalence of metabolic syndrome (MetS). MetS is one of the most prevalent epidemics across the world, affecting around a quarter of the world's population. It is diagnosed when three of five signs exist, including elevated fasting blood glucose (FBG) level or insulin resistance (IR), central obesity, high triglycerides (TG), high blood pressure and low high-density lipoprotein (HDL) level. Those diagnosed with MetS have a high incidence of developing myocardial infarction or stroke, at high risk of cardiovascular diseases (CVD) and have five times the chance of having diabetes mellitus (T2DM). Moreover, diabetes cases are expected to increase 2-fold by 2025 and, in 2030, will become the seventh most common cause of mortality worldwide (Pieńkowska et al. 2020). The World Health Organisation has agreed to aim to halt the rise in diabetes and obesity by 2025 (WHO 2020).

Intermittent fasting (IF) in its several forms has been suggested to be one of many strategies to prevent or alleviate the consequences of MetS by decreasing body weight, reducing body fat, and reducing energy consumption (Wilkinson et al. 2020). On the other hand, starvation or prolonged fasting is a known model that induces IR by stimulating lipolysis and fat oxidation that shifts fuel utilisation in the musculoskeletal system from glucose to free fatty acids (FFAs) to save glucose for the central nervous system (Hoeks et al. 2010). It is possible that time-restricted eating (TRE) could positively affect metabolic health and muscle mass. Given that many people worldwide practice Ramadan annually, this presents a suitable model to study the effects of TRE on metabolic health. This thesis aims to use the Ramadan fasting (RF) model to study the metabolic changes that could occur from this common annual religious practice among Muslims. It aims to use non-invasive MRI technology and

validate and optimise automatic segmentation of MR images to record skeletal muscle and fat volume changes. Finally, it aims to measure abdominal adipose fat volumes and skeletal muscle and liver ectopic lipids changes due to RF. In addition, fasting blood samples to monitor FBG, FBI (fasting blood insulin), and lipids profile will be measured. The aim is that this thesis will contribute to the development of strategies and guidelines to improve metabolic health via monitoring of muscle mass and body lipids.

1.2 Muscle Volume and Body Metabolism

Weight loss is mostly driven by modifications in dietary intake and exercise. Many people practice these strategies to achieve an optimal BMI and to improve metabolic health. Although body weight reduction aims to improve quality of life and metabolic health, it may cause potentially negative consequences, such as skeletal muscle mass reduction. The optimal result from any weight-loss plan is a reduction in fat mass and preservation of skeletal muscle mass. This outcome would improve markers of metabolic health, such as increased insulin sensitivity and improved blood lipids profile (McCarthy and Berg 2021). Skeletal muscle is the largest insulin-sensitive tissue in the body, forming approximately 40-50% of total body mass and responsible for 75-95% of all insulin-mediated glucose disposal under insulin clamps conditions. It is also responsible for lipid oxidation, and any change in skeletal muscle mass will significantly affect the body's energy stores and metabolism. Also, cardiovascular diseases (CVD) and MetS are strongly associated with decreased physical activity, that leads to the reduction in muscle mass and strength, independent of BMI and age (Stump et al. 2009). Additionally, increasing intermuscular adipose tissue (IMAT) and

decreasing muscle volume are associated with increasing fasting blood glucose (FBG) concentration (Kim et al. 2017).

Although it has been established that body mass index (BMI) is a marker of metabolic health, it does not differentiate between fat mass and fat free mass. A reduction in muscle mass and an increase in body fat are more strongly associated with an increased risk of MetS than BMI alone (Lang et al. 2015). A few days of limb immobilisation or inactivity caused a significant decline in muscle mass (Kilroe et al. 2020) and muscle strength (Demangel et al. 2017). Muscle atrophy is associated with many biological conditions such as ageing, disuse or inactivity and metabolic diseases, e.g., diabetes. This decline in muscle mass reduces glucose disposal in skeletal muscle and leads to muscle insulin resistance (Stephens et al. 2015; Dirks et al. 2016). These studies investigated the link between muscle atrophy and insulin sensitivity. *Dirks et al. (2016)* studied the effect of one-week of bed rest on the body composition of healthy young men. They measured the thigh muscle cross-sectional area (CSA), IMAT, abdominal visceral fat (AVF) and subcutaneous fat (ASF) using a CT scan. Also, whole-body insulin sensitivity was measured using a hyperinsulinemic-euglycemic clamp, and due to the hyperinsulinemia, the whole-body insulin sensitivity reflected peripheral insulin sensitivity. After 7 days of bed rest, they detected a significant decline in body weight (1.4±0.2 kg), total lean mass and thigh and arm muscles, as assessed by DXA. A CSA of one slice (3 mm thickness) from the CT images revealed the following: there was a decline of the total thigh CSA (-2.2±1.0%), abdominal muscle (-0.8 cm^2) and ASF(-0.04cm^2). These observations occurred in conjunction with an increase in whole-body insulin resistance (IR) and decreased muscle oxidative capacity; however, no other lipids accumulation was observed (Dirks

et al. 2016). *Stephens et al. (2015)* reported muscle protein synthesis decline due to intravenous lipid infusion that causes IR of skeletal muscle (Stephens et al. 2015).

Other studies have linked IR with body lipids accumulation; both ectopic lipids and adipose fats, e.g., abdominal visceral fat, was found to be associated with IR (Hoeks et al. 2010; Chee et al. 2016). For instance, *Thomas et al. (2012)* reported that muscle and liver ectopic lipids strongly correlate with AVF. However, this study did not include the measurement of total muscle mass. Also, it stated that subcutaneous fat has a beneficial role in preventing glucose and lipid metabolic risk (Thomas et al. 2012). This effect can be seen in the case of lipodystrophy disease, which is described as a partial or complete absence of subcutaneous adipose tissue (SAT) associated with metabolic perturbances and an increased risk of diabetes mellitus (Savage et al. 2019).

Furthermore, 2 days of thigh immobilisation caused a decline in whole thigh muscle volume of 1.7%, which increased to 5.5% after 7 days in physically fit young men aged 20±1 years (Kilroe et al. 2020). This study highlights the negative effects of physical inactivity on muscle mass while maintaining energy balance. Ageing, chronic sedentary behaviour, or inappropriate frequent weight loss events can contribute to sarcopenic obesity (a normal BMI but high fat mass and low muscle mass) that could lead to an increased risk of metabolic disease (McCarthy and Berg 2021).

1.3 Lipid metabolism in the skeletal muscle

Skeletal muscle is not only a crucial organ for body movement. It also represents around 40% of total body weight, consumes about 30% of basal energy and plays a pivotal role in regulating protein, lipid and carbohydrate metabolism in the human body. The skeletal muscle acts as a machine that stores and consumes energy.

Glucose and lipids are both fuel sources involved in complex metabolic processes with enzymes and proteins to produce sufficient energy required for body movement (Pagano et al. 2018). Skeletal muscle takes up lipid in the form of fatty acids by hydrolysis or lipolysis; the process or breaking down of the large molecule triacylglycerides (TAGs) into glycerol and energy-rich free fatty acids (FFAs). This process is stimulated in the presence of hormone-sensitive lipase. Skeletal muscle takes up the FFAs according to metabolic demand and lipid availability. Once the FFAs have entered the muscle tissue, they can undergo one of two processes. They either enter the β-oxidative process in the mitochondria to produce energy, or when the β-oxidation needs are exceeded, FFAs accumulate as lipid droplets LDs in skeletal muscle as an energy deposit store. However, excessive lipid deposition leads to lipotoxic stress or fatty infiltration (Morales, Bucarey, and Espinosa 2017).

Adipose tissue is an essential structure in the human body and is not merely used as an energy storage system. It is considered a major endocrine system that produces several types of proteins known as adipokines. In the human body, there are two main locations for fat deposits: visceral adipose tissue (VAT), which is the fat of the intra-abdominal cavity, and subcutaneous adipose tissue (SAT), which is the fat layer under the skin (Komolka et al. 2014). However, fat is also located in non-adipose tissues such as the heart, liver, pancreas and skeletal muscle. These organs which contain non-adipose tissues act as additional storage sites for lipids in addition to subcutaneous and visceral tissues. Lipids stored in non-adipose tissue are referred to as ectopic lipids, for instance, intrahepatocellular lipids (IHCL), intracardiomyocellular lipids (ICCL) and intramyocellular lipids (IMCL) refer to lipid deposition in hepatocytes, cardiac muscle cells and skeletal muscle cells, respectively (Loher et al. 2016). Musculoskeletal (MSK) intermuscular adipose tissue (IMAT) and extramyocellular lipid

(EMCL) are additional types of lipids (Pagano et al. 2018). Ectopic lipids, e.g., in skeletal muscle, can be considered as fuel storage, therefore, can be depleted by specific diet or physical exercise and repleted by (over) nutrition. Ectopic lipids can also be an indication of various metabolic diseases (Loher et al. 2016). Insulin resistance (IR) is one of the main cardiometabolic risk factors linked to ectopic lipid infiltration in liver, muscle and pancreas (Trouwborst et al. 2018). An interesting study examined the effect of a low-calorie diet (60% carbohydrate, 25% fat, 15% protein, total energy intake 27.9 kcal/kg of ideal body weight (IBW= 22.2 kg/m^2 , 21.9 kg/m^2 for men and women, respectively), and exercise, on insulin-sensitivity in people with T2DM (with no other diseases or complication). Total energy intake for 2 weeks was 1628.6 Kcal/day in the diet alone (non-exercise) group and 1657 Kcal/day in the diet and exercise group. In the diet and exercise group, subjects were asked to complete 2-3 sessions of 30 min walking per week. IMCL significantly decreased by 19% (measured using MRS technology), combined with a significant increase in skeletal muscle insulin sensitivity as measured by an increase in glucose infusion rate during the hyperinsulinemic-euglycemic clamp in the exercise group only. Both groups showed a significant reduction in IHCL by 27%. BMI was reduced by 0.4 kg/m^2 in the diet group and 0.7 kg/m^2 in the diet+exercise group. Body fat decreased by 2.4 and 2.8 in diet alone and diet+exercise groups, respectively. Also, the blood lipid profile improved in diet+exercise group. However, no information has been reported about muscle mass (Tamura et al. 2005) this study indicates the importance of combining these two factors (diet and exercise) in promoting heath and preventing MetS (Bergens et al. 2020).

1.4 The importance of measuring lipids and skeletal muscle volume

Interest in measurements of skeletal muscle and lipid volumes has increased in clinical research (Addeman et al. 2015). Lipid deposits have an intrinsic property and act as active groups of endocrine organs (e.g., subcutaneous, visceral, or intra-abdominal, and intermuscular adipose tissues) and organelles (e.g., IMCL and EMCL) (Komolka et al. 2014). Also, skeletal muscle has an important role as a carbohydrate and lipid metabolic regulator (Morales, Bucarey, and Espinosa 2017) and has a capacity for plasticity and adaptation. For instance, skeletal muscle rapidly responds to changes in physical activity or dietary alterations (Pagano et al. 2018). Skeletal muscle volume and degree of lipid infiltration are important factors in ageing and training as they are related to muscle strength (Manini et al. 2007). Many metabolic, cardiovascular, osteoarthritis, neuromuscular diseases, and inflammatory processes are linked to lipid and skeletal muscle volume changes (Marra et al. 2018; Karlsson et al. 2015; Hogrel et al. 2015; Addeman et al. 2015; Ikemoto-Uezumi et al. 2017). Significant developments in pharmaceutical and treatment strategies for muscular diseases have increased the demand for non-invasive, early disease detective surrogate biomarkers. Currently, there are many non-invasive quantitative methods for determining skeletal muscle and body fat volume or mass, such as bioelectrical impedance (BIA), air displacement plethysmography (BOD POD), dual-energy X-ray (DXA), computed tomography (CT) and magnetic resonance imaging (MRI). The first two are non-ionising radiation and non-expensive (Sirirat et al. 2020). DXA and CT are more reliable but are ionising radiation imaging modalities. MRI is non-ionising radiation, the most reliable and accurate imaging modality, which provides high resolution images and can be used as tool for assessing a wide range of anatomical and physiological characteristics (Borga et al. 2018). Medical imaging has improved our understanding

of biological changes in the human body (Komolka et al. 2014). Advanced imaging technology can provide quantitative measurements of tissue properties to aid the classification of disease severity and detect minor pathological changes over time. This technology allows the monitoring of specific treatment responses early (Carlier et al. 2016). Of the various types of medical imaging technologies, MRI and CT have shown high sensitivity and reproducibility in quantitative studies. Both technologies are non-invasive and provide high-resolution multi-projection images. However, unlike CT, MRI uses non-ionizing radiation. MRI also produces excellent contrast of soft tissues and provides wider options to study the anatomical and physiological properties of a specific organ (Carlier et al. 2016; Addeman et al. 2015). It is unclear which lipid deposits are most closely related to metabolic health and maintenance of muscle mass.

Quantification of ectopic lipids was historically assessed invasively with biopsy and examined via laboratory tools, such as electron microscopy and morphometry. Biopsy was the only gold standard method used to estimate ectopic lipids. Then after establishing the MRS technology, estimating ectopic lipids non-invasively became a wider and more reliable tool in research and clinical fields (Loher et al. 2016). Skeletal muscle biopsy was the gold standard and only method to assess ectopic lipids until *Schick et al. (1993)* discovered two magnetic resonance spectroscopy (MRS) peaks corresponding to fatty acids in the skeletal muscle, one associated with the lipids in fat cells restricted between muscle fibres and the other associated with the lipids droplets inside muscle cells which are not restricted to muscle fibre orientation. After this interesting finding, *Boesch et al. (1997)* validated MRS as a non-invasive tool to assess ectopic IMCL lipids (Chris Boesch et al. 2006).

1.5 Lipids classifications in skeletal muscle

There are three types of musculoskeletal lipid deposits. They are classified according to their storage site: intermuscular adipose tissue (IMAT), extramyocellular lipid (EMCL) or intramuscular fat (IMF), and intramyocellular lipids (IMCL). **Figure 1.5** illustrates the three different lipids' distribution in the skeletal muscle (Komolka et al. 2014).

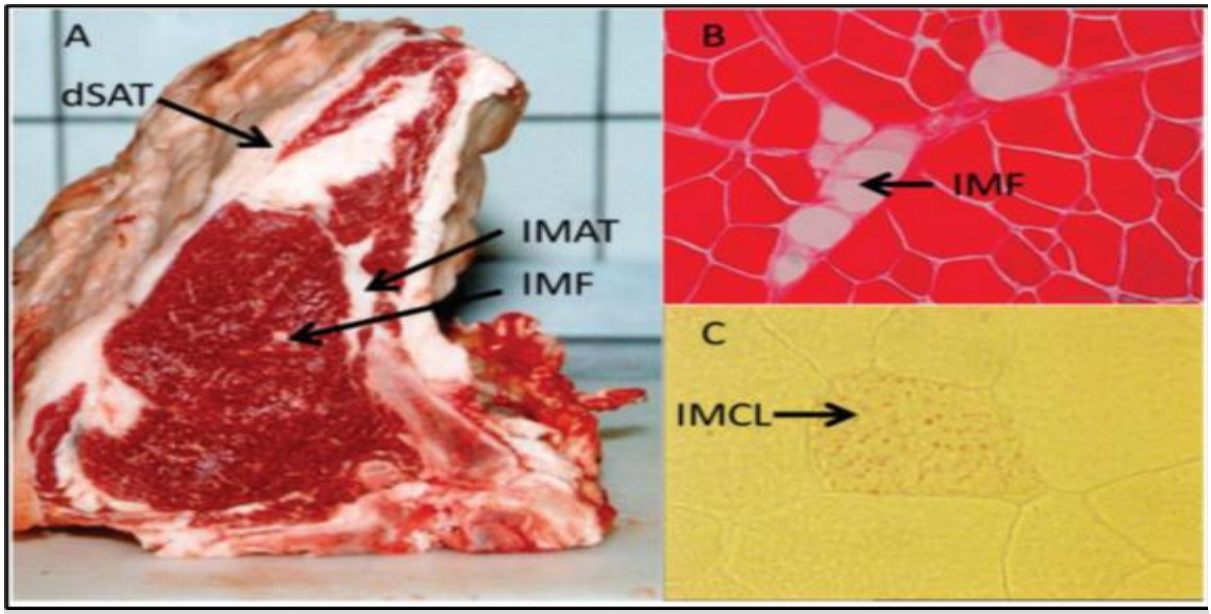

Figure 1.5 Illustration of different muscle-related adipose tissue depots. (A) Deep subcutaneous adipose tissue (dSAT) intermuscular adipose tissue (IMAT), intramuscular fat (IMF), (B) Cellular structure of IMF, (C) Intramyocellular lipids (IMCL, red dots, Oil-red O stained) in a muscle cell (Komolka et al. 2014).

1.5.1 Intermuscular adipose tissue (IMAT)

IMAT consists of adipocytes located between distinct muscles (Komolka et al. 2014). These fat cells are located under the epimysium (between bundles of muscle fibres)

and under the perimysium (between muscle fibres) as illustrated in **Figure 1.5.1** (Pagano et al. 2018).

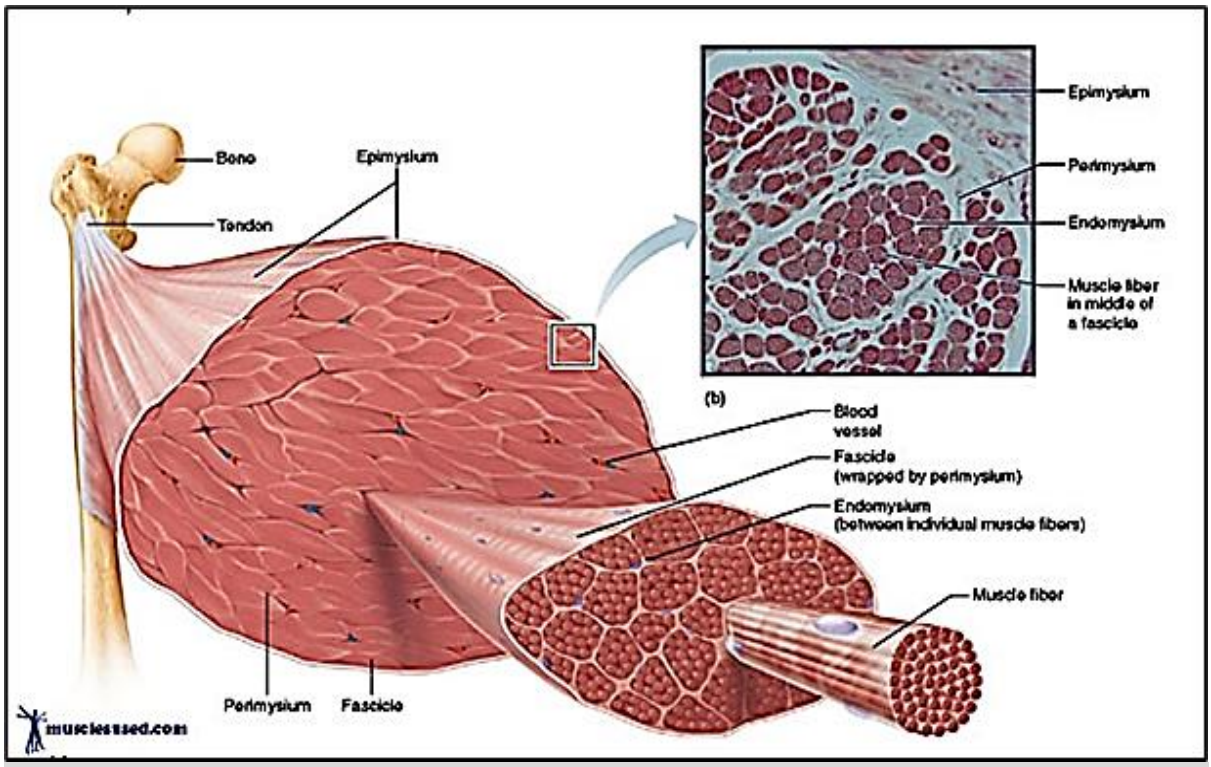

Figure 1.5.1. A skeletal muscle cross sectional view shows the sites of Intermuscular adipose tissue (IMAT) under epimysium and perimysium; Extramyocellular lipid (EMCL) under endomysium (Stovall 2013).

In an MRI image, it is visible as white lines between muscle groups and beneath muscle fascia (X. Y. Ruan et al. 2007). Although IMAT is normally present in the skeletal muscle, an increase in its infiltration rate is believed to be an important factor in muscle deconditioning (i.e., loss of muscle strength and power), as the loss of muscle mass alone is not sufficient to identify muscle deconditioning. Indeed, many observations suggest that loss of muscle power and strength usually exceeds the loss of muscle mass in many metabolic related cases, for instance, muscle inactivity,

denervation, diabetes, tenotomy and sarcopenia (Pagano et al. 2018). Moreover, in the case of sarcopenia, raised IMAT levels in a geriatric group are considered to be a good surrogate marker of bone fracture (Hamrick, McGee-Lawrence, and Frechette 2016).

In addition, IMAT accumulation is negatively correlated with the degree of inactivity (Pagano et al. 2018). *Manini et al. (2007)* concluded that after 4 weeks of immobilisation, an increased IMAT level was related to the loss of muscle strength in the thigh and calf. The cytokines protein secreted from IMAT are linked to muscle mass reduction (Manini et al. 2007). Together with previously discussed studies, it suggests that increased IMAT volume is more sensitive, or is an early biomarker, for decreased muscle function compared with decreases in skeletal muscle volume. It has been suggested that fat deposits localised outside muscle cells (EMCL and IMAT) are related to the ageing process and loss of muscle strength as well as IR (Pagano et al. 2018). IMAT accumulation is also related to skeletal muscles injury in the animal model (McHale et al. 2012) and inactivity in the human model (Pagano et al. 2018). Also interestingly, *Yim et al. (2007)* have linked IMAT and visceral adipose tissue accumulation with an increase in cardiovascular risk factors (Yim et al. 2007). However, the link between infiltrated muscle lipids and metabolic syndrome or IR is controversial, for example, *Dirks et al. (2016)* did not detect any changes in IMAT or total body fat after one week bed rest of young healthy men, but they detected a significant decline in muscle mass and insulin sensitivity (Dirks et al. 2016). Also, ageing *per se* is not strongly related to the accumulation of IMAT and the decline in muscle mass and strength (Marcus et al. 2010). Physical inactivity associated with ageing contributes to muscle decline, increases IMAT and lowers muscle strength. A study on the active elderly population has revealed that repeated intensity exercise

prevents muscle mass and strength decline and IMAT elevation (Wroblewski et al. 2011).

1.5.2 Extramyocellular lipid (EMCL) or intramuscular fat (IMF)

EMCL or IMF is located inside the muscle tissue and between myocytes or muscle fibres. It is also a type of adipose tissue or fat cells found adjacent to muscle tissues and outside muscle cells like IMAT. Its structure is restricted by the longitudinal form of muscle fibres bundles and thus is shaped like tubes, unlike IMCL which is spherical in shape. This difference allows MRS technology to differentiate and quantify each one separately. A study by *Goodpaster et al. (2000)* found a positive correlation between the volume of the adipose tissue interspersed around and between the skeletal muscle and insulin resistance. However, this relation was not found with subcutaneous fat in the same subjects. These findings highlight the important role of muscular lipids compared to other fatty deposits (Goodpaster, Thaete, and Kelley 2000). In standard T1 weighted spin echo MRI images (See 1.7.1 for definition), IMAT and EMCL appear as white lines diverging between and inside muscle tissues (Akhmedov and Berdeaux 2013)**.** They show the same image contrast as subcutaneous adipose tissue (SAT), see **Figure 1.5.2.**

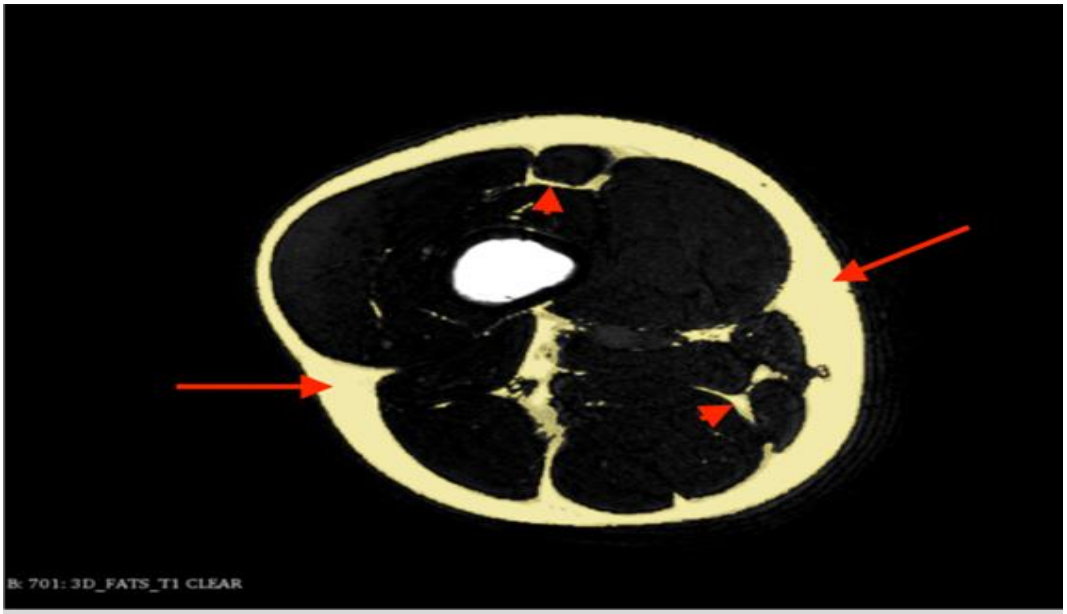

Figure 1.5.2. MR 3D FATS image, an axial slice of thigh. Shows fat segmentation post process, based on signal intensity variation between fat and muscle. Automatic segmentation includes IMAT (arrows heads), and SAT (long arrows) slicer post image processing programme.

1.5.3 Intramyocellular lipid (IMCL)

Intramyocellular lipid is lipid droplets (LDs) like vesicle intracellular structures covered with different types of proteins and enclosing several kinds of lipids referred to as IMCLs. LDs located in the sarcoplasm of myocytes (muscle cells) are found between sarcomeres near the mitochondria as shown in **Figure 1.5.3.** They act as local energy pools in the case of acute or chronic exercise, high lipid feeding and prolonged fasting (Morales, Bucarey, and Espinosa 2017). Furthermore, within MRS studies, LDs have been investigated in many vital organs, such as the heart, liver and pancreas. LDs are involved in different metabolic processes such as lipid storage, lipid transaction between organelles and cell (stimuli) signalling (Loher et al. 2016). In skeletal muscle, LDs are considered biologically active organelles and not just local lipids storage, covered by proteins with different biological functions. Proteomic studies explored 324

lipid droplet-proteins responsible for many biological functions such as lipid storage, metabolism and exchange between cell organelles, cell membrane traffic and signalling, which control the entry and exit of substances into the cell e.g., glucose uptake or insulin signalling. Also, LDs proteins interact with mitochondria and have a role in the cell autophagy process (a cell degradative process of damaged organelles to produce newer and healthier replacements). This process is important, for example, in skeletal muscle to remove dysfunctional mitochondria that cause oxidative stress and that reduce skeletal mass and strength (Komolka et al. 2014; Morales, Bucarey, and Espinosa 2017). IMCLs inside LDs consist of four lipids forms: triacylglycerol (TAG), long-chain acyl-CoA, diacylglycerol (DAG), and ceramides; the last three are related to muscle lipotoxic effects that are a risk factor for poor metabolic health (see 'Lipid Toxicity' section 1.6.1).

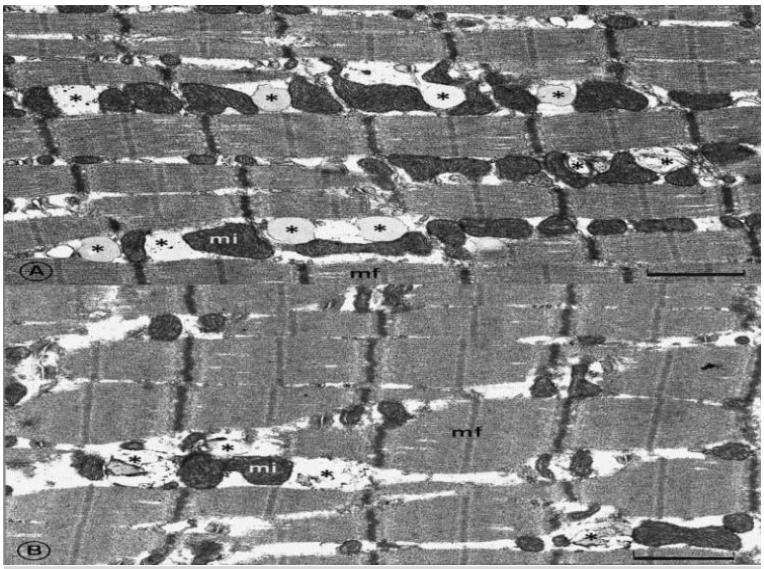

Figure1.5.3. Electron micrographs image of IMCL droplets (*) close to mitochondria (mi) sample biopsy were taken from tibialis anterior muscle. (A) at rest condition. (B) 48 hrs after exhaustive exercise. mf, Myofibrils (Howald et al. 2002).

Table 1.5.3 provides a brief comparison of prolonged fasting studies that includes IMCL measurements and the relationship between IMCL change and other metabolic changes. IMCL concentration is reported to have a significant association with insulin resistance; lipids intermediates such as diacylglycerol (DAG) and ceramide but not triacylglycerol (TAG), the normal fuel source for mitochondria (Chee et al. 2016).

Table 1.5.3. IMCL and prolonged fasting articles findings.

Article	Fasting hrs	Subjects	FBG	FBI	Insulin sensitivity	IMCL	FFA	TG	3-hydroxy butyrate
Stannard. 2002	72 h	6 healthy physically active males	↓	↓	No info	↑	↑	↑	↑
Hoeks. 2010	60 h	12 healthy males	↓	↓	↓	↑	↑	No info	No info
Thankamony. 2018	28 h	24 healthy males	No info	No info	No info	↑	↑	No info	No info
Johanson. 2006	67 h	7 healthy physically fit males	↓	↓	↓	↑	↑		↑

FBG: fasting blood glucose. FBI: fasting insulin. FFA: free fatty acid. TG: triglycerides.

1.5.3.1 IMCL characteristics in muscle cells (sarcoplasm) and its interaction with other lipid pools

Interpreting muscle or general body health status from only a determination of IMCL level is not a reliable approach (Loher et al. 2016). However, IMCL levels have been found to be linked to metabolic disease prevalence, for example, obesity, cardiovascular diseases, and IR (Komolka et al. 2014; Morales, Bucarey, and Espinosa 2017). Several hormones and proteins regulate IMCL concentration within a subject. In addition, IMCL level differs between subjects according to sex, age, muscle group, training level, exercise intensity and duration, fasting duration, diet, obesity, insulin, and growth hormones. Insulin strongly inhibits lipolysis. Hence, during

exercise, insulin secretion decreases, which, in conjunction with increased growth hormone, promotes lipolysis, thus increasing FFA in plasma and elevating IMCL levels in working tissues after exercise (Loher et al. 2016). IMCL is influenced by diet and physical exercise. They have been extensively studied and are now well-known as a fuel store for muscle, which is depleted after an acute bout of physical exercise and then repleted in rest (Loher et al. 2016).

However, an interesting phenomenon in an athletic population (endurance athletes) called the “athletes’ paradox” presents as high IMCL levels in skeletal muscle and also high insulin sensitivity (Komolka et al. 2014). This contrasts with healthy lean subjects where IMCL levels are negatively correlated to insulin sensitivity, i.e., high IMCL levels are associated with insulin resistance in healthy lean subjects. IMCL levels in an athletic population are similar to those of obese and insulin-resistant subjects (Stannard et al. 2002). However, athletes’ IMCL deplete faster during exercise, and LDs’ location within the myocyte are mainly adjacent to the mitochondria. The complexity and contradictory reports of IMCL levels in several situations reflect the lack of clarity of IMCL effects. Moreover, there is growing evidence of the stronger role of diacylglycerol and ceramide than triglyceride on insulin resistance (Loher et al. 2016). The accumulation of these intermediates in subsarcolemmal (SSL) can disrupt muscle glucose uptake and reduce muscle insulin sensitivity (Chee et al. 2016). Finally, prolonged fasting is a well-known physiological situation that promotes IR and increases IMCL levels (Morales, Bucarey, and Espinosa 2017; Hoeks et al. 2010; Stannard et al. 2002). A prolonged fasting study (60hrs) of healthy young men resulted in increased IMCL by 2.8-fold and increased IR by 55%. However, microscopic analysis revealed that individuals with more LDs associated with a special protein called perilipin5 (PLIN5) have an increased size and number of LDs, showed less

reduction in insulin sensitivity and mitochondrial function in fasting conditions which reduces lipotoxicity, in contrast to the individuals with less LDs coated with PLIN5 which result in no changes in LDs size and number but were more IR. Also, the author linked these results with trained athletes (the high IMCL levels and insulin sensitive population) that showed a high level of Perilipin 5 protein (Gemmink et al. 2016).

1.6 Skeletal muscle, liver and adipose tissue homeostasis of glucose and lipid

Skeletal muscle, adipose tissue, liver, brain, pancreas and intestine share a sophisticated mechanism for controlling body glucose levels and lipid metabolism (Röder et al. 2016)**.** Skeletal muscle and liver glucolipid homeostasis are important as they are considered major storage deposits for glucose in the form of glycogen and ectopic lipids in the form of triglyceride (Rigby and Schwarz 2001; Pola et al. 2012). Subsequently, the reduction of insulin action in skeletal muscle, liver and adipose tissue may lead to the development of T2DM (Morales, Bucarey, and Espinosa 2017). Liver and skeletal muscle are target organs for insulin action, and ectopic lipids in these two organs are linked to impaired insulin action (Loher et al. 2016). However, skeletal muscle has a greater role in developing insulin resistance as it is the main site of glucose disposal after meals (Savage et al. 2019). One example of the role skeletal muscle plays in insulin sensitivity is demonstrated by *Tsintzas et al. (2006).* This study reported a unique adaption of skeletal muscle during starvation of 48 hours or more, with increasing fatty acids influx into skeletal muscle, indicating a shift of fuel utility from glucose to fat. This shift in fuel utilisation during starvation coincided with decreased insulin sensitivity and decreased skeletal muscle glucose uptake (Tsintzas et al. 2006), which reflects the metabolic flexibility of skeletal muscle.

Non-alcoholic fatty liver disease (NAFLD) is one of the most prevalent epidemic diseases related to obesity and a sedentary lifestyle (Mindikoglu et al. 2017). It is also strongly correlated with liver disorders and T2DM, even more than waist circumference (WC) or obesity (Drinda et al. 2019). Previous research has shown that values of hepatic triglycerides or Intrahepatocellular Lipids (IHCL) determined by MRS significantly increased after 5-days of a high-fat diet in healthy young males. At the same time, no changes in SAT and VAT deposits were observed (Bakker et al. 2014). These indicate the importance of assessing ectopic lipids, e.g., IHCL, IMCL and IMAT lipids infiltrations, as a surrogate biomarker for metabolic syndrome, e.g., insulin resistance (IR) and T2DM (Kovanlikaya et al. 2005; Bakker et al. 2014)

1.6.1 Lipid toxicity and metabolic health

Lipid toxicity is a term used to describe the imbalance between lipids uptake and consumption or oxidation. Broadly speaking, an increase in plasma fatty acid leads to lipid infiltrations or accumulation in organs, e.g., muscle, liver, pancreas or heart. Excessive storage of ectopic lipids, e.g., IMCL or IHCL, in the cell leads to cell damage. Once fatty acids enter the cell, they are stored in LDs in the form of triacylglycerol (TAG), or in other forms called intermediates (diacylglycerol, ceramides and fatty acyl-CoAs) which cause cellular damage and are linked to insulin resistance (Akhmedov and Berdeaux 2013; Morales, Bucarey, and Espinosa 2017; Rui 2014). Excessive lipid infiltration in skeletal muscle has been linked to insulin resistance (IR) in obese, older populations (Chee et al. 2016). This in turn increases the accumulation of DAG and ceramide in the subsarcolemmal (SSL) region is strongly associated with IR (Chee et al. 2016) oxidative stress (due to damaged mitochondria), muscle atrophy, and muscular weakness (Morales, Bucarey, and Espinosa 2017). Prolonged fasting is a

physiologically well-known model for inducing IR. A study of 60 hrs fasting concluded that prolonged fasting for more than 48 hrs induced elevated plasma FFA and intramyocellular triglyceride (IMTG) or IMCL level (as assessed by muscle biopsy) and increased whole-body fat oxidation. This occurred with an observed reduction in mitochondrial function in skeletal muscle and reduced insulin sensitivity, without hyperinsulinemia or hyperglycaemia that is usually associated with T2DM. (Hoeks et al. 2010). Another 60 hrs fasting study showed similar findings. It proposed a role of a specific protein (PLIN5) that covered LDs and increased the capacity of LDs to store more IMCL. This study concluded that subjects with higher IMCL level after fasting showed a lower reduction in insulin sensitivity and mitochondrial function. The redistribution of PLIN5 protein to attach to LDs surfaces is an adaptive response to lipid-induced IR caused by prolonged fasting to improve mitochondrial function (Gemmink et al. 2016). These two previous studies were conducted on young, healthy men subjects. LDs are associated with autophagy (a degeneration cellular process of damaged cell organelles) (Morales, Bucarey, and Espinosa 2017). Patients with T2DM and hypertension (HT) have significantly elevated levels of fat infiltration in skeletal muscle, liver and pancreas, as assessed by MRI Dixon imaging. Ectopic fat infiltration in these organs positively correlated with BMI and waist circumference (WC). However, fat infiltration of skeletal muscle showed the strongest correlation with WC. Comparing three groups of patients who have (i) T2DM and high blood pressure the hypertension disease HT, (ii) T2DM or HT only, and (iii) neither T2DM nor HT, ectopic lipids infiltration was highest in all three organs in group 1 (T2DM and HT) than in group 2 (T2DM or HT) and the lowest level was in group 3 (neither T2DM nor HT). The authors suggested that MRI can be used to measure early metabolic changes (Pieńkowska et al. 2020). *Thomas et al. (2012)* have linked the relationship between

adipose tissue and ectopic fats using MRI. They found that IHCL, soleus and tibialis IMCL were correlated with abdominal visceral adiposity. Also, there was a strong positive correlation between age and IMCL and IHCL in males and females. Males showed higher IHCL and abdominal visceral fat, while females showed higher subcutaneous fat, reflecting sex differences in fat distribution (Thomas et al. 2012).

A high thigh subcutaneous fat is associated with lower glucose levels in men and better lipid profiles in women (Snijder et al. 2005). Conversely increased visceral abdominal and ectopic lipids are show a stronger correlation to metabolic risk than subcutaneous fat (Demerath et al. 2008). Although IMCL and abdominal VAT correlated with whole body IR, the hepatic ectopic lipid was reported to display a stronger association with peripheral IR than IMCL and abdominal VAT. Also, no correlation has been found between abdominal SAT and IR, thus revealing the effect of IHCL on other tissues' IR (Hwang et al. 2007).

1.7 MRI sequences used in skeletal muscle and lipid quantification studies

Body mass index (BMI) and waist circumference (WC) are common health markers. Still, these measurements are not sensitive to detect the changes in muscle and fat amounts and do not provide information on lipids infiltration (N. Khan et al. 2017; Lang et al. 2015)**.** Magnetic Resonance Imaging (MRI) is considered the most sensitive and safest tool for studying lipids accumulation or infiltration in specific body regions. MRI is also the most reliable imaging modality for measuring changes in muscle volume (Addeman et al. 2015; Kim et al. 2017). This section will introduce the MRI techniques for assessing muscle and fat in the human body.

1.7.1 T1 weighted images (T1-WI)

MRI image contrast depends on many factors categorised into two parameter groups; intrinsic (inherent to the body's tissues) or extrinsic (can be controlled by an operator). T1 weighting is one of the MR intrinsic parameters that affect image contrast. It is based on the differences in the T1 recovery time between fat and water. T1 recovery time is a constant. It represents the time taken for 63% of total hydrogen atoms of a specific tissue to reach equilibrium status after radiofrequency (rf) excitation. Relatively large molecules of fat have shorter T1 recovery time than water. Therefore, the effect of a static magnetic field on the fat hydrogen atoms leads them to recover more quickly than water hydrogen to an equilibrium state after radiofrequency (rf) excitation (Westbrook, Roth, and Talbot 2011).

T1-WI is the standard imaging sequence that shows high contrast between fat and water. Fat is shown as high intensity and water as low intensity within the images (Lloyd-Jones 2017). The MR T1-WI sequence is characterised by two main extrinsic parameters; short echo time (TE), i.e. the period between applying rf pulse and signal induced in the coil, and short repetition time (TR), i.e. the period between two rf pulses. T1-WI provides sufficient contrast between fat and water, making it the preferred MR imaging technique for assessing organ anatomy, for example, the volume or cross-sectional area. However, internal adipose tissue that is interstitial in the organ, intermuscular adipose tissue (IMAT) or visceral fat, is challenging to segment (highlighting specific tissue to distinguish it from other adjacent and different contrasting tissues) on T1 weighted images because signals from adipose tissues are slightly attenuated due to the variation of signal intensities caused by MR static field (B0) and radiofrequency magnetic field (B1) inhomogeneity (Burakiewicz et al. 2017).

The disadvantage of T1-weighted images is that the fat signal intensity is inherently weaker than fat-only or water-only images and cannot be adequately segmented by the thresholding technique, as there are attributed signals from unwanted tissues which not completely saturated. In contrast, the 3-point Dixon or IDEAL (see section 1.7.3) produces accurate fat estimation independent of hardware differences. Repeatable fat quantification results from this technology with high image contrast images can therefore be produced from multiple centres with high reproducibility (Addeman et al. 2015).

1.7.2 Fat and water imaging technique

MRI technology provides a versatile imaging technique with special characteristics and tissue contrasts. Techniques with fat-only images and water-only images greatly benefit MR image contrast and allow for quantitative studies. These techniques provide a higher contrast to noise ratio (CNR) and produce fat or water-only images. A chemical shift selective (CHESS) imaging technique and water excitation Spatial-spectral pulses (WATS) are examples of two MRI sequences that exploited the chemical shift difference between fat and water and selectively excite a certain spin (fat or water) to suppress specific tissue signal from the image and improve CNR (Bley et al. 2010; Muhaimin et al. 2019), which improve thresholding segmentation of fat or muscle in the MR image.

1.7.3 multi-point Dixon imaging technique

In 1984, Dixon created an MRI technique that takes advantage of the differences in precessional frequencies (oscillating perturbation or Larmor frequency) between fat and water (Grimm et al. 2018; Westbrook, Roth, and Talbot 2011). Under a magnetic field, different molecules resonate at different frequencies. The exact fat-water

frequency difference is a product of multiplying the Larmor frequency (the precession speed of a specific hydrogen nucleus around the static magnetic field B0 axis) by the chemical shift value. The precessional or Larmor frequency value is calculated from the Larmor equation as following:

$$\omega_0 = \gamma B_0$$

ω_0 is the precessional or Larmor frequency.

B_0 is the magnetic field strength of the magnet.
γ is the gyromagnetic ratio of Hydrogen atom, which is constant =42.57 MHz at 1Tesla magnetic field.
at magnetic field = 1.5 Tesla, ω_0 = 42.57 x 1.5= 63.86 ≈ 64 MHz.
at magnetic field=3 T Tesla, ω_0 = 42.57 x 3= 127.72 ≈ 128 MHz.
Although fat and water contain hydrogen, they have different chemical environments. Fat hydrogens bind with carbon, while water binds with oxygen. These result in differences in fat and water precession (chemical shift), which is proportional to the magnetic field. The amount of chemical shift is usually expressed in part per million (ppm), and its value is constant for fat and water (3.5 ppm). The difference in chemical shift between fat and water can be calculated at different fields directly by multiplying Larmor frequency by 3.5 (**ω_0 x 3.5).** For example**:** at 1.5 T precession frequency difference between fat and water = 63.86X 3.5= 220 Hz, fat precession is 220Hz lower than water at 1.5T and around 440 Hz lower than water at 3T (Westbrook, Roth, and Talbot 2011), see **Figure 1.7.3.** However, in order to determine the exact fat-water frequency difference, the precise MRI static magnetic field should be calculated. Owing to the different frequencies between water and fat components, two separate MR map images (water only and fat only) can be produced (Grimm et al. 2018).

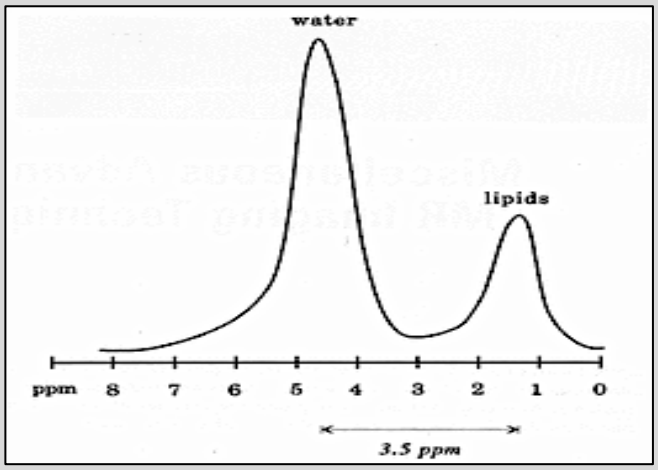

Figure 1.7.1. The chemical shift difference between the water and fat spectral peaks ('Fat-Water Chemical Shift - Questions and Answers in MRI' 2021)

The Dixon technique has been extensively used in muscle and fat measurements. Recently, it has been considered the most successful method to suppress fat or water signals and produce fat-only or water-only images (Mccurdy 2014; Addeman et al. 2015; Hogrel et al. 2015). Thus, one sequence provides two types of images **(Figure1.7.2)**. Furthermore, the Dixon technique produces a higher signal-to-noise ratio (SNR) and homogenous fat or water suppression images that are superior to other sequences such as inversion recovery pulse sequences, e.g. short tau inversion recovery (STIR) and chemically selective fat saturation (FAT-SAT) which produce only fat or water suppressed image, rather than both simultaneously (Guerini et al. 2015). Indeed, the modified 3-point Dixon technique is unique in producing an excellent homogeneous image independent of radiofrequency (B1) field or static field B0 inhomogeneity. Also, it can be combined with any MR weighting, e.g., T1, T2 or proton density, also any MR sequence, e.g., spin echo or gradient echo. In particular, the 3-point Dixon proton density (PD) gradient echo sequence has been used extensively in the last few years in musculoskeletal studies, for example, to examine how muscle

atrophy and fat infiltration relate to muscular diseases, e.g., Oculopharyngeal muscular atrophy (Gloor et al. 2010) and Duchenne muscular dystrophy (Wokke et al. 2014). Also, it has been exploited in various cross-sectional studies of skeletal muscle volume and IMAT differences in young and older men and women, healthy populations (Hogrel et al. 2015) and exercise studies (Fischmann et al. 2012).

Fat-only and water-only images and fat fraction maps (FF%) can be produced using 3-point Dixon, which uses three or more echo times and is an ideal method for musculoskeletal lipid measurements. However, when a 2-point Dixon technique is used, more care should be taken to acquire the two echoes exactly in-phase and opposed-phase to accurately separate the fat and water signals, while echo timings are more flexible in the 3-point Dixon (Grimm et al. 2018). The 3-point Dixon images are more robust and reproducible in terms of lipid measurement regardless of hardware changes. The 3-point Dixon technique also solves the problem of MR field inhomogeneity that creates signal intensity variation and causes fat signal deterioration. The 2-point Dixon in contrast is sensitive to B0 or static magnetic field inhomogeneity, thus making it less accurate than the 3-point Dixon technique (Hogrel et al. 2015; Addeman et al. 2015).

In skeletal muscle, 3-point Dixon proton density fat fraction (PDFF) images provide a regional estimation of fat fraction content that includes signals from IMAT, EMCL and IMCL. This is in contrast to visual threshold MR image segmentation, which presents intermuscular adipose tissue (IMAT) and roughly extramyocellular lipids (EMCL) only, which underestimates the total lipid deposition in the muscle (Grimm et al. 2018). The latest advance of the Dixon technique is the 6-point Dixon that is achieved when applying 6 echoes. This method, known as the Iterative Decomposition of water and fat with Echo Asymmetry and Least-square estimation (IDEAL) and T2*-IDEAL, is

considered the most advanced modification of the Dixon technique. The IDEAL sequence provides more precise measurements of hydrogen fat fraction. It has the ability to determine the changes in the lipid spectrum that could be due to obesity, neuromuscular diseases and muscular injuries (Carlier et al. 2016; Kovanlikaya et al. 2005; Matsumura et al. 2017). High-resolution 6-point Dixon or IDEAL sequence results are in agreement with values generated by magnetic resonance spectroscopy (MRS), which is considered the gold standard for lipid quantification (Grimm et al. 2018). Musculoskeletal lipid studies utilising MRS will be discussed in the next section.

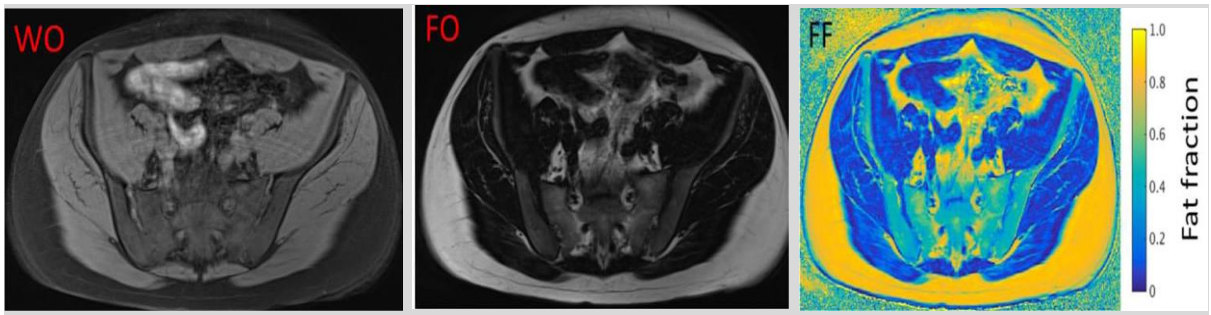

Figure1.7.2. An example of MRI Dixon images and fat fraction map (FF%). Dixon sequence produces water-only (WO) and fat-only (FO) images and quantitative measurements of fat deposition (Bray et al. 2018).

1.7.4 1H MR spectroscopy

Since 1993 when Schick et al. observed two fatty acid compartments in the human skeletal muscle with a resonance frequency shift of 0.2 ppm, MRS has gained increasing attention in musculoskeletal studies. Following this finding, Boesch et al. (2002) classified the two compartments as intramyocellular lipids (IMCL) with a peak at 1.28 ppm and extramyocellular lipids (EMCL) at approximately 1.48 ppm **(Figure 1.7.3).** The resonance separation of these two compartments is due to the distinction

in shape and location: IMCL is located inside the sarcoplasm as sphere droplets, and EMCL is located outside the sarcoplasm between muscle fibres in a tubular structure. Hence, due to the tubular structure of EMCL, it undergoes a specific phenomenon called “bulk susceptibility magnetic shifts” (BMS) that changes the local magnetic field, and this change depends on the geometry and type of tissue (C Boesch et al. 2006). 1H MRS is a widely accepted and validated method for measuring IMCL (Howald et al. 2002; Loher et al. 2016). The common MRS sequences for measuring IMCL are; stimulated echo acquisition mode (STEAM), point-resolved spectroscopy pulse sequences (PRESS) and chemical shift imaging (CSI) (Hu and Kan 2013). It is difficult to measure EMCL via MRS because the EMCL level is strongly affected by voxel positioning due to the geometric tubular shape that causes bulk susceptibility magnetic shifts (BMS) and alters the magnetic field strength experienced by EMCL nuclei (C Boesch et al. 2006). However, EMCL can be estimated as total lipids infiltration by the Dixon technique, which provides a percentage measurement of proton-density fat fraction (PDFF%). Thanks to the advances of MRS in the last few years, it is possible to estimate the degree of (un)saturation of fatty acid chains, which is suggested as a biomarker for different diseases such as osteoporosis, obesity and diabetes (Ruschke et al. 2016). Several studies indicate that saturated fatty acids are a risk factor for many diseases, while unsaturated fatty acids are linked to good health status (Lindeboom and de Graaf 2018). The drawback of MRS is the difficulty of measuring IMCL in obese subjects due to the large contamination of EMCL. The correct placement of the MRS voxel is crucial to successfully separate IMCL from EMCL spectra (Hu and Kan 2013).

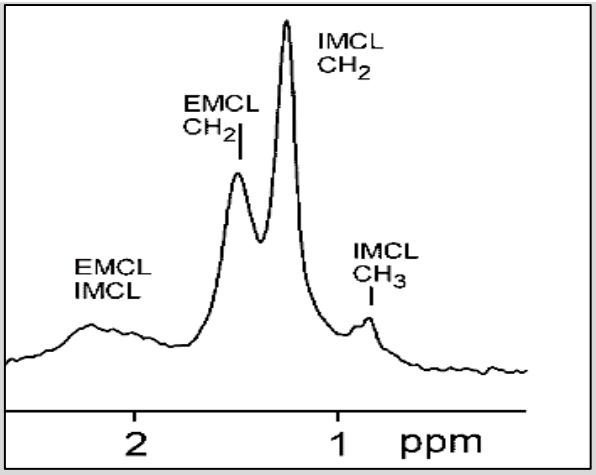

Figure1.7.3. 1H-MR spectrum, PRESS sequence single voxel in the m.tibialis anterior shows the splitting of the Methylene=CH2 resonances of fatty acid into two compartments IMCL/EMCL (Chris Boesch et al. 2006).

1.8 Liver ectopic lipids quantification methods

The gold standard method for quantification of liver fat was using biopsy. However, the invasiveness of this procedure makes it inappropriate for repeated measurements (Clarke et al. 2017). Liver ectopic lipids MR quantification methods are similar to muscle. Multi-point Dixon (IDEAL) and 1HMRS sequences have been approved and widely used in clinical and research fields (Bray et al. 2018). Liver proton density fat fraction (PDFF%) can be acquired from multipoint Dixon, and Intrahepatocellular Lipid (IHCL) concentration can be acquired from a single-voxel MRS called HISTO with the stimulated echo acquisition mode (STEAM) sequence. Both liver fat evaluations can be conducted automatically from an MRI workstation using vendor-supplied software (Zhao et al. 2019)**.** Hepatic steatosis (increased fat deposition in the liver) is strongly associated with MetS (Bray et al. 2018) and decreased liver fat has been strongly associated with improved insulin sensitivity (Müller et al. 2012). Multi-point, or multi-echo Dixon, correlates strongly and agrees with MRS in liver fat quantification (Zhao et al. 2019). Currently, liver MRS and Dixon sequences are quick and safe for liver fat

assessment, and they can be conducted within a few minutes (5-7 mins). Furthermore, compared to other imaging modalities, e.g., CT and Ultrasound, MRI provides qualitative and quantitative diagnostic information with the highest accuracy and reproducibility (Frittoli et al. 2020).

1.9 Ramadan fasting model

Recently two intermittent fasting (IF) strategies have gained interest for weight management and improving markers of metabolic health; intermittent energy restriction (IER) involving two days of energy restriction or fasting per week (alternate days or 2-consecutive days) and unrestricted or less restricted energy intake on the other 5 days (Gao et al. 2022). Time restricted eating (TRE) involving refraining from food (fasting) for ≥12 hours each day (Antoni et al. 2017; Mindikoglu et al. 2017). Fasting is a ritual practice in some religions, such as Judaism, Christianity and Islam, although the form of fasting differs (Kul et al. 2014). In Islam, fasting is a form of worship that Muslims have been encouraged to practice on various occasions, for instance, two days per week or three days per month (A. Khan and Muzaffar Ali Khan Khattak 2002). Ramadan, the obligatory fasting month, is the ninth lunar month. During this month, adult Muslims refrain from eating, drinking, smoking and having sexual relations from about one hour before sunrise until sunset. As a result of geographic and astronomical differences in the lunar system, the Ramadan month can be 29 or 30 days, and the fasting duration per day can last from 8-19 hours. Children, women in the menstrual period, pregnant or breastfeeding, and those suffering from illness or travelling are exempt from Ramadan fasting (Saleh et al. 2005; N. Khan et al. 2017; Ongsara et al. 2017). Intermittent fasting (IF), which includes Ramadan fasting (RF), time-restricted eating (TRE) and intermittent energy restriction (IER), has gained

significant attention in the last two decades as a dietary strategy that could change body metabolic markers, e.g., body weight, blood glucose, lipid profile (Rothschild et al. 2014; A. Khan and Muzaffar Ali Khan Khattak 2002). Moreover, RF has been associated with the anticancer proteomic signature preferentially altering, gene protein products of glucose and lipid metabolism, insulin signalling, circadian clock, DNA repair, cytoskeleton remodelling, immune system, and cognitive function (Mindikoglu et al. 2020).

Studying the effect of Ramadan fasting is of interest, as a large Muslim population (1.5 billion) across the world engages in this religious worship every year (Nachvak et al. 2018). Several studies have focused on Ramadan fasting, mainly in the Middle East or Southeast regions, with the fasting durations varying between 12 and 17 hours (Ongsara et al. 2017; Saleh et al. 2005; Akhtar et al. 2020; Mohammadzade et al. 2017). Other IER studies reported on fasting periods of up to 20 hrs/day every other day for two months (Carlson et al. 2007; Stote et al. 2007). Such studies have reported a range of metabolic changes summarised in **Table 1.9.** Although the effect of TRE or IER is shown to be beneficial in animal models, this has not yet been consistently shown in humans (Antoni et al. 2017; de Cabo and Mattson 2019; Faris et al. 2020). Furthermore, according to recent reviews, there is heterogeneity in reporting, with either no significant effects or a report of both advantages and disadvantages of TRE, Ramadan fasting, and IER, on markers of metabolic health (Rothschild et al. 2014; Kul et al. 2014; Antoni et al. 2017; Santos and Macedo 2018; Cioffi et al. 2018; Fernando et al. 2019; Faris et al. 2020; Wilkinson et al. 2020). The uncertainty of Ramadan fasting effects may be due to the variability in study design and fasting duration, which varies depending on geographical location and weather season that changes periodically according to the lunar system. In addition, the assessments of energy

intake and expenditure in many trials were not included or done imprecisely (Nachvak et al. 2018; N. Khan et al. 2017). Thus, more precise human studies are required to either control or accurately record variables such as age, sex, physical activity, and total energy intake (Longo and Mattson 2014; Fernando et al. 2019; Cioffi et al. 2018; Rothschild et al. 2014; Santos and Macedo 2018; Faris et al. 2020). Most Ramadan studies were done on healthy subjects with a wide range of ages. The oldest RF study we recorded was in 1997 (Adlouni et al. 1997), and they studied the temporal effect of RF of 12 hrs/day on healthy men aged 25-50 yrs. The data were collected one week before, one month after and on days 8, 15, 22 and 29 of RF. Fasting blood samples were taken between 10-12 hrs fasting in all phases. A significant weight loss was started on day 22 of RF, and the decline continued until the end of RF.

Also, fasting blood glucose (FBG), cholesterol, and triglycerides (TG) significantly declined. The declining pattern fluctuated but was significantly lower than pre-RF. HDL and LDL fluctuated during the RF phases, and the last reading on day 29 showed a significant increase in HDL and a decrease in LDL. The authors attributed these physiological changes to habitual changes in Ramadan, including nocturnal feeding, meal frequency, which were mainly two large meals (one after sunset and another after midnight or early morning before sunrise), sleep pattern as well as macronutrient intake, and food quality. Generally, during Ramadan, people tend to consume more sugary food (Adlouni et al. 1997). However, eating habits differ among populations and individuals. In this study, daily energy intake, carbohydrates, protein and monounsaturated fatty acids (MUFA) increased significantly during Ramadan, whereas saturated fatty acids decreased. After a month from the end of RF, cholesterol and LDL were lower than pre-RF, HDL higher, and FBG returned to pre-RF level (Adlouni et al. 1997). In addition, the increase in total energy intake during

Ramadan occurred with a decline in body weight and improved blood lipid profile. This improvement was also linked to food quality (high PUFA and low SFA), not RF *per se*. Similar glycaemic and lipid profile findings were reported in previous studies (Larijani et al. 2003; Fakhrzadeh et al. 2003; Saleh et al. 2005; Mohammadzade et al. 2017; Akhtar et al. 2020), while other studies reported no significant changes in these variables (Ongsara et al. 2017; Mindikoglu et al. 2020), see **Table 1.9**. This discrepancy may relate to the food quantity and quality, fasting period and timing of sample taken.

Moreover, most RF studies reported a significant decline in body weight, skeletal muscle and adipose fat measured by Bioelectrical impedance (BIA) (Norouzy et al. 2013; Nachvak et al. 2018). *Sadia et al. (2011)* reported a significant increase in FBG due to RF in patients with MetS. A randomised crossover design study of two months was undertaken with TRE 20hrs/day fasting (1 meal per day) versus a control (3 meals per day) with controlled equivalent energy and macronutrient content, no changes in physical activity among groups, and there was 11 weeks washout period between the two diets. The findings of the TRE group compared with the control group were the following: a significant decline in body weight and body fat, no change in lean body mass and a significant increase in FBG, TC, LDL and HDL with a trend towards decreasing insulin sensitivity as measured by oral glucose tolerance test (OGTT). The authors' explanation of the physiological mechanism behind TRE was that consuming one large meal in a short TRE window (4 hrs/day) causes an increase in free fatty acids (FFAs) net flux from adipose tissues leading to hepatic gluconeogenesis (a process of producing endogenous glucose from the breakdown FFAs and amino acids, in response to depleted liver glycogen stores) (Carlson et al. 2007; Stote et al. 2007).

Table 1.9. A brief comparison of Ramadan fasting studies on healthy and metabolic syndrome subjects. The recorded changes were at the end of the intervention period.

References	Region/ Gender /health status	Age (years)	Fasting hrs/days, & study duration	Changes in BMI Kg/m^2 weight or WC	Body fat mass/Tool	Muscle change	FBG	FBI Insulin &HOMA-IR	FFA change
Adlouni.1997 (Ram)	Morocco, healthy 23 males	**25-50**	**12hrs, month**	Weight sig. decrease 1.8 kg	No.info	No.info	Sig. decrease	No.info	TC sig. decrease TG sig. decrease LDL sig. decrease HDL sig. increase
Fakhrzadeh. 2003 (Ram)	Iran, healthy 50 males,41 females	males19.9±1.8 females 21.9±3.9	**12hrs, month**	males BMI. sig. decrease (BMI-0.4,1.3kg) females only WC. sig decrease 3.1 cm	No.info	No.info	Sig. decrease	No.info	TC sig. decrease TG sig. decrease LDL sig. decrease HDL sig. increase
Larijani.2003 (Ram)	Iran, healthy 67males 48 females	21.2±4.3 years	**12hrs, month**	No.info	No.info	No.info	Sig. decrease	No.info	No.info
Saleh.2005 (Ram)	Kuwait, healthy 41 males, 19 females	Male 24-56 (37±8.6) Female 23-33 (27.7±3.4)	12hrs, month	WC Sig. decrease Males 2.7cm Females 2.6cm	No.info	No.info	No. sig change in both genders	No. info	Male: TC, LDL (sig. decrease) TG, HDL, VLD (no. sig) Female: TC, LDL, TG, HDL & VLDL (no. sig)
Sadiya,2011 (Ram)	UAE, 5 males, 14 females, (MS)	37.1 ± 12.5	14 hrs, month	Sig. decrease Weight1.8kg BMI 0.2	BIA No. sig. decreased	No. sig decreased	sig. increase P<0.05	No. sig change	TG, HDL & LDL (No. sig change)
Norouzy.2013 (Ram)	Iran, 158 males, 82 females	40.1±0.7	14 hrs, month	Sig. decrease, males' weight 2.2kg, BMI 2.1 female weight 1.4kg, BMI1.5	BIA. sig. decreased Males 2.5% Females 1.1%	Sig. decrease Males 2.1kg Females 1.1kg	No.info	No.info	No info
Ongsara.2017 (Ram)	Thailand 21 Males, 44 Females, Healthy	19-24	12±0.15, month	No sig	No sig. Change in both gender	No. sig. change	No. sig	No. sig	TC LDL cholesterol TG HDL (All no. sig. changes both sexes)

Mohammadzade. 2017 (Ram)	Iran 30 Males, Healthy	20-35	16hrs, month	Sig. decrease Weight 2.3kg BMI 0.82	No info	No info	Sig. decrease	Sig. decrease	TC no. sig, TG sig. decrease HDL sig. increase LDL no. sig
Khan.2017 (Ram)	Pakistan 18 Male,17 females Healthy	21–23	15hrs, month	Sig. decreased in weight 0.03. no. sig BMI	No. info	No.info	No. sig change	No.info	TC no. sig TG no. sig HDL sig. decrease LDL sig. increase
Nachvak.2018 (Ram)	Iran,160 Males, Healthy	21-63	17hr, month	Sig. decrease In weight 2.1 kg & BMI 0.73	BIA Sig. decreased 0.37%	Sig. decreased 1.37kg+TBW 0.98%	Sig. decrease	Sig. increase	TC sig. increase TG sig. decrease HDL no. sig LDL sig. increase
Mindikoglu.2020 (Ram)	US 13 Male, 1 female, Healthy	Mean32	12:30 hrs, month	No sig	No info	No info	No. sig	No sig	TC, TG, HDL, LDL (No. sig)
Akhtar.2020 (Ram)	India 100 Males, Healthy	20-74	10-11hrs, month	No info	No info	No info	No. info	No info	TC sig. decrease HDL sig. increase TG sig. decrease
Dundar.2021 (Ram)	Turkish,28 males,6 females, non-healthy	19-68	14 hrs, month	No. info	MRI. Hepatic FF%, no sig increased	No.info	No. info	No.info	TG sig. decrease HDL sig. decrease LDL sig. increase TC sig. increase

Abbreviations:
(MS) Metabolic Syndrome
(WC) Waist circumference
(FFA) Free fatty acid
(TC)Total Cholesterol
(TG) Triglyceride
(TG) Triglyceride
(HDL)High Density Lipoprotein
(LDL)Low Density Lipoprotein
(VLDL) Very-low-density lipoprotein
(BIA) Bioelectric Impedance Analysis
(TBW) Total body water
No. sig= No significant changes
No. info= no information given in study description
Sig= represented a significant change, $P<0.05$
(IF) Intermittent fasting
(Ram) Ramadan fasting

1.10 Other non-Ramadan fasting models

Growing evidence from many studies and reviews that show the beneficial health outcomes of IF including weight loss, reduced IR and improved lipid profile that have been related to Mets (Anton et al. 2021; Aragon and Schoenfeld 2022; Dong et al. 2020; Peeke et al. 2021; Soliman 2022; Varady et al. 2022; Vasim, Majeed, and DeBoer 2022; Elortegui Pascual et al. 2023). Over the last few years, the different models of IF, e.g., early or delayed time-restricted eating (eTRE) or (dTRE), alternate-day fasting (ADF) and twice weekly 5:2 fasting, have been investigated intensively and compared with the traditional caloric energy restriction regime (CER). These types of regimens showed a similar effect to calorie-restricted strategy without intentionally manipulating calorie intake (Aragon and Schoenfeld 2022). In CER, the individual is reducing their daily energy intake by 500-750 kcal of normal requirements, which are around 1800-2200 kcal in middle-aged women and 2200-3000 kcal in middle-aged men (Ryan and Heaner 2014). The idea premise of IF strategies is to restrict the period available for eating and not calculate the energy intake or restrict the calorie intake from 0-25% of calorie needs in 2 days/week (Welton et al. 2020). However, other studies have combined CER and IF model (Peeke et al. 2021), as explained in the following section 1.10.1.

1.10.1Time-restricted eating (TRE)

TRE is a popular form of IF, currently being studied with several eat timing windows. We compare two randomised control TRE studies, see **Table 1.10**, one with healthy young men (Zeb et al. 2020), and another with an overweight and obese cohort (BMI> 27 and <43) (Lowe et al. 2020). The fasting duration was 16hrs, starting in the evening and ending in the afternoon, thus skipping breakfast. Both studies reported significant

weight loss. However, the healthy young men showed beneficial improvement in their lipid profiles and decreased body fat with a significant reduction in total energy, carbohydrate, fat, and protein intake (Zeb et al. 2020). The overweight and obese group showed significant lean mass reduction using DXA with no change in body fat or lipid profiles, and also no significant changes in total energy, carbohydrate, fat, and protein intake (Lowe et al. 2020). Neither recorded any change in FBG or FBI.

A further study looked TRE effect in a cohort of obese males and females. An 8-week randomised control study of two groups fasting for 12hrs or 14 hrs daily was conducted (Peeke et al. 2021), see **Table 1.10**. Fasting started between 17:00-20:00. Participants had a controlled diet (500-1000 kcal energy reduction regimen) and engaged in physical activity which involved walking 7,000-10,000 steps during the day. There was a significant reduction in body weight by 8.9kg in the 12hrs and 10.9kg in the 14hrs fasting groups. Also, the researchers recorded a significant FBG reduction in the 14hrs fasting group (−7.6 mg/dl; $P<0.05$) but not a significant reduction in the 12 hrs fasting group (−3.1 mg/dl; $P=0.36$) In addition, both interventions recorded significant FBG decrease in pre-diabetic participants (FBG ≥100 mg/dl), with a reduction of 11.2mg/dl ($P= 0.029$) for the 12hrs group and a reduction of 17.6mg/dl ($P=0.008$) for the 14hrs group (Peeke et al. 2021).

Moreover, a recent 16:8 hrs TRE study on healthy young men (McAllister et al. 2020) compared *ad libitum* against isocaloric (<300 difference from baseline) diets, both groups conducted TRE. However, there was no significant differences in total calorie intake between the two groups, which indicates the potential effect of TRE in decreasing food intake unconsciously and mimicking isocaloric condition. In both groups, there was a significant reduction in body weight, muscle and fat as measured by BOD POD and HDL. However, there was a significant increase in FBI and LDL in

the TRE ad libitum group only. These differences may be attributed to the numerical but not statistical increase in total calorie intake in the *ad libitum* group 2151 Kcal compared to 1839 Kcal in the isocaloric group. This discrepancy may indicate that the 3-day dietary record was insufficiently detailed in exactly recording the total calories and macronutrients. Furthermore, physical activity was not monitored (McAllister et al. 2020).

Another 16:8 hrs TRE study recorded an increase in LDL and TC in healthy old participants without any changes in body weight, calorie intake and FBG (Martens et al. 2020). A crossover-controlled study of 18hrs early fasting with a fixed diet to maintain weight (50% carbohydrate, 35% fat, 15% protein) in control and fasting groups was conducted. The eating window in the fasting group was between 8:00-14:00 for 4 days. The study resulted in decreased FBG, FBI and mean continuous glucose monitor CGM, but increased TC, HDL and LDL in fasting. The author associated the blood lipid increase with the larger dependency on fat oxidation due to prolonged fasting (Jamshed et al. 2019), see **Table 1.10**.

1.10.2 (5:2) intermittent energy restriction and alternative day fasting

Alternative day fasting (ADF) and 5:2-day fasting have become two recognisable forms of IF. The ADF rule is based on fasting for one day followed by a non-fasting ad libitum or no food-restricted day. ADF is conducted in two ways, one with zero calories on the fasting day and the second with 20-30% only calorie intake on the fasting day. The 5:2 method allows 5 days per week of normal food intake and 2 non-consecutive days of fasting or reduced calorie intake (Elortegui Pascual et al. 2023). One study conducted on 13 healthy young females who participated in a 5:2 fasting

study showed a significant increase in average Beta-hydroxybutyrate (βHB), a type of ketone bodies substrate, and it was higher on the first fasting day than the second one. In addition, it increased gradually. On the morning of the fasting day, it was low then increased in the evening and was highest in the morning following the fasting day. However, average blood glucose results had opposite βHB results. The average blood glucose level was lower on the first fasting day than on the second day, and it had a gradually decreasing pattern during the fasting day from morning until evening and was at the lowest level in the following morning after waking up and at the end of around 20hrs fasting. After the 7 days of intervention, participants lost an average of 0.8 ± 0.9 kg of their weight except for 2 participants who increased their energy intake and gained 0.2kg and 1.5 kg of weight respectively. This study suggests that short term fasting leads to ketogenesis (an increase in ketone bodies). Body metabolite acutely reacts to fasting as the changes in blood glucose and βHB were higher on the first fasting day than the second one. Weight loss was not expected in this short intervention and the authors referred to the depletion of glycogen stores and the associated dehydration or a recorded 225 kcal lower energy intake than the requirement in the study sample during non-fasting (Cerniuc et al. 2019).

Gao *et al.* (2021) was conducted a randomised study consisting of a parallel 2-week 5:2 intermittent energy restriction (IER) with non-consecutive days of fasting in the form of a 70% energy-restricted diet and compared it with a continuous energy restriction (CER) diet in the form of a daily 20% energy restriction. Over the 2 weeks, the two diets had the same total energy intake. Both forms of diet resulted in a lower body weight and improved insulin sensitivity (IS) with greater improvement in the 5:2 IER group, see **Table 1.10**. The authors attributed the improvement in IS to the hepatic IS improvement (Oh et al. 2018).

Furthermore, an ADF study was carried out on healthy middle-aged overweight and obese individuals for 8 weeks. The participants were divided into four groups: ADF, exercise without ADF, exercise with ADF, and control. On the three interspersed fasting days, they consumed only (400-500Kcal) and were ad libitum on the remaining four days. The exercise intervention included 3 days/week sessions of resistance training for 40 minutes and aerobics training for 20 minutes. All intervention groups had decreased body weight and waist circumference (WC). The ADF with exercise and ADF only groups lost significant amounts of weight: 3.3kg and 2.4kg respectively. The ADF with exercise group recorded a significant decrease in body fat mass measured by BIA, which suggested the superior effect of combining exercise with ADF or other forms of dietary interventions. However, there was a non-significant muscle mass reduction in all groups, especially in the ADF group. There was a significant blood metabolic index (FBG, FBI and lipid profiles) improvement in the ADF with exercise group, but not in the ADF, and exercise-only groups (Oh et al. 2018), see **Table 1.10**.

Table 1.10. A brief comparison of intermittent fasting (IF) studies on healthy and metabolic syndrome subjects. The recorded changes were at the end of the intervention period.

References	Region/ Gender /health status	Age (years)	Fasting hrs/days, & study duration	Changes in BMI Kg/m^2 weight or WC	Body fat mass/Tool	Muscle change	FBG	FBI Insulin &HOMA-IR	FFA change
Carlson.2007 & Stote.2007 (dTRE)	US, Healthy 5 male,10 female	40-50	20hrs from 21:00 to17:00, 2 months	Sig. decrease 1.4 kg	BIA Sig. decrease 2.1kg	No sig change	Sig. increased	No. sig	TC sig. increase LDL sig. increase HDL sig. increase
Wilkinson .2020 (TRE)	US, obese, MS 13 males,6 females	59±11.14	16hrs,3 months Start time not specific	Sig. decrease Weight 3.3kg BMI 1.09	BIA Sig. Visceral decreased 3%	No.info	Trend. decreased HbA1c sig. decreased	Trend. decrease	TC Sig. decrease TG no. sig LDL sig. decrease HDL sig. decrease
Zeb.2020 (dTRE)	China, healthy, 56 males	Young international university students	16hrs from 3:30 to 19:30 for 25 days	BMI sig. decrease 2kg/m^2	Sig. decrease 5.9% Tool. No.info	No.info	No.info	No.info	TC sig. decrease TG sig. decrease HDL sig. increase LDL no. sig change
Lowe.2020 (eTRE)	USA, overweight &obese ,116, males & Females. TRE(n=59)	18-64 yrs	16hrs From 20:00 to 12:00 for 3 months	sig. decrease weight 0.94kg	No. sig change/ DXA	Sig. decrease	No. sig change	No. sig change	TC TG HDL LDL All no. sig change
Peeke.2021 (eTRE)	USA, obese,60 males &females	18-64yrs	12hrs Or 14 hrs Start from 18-20 2months	Sig. decrease 8.9 kg in 12hrs 10.7kg in 14hrs	No.info	No.info	Sig. decrease	No.info	No.info
McAllister. 2020 (TRE) pilot	USA, healthy 22 males	22±2.5yrs	16hrs Start time not specific. 28 days	Sig. decrease, no numerical info	Sig. decrease /BOD POD	Sig. decrease	No. sig	Sig. increase	TC sig. increase TG no. sig HDL sig. increase LDL sig. increase

Martens. 2020 (eTRE)	USA, 22 healthy males and females	55-79yrs	16hrs Start 18:30 To 10:30 6weeks	no. sig	No.info	No.info	No. change	No.info	TC sig. increase TG no. sig HDL no. sig LDL sig. increase
Jamshed. 2019 (eTRE)	USA,18 healthy males and females	20-40yrs	18hrs Start 8:00 To 14:00 For 4days	No.info	No.info	No.info	Sig. decrease	Sig. decrease	TC sig. increase TG no. sig HDL sig. increase LDL sig. increase
Cerniuc .2019 (5:2 IER)	Germany,19 healthy females	18-30yrs	2 complete & separated days fasting	Sig. decrease	No.info	No.info	Sig. increase	No.info	No.info
Gao.2021 (5:2 IER)	UK,16 healthy males	20-35yrs	2 separated days 70% ERD /week For 2 weeks	Sig. decrease 2.5kg	No.info	No.info	Sig. decrease	Sig. decrease	TC TG HDL LDL All no. sig
Oh.2018 ADF	Korea, overweight & obese,45 males &females	32-40yrs	3 alternate days (400-500kcal) fasting	Sig. decrease 2.4kg	Sig. reduce 1.3%/ BIA	No. sig	No. sig	No. sig	TC TG HDL All no. sig

TRE: Time restricted eating IER: Intermittent energy restriction ERD: Energy restricted diet ADF: Alternate day fasting	(TG) Triglyceride (HDL)High Density Lipoprotein (LDL)Low Density Lipoprotein (BIA) Bioelectric Impedance Analysis	No. sig= No significant changes No. info= no information given in study description Sig= represented a significant change, $P<0.05$

1.11 The role of Circadian rhythm

The Circadian clock, also known as a circadian system and circadian rhythm, is a 24-hour human body process that involves the sleep and waking pattern, body activity metabolism and physiological mechanisms (Zeb et al. 2020). The suprachiasmatic nucleus (SCN) in the anterior part of the hypothalamus in the brain is the circadian rhythms' master regulator which is influenced by the light-dark cycle. Peripheral circadian rhythms which regulate peripheral organs, for example, the liver, skeletal muscle, adipose tissues, the pancreas, and intestines are synchronised by the SCN. However, the peripheral circadian rhythms are not directly influenced by light-dark, they are more sensitive to the fasting-feeding cycle (Regmi and Heilbronn 2020). Disruption to the circadian clock is linked to many metabolic diseases including diabetes and obesity (Bass and Takahashi 2010). This effect can be seen in night shift workers as they are more prone to obesity, diabetes, and cardiovascular disease (Gibson et al. 2015; Scheer et al. 2009).

A delayed time-restricted eating study with an eating window of 4 hours started in the evening resulted in a decrease in body weight and body fat and raised HDL. However, there were increases in FBG, TC and LDL. Although diet was controlled in this crossover study, there were non-beneficial metabolic marker changes (Carlson et al. 2007; Stote et al. 2007). Another delayed TRE study of 16 hours fasting that started from dawn until night (from 03:30 until 19:30) reported decreased body weight and body fat, an improved blood lipids profile, decreased TC and TG, and increased HDL, see **Table 1.10**. These effects were associated with decreased total energy intake which was significantly lower in the TRE group (1512kcal) compared to the non-TRE group (2018kcal) (Zeb et al. 2020). However, early TRE studies also reported discrepancies in reporting FBG, FBI and blood lipid profiles, see **Table 1.10**.

1.12 Overarching thesis aims and hypotheses

The primary aim of this thesis is to comprehensively examine metabolic changes resulting from Ramadan fasting (RF) with less invasiveness methods. RF serves as a model for time-restricted eating (TRE). Time-restricted eating (TRE), which involves eating during a limited number of hours and fasting for the remainder of the day for a month or more, is a suggested strategy to enhance cardiometabolic health. However, prolonged fasting (fasting for over 24 hours up to 3 days) can result in lipolysis and impaired insulin sensitivity. The impact of RF and other forms of TRE and intermittent fasting (IF) on metabolic health remains insufficiently understood, as evident from **Tables 1.9 and 10.1.**

The secondary aim is to optimise advanced non-invasive MR imaging techniques and post-processing methods to detect changes in skeletal muscle and adipose tissue volumes as well as levels of liver and muscle ectopic lipids infiltration.

The overarching hypothesis guiding this research posits that the implementation of an 18-hour RF regimen, as a form of TRE, induces metabolic changes. It is postulated that the shorter eating window during RF, coupled with reduced energy intake and decreased physical activity, contributes to metabolic changes in BMI, muscle, and fat volumes, ectopic lipids, FBG, FBI, and blood lipid profiles.

Chapter 2

General methods

2.1 Overview

Data collection in chapter 3 was done by co-researchers. In chapter 4, data were collected in different years, Ramadan 2019 and 2021. Due to the COVID-19 pandemic lockdown, data could not be collected for Ramadan 2020. This chapter summarised all methods and procedures used in all chapters.

2.2 Human volunteers

Healthy females and males participated in all studies and were recruited by advertisement and word of mouth. The participants were from Exeter University students' and the general population. These studies were approved by The University of Exeter's Sport and Health Sciences Research Ethics Committee in accordance with the Declaration of Helsinki (World Medical Association 2013). Before participating in the study, the participants received an information sheet and the consent form at least 48 hours before the study started. The study purpose, procedures and potential risks were explained verbally thoroughly and provided in the information sheet. A written consent was checked and signed by the participants, and a copy was given to them. They were aware they could withdraw from the study at any time. In chapter 3, for studies 1 and 2, the inclusion criteria were healthy young males (aged 21±1 years) sedentary for the last 6 months prior to the study. The exclusion criteria were any musculoskeletal injury, using medications such as non-steroidal anti-inflammatory drugs, taking nutritional supplements, diagnosed metabolic or cardiovascular impairment, or motor disorders.

The participants' inclusion criteria in chapters 4 and 5 were healthy females or males, with an age range from 18-40 years, intended to fast during the Ramadan month in

Exeter. The exclusion criteria were any chronic disease, musculoskeletal injury to the thighs within the last six months prior to the study and pregnancy for women. All participants in all thesis chapters also did not have any contraindication for an MRI exam (e.g., heart pacemaker, cochlear implants, medication pumps, surgical clips, plates, screws or claustrophobia). In 2021, and during the COVID-19 pandemic, additional COVID-19 information was provided on the potential risk of infection. During the pandemic, the participants were asked to follow the UK government guidance, and additional consent check lists regarding the pandemic were added to the consent form. Furthermore, the participants were asked to do two COVID tests within 72 hrs prior to each laboratory visit.

2.3 Habitual diet analysis

In chapter 4, all participants completed an arbitrary three-day diet diary during Ramadan month and one month after the end of Ramadan. It was assumed that people follow a similar diet throughout the Ramadan month so any three-day interval would be representative of the whole period. The dietary intake data was analysed via online software (Nutritics, Swords, Co. Dublin, Ireland). The 3 days of habitual diet activity data were compiled into an individual day average for each participant.

2.4 Physical activities

In chapter 4, participants wore a GENEActiv original accelerometer (Activ insights, Kimbolton, UK), a wrist-worn device that measures four daily physical activity intensity types. The device was worn on their non-dominant wrist for 3 consecutive days for two periods (during Ramadan month and one month after the end of Ramadan). The data

from the GENEActiv monitors were processed using GENEActiv excel macros. The metabolic equivalent of task (MET) of the following physical activities; sedentary, mild, moderate and vigorous were calculated separately. The 3 days of each habitual physical activity data were compiled into individual day averages for each participant.

2.5 Body hydration

In chapter 5, body hydration was assessed through two methods: serum calcium concentration in each Phase. Dehydration can cause an increase in the calcium concentration in blood as calcium is a component of blood solutes (Parameswaran Rajeev 2022; Barley, Chapman, and Abbiss 2020) and measurements of consumed water amount recorded by participants during Ramadan and one month after the end of Ramadan for 3 days. Water amount was measured in millilitres using a digital kitchen scale that was given to each participant. Water consumption data for the 3 days were compiled into individual day averages for each participant. This method was used to directly compare the difference in the amount of water consumption during RF and non-RF periods.

2.6 Venous blood sampling

In chapters 4 and 5, in all four Phases (Pre-RF, a week and 3.5 weeks after RF and a month after the end of RF), blood samples were collected via an antecubital vein, either right or left arm. The participant rested in a semi-supine position on a bed whilst a butterfly needle was inserted into the superficial antecubital vein, and approximately 2 ml of venous blood was drawn into a vacutainer. 20µl was immediately analysed for glucose concentration by a biochemical analyser assay. One ml of blood sample was

drawn into a lithium heparin-coated vacutainer for plasma. The samples were immediately centrifuged (at 4°C for 10 min), and the plasma fraction was then aliquoted into individual Eppendorf tubes and stored at -80 °C until further analysis. The other one ml was drawn into a serum separator tube (SST) and left at room temperature for at least 30 minutes, then centrifuged (at 4°C for 10 min). The serum fraction was then aliquoted into individual eppendorf tubes and stored at -80 °C until further analysis.

2.7 Continuous glucose monitoring

In chapter 5, during Ramadan and a month after the end of RF, continuous glucose monitoring was undertaken (CGM) (Dexcom G6, Inc., San Diego, CA, USA). A sensor was placed subcutaneously at the upper arm and connected via Bluetooth to an application installed on the participant's mobile phone (Dexcom G6). This device measures interstitial glucose concentrations (calibrated to blood glucose concentrations measured via finger prick 4 times per day) every 5 mins and records hypo and hyper glucose events. The readings were stored in the Dexcom iCloud, such that the operator could monitor the data and the analytical results from the Dexcom clarity healthcare professional's website account. The average of minimum one and maximum three days were compiled into an individual average glucose concentration for each participant. The same number of days was kept for the two compared periods.

2.8 Magnetic resonance imaging

Magnetic resonance images (MRI) in Chapter 3 (study 1, 2) and a subset of the images in chapter 4 were acquired via a 1.5 Tesla (T) (Intera, Phillips, The

Netherlands) MRI scanner. The MR sequence used in Chapter 3, study 1, was a T1-weighted turbo spin echoT1-TSE, see section 3.3.1 for sequence parameters. In chapter 3, study 2, eight MR sequences were tested (2DT1-TSE, 3D T1-FATS, 3D T1-GRE, 3D T1-TSE, 3DT2-TSE, 3DT1-WATS GRE, PD-TSE, 3D T1-FATS-GRE), to find the optimal sequences that was most appropriate (provides most homogeneous signal intensities) to use with an automatic thresholding segmentation method (image post-processing method using a computer algorithm to separate pixels of different signal intensities and calculate the volume of the pixels of similar intensities values, depending on the chosen image threshold range), to allow direct volume measurements of skeletal muscle and fat volumes separately (Wokke et al. 2014), see **Figure 2.8**. Eight bilateral images of the thighs were acquired using the eight suggested MR sequences. The choices of MR sequences depended on the acquisition duration, which should be acceptable, providing high tissue contrast images and having high and homogenous signal intensity. As a result, two MR sequences, 3DT1-WATS GRE for the muscle image and 3D T1-FATS for the fat image, were chosen. The parameters of these two MR sequences are detailed in chapter 3, section 3.3.2.

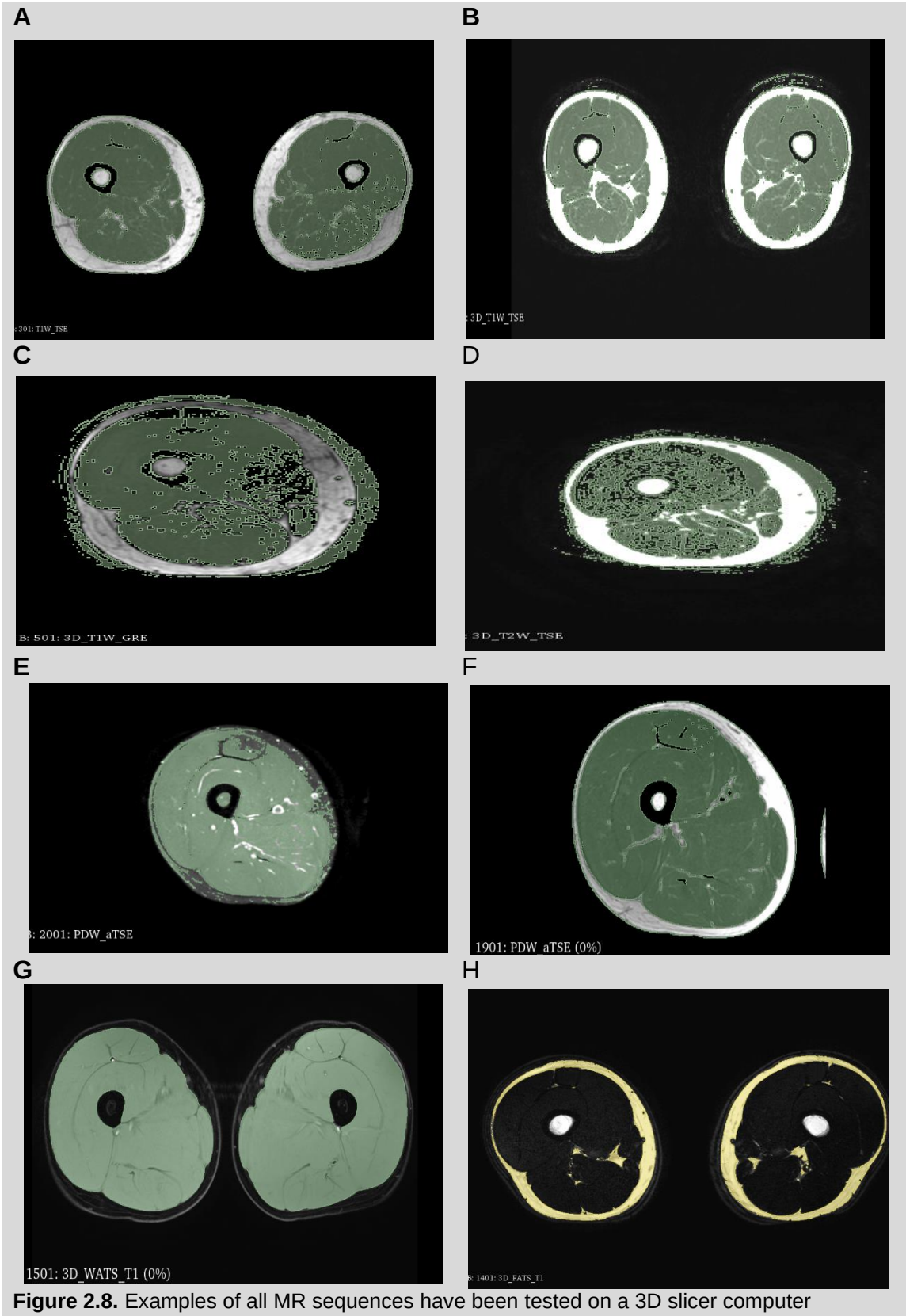

Figure 2.8. Examples of all MR sequences have been tested on a 3D slicer computer programme to depict the most appropriate sequences for water and fat measurements using the threshold segmentation technique. (A) 2D T1-TSE, (B) 3D T1-TSE, (C)3D T1-GRE, (D) 3D T2-TSE, (E) PD-saturated fat-TSE,(F) PD-TSE, (G) 3D T1-WATS, (H) 3D T1-FATS. The last two were chosen for muscle and fat measurements.

In Chapter 4, during Ramadan 2019, the 1.5 T (Intera, Phillips, The Netherlands) MRI scanner was used. The MR sequences were 3D Gradient Echo T1 weighted with selective water excitation (3D GRE T1_WATS); field of view FOV= 826 x 632 mm, Reconstructed matrix=864 x 864, 0.49 x 049mm, echo time TE=8.3ms, repetition time TR=20ms, Flip angle=25^{o} , echo train length ETL=1, Acquisition duration=270ms, Slice thickness 10mm, Slice spacing=5mm, number of slices=21), to determine thigh muscle, and 3D Gradient Echo T1 weighted with selective fat excitation (3D GRE_T1 FATS); FOV=208 x 162 mm, Reconstruction matrix=256 x 256, 1.76 x 1.76mm, TE=67ms, TR= 794.9, Flip angle=45^{o}, ETR=16, Acquisition duration= 12.70ms, Slice thickness=10mm, Slice spacing=5mm, number of slices= 21), to determine abdominal fat areas. Subjects lay in a supine position, with feet first for thigh images and head-first for abdomen images.

In 2021 a 3 T Siemens (MAGNETOM Prisma, Erlangen, Germany) MRI scanner was used. The MR sequences were 3-point-Dixon, 3D Proton density fat fraction Spoiled Gradient echo (3D-PDFF-SGE); FOV=420mm, TE 1=2.46ms, TE2=3.69. TR=6.44, Flip angel=12^{o}, ETL=2, number of averages=1, slice thickness=1.5mm, Slice Spacing=0.9mm_20% of thickness, number of slices=104), for thigh images. And 3 points-Dixon (3D-PDFF-SGE); FOV=380, TE1=1.29, TE2=2.52 ms, TR=4.05, Flip angle=9^{o}, ETL=2, number of averages=1, Slice thickness=3mm, Slice spacing=1.09 mm _20% of thickness, number of slices=80), for abdomen images. The subjects' position was supine head-first for both anatomical regions.

In chapter 5, the 3 T Siemens MRI scanner was used for all MR data collected in 2021. Three MR sequences were analysed; 1) 3 point-Dixon, 3D Proton density fat fraction Spoiled Gradient echo (3D-PDFF -SGE) for a region of interest (ROI) thigh FF% quantification, 2) MR-Spectroscopy (1H MRS) was Point RESolved

Spectroscopy with single-voxel Spectroscopy (PRESS-SVS) for muscle IMCL measurements, 3) 3 points-Dixon, proton density fat fraction (PDFF) within the Siemens designed Liver lab package, for liver FF% quantification. The detailed parameters for these three sequences are in the related chapter.

2.9 Image post-processing

In chapter 3, study 1, the manual segmentations were conducted by a co-researcher using Philips online MRI software (Kilroe et al. 2020). All other MRI images in chapters 3,4, and 5 were automatically segmented using a free, open-source 3D slicer software package (version 4.10.0 and 4.11.0; https://www.slicer.org/) (Fedorov et al. 2012). Automatic volume measurements were conducted via a modified threshold image technique that provides a convenient method to correct thresholding errors. This was a challenging issue when this method was first run. The threshold technique is used on digital images to segment the image structures based on pixel intensity values. The regions with similar intensity pixels value accounted as one segment, and these pixels were allocated the same label colour (Sujji, Lakshmi, and Jiji 2013). The 3D slicer software threshold values were set up manually to choose the area of interest in each slice. After that, additional thresholding correction tools (e.g., smooth edge and removal unwanted islands effects) were selected to automatically correct the errors that emerged from the MR images' slight signal inhomogeneity. Finally, the volume of the segmented area was automatically estimated by 3D slicer software.

In chapter 5, MRS data were analysed using the Software package JMRUI v.5.2. Liver and muscle fat fractions were calculated directly from the Siemens workstation.

2.10 Statistical analysis

In chapter 3 (studies 1 and 2) the Bland-Altman test was used, as it is a preferable tool for comparing biological measurement methods in clinical settings (Martin Bland and Altman, 1986). All studies presented within this thesis (Chapters 3,4,5) employed parallel group design. A Two-factor analysis of variance (ANOVA) was used to identify the main effect or interaction between factors. The main effects in chapter 3, study 1 were method X time, and study 2 were sequence X time. The main effects in chapters 4 and 5 were sex X time. A mixed-effects model was applied when analysing data sets with missing values. Tukey's or Šídák's post hoc multiple comparisons test was used to locate individual differences. $P<0.05$ indicated statistical significance. Pearson's correlation test was used to assess if there is a correlation between the changes in FBG and IMCL or FBG and IHCL. GraphPad Prism version 9.3.1 was used for all statistical analyses. All data in text and tables are presented as mean ± standard deviation (SD) and in figures presented as means ± standard error (SEM).

Chapter 3

Optimising the automated analysis of non-invasive MRI measurements of skeletal muscle volume in humans

3.2 Introduction

Magnetic resonance imaging (MRI) is a gold standard tool for measuring muscle volume. Many manual and automated volume measurement techniques have been developed to estimate muscle volume and are used widely in both clinical and research fields. The validity and reliability of measurement techniques are essential to produce true measurements and the same value repeatedly (Pons et al. 2018). A recent systematic review by Pons *et al.* (2018), showed that, the validity of automatic segmentation was moderate to excellence compared to slice by slice manual segmentation. The reliability of automatic segmentation was also found to be good (Pons et al. 2018). Automated 3D slicer software has been used to measure muscle volume changes under physiological states e.g., muscle leg immobilisation and leg damage (Jameson et al. 2021). Muscle volume quantification is an important monitoring tool in many clinical conditions (Hogrel et al. 2015) and physiological studies that include exercise interventions, immobilisation, or observations in ageing and neuromuscular pathology conditions (le Troter et al. 2016). It is measured in conjunction with other biomarkers, e.g., muscle strength per unit of muscle area and muscle fat infiltration, to obtain a picture of overall muscle quality (Culvenor et al. 2017). The estimation of muscle mass can be conducted via computed tomography (CT), magnetic resonance imaging (MRI), and indirectly by measuring total lean body mass using dual-energy X-ray absorptiometry (DXA) and. However, MRI provides higher resolution and high soft tissue contrasts and is non-ionising, making it the preferred choice in research and many clinical applications (Franchi et al. 2018; Moser et al. 2009).

The manual segmentation of radiology images (MRI or CT) is the gold standard method; however, it is time-consuming as it effectively involves the researcher tracing

the boundaries of each tissue of interest on every slice or every few slices. Therefore, it is unsuitable for large trials and relies on operator anatomical knowledge and skills that lower the reproducibility of measurements between operators (Berg et al. 2020; Kilroe et al. 2020)**.** The development of computer sciences and image analysis software have greatly improved medical image post-processing and quantification, which benefits clinical and pre-clinical studies. Automated segmentation is a method that uses computer algorithm-based thresholding of pixels of similar intensity to estimate the volume of the tissue of interest, i.e., it mainly depends upon image signal intensity rather than the judgement of the person undertaking the analysis (Wokke et al. 2014).

The T1-weighted spin-echo sequence (T1-SE) is one of the more routine MRI techniques and is commonly used for showing anatomical structures. The properties of the T1-SE sequence allow for excellent tissue contrast and a high signal-to-noise ratio (SNR). In T1-weighting images, the contrast depends on the differences in the T1 times between fat and water. Fat protons recover (return to equilibrium status by giving up the energy that has been gained from rf excitation) faster than water protons and produce a high T1 signal (bright), while water protons have a low T1 signal (dark) (Westbrook, Roth, and Talbot 2011). A Turbo or fast spin echo (TSE) sequence, the modified faster version commonly used instead of the original SE, is a part of the routine protocol in most clinical applications, including musculoskeletal imaging. It provides image contrast similar to SE and takes less scanning time, which lowers the chance of motion artifacts (McMahon, Cowin, and Galloway 2011). However, MR-signal intensities lack uniformity. In T1-TSE images, the slices further from the central slice are prone to signal intensity (SI) inhomogeneities, especially at the edge of the

images, due to a slight static magnetic field (B0) change. Also, the variation in the radiofrequency field (B1) induced by the rf pulses is a potential source of SI inhomogeneity that can cause errors in threshold segmentation and need correction or yield inaccurate volume estimation (Preim and Botha 2014).

MR signal intensity variations across an image are challenging when using automated segmentation. Intensity variation in the range of 10-20% does not affect visual diagnosis, but it severely affects the performance of intensity-based segmentation algorithms. MR signal intensity depends on many factors, e.g., sequence type and parameters (Preim and Botha 2014). It is possible to improve the signal intensity of a selected tissue (fat or water) by selectively exciting certain molecules, e.g., fat or water using CHESS pulse sequences. The saturation rf pulse is centred at the main selected component peak (e.g., fat or water). All longitudinal magnetisation of the unwanted peak will move to the transverse plane. Then another pulse spoils all the transverse magnetisation components, leaving only the wanted component in the longitudinal plane, which results in one type of signal from the selected pool (fat or water) being detected by the receiver MR coil (Bley et al. 2010; Shetty et al. 2019). Another technique for water excitation is called a Spectral selective pulse sequence, which excites the water and leaves the fat and all other spins without any excitation. The water excitation scheme is faster than CHESS, as there is no need for an additional spoiler gradient. Also, it provides higher SNR and CNR and is insensitive to B1 heterogeneity (Grande et al. 2014). Thus, it is possible to exploit the advantage of the water excitation sequence that provides higher image SNR and assess whether it is more compatible with automated segmentation methods. Chemical shift selective-fat images (CHESS) and water excitation spatial-spectral pulse (WATS) imaging techniques are fairly standard MR sequences for clinical diagnostic purposes. They

can selectively eliminate fat or water signals allowing for decreased MR receiver bandwidth (a range of received frequencies per millisecond which is inversely proportional to SNR and scanning time) (Graessner 2013), leading to improved (SNR) and contrast-to-noise ratio (CNR). **Figure 3.2** compares a routine T1-TSE image against fat and water images provided by CHESS and WATS sequences.

A.3D T1-WATS GRE **B. 2 D T1-TSE,** **C. 3D T1-FATS GRE**

Figure 3.2. (A) 3D T1-WATS GRE, high muscle tissue signal with full suppression of fat; (B) 2 D T1-TSE, the muscle tissue and fat tissue signals are medium intensity; (C) 3D T1-FATS GRE, the high-fat signal intensity with full suppression of muscle signal.

3.2.1 Study aims

The first aim of the present chapter was to validate an automated measurement of temporal muscle volume changes by comparing it with the gold standard manual segmentation method. Although there are other software packages tested in research, e.g. Osirix, MIPAV and ImageJ (Fedorov et al. 2012), 3D slicer (https://www.slicer.org/) was chosen in the current study to provide automated segmentation measurements for muscle volume changes in the thigh and the adjacent fat deposits; subcutaneous adipose tissue (SAT) and intramuscular adipose tissue (IMAT). 3D slicer is an example of a medical image computing programme that is free and open source. It is convenient, interactive, and mimics the radiology workstation's

with many straightforward analysis tools that can correct the post-segmentation errors caused by slight MR field heterogeneity. In order to induce a measurable change in muscle volume, a unilateral leg immobilisation model was used. Immobilisation is a well-known model for inducing muscle volume atrophy, and temporal detection of these changes is well established using a gold standard manual segmentation of T1-TSE MR images (Kilroe et al. 2020). Our hypothesis is that automated segmentation is comparable to manual segmentation in detecting temporal muscle volume changes.

The second aim was to optimise the automated segmentation method by using an alternative MR water excitation sequence (Spatial-spectral) 3D-T1 WATS GRE that provides a high and uniform signal intensity of muscle tissue and compare it with the routinely used T1-TSE sequence in detecting muscle volume changes. A unilateral limb immobilisation model was again utilised to induce muscle volume changes following muscle-damaging eccentric exercise. High-intensity eccentric exercise causes transient muscle inflammation and oedematous swelling (Jameson et al. 2021), which is analogous to various clinical and pathophysiological conditions where measures of muscle volume are desirable. Muscle quality and fat volume may also change under these conditions. The second hypothesis was that using automated segmentation methods with the 3D T1-WATS sequence would be quicker and more sensitive than 2D T1-TSE in detecting muscle volume temporal changes.

The third aim of this chapter was to assess the possibility of measuring muscle fat volume changes using a CHESS 3D T1-FATS sequence. Thus, the final hypothesis was that muscle SAT, and IMAT volume could be estimated by the automated threshold method.

3.3 Methods

3.3.1 Study 1 – Comparison of manual vs. automated methods for measuring muscle volume changes within a unilateral limb immobilisation study

3.3.1.1 Participant characteristics and study design

This study was part of a major study done by members of the Nutritional Physiology Research Group at the University of Exeter (Kilroe et al. 2020). 13 males (age = 20.2±0.6 years; BMI = 23.4±0.9 kg·m^2) took part in this study. Each participant had 3 bilateral MRI thigh scans: (1) prior to applying a cast on one leg; (2) after two days of immobilising one leg; and (3) after seven days of immobilising the same leg. Scanning was undertaken using a 1.5 Tesla (T) MRI system (Intera, Phillips, The Netherlands) employing an axial T1- weighted turbo spin echo T1-TSE sequence (TR= 645.39 ms, TE =15 ms, slice thickness = 5 mm, slice spacing = 10 mm, acquisition matrix= 376× 376mm) with the participants in a supine position. The study was approved by the University of Exeter Sport and Health Sciences ethics committee (151021-B-02). Participants' characteristics are shown in **Table 3.3.1.1.**

Table 3.3.1.1. Participant characteristics (*n*=13).

Age (y)	20.2±0.6
Body mass (Kg)	79.21±0.03
Height (cm)	178±7.6
BMI (kg·m^{-2})	25±6

Values are presented as mean±SD

3.3.1.2 Immobilisation protocol

One leg was immobilised using a unilateral leg brace (X-ACT Donjoy brace, DJO Global, Vista, CA, USA), with the participant ambulating on crutches (after receiving instructions) during the immobilisation period. The immobilised leg was counterbalanced for leg dominance, and the non-immobilised leg considered as a within-participant control. The knee was fixed at an angle of 40° flexion (i.e., full knee extension being considered as 0°) by the locking hinge of the brace to ensure no weight-bearing occurred. Participants were instructed that all ground contact and muscle contraction (except for ankle rotation exercises twice daily to activate the venous muscle pump) in the immobilised leg were avoided. Participants were given a plastic cover to wear over the brace when showering. Daily contact was maintained with the participants throughout the study to ensure compliance, and only the researcher could adjust the brace fitting.

3.3.1.3 Image Analyses

Phantom image validation

An MR image of known measurements phantom was analysed by 3D slicer to compare the measurement with true volume. Volume estimation was close to the true volume with only 1.6 cm^3 difference. The actual phantom diameter was 907.2 cm^3, and the automated 3D Slicer measurement was 908.8 cm^3. The percentage difference between the two methods was 0.18%.

Validating automated volume measurement of MRI thigh images

Automated and manual segmentations were compared on the MRI thigh images of the 13 participants. The number of slices analysed was kept the same in both

segmentation methods for each participant and each visit and was in the range of 7-13 slices at the mid-thigh. In the manual segmentation method, one operator from the research group manually drew around each muscle on each third slice for mid-bilateral thighs (non-immobilised or control and immobilised legs). Then the cross-sectional areas for the selected slices were summed (Kilroe et al. 2020). Total volume was determined by multiplying anatomical cross-sectional areas (ACSA) by the distance between measured slices (incorporating the slice thickness and gap between slices) (Franchi et al. 2018).

$$\text{Total volume} = \Sigma \text{ ACSA} \times (\text{slice thickness} + \text{slices gap})$$

For the automated method, the researcher used 3D slicer software (Version 4.10.0; https://www.slicer.org/) (Fedorov et al. 2012), which uses an image intensity thresholding basis for selecting whole mid-thigh muscles (a computer estimation of the digital image signals' intensity difference), which utilised all of the slices collected (true measurement, no slices were missing) and read in the slice thickness and gap from the image header file thereby automatically produce a segmented image of the tissue of interest. The operator selected a range of threshold values to cover the desired tissue automatically, then chose post-segmentation correction by selecting specific correction tools (e.g., remove isles, smooth extrusion), see, **Figure 3.3.1.1**. Volume measurements were determined for total thigh muscles for all three visits using manual and automated methods. The number of slices selected depended on the image contrast quality of each participant's images that were evaluated on 3D Slicer. Image contrast varies depending on the participant's thigh size and static (B0) and RF (B_1) fields inhomogeneity that leads to SI variation in the peripheral slices (MR-TIP.com n.d.), which affects the thresholding segmentation. **Figure 3.3.1.2** shows the

thresholding segmentation defect caused by SI variation. A final 3D image illustrating muscle volume segmentation after applying correction effects is shown in **Figure 3.3.1.3**.

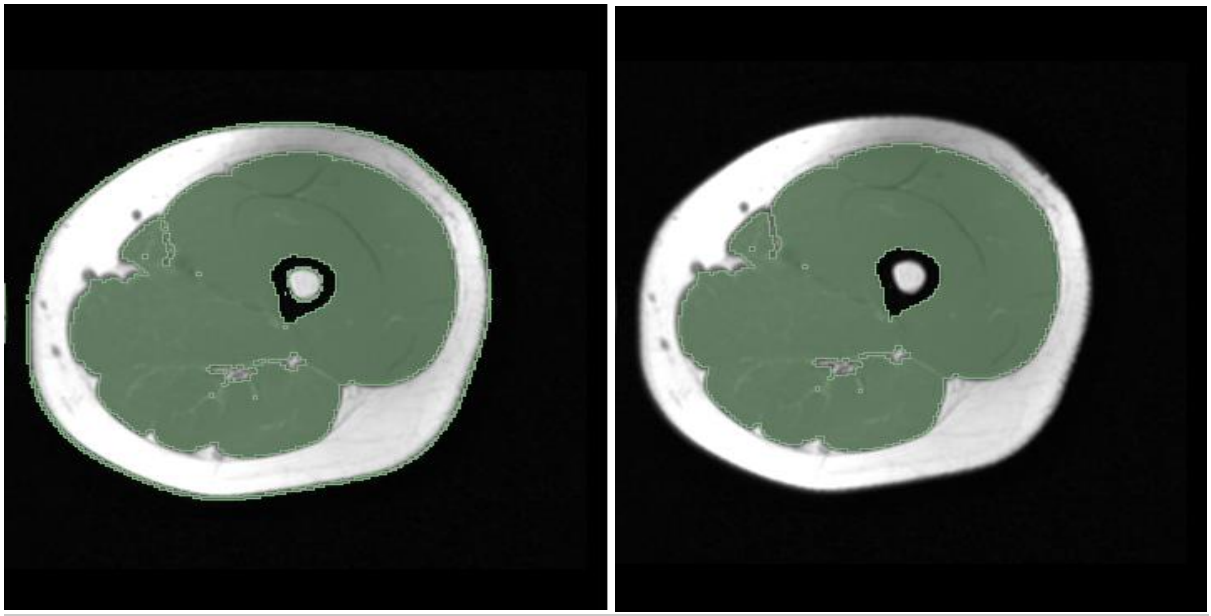

Figure 3.3.1.1 Illustration of the automatic segmentation. The left image does not include threshold correction effects (unwanted segmentations around the whole thigh and bone marrow). The right image incorporates threshold correction effects resulting in only segmenting the muscle area.

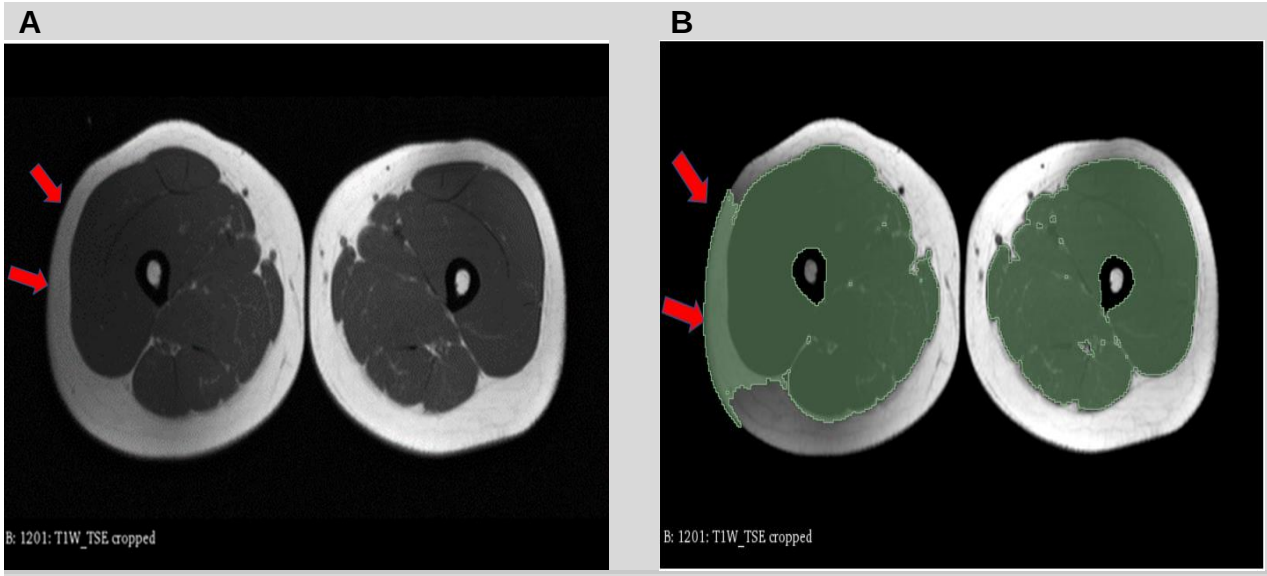

Figure 3.3.1.2. MRI T1TSE image showing (A) signal intensity degradation in the edge of the peripheral slice resulting in the dark area on the right thigh (left side of the image), and (B) the impact of this degradation on automated thresholding segmentation of the muscle.

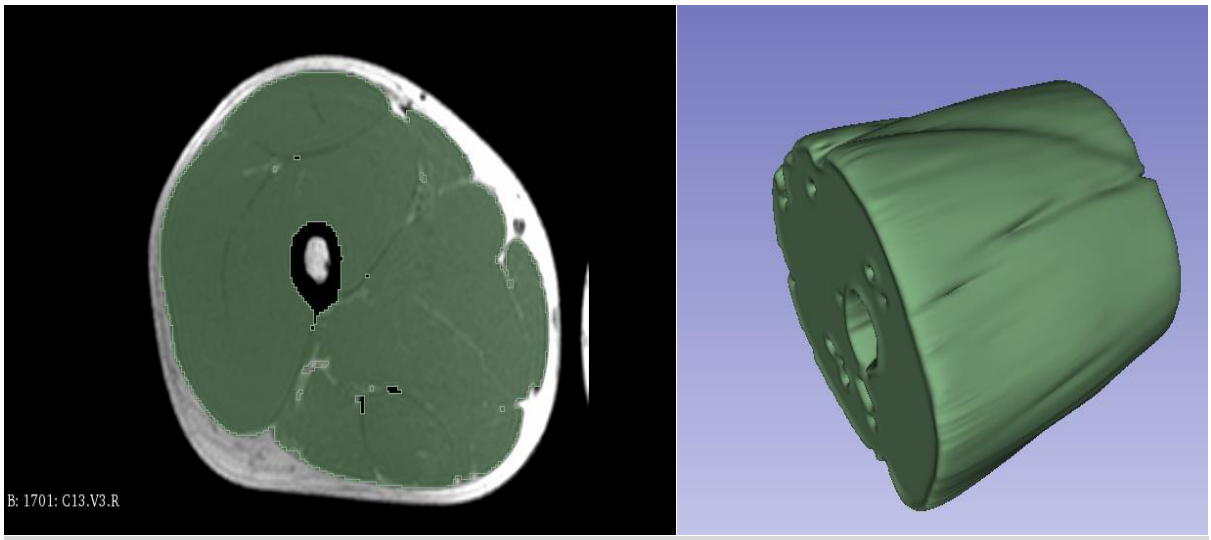

Figure 3.3.1.3. Example of 3D segmentation of the thigh muscle.

3.3.2 Study 2 – Optimising MR sequences for automated measurements of muscle volume changes using a unilateral limb damage-immobilisation study

3.3.2.1 Participant characteristics

Seven young, healthy males (age: 20±2 y, BMI: 25±6 kg·m^{-2}) volunteered for the study. Participants' characteristics are shown in **Table 3.3.2.1.** The study was approved by the Sport and Health Sciences ethics committee of the University of Exeter (REF NO. 151021/B/02 and 171206/B/08). The study was registered at ClinicalTrials.Gov (IDs: NCT02984332 and NCT03559452).

Table 3.3.2.1. Participants' characteristics (*n*=7).	
Age (y)	20±2
Body mass (Kg)	79±18
Height (cm)	176±8
BMI (kg·m^{-2})	25±6
Values are presented as mean±SD	

3.3.2.2 Experimental protocol

This study was a part of a major study done by members of the Nutritional Physiology Research Group at the University of Exeter (Jameson et al. 2021). More experiment details and analytical procedures are presented in sections 2.2, 2.8 and 2.9. Participants received a detailed explanation of the exercise protocols at least 48 hrs before the study began. The study consisted of three MRI visits. The first bilateral thigh muscle MRI scan was performed on day one at 8:30 am. Then participants underwent a bout of 300 bilateral and maximal eccentric muscle contractions of the knee

extensors. This was immediately followed by immobilisation of the dominant leg for seven days. The second MRI scan was performed on day-2 of immobilisation, and the third scan on day-7 of immobilisation. Participants were transported to and from the MRI scanner via a wheelchair to ensure no contractions or weight bearing for the immobilised leg.

3.3.2.4 Image acquisition and analysis

Three MR sequences were performed using a 1.5T MRI scanner (Intera, Philips, The Netherlands). All generated bilateral thigh axial images. The first used was a T1-weighted turbo spin echo (T1-TSE) sequence (field of view 500 x 500 mm, reconstructed matrix 512 x 512 mm; echo time (TE)= 15 ms, repetition time (TR)= 645 ms, slice thickness 5 mm, slice gap 10 mm) number of slices= 51, acquisition duration= 309 ms). The second was a 3D water selective excitation T1-Gradient echo (3D-WATS-GRE) sequence (field of view 500 x 500 mm, reconstructed matrix 960 x 960 mm, TE=11.73 ms, TR=20 ms, flip angle= 25º, slice thickness=10mm, slice gap= 5mm, number of slices=29, Acquisition duration= 349ms). The third was a 3D fat selective excitation T1-Gradient echo (3D-FATS-GRE) sequence (field of view 500 x 500 mm, reconstructed matrix 960 x 960 mm, TE=7.1 ms, TR=20ms, flip angle=25º, slice thickness=10mm, slice gap=5mm, number of slices=29, Acquisition duration=352 ms). Comparisons of muscle volume measurements of the control and immobilised thigh and the muscle volume percentage changes in the immobilised thigh across visits were conducted between the T1-TSE and 3D-WATS-GRE sequences. During volume measurements, the operator was blinded as to which thigh was control or immobilised. Due to the differences in slice thickness and slice gap between the two sequences, the number of slices to cover the same length were different for the

T1-TSE sequence (14 slices to cover 140mm of thigh length) than for the T1-WATS sequence (29 slices to cover 145mm of thigh length). **Figure 3.3.2.1** shows a comparison between the two sequences in producing 3D segmentation images (A) and the images' weighting and contrast differences (B). Five central slices from the 3D-FATS-GRE image were segmented for fat measurements to calculate total fat volume. Example images and segmentation are shown in **Figure 3.3.2.2**.

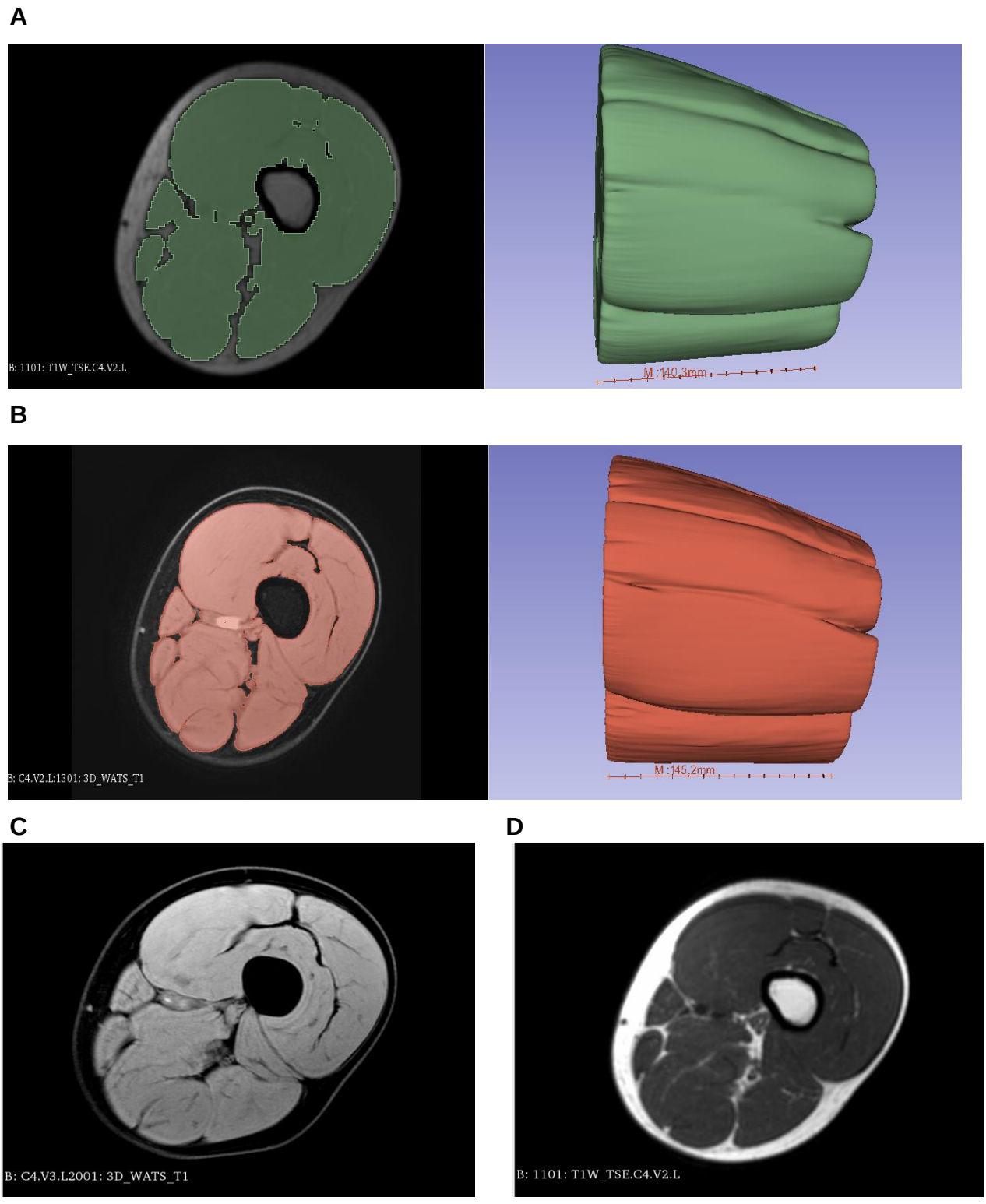

Figure 3.3.2.1. A comparison between images obtained and analysed with A) a T1-TSE sequence (slice thickness 5 mm, slice gap 10 mm) and (B) a T1-WATS sequence (slice thickness=10mm, slice gap= 5mm). Due to the differences in slice thickness and slice gap, the number of slices covering relatively similar but not exact areas differed between the two sequences. 14 slices were used for the T1-TSE sequence to cover 140mm, and 29 slices of the T1-WATS sequence to cover 145mm were used for the segmentation analysis. Images were taken from the same thigh. (C) example of a raw T1-WATS image, (D) example of a raw T1-TSE image.

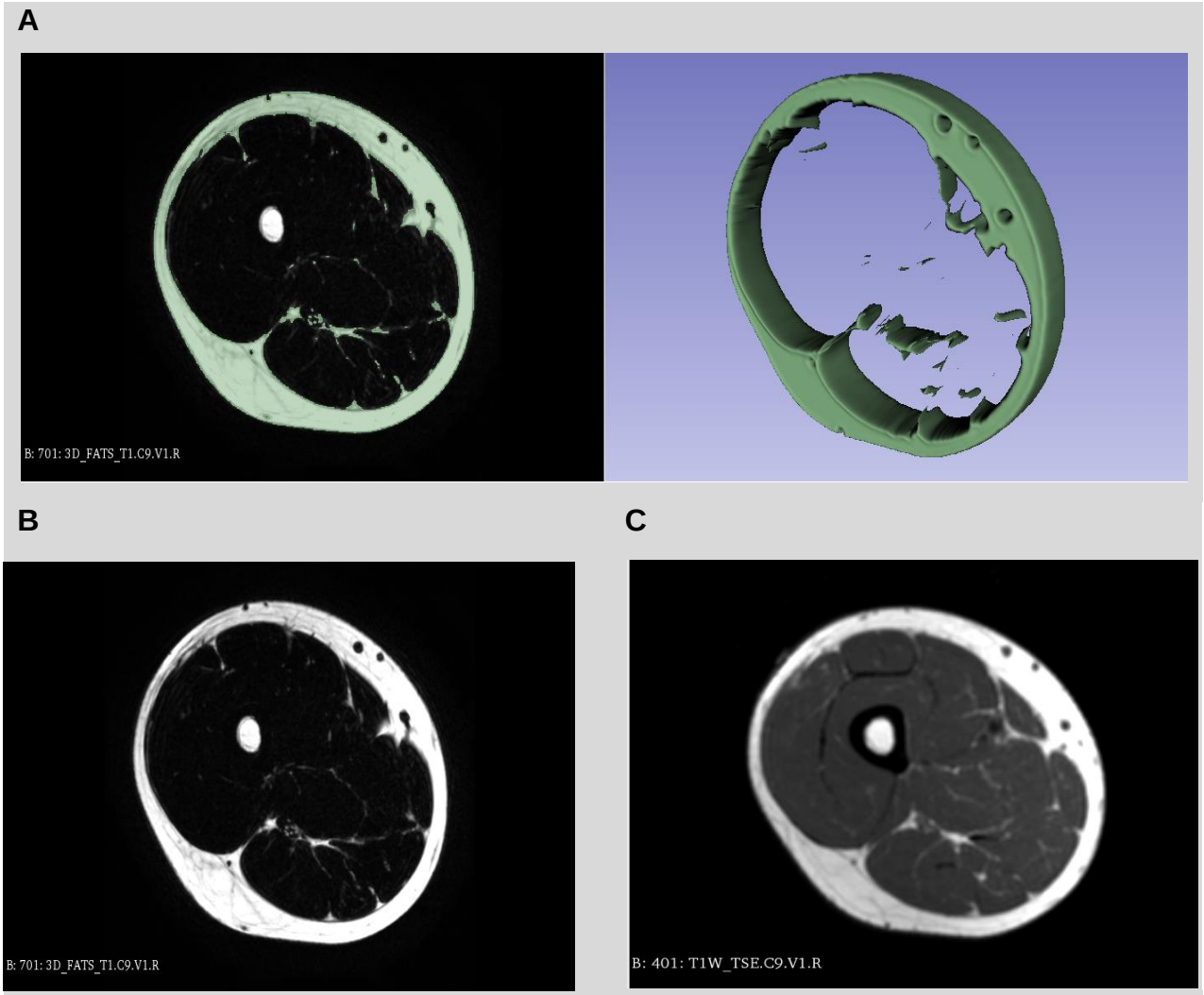

Figure 3.3.2.2 (A)T1-FATS image segmentation, 5 central slices were used. (B) T1-FATS image, (C) T1-TSE, the tissues contrast in T1-FATS is higher than in T1-TSE.

3.3.3 Statistical analysis

All statistical analysis procedures and calculations are presented in **chapter 2, Section 10.** Statistical analysis was undertaken to assess the agreements and differences between the two segmentation methods which were done by different operators. in study 1 and two MR sequences in study 2. A coefficient of variation (CV%) was calculated for the control thighs (3 visits, 2 methods and 3 visits, 2 MRI sequences) to directly compare the percentage of measurement errors and the relative variability to each sample mean from the two methods. A Bland-Altman test was used to estimate the agreement between manual and automated methods and between the two MR sequences. If the bias value of this test is close to zero, the two methods or two MR sequences are systematically producing the same results. A repeated-measure two-factor analysis of variance (Two-way ANOVA) was used to analyse time X segmentation method differences between the two methods in measuring muscle volume changes in the immobilised leg during the three visits (baseline, 2-day, 7-day). Due to missing values, a mixed model of repeated measures was used instead of Two-way ANOVA to analyse time x MR sequence differences for the damaged immobilised leg. Tukey's post hoc test was used when time, treatment or interaction effects were significant. All statistical analyses were conducted using GraphPad Prism 9.3.1 (GraphPad Software, San Diego, California, USA). $P<0.05$ was considered statistically significant, with all data in text and tables expressed as mean±Stdv and in figures expressed as mean±SEM.

3.4 Results

3.4.1 Study 1 - Comparing manual with automated segmentation methods

Muscle volume measurements of the control thighs and percentage changes of the immobilised thigh from pre-immobilisation, 2-day and 7-days are presented in **Table 3.4.1**. For the control thighs, the mean CV% for muscle volume over the 3 visits for the 13 participants was 1.60% for automated and 1.07% for manual methods.

The Bland-Altman test of agreement yielded 101.1 cm^3 bias, and 95% limits of agreement were [-28.54, 230.6] between automated and manual methods in measuring the thighs volume of the control legs, see **Figure 3.4.1.1.** In the immobilised legs, the bias values between the two methods after 2 and 7 days of immobilisation were -0.3±1.7% and -0.02±1.7%, respectively. The 95% limits of agreement were [-3.63, 2.96] and [-3.30, 3.26], respectively, see **Figure 3.4.1.2 and Figure 3.4.1.3**. In the immobilised leg, there were significant muscle volume changes with time after 2 and 7 days in both manual and automated methods; the time interval was $P < 0.0001$, methods interval $P = 0.4$, and interaction $P = 0.9$, see **Figure 3.4.1.4**. The automated method detected muscle volume changes significantly in two-time points, 0-7 days ($P<0.001$) and 2-7 days ($P<0.001$), but the decrease after 2 days (0–2 days) was not significant (P=0.1). For the manual method, the decrease was significant at all time points (0-2, $P<0.01$), (0-7, $P<0.001$) and (2-7, $P<0.001$).

Table 3.4.1. Muscle volume measurements of control and immobilised thighs and percentage muscle volume changes of the immobilised thigh over two-time intervals. Values are given for both automated and manual segmentation.

Total volume (cm^3)	**Automated**	**Manual**	**%Difference between methods**
Control-leg mean of 3 visits	1577±2.0	1475±4.2	7%
Pre-immobilisation	1604.5± 342.0	1494.5± 333.6	7.4%
2-Day immobilisation	1583.3± 338.7	1469.0± 325.7	7.8%
7-Day immobilisation	1509.7± 326.9	1402.9± 306.0	7.6%
%Change (0-2) interval	-1.3	-1.7	
%Change (0-7) interval	-5.9	-6.1	
% Change (2-7) interval	-4.6	-4.5	

Values present mean±Stdv.

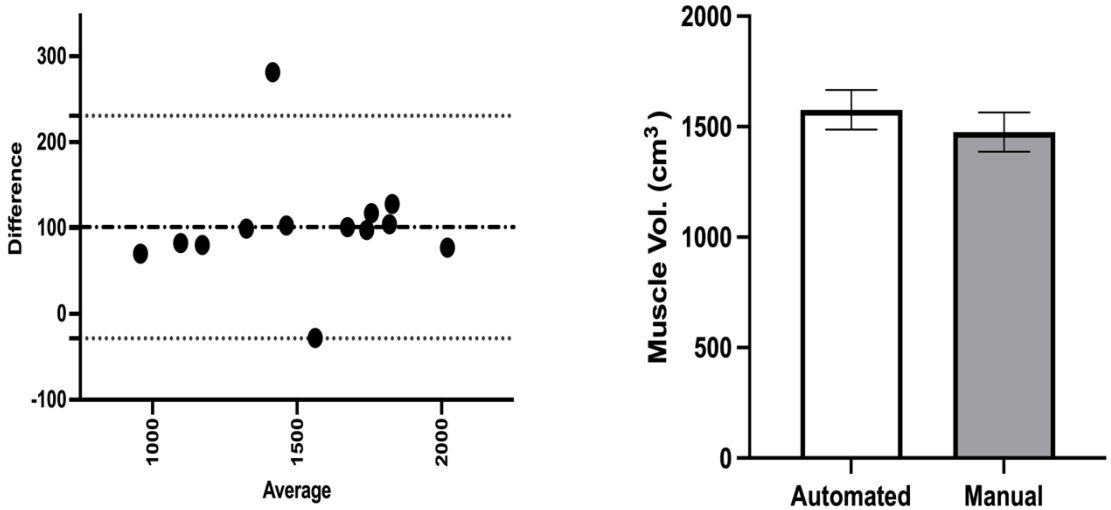

Figure3.4.1.1. An average muscle volume difference between two segmentation methods (automated vs manual). An MRI T1-TSE imaging sequence was post-processed to estimate muscle volume using the two segmentation methods. A direct comparison of thigh muscle volume measurements of the control leg at baseline. Statistical analysis was performed with Bland-Altman, (n=13).

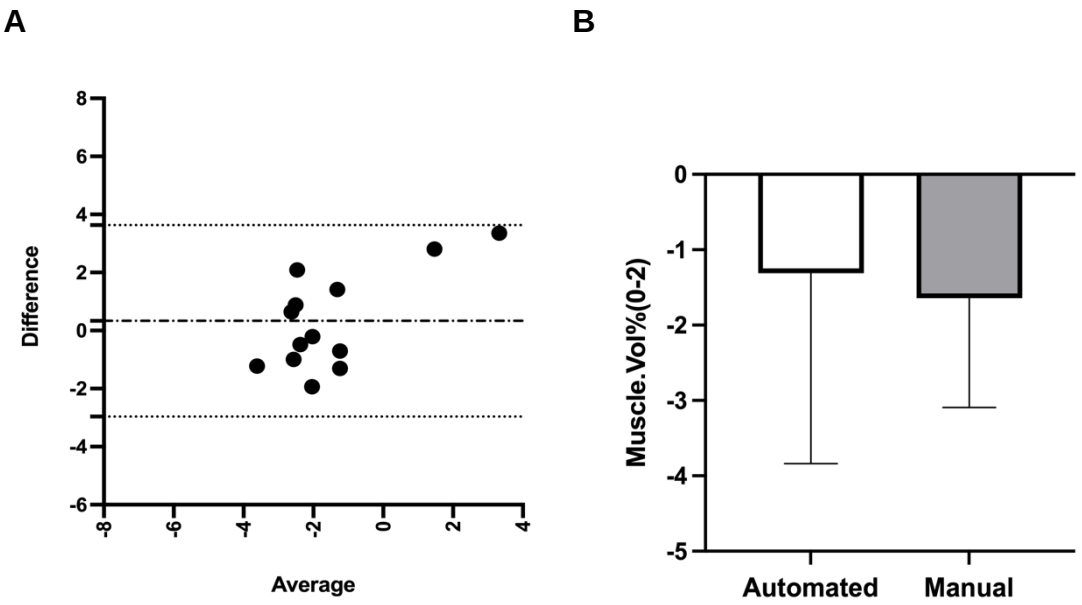

Figure 3.4.1.2. Average muscle volume %change was calculated from automated and manual methods. Percentage change of thigh muscle volume after 2-days of leg immobilisation. Data are represented as % differences with error bars (standard error). Statistical analysis was performed with the Bland-Altman test (n=13).

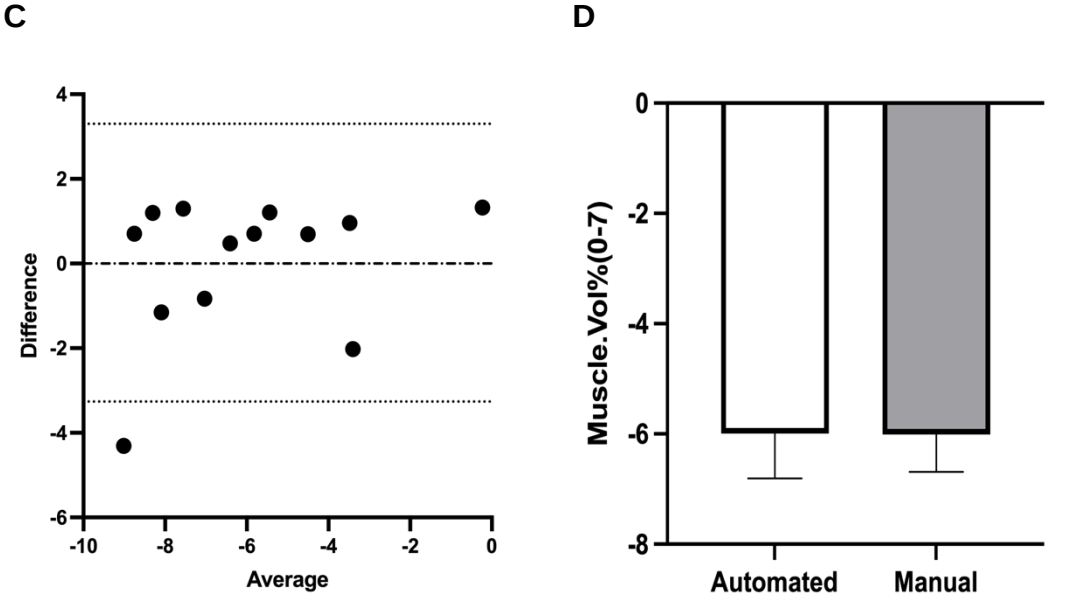

Figure 3.4.1.3. Average muscle volume %change was calculated from automated and manual methods. Percentage change of thigh muscle volume after 7-days of leg immobilisation Data are represented as % differences with error bars (standard error). Statistical analysis was performed with the Bland-Altman test (n=13).

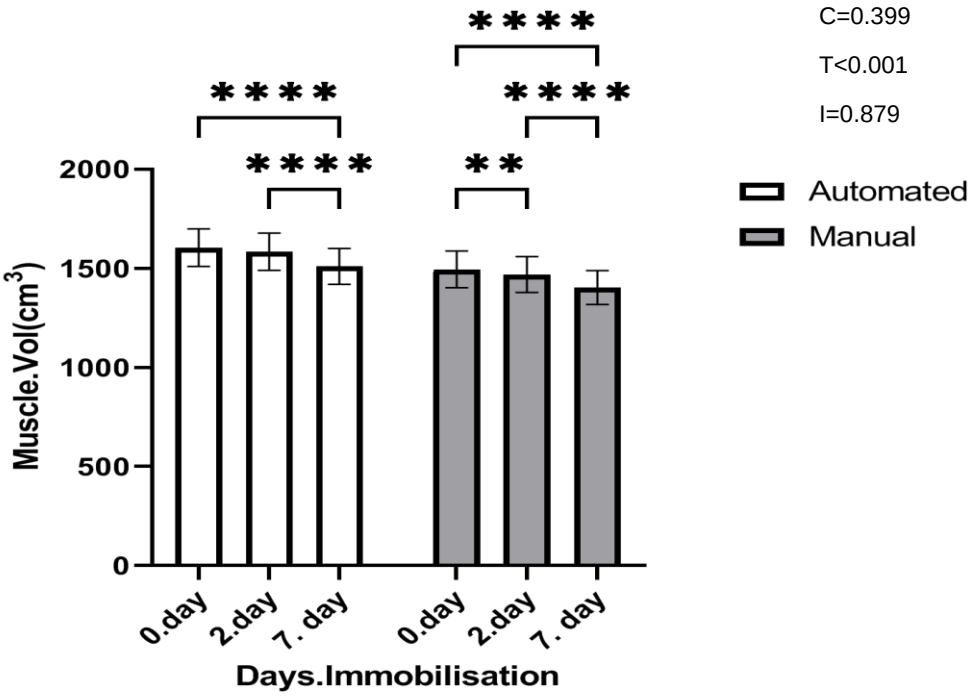

Figure 3.4.1.4. Average muscle volume determinations from two different methods (Automated Vs manual). MRI was done three times; pre-immobilisation, 2-day, and 7-day immobilisation. Data are presented as means with error bars representing standard error. Statistical analysis was performed with two-way repeated measures (Two-way ANOVA) (method *x* time) and time (T), condition (C) (i.e. Method) and interaction (I) effects are displayed on the graph. (*) represent the significant difference between pre-and post-2 and 7 days immobilisation (main effect). Two symbols $P<0.01$, four symbols $P<0.0001$, ($n=13$).

3.4.2 Study 2- Optimising image sequences for the automated segmentation method

The 3D T1-WATS sequence was more efficient and time-saving than T1-TSE when using the automated segmentation method. It required less post-segmentation correction, resulting from a higher CNR and being less sensitive to B1 heterogeneity than T1-TSE. All volume measurements and differences between the two MR sequences estimation are represented in **Table 3.3.2.** Volume measurements of the control (damaged non-immobilised) legs from the two sequences were comparable, CV% of WATS= 2.7% and T1-TSE= 2.3%. The Bland-Altman test of agreement between the two MRI sequences in measuring thigh volume of the control legs at the baseline visit yielded 101.0±47.4 cm^3 bias and [8.0, 193.8] 95% limits of agreement as shown in **Figure 3.4.2.1.** The relative percentage change after 2-days and 7-days of damage and immobilisation was -0.3±2.2%, [-4.7, 4.1] and -0.9±1.1%, [-3.1, 1.2] respectively, see **Figure 3.4.2.2** and **Figure 3.4.2.3**. There was a significant change in muscle volume in the damaged-immobilised leg recorded by both sequences (*P*=0.003, interaction; *P*=0.48). **Figure 3.4.2.4. A** shows the temporal muscle volume changes in the damaged-immobilised thigh during the three-time points. However, the T1-WATS GRE sequence was more sensitive in detecting changes than T1-TSE. Thigh muscle volume changes of the damaged immobilised leg were significant for T1-WATS when comparing baseline to day 2 and day 2 to day7 (*P*< 0.02) in both time points. The changes in T1-TSE were significant between baseline and day 2 (*P*<0.03) only and trending between day 2 and day 7 (*P*=0.05). No significant muscle volume differences between baseline and day 7 were detected by either sequence (T1-WATS, *P*=0.2, T1-TSE, P=0.9). Furthermore, in the damaged non-immobilised leg, no significant differences across time points were detected by either sequence (*P*=0.2,

interaction; *P*=0.9). **Figure 3.4.2.4.B** shows the temporal muscle volume changes in the damaged-non immobilised thigh over the three-time points. For the T1-FATS sequence, there were no significant changes in thigh muscle fat volume due to damage or immobilisation at any time points in both damaged thighs (non-immobilised and immobilised) (*P*=0.4, interaction; *P*=0.9). **Figure 3.4.2.5** shows the temporal fat volume changes in the damaged-immobilised and damaged-only thighs.

Table 3.4.2. Automated muscle volume measurements from two MRI sequences (T1-WATS Vs T1-TSE). A comparison between the sequences in measuring muscle volume in (damaged-non immobilised) and (damaged immobilised) thighs and temporal muscle volume %change of the damage-immobilised thigh.

Total volume (cm^3)	**T1-WATS**	**T1-TSE**	**%Difference between sequences**
Control-leg mean of 3 visits	2050.7± 22.8	1946.3± 25.8	5.4%
Pre-immobilisation	2049.5± 386.4	1917.1±349.7	6.9%
2-Day immobilisation	2103.6± 422.5	1965.4±370.5	7.0%
7-Day immobilisation	2021.7± 371.5	1909.6±336.7	6.3%
%Change (2-0)	2.64	2.52	
%Change (7-0)	-1.36	-0.39	
%Change (7-2)	-3.89	-2.84	
Values are presented as mean±SD			

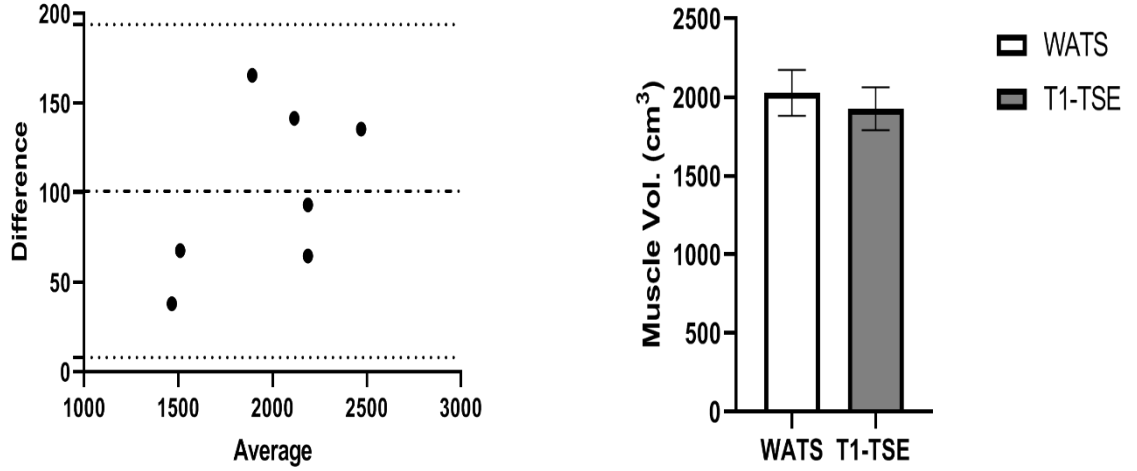

Figure 3.4.2.1. Average muscle volume difference between two MR-sequences (T1-WATS vs T1-TSE). A comparison of thigh muscle volume of control legs at baseline. WATS images (29 slices, covered 145 mm length), T1-TSE image (14 slices, covered 140mm length). Measurements were conducted by 3D slicer software (automatic thresholding technique). Data are presented as mean with error bars representing standard error (SEM) (*n*=7). Statistical analysis was performed with Bland-Altman analysis.

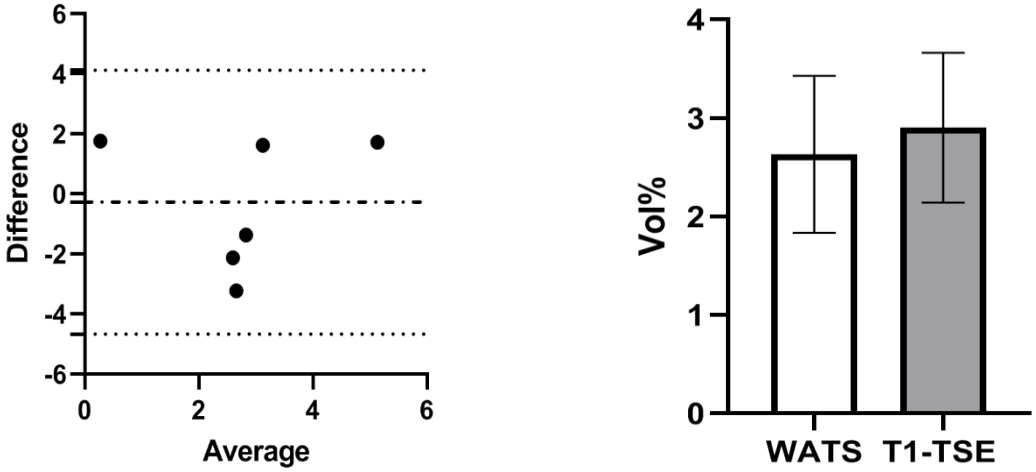

Figure 3.4.2.2. Average muscle volume %change after 2-day of thigh muscle damage and immobilisation. Measurements were calculated from T1-WATS and T1-TSE image sequences. A comparison between the two MRI sequences; T1-WATS (29 slices covered 145 mm length) and T1-TSE (14 slices covered 140mm length). Data are presented as mean with error bars representing standard error (SEM) (*n*=7). Statistical analysis was performed with Bland-Altman analysis.

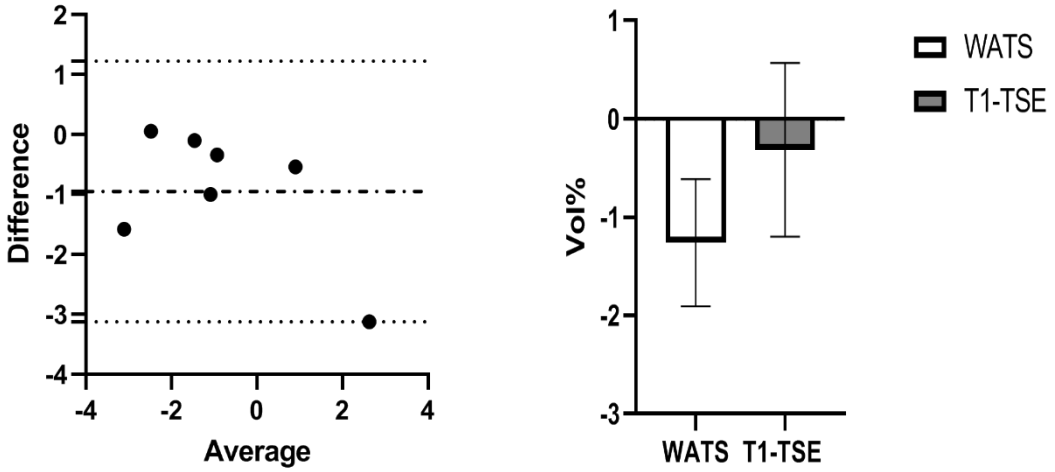

Figure 3.4.2.3. Average muscle volume %change after 7-day of thigh muscle damage and immobilisation. Measurements were calculated from T1-WATS and T1-TSE image sequences. A comparison between the two MRI sequences. T1-WATS image (29 slices, covered 145 mm length), T1-TSE image (14 slices, covered 140mm length). Data are presented as mean with error bars representing standard error (SEM) (n=7). Statistical analysis was performed with Bland-Altman analysis.

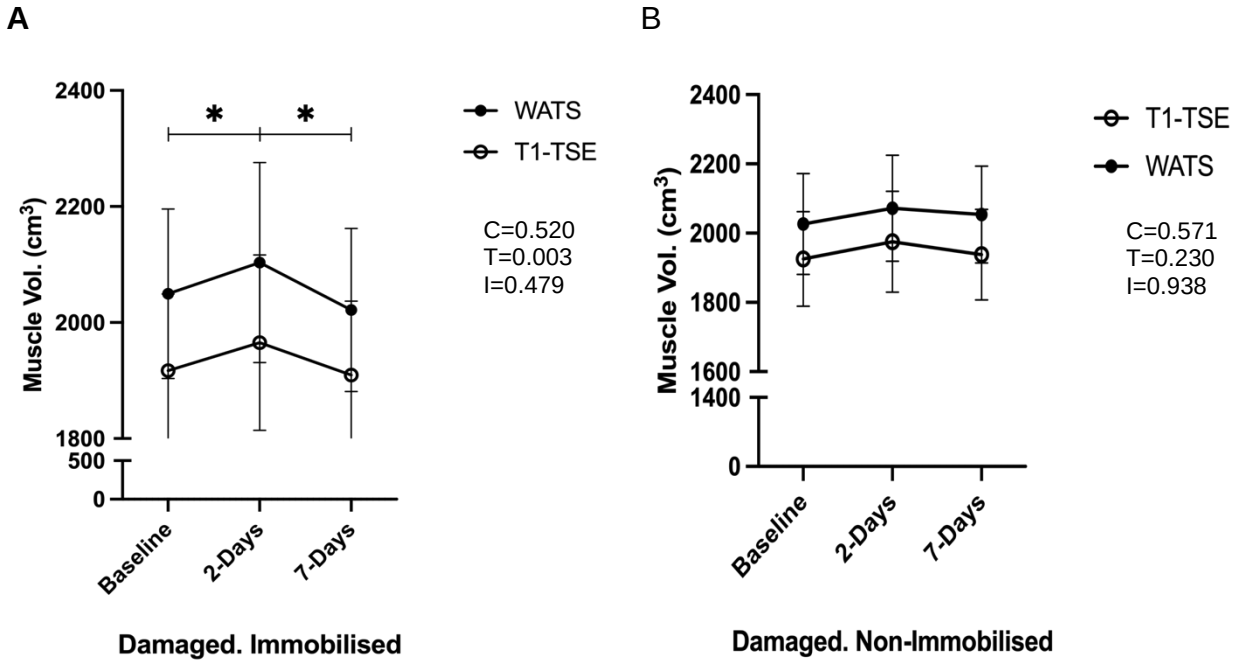

Figure3.4.2.4. (A) Damaged. Immobilised leg, (B) Damaged. Non-immobilised leg. Thigh muscle volume change at three-time intervals, baseline, 2-day and 7-day. A comparison between the two MRI sequences (T1-WATS and T1-TSE). T1-WATS images (29 slices, covered 145 mm length), T1-TSE images (14 slices, covered 140mm length). Statistical analysis was performed with Mixed-effect analysis (sequence *X* time) and time (T), condition (C) (i.e. sequence) and interaction (I) effects are displayed above on each graph. Data are presented as mean with error bars representing standard error (SEM) (n=7). (*) represents the significant difference between time points (main effect) and one symbol ($P<0.05$).

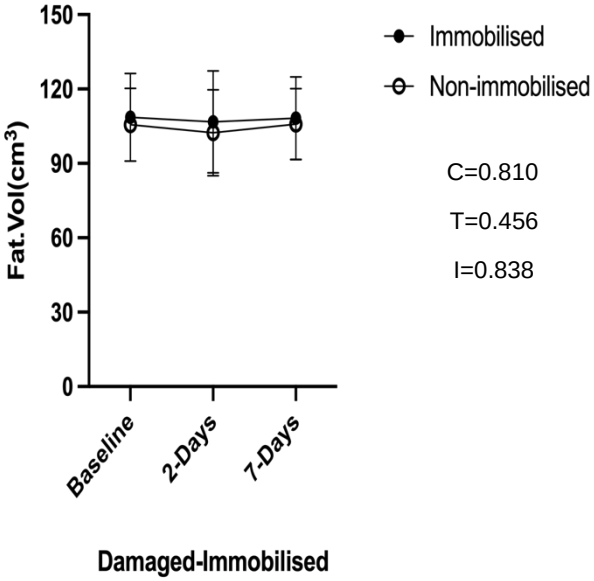

Figure 3.4.2.5. A comparison of total thigh fat volume change of damaged immobilised thigh. Images were taken at baseline (pre-immobilisation), after 2 and 7 days of immobilisation, 5 central slices were used. Data are presented as means with error bars representing standard error (SEM) (*n*=6). Statistical analysis was performed with Mixed effect analysis (leg X time) and time (T), condition (C) (i.e., leg) and interaction (I) effects are displayed on graph.

3.5 Discussion

Automated measurements of T1-TSE MR-images using thresholding and post-thresholding correction effects resulted in very good agreement with the gold standard manual method in detecting muscle volume changes. The biological measurements between automated and manual methods from MR- T1-TSE images of 13-control thighs were comparable. CV% estimates of the repeatability of measurement for both methods was good and comparable for both methods; CV%=1.6 for the automated and CV%=1.07 for the manual methods, which means that the error of measurements was low and similar in both methods, both under 5%error.

However, the automated segmentation slightly overestimated the total volume compared to the manual method. The bias between the two methods was 101.1 cm^3 when comparing control thighs **(Figure 3.4.1.1)**. The average volume of control thighs from automated and manual methods were 1577±2 cm^3 and 1475±4 cm^3 , respectively corresponding to an approximate 7% difference in estimated muscle volume between the two methods. The most important test in this study is the agreement between the two methods in detecting muscle volume change over time. The bias of the volume changes between the two methods after 2 and 7 days of immobilisation was 0.3 and 0.02 %, respectively, indicating excellent agreement in detecting temporal muscle volume changes as shown in **Figure 3.4.1.2** and **Figure 3.4.1.3**. Finally, both methods detected muscle volume reduction due to immobilisation which was significant over time, $P<0.001$, with no differences or interaction between the methods P=0.9 **(Figure 3.4.1.4).** The volume measurements were done manually by one operator and automatically by another one. The interobserver differences can cause variability in muscle volume measurements which can affect the accuracy and reliability (Pons et al. 2018).

In this study, we were able to validate the new automated segmentation method to measure muscle volume change. The main advantage of using the automated method is the lower time burden compared to the manual method. Total muscle volume was calculated within minutes using the automated method versus hours in the manual method. Thus, automated segmentation is more effective than manual one in terms of time-saving and can potentially improve the efficacy of using muscle volume measurements as a biomarker (Berg et al. 2020).

3D slicer software is designed to overcome segmentation problems, provide all correction tools required for the automatic correction of segmentation errors and produce a robust coverage of muscle area within a reasonable time. In the automated method, we used post-threshold correction effects, which easily amend the threshold segmentation errors and result in sensitive and accurate muscle volume measurements corresponding to the manual method, as illustrated in **Figure 3.3.1.1**. However, the automated method using the T1-TSE images appeared less sensitive than the manual method when detecting early changes due to immobilisation (days 0-2). The reduction in muscle volume was significant in the manual ($P<0.01$) but not in the automated ($P=0.1$). Also, IMAT segmentation could not be conducted from T1-TSE due to the low CNR of this pool in the image.

The important aims of the second study were to improve the quality and the sensitivity of the automated segmentation method and to compare T1-WATS with the routinely used T1-TSE MR images to assess the correspondence and the agreement in detecting muscle volume changes. In this study, the change of muscle volume after induced quadriceps muscle damage from a bout of 300 bilateral and maximal eccentric muscle contractions of the knee extensors immediately followed by unilateral leg immobilisation for 7-days were measured. There was strong agreement between the

two sequences' estimation of muscle volume change after 2-days and 7-days (bias = 0.27±2.2%, 0.9±1.1%), respectively. Both MR sequences showed significant muscle volume changes with time. However, T1-WATS showed more muscle volume and inflammatory changes that caused by muscle damage (oedematous swelling) than T1-TSE in the damaged immobilised thigh. The increases in muscle volume after 2 days of intervention were 2.6% (P<0.02) in T1-WATS and 2.5% (P<0.03) in T1-TSE, which were similar and significant in both sequences. However, when comparing the changes between day 2 and day 7, the atrophy and the swelling reduction were more obvious and significant in T1-WATS (-3.9%, P<0.02) compared to T1-TSE (-2.8%, P=0.05).

In summary, we have proposed an alternative MRI sequence (T1-WATS GRE) that provides higher image contrast (CNR) and signal intensity (SI) (Muhaimin et al. 2019), which helped to reduce the need for post-segmentation correction and to speed up segmentation time, also, improved measurement sensitivity. Also, we have introduced the possibility of measuring thigh muscle fat automatically from T1-FATS images.

There were differences in image parameters between the two MR sequences, specifically slice thickness and slice gap, which resulted in different volumes being measured. T1-WATS GRE covered 14.5 cm length of the mid-thigh with 29 slices, the slices gap was only 5mm, and slice thickness was 10mm. While T1-TSE covered 14.0 cm with only 14 slices along the mid-thigh length as the slice gap was 10mm and slice thickness 5mm. Consequently, there were about 5.4- 7% differences in estimating muscle volume. This difference may be diminished if similar geometric parameters were set up. This bias in estimating muscle volume was consistent, within 5.4-7% between the two sequences over the three visits. T1-WATS volume measurements

were higher than T1-TSE, though the coefficients of variation CV% of the control legs were quite similar, CV% = 2.7% and = 2.3% for T1-WATS and T1-TSE, respectively.

In the damaged non-immobilised thigh, no muscle volume change was detected by either MR sequence showing no significant muscle volume changes due to induced damage. From these findings, we suggested that muscle damage *per se* did not cause muscle volume changes, while the immobilisation of damaged muscles due to eccentric exercise increases the inflammatory fluids in the first 2 days.3D T1-WATS is a gradient echo pulse sequence modified by adding a water-selective excitation pulse. This selectively excites fluids only and suppresses fat signals by taking advantage of a chemical shift between water and fat. Subsequently, fluid changes are more prominent in this image type (Muhaimin et al. 2019). Muscle damage was induced in both legs, but there was a significant increase in muscle volume of the immobilised leg only after 2-days recorded by two sequences, T1-WATS ($P<0.02$) and T1-TSE ($P<0.03$). Also, muscle volume declined when comparing day 2 with day 7 in the damaged-immobilised thigh, which was significant in the T1-WATS ($P<0.02$) but trending in the T1-TSE ($P=0.05$) images. Furthermore, the exercise preserves muscle volume; no significant change was detected in either of MR sequences between baseline and post 7 days in the damaged immobilised group (*$P>0.05$*).

When assessing T1-TSE and T1-WATS correspondence in detecting muscle volume changes, we found T1-WATS GRE more efficient to use with the automated thresholding measurement. It provides higher SNR and CNR and is less sensitive to B1inhomogenity than T1-TSE **(Figure 3.2).** As a result, it requires less segmentation time (less segmentation correction) than T1-TSE (Grande et al. 2014). On the other hand, T1-FATS was deemed insufficient to measure thigh muscle fat changes in normal healthy participants with a very small amount of IMAT pool. Also, the image

resolution of this pool appeared low and difficult to detect by the automated thresholding method. We could not analyse the whole block (29 slices) of T1-FATS images due to practical difficulties, which were parallel to T1-WATS and so only the 5 middle slices were examined. Assessing muscle fat with more rigorous MR sequences such as Dixon and MRS is an aim in future studies. Quantitative and qualitative fat and muscle information can be gathered from Dixon images. Furthermore, deeper and microscopic information about fat infiltration can only be detected by using MR-spectroscopy (MRS).

Limitations

The automatic segmentation overestimates total muscle volume compared to the manual either because of inherent calculation differences or because it includes the adjacent vessels and connective tissues between muscles, as shown in an example of vessels included in thresholding segmentation **(Figure 3.5).** If the difference does lie in the inclusion of vessel volumes, these remain constant, unlike muscle volume, which changes due to a range of intervention factors. The other suggestion of this difference is that the manual segmentation, which included only every third slice and assumed all the three slices' areas were equal, causes an error as the shape of the muscles differs across slices. Overall, any overestimations are not a major problem as they are constant and do not affect the sensitivity to monitoring changes in muscle volume. Furthermore, it was not possible to compare muscle volume measurements directly with two different MR images due to the different geometric parameters. Instead, we compared the temporal volume changes, and there was strong agreement between 3D T-WATS and T1-TSE.

Figure 3.5 Automated segmentation of thigh muscle using the thresholding technique. The area inside the red circle is an example of the vessels included in total muscle estimation.

Conclusion

Automated segmentation is in demand in the research and clinical fields, as it saves time and can produce accurate measurements for muscle volume changes. In this study, we validated the automated segmentation for muscle volume changes.

3D T1-WATS was more convenient with automated thresholding-based segmentation, as it consumes less time to segment than the routine T1-TSE imaging sequence. However, using the same segmentation method with different MR images with different parameters yielded different volume estimations. However, it did not affect the agreement between the sequences in detecting muscle volume changes. Automated muscle fat measurement using 3D T1-FATS was not satisfied in normal healthy participants owing to the difficulty in detecting and measuring very small IMAT

areas with very low spatial resolution using the same number of slices as was used for the T1-WATS sequence (29 slices). We analysed only 5 central slices as the slices further from the centre largely suffered from MR field inhomogeneity. Using only 5 central slices, we did not detect changes in total fat volume, which might be because of a small number of slices, or the subjects were young and healthy males with little fat tissue, which caused an additional limit to detect fat volume changes from only a few slices. Or there is no change in subcutaneous and IMAT fat depots. Also, the sample size was small.

Chapter 4

18 hours of restricted eating during the fasting month of Ramadan increases fasting glucose concentration and reduces muscle volume

4.2 Introduction

Intermittent fasting (IF) strategies have gained interest for weight management and improvement of metabolic health markers comparable to a calorie restriction regime (Dong et al. 2020). There is growing evidence of the beneficial effect of IF in preventing and boosting the treatment of Mets (Zeb et al. 2020). There are several forms of IF for example, time-restricted eating (TRE) is a popular form of fasting for 16 hours incorporating a sleep period and eating for 8 hours. The other forms include early time-restricted eating (eTRE) with food consumed before evening and delayed time-restricted eating (dTRE) that allows an evening meal before fasting, alternative day fasting (ADF) with three interspersed days per week of total fasting or energy restriction and 5:2 intermittent energy restriction (5:2 IER) with two consecutive or non-consecutive fasting days per week (Aragon and Schoenfeld 2022).

Fasting during the Ramadan month, one of five Islamic pillars that has been practised annually for more than 1440 years, is categorised as evening or delyed TRE (Antoni et al. 2017) (Mindikoglu et al. 2017).

As previously mentioned, IER and TRE have received attention in the last decade, with a recent study reporting an increased life span in rodents that consume a calorie-restricted diet within a few hours, followed by a fasting period of up to 20 hours, during which ketone bodies in the blood increased (de Cabo and Mattson 2019). There is growing evidence demonstrating the beneficial effects of Ramadan fasting, or TRE, on metabolic health, such as significant weight loss of approximately 1.4-2.3 kg at the end of Ramadan (Adlouni et al. 1997; Norouzy et al. 2013; N. Khan et al. 2017; Mohammadzade et al. 2017; Nachvak et al. 2018). The reduction in body weight is due to a decrease in fat and/or muscle mass as measured by bioelectrical impedance analysis (BIA) **(Chapter 1, Table 1.9)**. This suggests that TRE could be used as a

strategy to reduce body weight without consciously intending to reduce calorie consumption or increase physical activity levels (Longo and Mattson 2014; Faris et al. 2020; Wilkinson et al. 2020). In some Ramadan studies, there has been a slight reduction in calorie consumption, mainly from reduced protein intake, which leads to a higher intake of carbohydrates and fat during Ramadan (Sadiya et al. 2011; Norouzy et al. 2013; Mohammadzade et al. 2017; Nachvak et al. 2018). A study by *Adlouni et al. (1997)* reported a reduction in body weight despite increased calorie, carbohydrate and protein intake. In addition, they found that saturated fatty acid (SFA) consumption was significantly reduced, and monounsaturated fatty acid (MUFA) significantly increased during Ramadan (Adlouni et al. 1997). *Stote et al. (2007)* conducted a form of dTRE study examining the impact of 8 weeks of 20 hrs/day. This study allowed a 4-hr eating window (5:00-10:00 pm) and the calorie-free drinks were permitted during the fasting period. Unlike Ramadan fasting, which forbids the consumption of any foods or drinks. Also, the authors controlled the energy and macronutrient intake, which were kept the same during TRE and non-TRE periods. It was found that subjects lost weight during the TRE period compared to non-TRE and most of the reduction came from fat mass estimated by BIA (Stote et al. 2007). In contrast, other Ramadan studies reported no change in BMI, body weight or body composition. However, these studies did not report any information about energy intake (Ongsara et al. 2017; Mindikoglu et al. 2020).

Most Ramadan studies reported decreased or no significant changes in fasting blood glucose (FBG) **(Chapter 1, Table 1.9)**. Two studies reported increased FBG; one of which included 20 hrs/day over two months of TRE, and the other Ramadan fasting in people with metabolic syndrome (Stote et al. 2007; Sadiya et al. 2011). Most Ramadan studies have reported no changes in fasting insulin (FBI) level or insulin sensitivity (as

measured by HOMA-IR). One study reported an improvement in insulin sensitivity: reduced insulin resistance (i.e. by decreasing FBG and FBI) at the end of Ramadan (Mohammadzade et al. 2017). Another study reported increased FBI and HOMA-IR, despite a reduction in FBG. However, these results may be due to the subjects' wide age range (21-63 years) (Nachvak et al. 2018). It is well-known that a younger population is more insulin sensitive than an older one (Chee et al. 2016). The wider age range may therefore be a confounding factor. No consideration was given to the age factor in the study design and in the interpretation of the results. It would be better to separate the group into young and older groups. The effect of Ramadan fasting and TRE on blood lipid profile is also heterogeneous among studies **(Chapter 1, Table 1.9)**. In some studies, Ramadan fasting beneficially altered blood lipid profile, especially when the fasting duration was around 12 hrs (Adlouni et al. 1997; Fakhrzadeh et al. 2003; Akhtar et al. 2020; Saleh et al. 2005). However, other Ramadan fasting studies reported no significant changes with similar fasting hours (~12hrs/day) (Ongsara et al. 2017; Mindikoglu et al. 2020). Ramadan fasting with a duration of 16hrs/day was reported in some studies to lead to a beneficial decrease in total triglyceride (TG) and increased high-density lipoprotein (HDL) (Mohammadzade et al. 2017), whereas other studies with a fasting time range of 15-17 hrs/day reported no beneficial alteration of blood lipid profile (N. Khan et al. 2017; Nachvak et al. 2018).

To our knowledge, only one study highlighted the temporal effects (changes recoded at specific time points) of Ramadan fasting (Adlouni et al. 1997). Furthermore, although some studies have used BIA to determine fat free mass (muscle) and fat mass changes (Santos and Macedo 2018), no studies have included MRI assessments of altered muscle volume and lipids deposits **(Chapter 1, Table 1.9)**. Changes in body composition (muscle and fat masses) are associated with changes

in the body's metabolic markers and capacity for blood glucose disposal (Dirks et al. 2016).

Most Ramadan studies included males only or had unequal numbers of each sex. Analysis was subsequently undertaken considering the group as a whole, which could explain the inconsistent effect of Ramadan fasting. In fact, women of fertile age will suspend Ramadan fasting according to the duration of their menstrual period, unlike men who are expected to fast the whole Ramadan month. This should be considered when interpreting studies examining the effects of fasting during Ramadan.

4.2.1 Study aims

The primary aim of this study is to examine the effect of an 18-hour RF on; BMI, skeletal muscle volume, FBG, FBI, AVF and ASF, and blood lipid profiles through the measurement of these markers Pre-RF, after one week and 3.5 weeks of commencing fasting. The study enrolled healthy adult Muslims who intended to practice RF in the United Kingdom.

The secondary aims are to compare sex-based differences in response to RF by comprising an equal distribution of female and male participants, and examine any lingering effects of RF by reassessing the same participants one month after the end of Ramadan and during normal habitual energy intake (non-fasting period). Finally, the study aims to compare daily habitual dietary intake and physical activity during Ramadan and the non-fasting period to determine differences in energy and macronutrient consumption as well as physical activity that may impact the identified biological markers.

4.3 Methods

4.3.1 Participants

After potential participants expressed interest in taking part, they were contacted, and the requirements of the study were explained via email or other electronic communication. The information sheet and consent forms were sent at least 48 h before the first visit. The study design and the participants' specific tasks in each Phase are displayed in **Figure 4.3.2**. Thirty-eight healthy middle-aged Muslims (19 females and 19 males) that intended to fast for the Ramadan month during daylight hours in the UK enrolled in the study. All participants underwent daytime fasting, i.e. time-restricted eating (TRE), during Ramadan month. However, females do not fast during their menstrual cycle as it is religiously forbidden; therefore, generally, females did not fast over the month for between 0 and 10 days. One female did not have a period in Ramadan and fasted the whole Ramadan month, and one female was excluded due to her long menstrual cycle (15 days). Sixteen of the males fasted for the entire month. Of the remaining three, one man broke for one day due to tiredness, another for two days and the third for six separated days due to travelling. Recruitment for the study was undertaken in 2019 (total n=16, 8 males and 8 females) and in 2021 (total n=21, 10 females and 11 males), and was approved by the Sport and Health Sciences ethics committee, University of Exeter (Ref No: 190327/A/02 for 2019) (Ref No: 200325/A/04 for 2021). Ramadan in 2019 was 29 days (started on 6th May and ended on 4th June), and Ramadan in 2021 was 30 days (started on 13th April and ended on 12th May). Participants' characteristics are shown in **Table 4.3.1.**

Table 4.3.1 Participant Characteristics		
Sex	**Females (n=18)**	**Males (n=19)**
Age (y)	31±5	32±6
Body mass (kg)	67±14	79±17
Height (cm)	161±6	173±6
BMI (kg.m^{-2})	25.5±4.4	26.5±5.6
Total fasted days	22±6	29±1
Values represented mean±Stdv. BMI = body mass index		

4.3.2 Experimental Protocol

All experimental and analytical procedures details are presented in **Chapter 2, sections 2.2-2.10**. An overview of the study design is shown in **Figure 4.3.2**. The study was split into four main phases. Phase 1 was completed before Ramadan fasting commenced, Phase 2 was completed one week after commencing Ramadan fasting, Phase 3 was completed 3.5 weeks after commencing Ramadan fasting, and Phase 4 was completed one month after the end of Ramadan fasting. Participants attended the lab on four occasions, once during each Phase of the study. Participants attended the Nutritional Physiology Research Unit (NPRU), St. Luke's Campus, University of Exeter in 2019, and Mireille Gilling's Neuroimaging centre, Royal Devon & Exeter hospital in 2021 for their study visits.

For all visits, participants had fasted for 8-12 h from their last meal. The non-Ramadan fasting Phases (1 and 4) were more flexible in terms of visits schedule and these Phases were completed over four days in each Phase, with the daily schedule designed to accommodate one participant every 45 minutes. The first appointment started at 8:15 am and the final at 12:00 pm. The Ramadan phases (Phases 2 and 3) were stricter and completed within two days in each Phase to allow just one day difference between subjects. The first appointment started at 9:30 am, and the final

appointment at 5:15 pm, to allow an 8-12 h fasting period for each participant. No early morning appointments were made as Muslims eat Suhur meal after midnight (1-2 am).

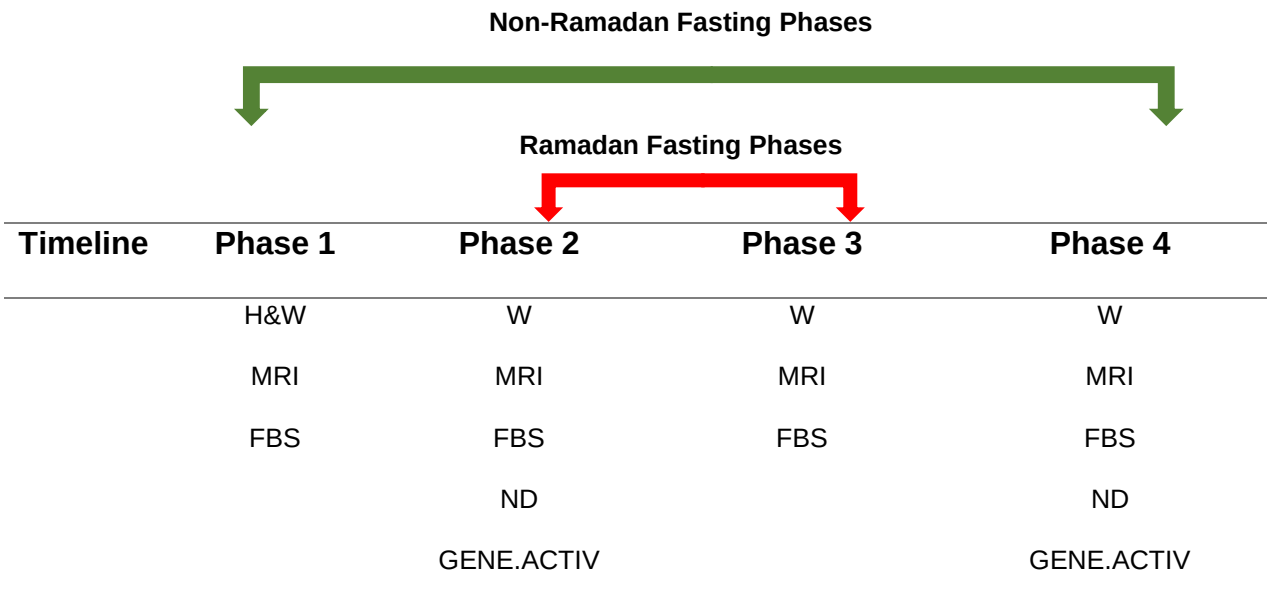

Figure 4.3.2. Study Design represents study tasks for each Phase. Phase 1 (Pre-Ramadan), Phase 2 (one week after commencing Ramadan fasting), Phase 3 (3.5 weeks after commencing Ramadan fasting), and Phase 4 (one month after end of Ramadan fasting). Participants' visits were within four days in non-fasting stages (Phase 1) and (Phase 4) and within two days in the fasting stage. Abbreviations: W&H: Height and Weight, W: weight, MRI: Magnetic resonances imaging FBS: Fasting blood samples, ND: Nutritional Diary, GENE.ACTIV: Activity watch.

4.3.3 Images acquisition and analyses

When the participants arrived at either the NPRU or Mireille Gilling's Neuroimaging centre, body mass was measured, followed by MRI scans on the abdomen and mid-thighs. A body array coil for both anatomical regions was used. Axial images were obtained for mid-bilateral thighs and mid-abdomen. In 2019, 1.5 T (Intera, Phillips,

The Netherlands) MRI scanner was used a 3D GRE T1_ WATS sequence was used for leg compositional analysis, the number of slices was 21 (Slice thickness 10mm, Slice spacing=5mm), for measuring mid-thigh muscle volume and a 3D GRE_T1 FATS sequence was used with 3 slices to estimate abdominal subcutaneous and visceral fat volumes. In 2021,3T Siemens (MAGNETOM Prisma, Erlangen, Germany) MRI scanner was used, MR sequence was 3 points-Dixon (3D PDFF-SGE) the number of slices was 104 (slice thickness=1.5mm, Slice Spacing=0.9mm) to cover same area, as the slice thickness and slice gap were different between the two sequences. The 3D PDFF-SGE was used for measuring thigh muscle and thigh fat volumes. However, for one female, due to an inadequate field of view, 75 slices were used for measuring thigh fat. 10 slices were measured for abdominal subcutaneous and visceral volumes. Slicer software (version 4.11.0; https://www.slicer.org/) was used for the MR images post processing to determine volumes.

4.3.4 Blood sample collection and analyses

Blood samples were collected from venipuncture of the antecubital vein. Two ml of blood was collected into vacutainer blood collection tubes (Becton Dickinson, Franklin Lakes, NJ, USA), with 20µl immediately–analysed for glucose concentration by a biochemical analyser assay (Biosen EKF-diagnostic GmbH, Barleben, Germany). According to the company website, Biosen analyser provides excellent accuracy with less than 2% CV over large measurement ranges (‘Biosen Lactate and Glucose Analyzer | EKF Diagnostics’ n.d.). One ml of each blood sample was collected into lithium heparin tubes (Becton Dickinson, Franklin Lakes, New Jersey, USA) and immediately centrifuged. The other one ml was collected into serum separator tube (SST) (containing spray-coated silica and a polymer gel for serum separation; Becton

Dickinson) and left at room temperature for at least 30 minutes. All tubes were centrifuged at 4º C and 4000 RPM, and aliquoted (one aliquot designated for each of the following analyses) plasma and serum were stored at -80º C. In 2019, aliquots of serum samples were transported to the Clinical Chemistry department of the Royal Devon & Exeter NHS Foundation Trust and analysed for insulin concentrations using the Roche Cobas 702 module of the Cobas e 801 analyser (Roche, Basel, Switzerland). According to the cobas e 801 system's manual, the precision of the immunoassay method to quantify human serum and plasma was determined using Elecsys reagents, pooled human sera and controls in a protocol (EP5-A3) of the CLSI (Clinical and Laboratory Standards Institute): 2 runs per day in duplicate each for 21 days (n = 84). and DRG ELISA kits (DRG International, Springfield, NJ, USA). Plasma aliquots samples were sent to the MRC Integrative Epidemiology Unit at the University of Bristol for metabolomics analysis by nuclear magnetic resonance (NMR) spectroscopy for blood lipids profile; Low-density lipoprotein (LDL), high-density lipoprotein (HDL), total blood cholesterol (TC), total triglyceride (TG) and albumin. NMR is a highly sensitive blood lipid quantitative method (Soininen et al. 2015). In 2021, all serum and plasma aliquots were sent to the Clinical Chemistry department of the Royal Devon & Exeter NHS Foundation Trust. Plasma was analysed for insulin concentration using the Roche Cobas 702 module of the Cobas e 801 analyser (Roche, Basel, Switzerland) Roche, Basel, Switzerland) and DRG ELISA kits (DRG International, Springfield, NJ, USA). Blood lipids concentrations were analysed using Roche/Hitachi Cobas c 701/702 analyser Quantikine ELISA kits (R&D Systems, Minneapolis, MN, USA). Blood lipid concentrations analyses method is widely accepted as a sensitive tool (Zeb et al. 2020). HOMA-IR was calculated from the equation proposed by Matthews et al (1985) and Wallace et al (2004).

HOMA-IR= FBG (mmol/l)* FBI(µlU/ml)/22.5

4.3.5 Habitual dietary and physical activity data

Habitual dietary intake and physical activity were recorded on two occasions: during Ramadan fasting and after one month from the end of Ramadan (after phase 4). The 3-day nutritional diary analysis was validated against the food frequency questionnaire (FFQ) and the 9-day nutritional diary. The 3-day nutritional diary showed high correlation and agreement with the other methods (Yang et al. 2010). 3-day nutritional diaries were given to participants to estimate habitual energy and macronutrient intake. The nutritional diaries were analysed for energy and macronutrient content using Nutritics (Nutritics Professional Nutritional Analysis Software, Swords, Dublin, Ireland). Monitoring physical activity using GENEActiv original accelerometer watch is validated against another tool called activPAL (Pavey et al. 2016). GENEActiv original accelerometer watches were given to the participants to record 3-day habitual physical activity levels and the metabolic equivalent of task (MET) of the following physical activities; sedentary, mild, moderate and vigorous. Participants wore GENEActiv watches on their non-dominant wrists. Physical activity data from the GENEActiv monitors were processed using GENEActiv excel macros. The 3-days of habitual energy and macronutrient intake, and also physical activity data were compiled into an individual average for each participant.

4.3.6 Statistical analyses

All statistical analysis procedures and calculations are presented in section 2.10. Statistical analyses were undertaken to study the effect of RF on female and male groups. A Two-factor analysis of variance (ANOVA) was used to analyse time X sex differences. There were two sets of comparisons; firstly, between Phases 1,2 and 3 to study the changes from baseline (pre-RF) to one week and 3.5 weeks of RF, then between Phases 1 and 4 to elicit any residual effects one month after the end of RF. A mixed-effects model was used instead of two-way ANOVA when some data were missing. One factor was matching/repeated measures (time) and one factor was not (sex)". The analyses were performed for BMI, thigh muscle volume, abdominal visceral and subcutaneous fat deposits (AVF and ASF), FBG, FBI, HOMA-IR, lipids profile, energy, macronutrients and METs of physical activities. Tukey's post hoc test was used when time or interaction effects were significant in a Two-way ANOVA or mixed-effect tests. All statistical analyses were conducted using GraphPad Prism 9.3.1 (GraphPad Software, San Diego, California, USA). $P<0.05$ was considered statistically significant, with all data in text and tables expressed as mean±Stdv and in figures expressed as mean±SEM.

4.4 Results

4.4.1 Body mass index

There was a significant reduction in BMI due to Ramadan fasting (RF) in both males and females (*P*<0.001, interaction; *P*=0.7; **Figure 4.4.1**). This reduction reached statistical significance after one week (8±1 days) and continuously declined after 3.5 weeks (26±1 days) of fasting, *P*<0.05 and *P*< 0.001, respectively, in males and females. There was a trend towards lower body mass one month after the end of Ramadan compared to pre-Ramadan (*P*=0.06, interaction; *P*=0.1). **Table 4.4.1** illustrates the biometric values in each phase and percentage differences from baseline.

Table 4.4.1. Body mass and BMI during the 4 Phases of the study.

Phases	**Females**		**Males**	
	Body mass (Kg)	**BMI (Kg.m^{-2})**	**Body mass (Kg)**	**BMI (Kg.m^{-2})**
Phase1	67±14	25.5±4.4	79±17	26.5±5.6
Phase 2	66±13	25.2±4.3	78±17	26.2±5.4
Phase 3	65±14	24.9±4.4	77±16	25.8±5.4
Phase 4	66±14	25.2±4.5	78±16	26.0±5.3
Phase (2-1) %	-1.0	-1.0	-1.33	-1.31*
Phase (3-1) %	-2.3	-2.4***	-2.61	-2.61***
Phase (4-1) %	-1.1	-1.1	-2.14	-2.03

Values present mean±Stdv. Phase1 (Pre-Ramadan), Phase2 (one week after commencing Ramadan fasting), Phase3 (3.5 weeks after commencing Ramadan fasting), and Phase4 (one month after end of Ramadan fasting). (*) represent the significant difference between time points, one symbol (P<0.05), two symbols P<0.01, and three symbols (P<0.001).

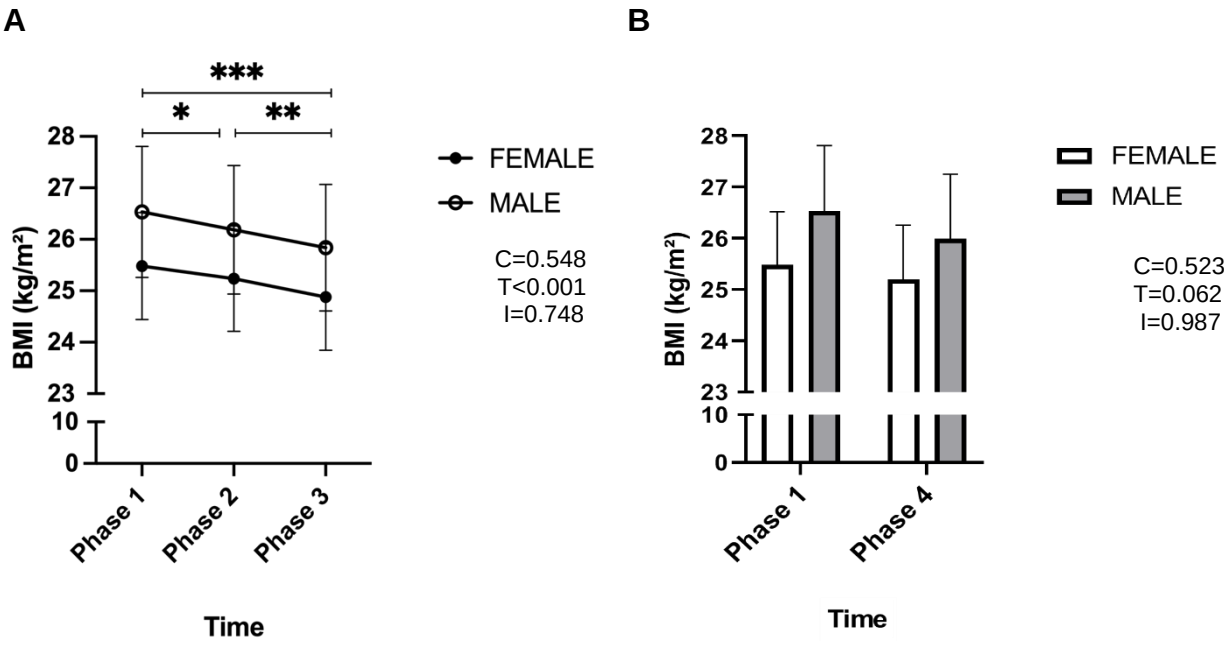

Figure 4.4.1. Comparisons of Body mass index (BMI). Phase1(Pre-Ramadan) compared to Phase2 (one week after commencing Ramadan fasting) and Phase3 (3.5 weeks after commencing Ramadan fasting) to show Ramadan fasting effect (A). Phase1 (Pre-Ramadan) and Phase4 (one month after end of Ramadan fasting) (B) to explore if the impact of Ramadan fasting is continuous one month later. Data are presented as means with error bars representing standard error (SEM) (n=18 females, n=19 males). Statistical analysis was performed with Two-way ANOVA (A) and Mixed-effects model (B) (sex *X* time) and time (T), condition (C) (i.e., sex) and interaction (I) effects are displayed above on each graph. (*) represent the significant difference between time points, one symbol (P<0.05), two symbols P<0.01, and three symbols (P<0.001), based on Tukey's pot hoc multiple comparisons test.

4.4.2 Skeletal muscle volume

Right thigh absolute muscle volumes are presented in **Figure 4.4.2**. Thigh muscle volume significantly decreased from phase 1 baseline (pre- Ramadan fasting) in males and females due to RF (time factor) (*P*=0.02, interaction; *P*=0.2). The reduction was significant after 3.5 weeks (*P*<0.01) in females and (*P*<0.001) in males. The reduction in thigh muscle volume did not recover completely one month after Ramadan fasting. There was a trend towards low thigh muscle volume one month after the end of Ramadan compared to pre-Ramadan in both sexes (*P*=0.08, interaction; *P*=0.9).

Table 4.4.2

displays the percentage change in thigh muscle volume in each Phase compared to phase 1 (pre-Ramadan fasting).

Table 4.4.2 Average percentages of muscle volume changes compared to Phase1(Pre-Ramadan fasting).

Phase compared to Phase 1	Female	Male
Phase 2	(-1.14)±(4.16)%	(-0.30)±(5.92)%
Phase 3	(-3.29)±(-0.72)%**	(-3.04)±(-3.69)%***
Phase 4	(-1.71)±(-0.20)%	(-1.84)±(-3.46)%

Values present mean±Stdv% of the percentage changes in right thigh muscle volume from the baseline Phase1 (Pre-Ramadan), Phase2 (one week after commencing Ramadan fasting), Phase3 (3.5 weeks after commencing Ramadan fasting), Phase4 (one month after end of Ramadan fasting) in the female and male groups. (*) represent the significant difference between time points, one symbol (P<0.05), two symbols P<0.01, and three symbols (P<0.001), based on Tukey's pot hoc multiple comparisons test.

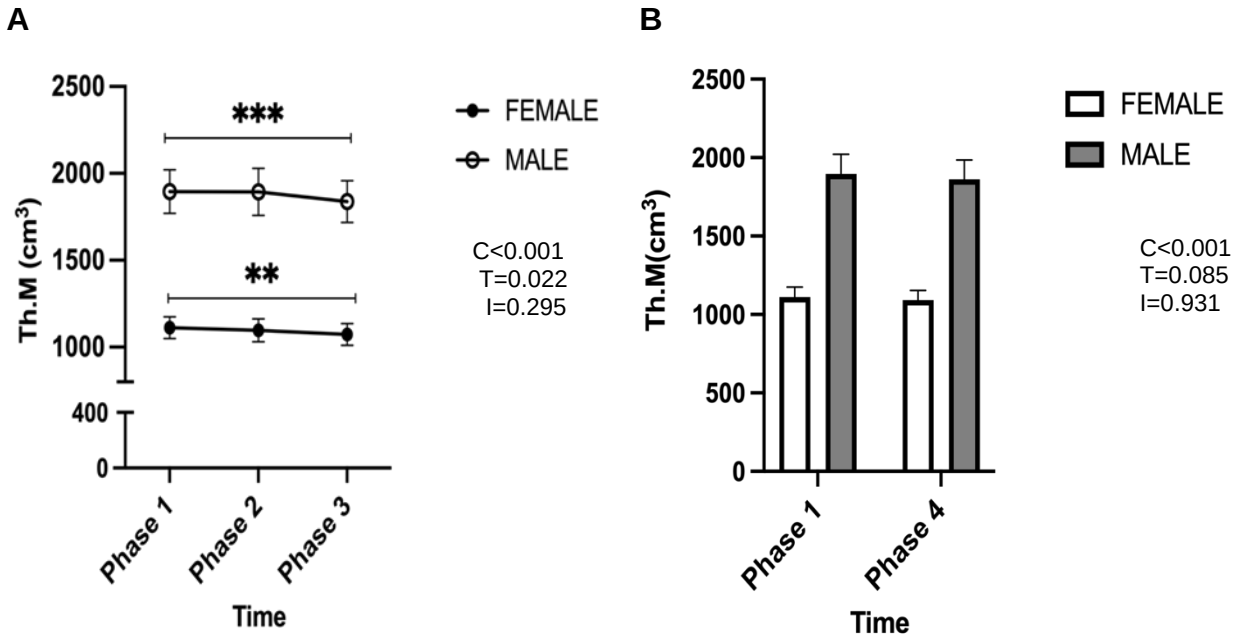

Figure 4.4.2. Comparisons of right thigh muscle volume (Th.M). Phase1 (Pre-Ramadan) compared to Phase2 (one week after commencing Ramadan fasting) and Phase3 (3.5 weeks after commencing Ramadan fasting) shows the effect of Ramadan fasting (A). A comparison between (pre-Ramadan) and (one month after end of Ramadan fasting) to elicit if the significant impact of Ramadan month fasting persists one month later (B). MR T1-WATS and Dixon-fat images of thigh muscle volume were measured automatically via thresholding technique using 3D slicer software. Data are presented as means with error bars representing standard error (SEM) (n=18 females, n=19 males). Statistical analysis was performed with mixed effect models (sex *X* time) and time (T), condition (C) (i.e., sex) and interaction (I) effects are displayed above on each graph. (*) represent the significant difference between time points (main effect), one symbol (P<0.05), two symbols P<0.01, and three symbols (P<0.001), based on Tukey's pot hoc multiple comparisons test.

124.4.3 Abdominal visceral fat

Abdominal visceral fat reduced significantly (*P*<0.01, interaction *P*=0.02). This reduction was significant after 3.5 weeks in the males' group only, phase-1 303.75±211.65 cm^3 (mean±Stdv) compared to phase-3, 273±199.73 cm^3 (*P*<0.01). No significant changes were seen between pre and one-month post-Ramadan fasting in either sex (*P*=0.6, interaction; *P*=0.5) (**Table, Figure 4.4.3**).

Table 4.4.3. Average percentage of Abdominal visceral fat changes during the timeline.

Phase 1 mean±Stdv volume (cm^3)	**Females**	**Males**
	158.7±90.9	303.8±211.7
Abdominal visceral fat volume change%		
Phase 2-1	-0.75± -6.65	-2.94 ± 2.37
Phase 3-1	-3.53± -8.05	-9.96 ± -5.63**
Phase 4-1	0.52± 0.49	-8.28 ± -1.97

The percentage changes in Abdominal visceral fat volume from the baseline Phase1(Pre-Ramadan) to Phase2(one week after commencing Ramadan fasting), Phase3 (3.5 weeks after commencing Ramadan fasting) and Phase 4 (one month after end of Ramadan fasting) in the female and male group separately. Values present mean±Stdv%. (n=18 females, n=19 males). (*) represent the significant difference between time points (main effect), two symbols P<0.01,

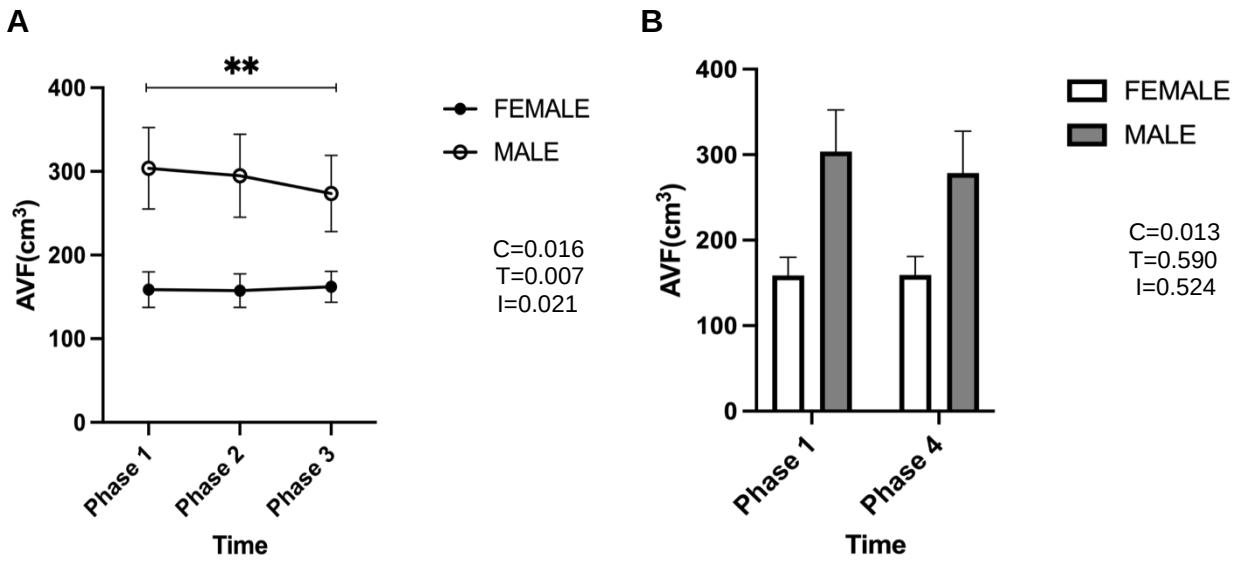

Figure 4.4.3. Abdominal visceral fat volume (AVF) comparison of three phases; Phase1 (pre-Ramadan), Phase2 (one week after commencing Ramadan fasting) and Phase3 (3.5 weeks after commencing Ramadan fasting), illustrate the effect of Ramadan fasting. The significant decline was in males only (A). Two phases comparison Phase1 (pre-Ramadan) and Phase4 (one month after end of Ramadan fasting) illustrate if the impact of Ramadan month fasting persists one month later (B). MR T1-FATS image (3-slices) or Dixon-Fat images (10-slices) of mid-abdomen measured automatically via thresholding technique using 3D slicer software. Data are presented as means with error bars representing standard error (SEM) (n=18 females, n=19 males). Statistical analysis was performed with mixed effect models (sex *X* time) and time (T), condition (C) (i.e., sex) and interaction (I) effects are displayed above on each graph. (*) represents the significant difference between time points (main effect), two symbols P<0.01, based on Tukey's pot hoc multiple comparisons test.

4.4.4 Abdominal subcutaneous fat

There was a trend toward decreasing abdominal subcutaneous fat at the end of Ramadan in both males and females (P=0.08, interaction; P=0.9). However, this reduction was not significant. Also, there were no significant differences between Phase 1 and Phase 4 (P=0.7, interaction; P=0.5) (Table, Figure 4.4.4).

Table 4.4.4. Average percentage of Abdominal subcutaneous fat changes during the timeline.		
Abdominal subcutaneous fat volume change%	**Females**	**Males**
Phase 2-1	0.90±5.34	0.87±1.77
Phase 3-1	-0.52±3.01	-2.20±0.15
Phase 4-1	0.47±4.80	-1.30±3.48

The percentage changes in Abdominal subcutaneous fat volume from the baseline phase1 (Pre-Ramadan) to Phase 2 (one week after commencing Ramadan fasting), Phase 3 (3.5 weeks after commencing Ramadan fasting) and Phase 4 (one month after the end of Ramadan) in the female and male group separately. Values present mean±Stdv%.

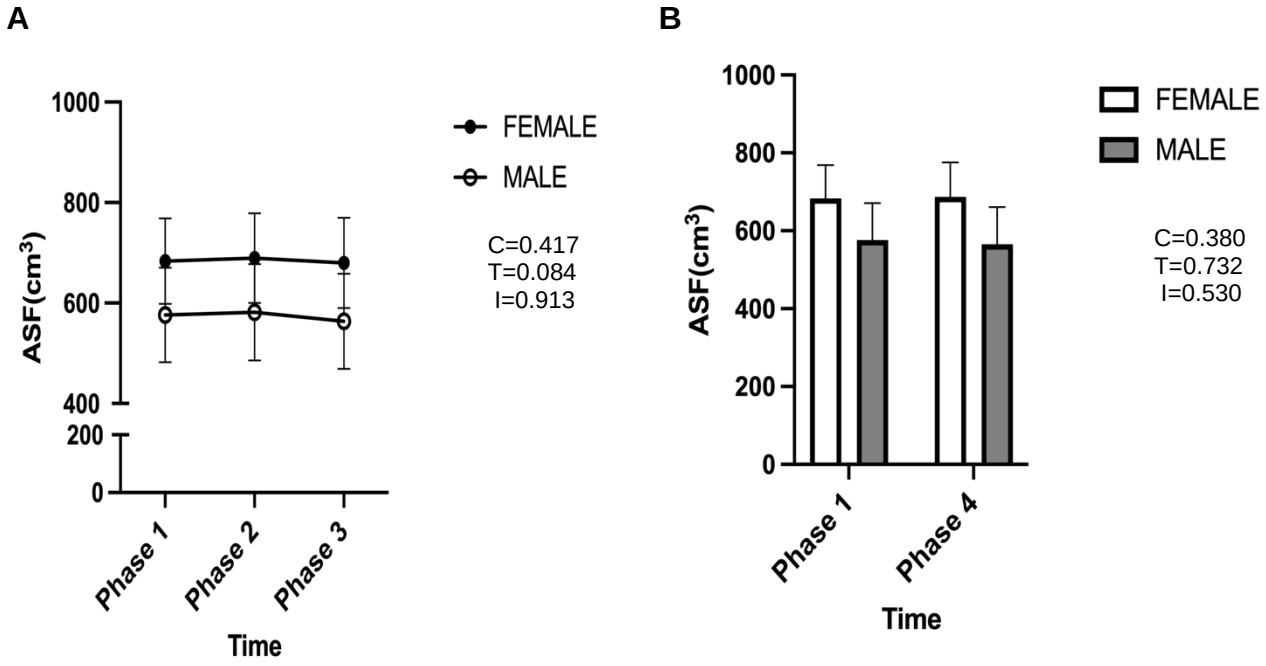

Figure 4.4.4 Abdominal subcutaneous fat volume (ASF) comparison of three phases; baseline (pre-Ramadan fasting), (one week after commencing Ramadan fasting) and (3.5 weeks after commencing Ramadan fasting), shows the effect of Ramadan fasting (A). A comparison of two phases (pre-Ramadan) and (one month after the end of Ramadan fasting) to elicit if the significant impact of Ramadan fasting persists one month later (B). MR T1-FATS image (3-slices) or Dixon-Fat images (10-slices) of mid-abdomen measured automatically via thresholding technique using 3D slicer software. Data are presented as means with error bars representing standard error (SEM) (n=18 females, n=19 males). Statistical analysis was performed with separate mixed effect models (sex *X* time) and time (T), condition (C) (i.e., sex) and interaction (I) effects are displayed above on each graph.

4.4.5 Fasting blood glucose

Fasting blood glucose (FBG) increased significantly at phase 3 (3.5-weeks after commencing fasting) in both males and females (time *P* <0.003), with no differences in response between the two groups (interaction *P* >0.5). However, there was no difference between baseline (Pre-Ramadan) and one month after the end of Ramadan fasting (*P*= 0.6, interaction; *P*=0.1) (**Table, Figure 4.4.5**).

Table 4.4.5. Absolute fasting blood glucose concentrations in four phases.

Timeline	Phase 1	Phase 2	Phase 3	Phase 4
Female	4.32±0.57	4.36±0.65	4.61±0.58	4.23±0.39
Male	4.23±0.55	4.48±0.45	4.72±0.70 *	4.41±0.55

Values present mean±Stdv of absolute fasting blood glucose concentrations (mmol/L) from the baseline, Phase1(Pre-Ramadan) to Phase2 (1-week after commencing fasting), Phase3 (3.5-weeks after commencing fasting) and Phase 4 (one-month after Ramadan fasting end) in the female and male group separately. (*) indicate the significant change.

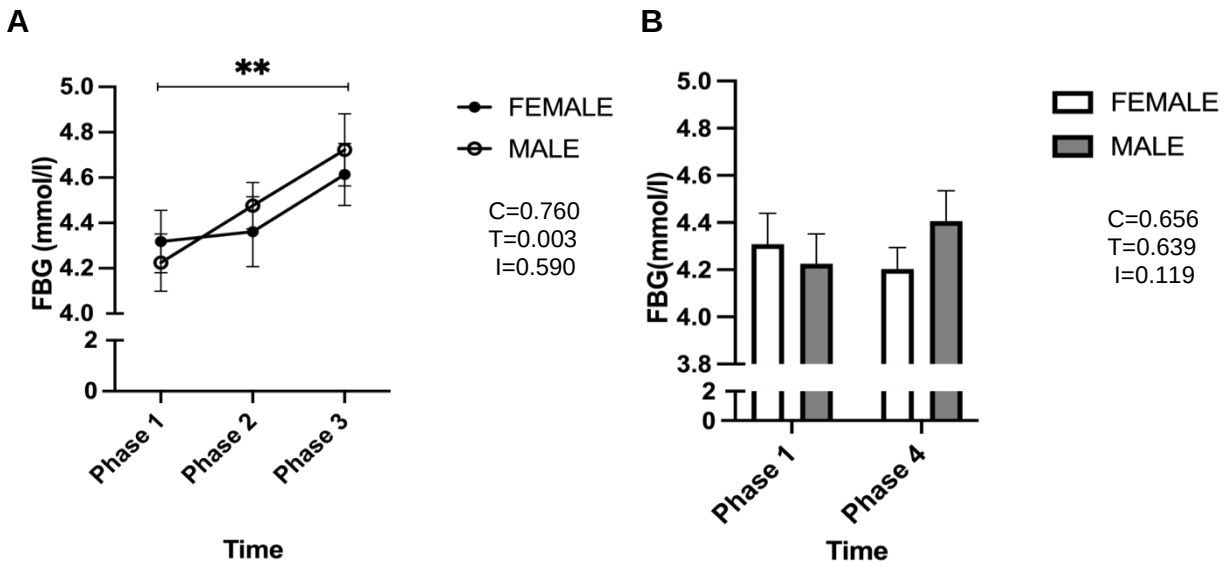

Figure 4.4.5. Fasting blood glucose concentration (mmol/l). Three phases comparison; Phase1 (pre-Ramadan), Phase2 (one week after commencing Ramadan fasting) and Phase3 (3.5 weeks after commencing Ramadan fasting), illustrate the effect of Ramadan month fasting (A). Two phases comparison, Phase1 (pre-Ramadan) and Phase4 (one month after end of Ramadan fasting) illustrate if the impact of Ramadan month fasting persists one month later (B). Data are presented as means with error bars representing standard error (SEM) (n=37, 18 females and 19 males). Because some values are missing this statistical analysis was performed with mixed effect models (sex *X* time) and time (T), condition (C) (i.e., sex) and interaction (I) effects are displayed above on each graph. (*) represents the significant difference between time points (main effect), two symbols P<0.01.

4.4.6 Fasting insulin and HOMA-IR

No significant changes were detected in both males and females in fasting insulin (time, *P*=0.391) and (interaction *P*=0.130) or HOMA-IR (time, *P*=0.611) and (interaction, *P*=0.162) during Ramadan. Furthermore, no differences between baseline and one-month post the end of Ramadan were detected (*P*=0.8, interaction; *P*=0.8) for insulin and (*P*=0.8, interaction; *P*=0.3) for HOMA-IR **(Figure 4.4.6), (Figure 4.4.7).**

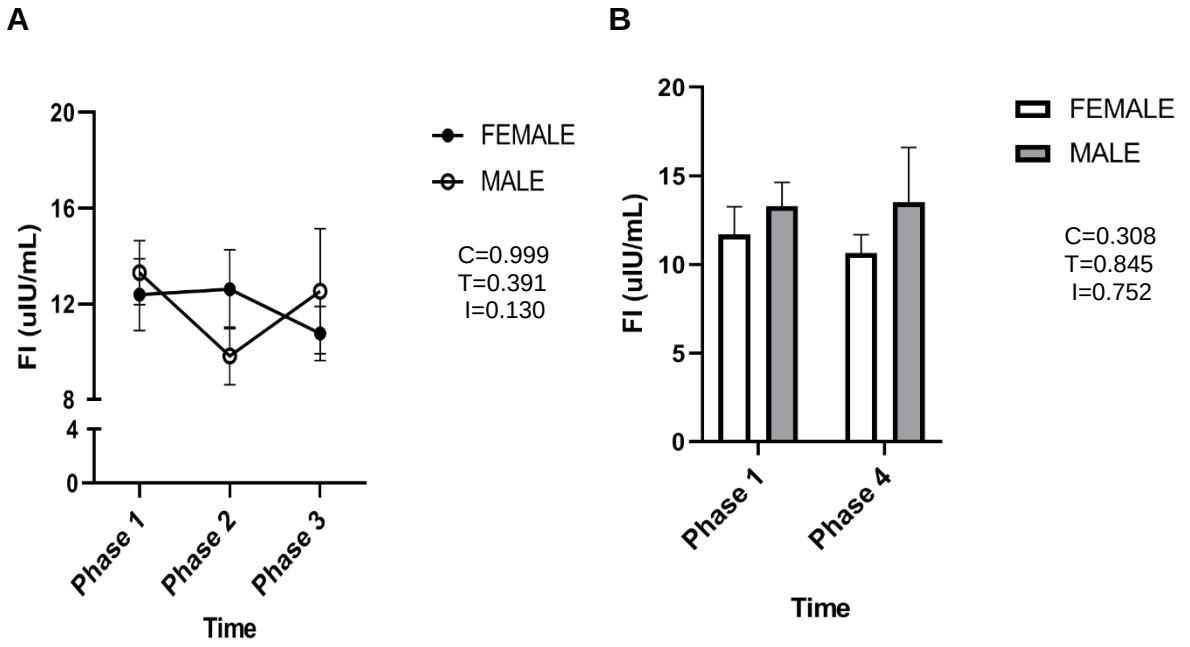

Figure 4.4.6. Fasting blood insulin concentration (mmol/l). Three Phases comparison; Phase 1 (pre-Ramadan), Phase2 (one week after commencing Ramadan fasting) and Phase3 (3.5 weeks after commencing Ramadan fasting), illustrate the effect of Ramadan month fasting (A). two phases comparison Phase1 (pre-Ramadan) and Phase4 (one month after end of Ramadan fasting) illustrate if the impact of Ramadan month fasting persists one month later (B). Data are presented as means with error bars representing standard error (SEM) (n=37, 18 females and 19 males). Statistical analysis was performed with separate mixed effect models (sex *X* time) and time (T), condition (C) (i.e., sex) and interaction (I) effects are displayed above on each graph.

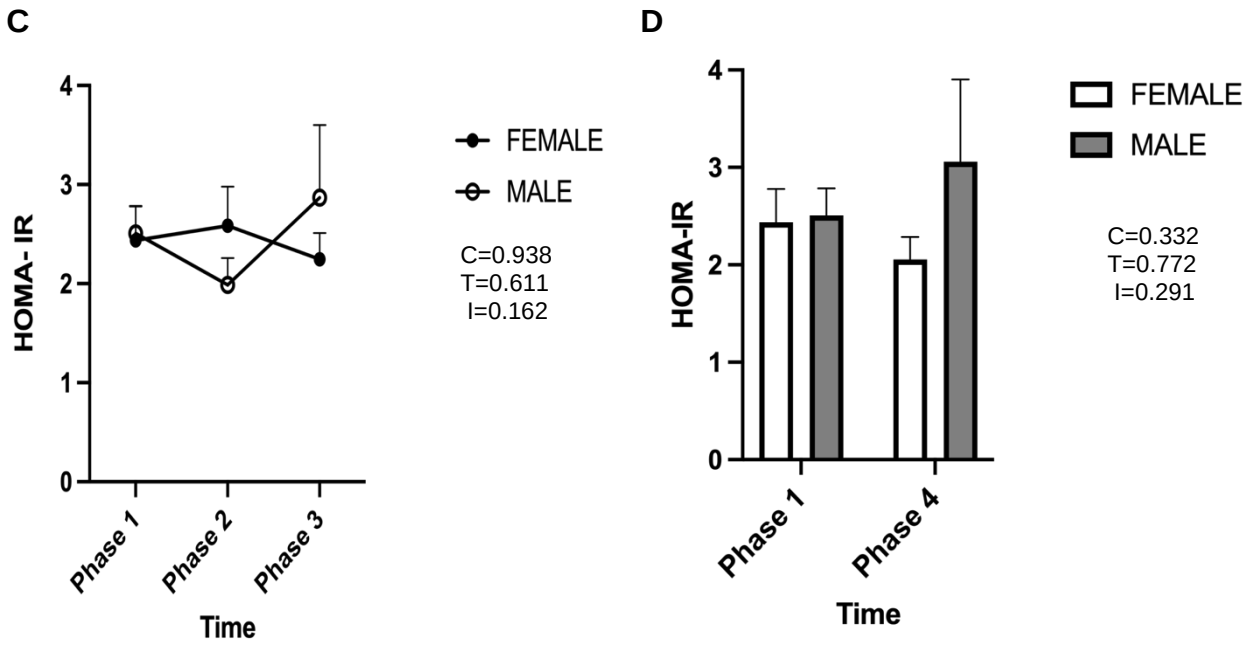

Figure 4.4.7. HOMA-IR, three Phases comparison; Phase 1 (pre-Ramadan), Phase2 (one week after commencing Ramadan fasting) and Phase3 (3.5 weeks after commencing Ramadan fasting), illustrate the effect of Ramadan month fasting (A). two phases comparison Phase1 (pre-Ramadan) and Phase4 (one month after end of Ramadan fasting) illustrate if the impact of Ramadan month fasting persists one month later (B). Data are presented as means with error bars representing standard error (SEM) (n=37, 18 females and 19 males). Statistical analysis was performed with separate mixed effect models (sex *X* time) and time (T), condition (C) (i.e., sex) and interaction (I) effects are displayed above on each graph.

4.4.8 Blood lipid profile

Low-density lipoprotein (LDL) increased in both males and females (P<0.05, interaction; P>0.4). However, it returned to baseline level (pre-Ramadan) one month after the end of Ramadan fasting (P>0.3, interaction; P>0.3) (**Figure 4.4.8**). There were no significant changes in total blood cholesterol (TC), total triglyceride (TG), high-density lipoprotein (HDL), or albumin at any time point during the study (P>0.05, interaction; P>0.05) **(Figure 4.4.9), (Figure 4.4.10)**. There was a trend of altering Acetoacetate concentration during Ramadan, (P=0.08, interaction=0.05), and post hoc test showed a significant increase after one week in the female group only (P<0.05). Also, there was a trend of increased acetoacetate concentration in both

groups at Phase 4 (one month after the end of Ramadan fasting) (*P*=0.08, interaction; *P*=0.2). No differences in beta-hydroxybutyrate during Ramadan (*P*=0.2, interaction; *P*=0.1), and after Phase 4 (*P*=0.7, interaction; *P*=0.3) were found **(Figure 4.4.11)**.

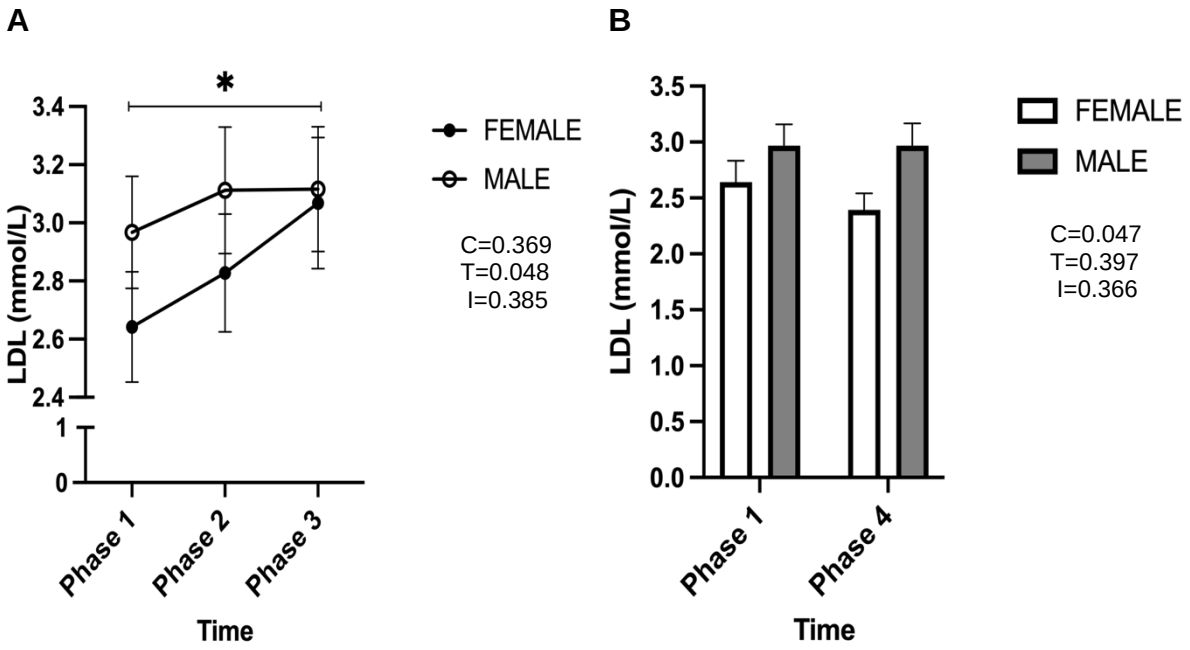

Figure 4.4.8. Low-density lipoprotein concentration (mmol/L). Three phases comparison; Phase1 (pre-Ramadan), Phase2 (one week after commencing Ramadan fasting) and Phase3 (3.5 weeks after commencing Ramadan fasting), shows the effect of Ramadan fasting (A). Two phases comparison; Phase1 (pre-Ramadan) and Phase4 (one month after the end of Ramadan fasting) to elicit if the significant effect of Ramadan fasting persists one month later (B). Data are presented as means with error bars representing standard error (SEM) (n=18 females, n=19 males). Statistical analysis was performed with mixed effect model (sex *X* time) and time (T), condition (C) (i.e., sex) and interaction (I) effects are displayed above on each graph. (*) represents the significant difference between time points (main effect), one symbol (P<0.05).

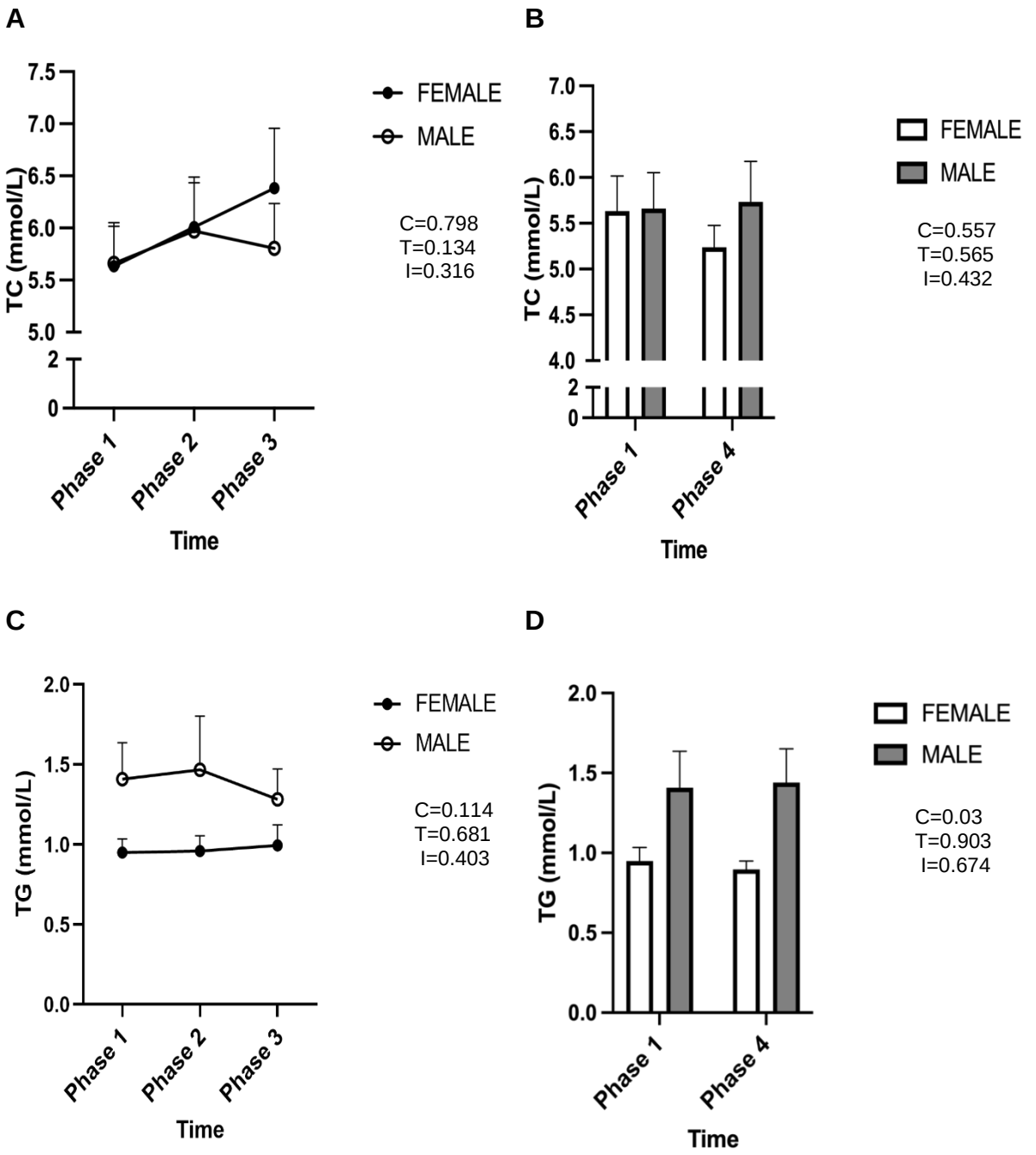

Figure 4.4.9. Total blood cholesterol (A), Total Triglycerides (B) concentrations changes. Three phases comparison; Phase1 (pre-Ramadan), Phase2 (one week after commencing Ramadan fasting) and Phase3 (3.5 weeks after commencing Ramadan fasting), shows the effect of Ramadan fasting. Two phases comparison; Phase1 (pre-Ramadan) and Phase4 (one month after the end of Ramadan fasting) to elicit if the significant effect of Ramadan fasting persists one month later (C), (D). Data are presented as means with error bars representing standard error (SEM) (n=18 females, n=19 males). Statistical analysis was performed with mixed effect model (sex *X* time) and time (T), condition (C) (i.e., sex) and interaction (I) effects are displayed above on each graph.

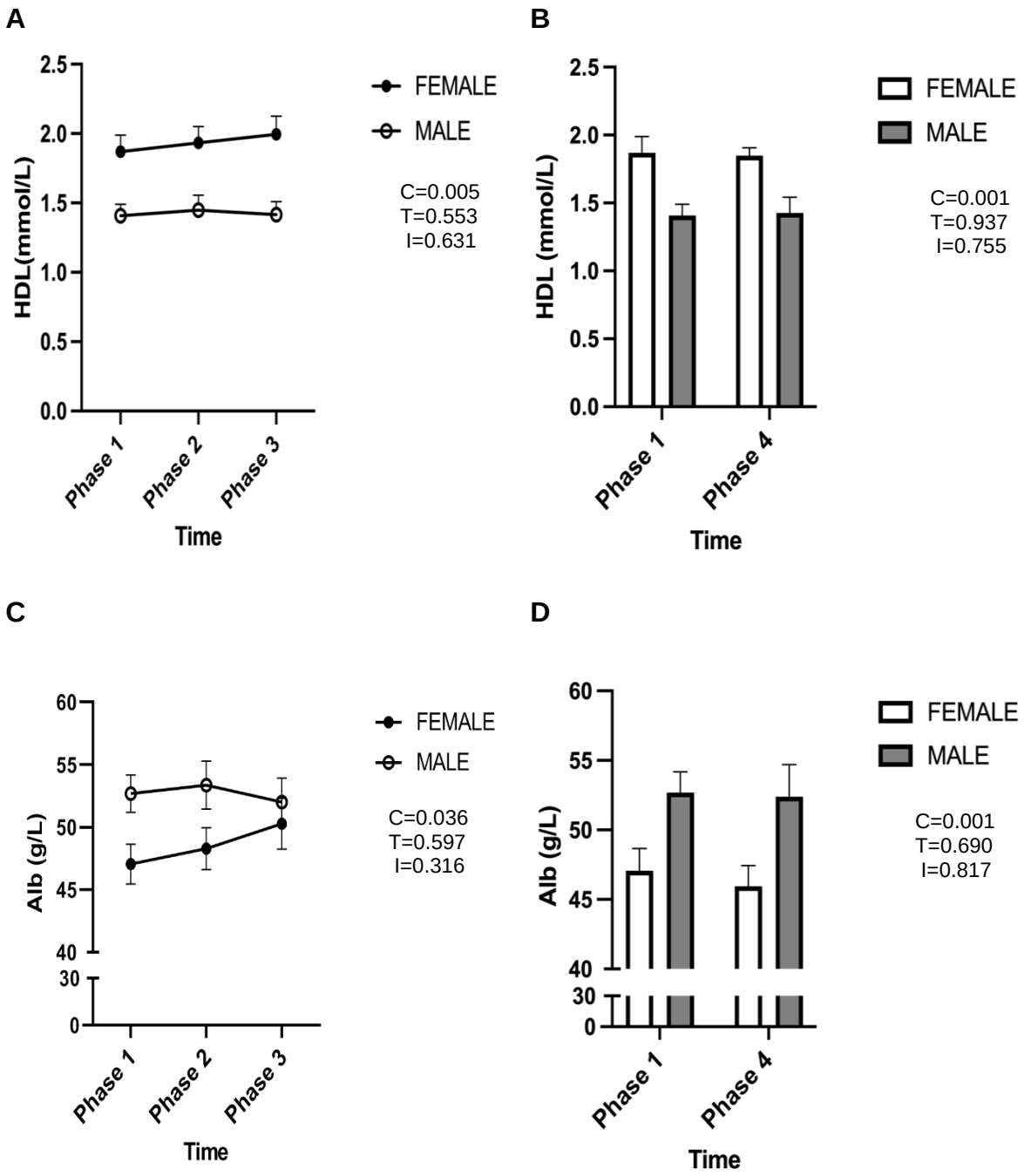

Figure 4.4.10. High density lipoprotein (A), and Albumin (B) concentrations changes. Three phases comparison; Phase 1 (pre-Ramadan), Phase 2 (one week after commencing Ramadan fasting) and Phase 3 (3.5 weeks after commencing Ramadan fasting), shows the effect of Ramadan fasting. Two phases comparison; Phase 1 (pre-Ramadan) and Phase 4 (one month after the end of Ramadan fasting) to elicit if the significant effect of Ramadan fasting persists one month later (C), (D). Data are presented as means with error bars representing standard error (SEM)(n=18 females, n=19 males). Statistical analysis was performed with mixed effect model (sex *X* time) and time (T), condition (C) (i.e., sex) and interaction (I) effects are displayed above on each graph.

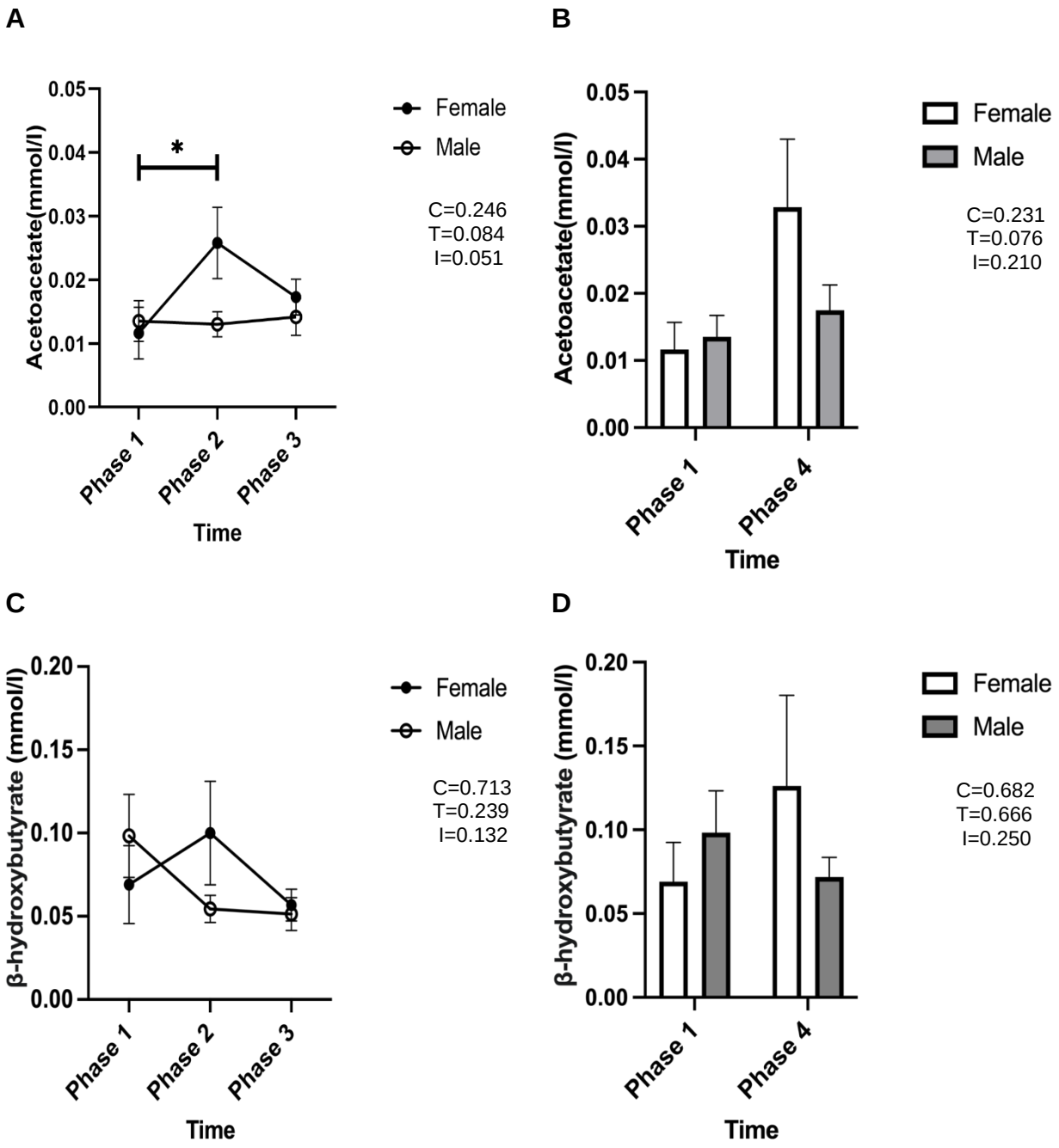

Figure 4.4.11. Acetoacetate (A &B), and β-hydroxybutyrate (C&D) concentrations change. Three phases of comparison; Phase1 (pre-Ramadan), Phase2 (one week after commencing Ramadan fasting) and Phase3 (3.5 weeks after commencing Ramadan fasting), show the effect of Ramadan fasting. Two phases of comparison; Phase1 (pre-Ramadan) and Phase4 (one month after the end of Ramadan fasting) to elicit if the significant effect of Ramadan fasting persists one month later (C), (D). Data are presented as means with error bars representing standard error (SEM) (n=8 females, n=8 males). Statistical analysis was performed with mixed effect models (sex *X* time) and time (T), condition (C) (i.e., sex) and interaction (I) effects are displayed above on each graph.

4.4.9 Habitual dietary analysis

In both groups, there were no significant differences in energy intake during Ramadan fasting compared to the non-fasting period (after Phase 4) (*P*=0.2, interaction; *P*=0.9). However, there was a significant difference in protein intake (*P*=0.01, interaction *P*=0.2), which was significantly lower during Ramadan, especially in males, post hoc (*P*<0.02). No differences in carbohydrate (*P*=0.9, interaction; *P*=0.2) or fat intake (*P*=0.3, interaction; *P*=0.5) were found **(Table 4.4.9)** (**Figure 4.4.12**).

Table 4.4.9. Comparisons of energy intake and macronutrient consumption during Ramadan and one month after the end of Ramadan.

Sex	**Female**		**Male**	
Diary intake	**Non-Fasting**	**Fasting**	**Non-Fasting**	**Fasting**
Energy (Kcal/d)	1887±601	1698±978	2736±983	2490±589
Carbohydrate (g/d)	210±88 g	189±71 g	297±95 g	316±110 g
Carbohydrate (% total energy)	44±11 %	47±11 %	45±10 %	51±13 %
Fat (g/d)	80±29 g	77±69 g	116±54 g	95±40 g
Fat (% total energy)	39±9 %	39±11 %	38±8 %	34±11 %
Protein (g/d)	70±26 g	58±36 g	126±75 g	90±35* g
Protein (% total energy)	15±4 %	13±3 %	17±5 %	14±5 %
Values present mean±Stdv				

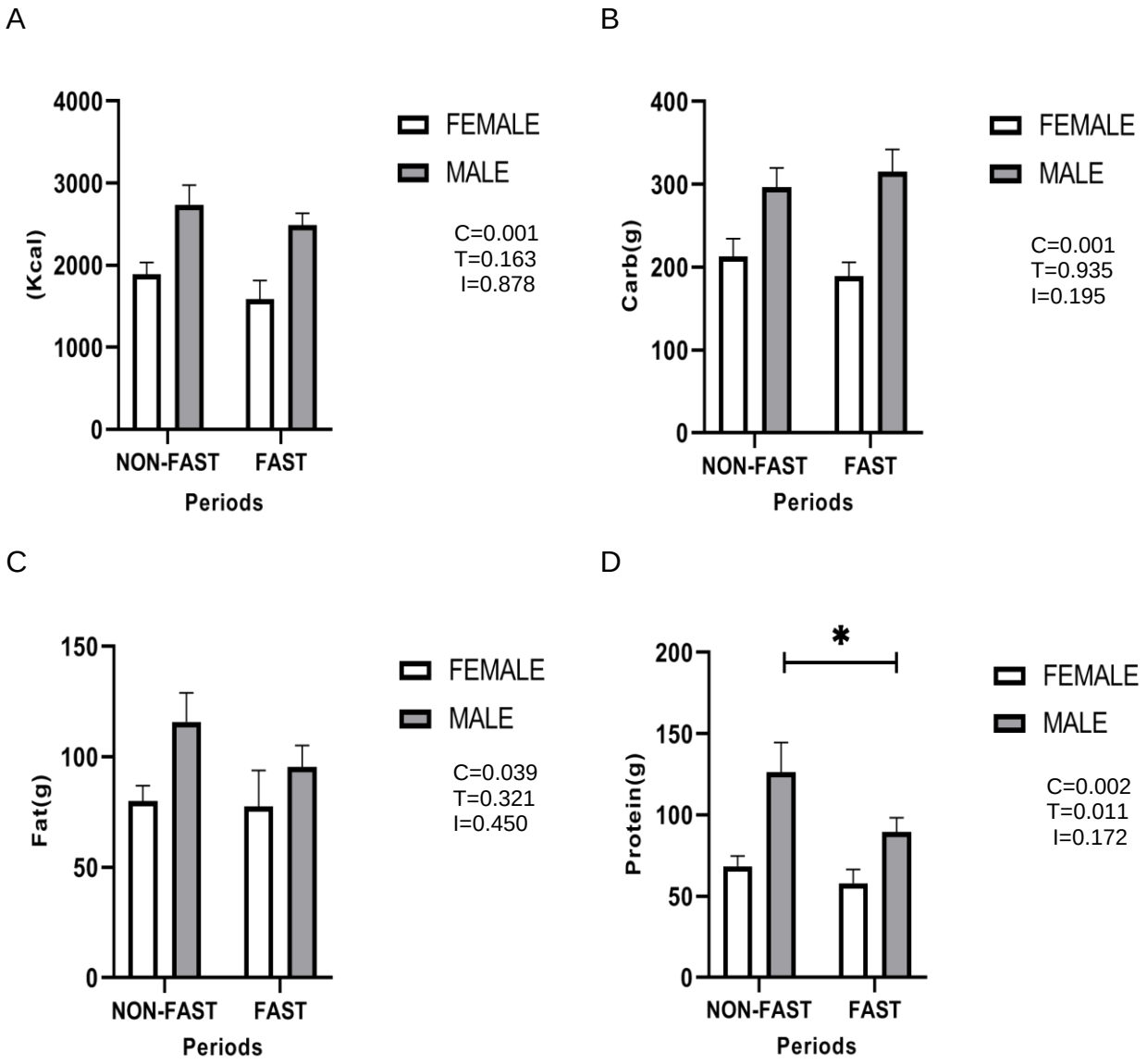

Figure 4.4.12. Comparisons of habitual energy consumption (kcals) and macronutrients intake (grams) between Ramadan fasting period (started after Phase 2) and non-fasting period (started after Phase 4). Energy consumption (A), carbohydrate intake (B), fat intake (C), and protein intake(D). Data are presented as mean with error bars representing the standard error of mean (SEM)(*n*=18 females, *n*=17 males). Statistical analysis was performed with two-way ANOVA. (*) represents the significant difference between time points (main effect), one symbol (*P*<0.05), based on Šídák's post hoc test.

4.4.10 Physical activity

There were no differences in metabolic equivalent of tasks between Ramadan fasting and non- Ramadan fasting periods in sedentary (*P*=0.3, interaction; *P*=0.6), light (*P*=0.4, interaction; *P*=0.2), moderate (*P*=0.1, interaction; *P*=0.7) or vigorous (*P*=0.2, interaction; *P*=0.8) activities (**Table 4.4.10)** (**Figure 4.4.13**).

Table 4.4.10. comparisons of the metabolic equivalent of tasks (MET) during and one month after the end of Ramadan.

Activities (MET.mins)	**Females**		**Males**	
	Fasting	**Non- Fasting**	**Fasting**	**Non-Fasting**
Total activity (MET.mins)	1003±186	1041±209	1110±247	1140±262
Light	146±54	139±49	110±41	136±86
Moderate	222±103	271±133	274±163	306±171
Vigorous	4±8	11±25	16±30	27±47
Sedentary	632±86	621±119	710±172	671±156

Mean±Stdv of 3-days mean, (n=36, females=18, males=18)

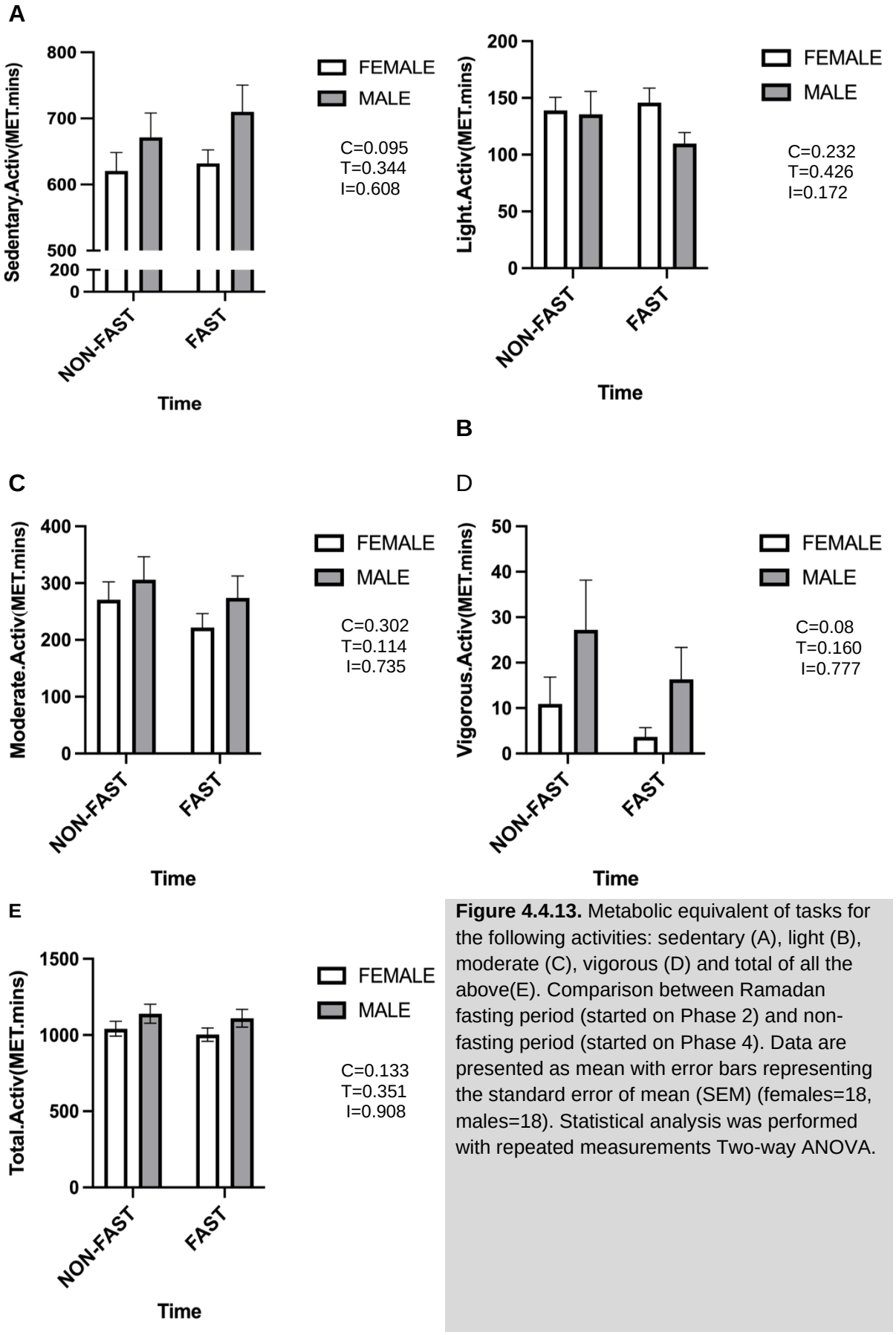

Figure 4.4.13. Metabolic equivalent of tasks for the following activities: sedentary (A), light (B), moderate (C), vigorous (D) and total of all the above(E). Comparison between Ramadan fasting period (started on Phase 2) and non-fasting period (started on Phase 4). Data are presented as mean with error bars representing the standard error of mean (SEM) (females=18, males=18). Statistical analysis was performed with repeated measurements Two-way ANOVA.

4.5 Discussion

The current study aimed to examine the effect of Ramadan fasting on metabolic health markers, including: BMI, thigh muscle volume, FBG, FBI, HOMA-IR, abdominal visceral and subcutaneous fat deposits (AVF and ASF) and blood lipids in males and females. This study also aimed to investigate any changes in habitual physical activity, energy intake and macronutrient intake during Ramadan.

To the best of our knowledge, this is the first study that used MRI to measure the changes in muscle, AVF and ASF volumes after Ramadan fasting. During spring-summer the Ramadan fasting duration is approximately 18 hrs/day in the UK, where data was collected, which is longer than most middle east and south Asia countries with a larger Muslim population. We detected some metabolic changes due to Ramadan fasting, including a significant reduction in BMI, and muscle volume, a trend of ASF reduction in both sexes, and a significant AVF reduction in males. Moreover, FBG was significantly elevated at the end of Ramadan with no differences in FBI or HOMA-IR. For lipid profile, only LDL significantly increased at the end of Ramadan. Acetoacetate significantly increased after one week of fasting in the female group, then decreased at the end of Ramadan**.** Acetoacetate also recorded a trend of elevation a month after the end of Ramadan in both sexes. Habitual energy intake and physical activity were the same during Ramadan and non-Ramadan periods, except for a significant reduction in protein intake in the male group during Ramadan.

The novelty of this study was the detection of various changes in response to TRE or Ramadan fasting both initially and after a prolonged period. This initial response after one week of RF represents a significant reduction in BMI with a percentage reduction of [-1.0%,-1.33%] and thigh muscle volume [-1.14%,0.30%] in females and males respectively, which continued to decline until the end of fasting with a BMI reduction [-

2.4%,-2.6%] and muscle volume reduction [-3.3%,-3.0%] in females and males respectively. These results are consistent with many observations from Ramadan fasting studies of 14 up to 17 hrs that detected a reduction in weight and BMI (**Chapter 1, Table 1.9)**. Previous studies have reported weight loss only at the end of Ramadan, stating that the reduction came from decreased muscle and fat mass (Nachvak et al. 2018; Norouzy et al. 2013). There was a small but not significant reduction in total energy intake during Ramadan, which may contribute to the decrease in body weight. Also, reduced protein consumption, which was reduced in both sexes and was significant in the male group, may explain muscle volume reduction at the end of Ramadan. However, we reported that the male group consumed a mean of 126g of protein in the non-fasting period and 90g in the fasting period. The current guideline for protein consumption is between 0.75-0.8 g/kg of body weight daily (EFSA 2017). It should be noted that there is a recommendation for increased protein consumption up to 1.6-2.4g/kg to maintain muscle mass during weight loss strategies including IF, as a small eating window can negatively affect daily muscle protein synthesis (McCarthy and Berg 2021; Lowe et al. 2020; Aragon and Schoenfeld 2022). Our results were consistent with a delayed TRE 16 hours fasting which reported a significant lean mass reduction in the TRE group compared to the control group. No dietary analysis was done on this study, but the authors speculate that TRE leads to a decrease in calorie and protein intake(Lowe et al. 2020). Self-reporting dietary intake is challenging. Participants might not report their actual intake properly and this might be the reason for non-significant changes of total energy intake, except for the protein intake in the male group. Perhaps more significantly, 3 days of food dietary reporting does not fully reflect the exact amount of food intake (McAllister et al. 2020).

In the current study, AVF was reduced significantly in the male group and non-significantly in the female group at the end of RF compared to baseline. Also, ASF decreased but not significantly in both sexes. These detected reductions in adipose fat tissues are signs which may explain the lipolysis process. Two Ramadan studies with a fasting time of about 12hrs/day reported a significant reduction in body weight and/or BMI, but no information about changes in body composition (Adlouni et al. 1997; Fakhrzadeh et al. 2003). However, other studies with 12hr/day fasting period reported no significant changes in body weight, BMI, or body composition (Ongsara et al. 2017; Mindikoglu et al. 2020). Despite the normal BMI, increasing AVF is associated with cardiometabolic risks and IR (Thomas et al. 1998; 2012) and AVF is beneficially reduced in our sample in male group. No study reported an increase in body weight following Ramadan **(Chapter 1,Table 1.9)**.

In the current study, FBG increased at the end of Ramadan, especially in the male group (*P*=.02), with no changes in FBI or HOMA-IR. This result contrasts with most Ramadan studies where FBG significantly decreased or showed no significant changes **(Chapter 1, Table 1.9)**. However, two studies reported increased FBG: Carlson *et al.* (2007) with dTRE 20hrs/day over two months in a healthy cohort, and Sadiya *et al.* (2011), a Ramadan study that included participants with metabolic syndrome. However, there were no significant changes in FBI and HOMA-IR (Sadiya et al. 2011; Carlson et al. 2007). RF study of 17hr/day conducted by Nachvak *et al*. (2018) showed increased FBI and HOMA-IR but decreased FBG. However, there was a large age range in this study, from 21-63 years, which has not been accounted for in the analysis as people above the age of 40-50 years may have unknown insulin resistance and manifest sarcopenia (Merz and Thurmond 2020). Also, Nachvak *et al*. (2018) referred these increased in FBI and HOMA-IR and decreased FBG in Ramadan

to the circadian pattern of insulin secretion as they collected blood samples at 6-8 pm in Ramadan and at 8-9 am pre-Ramadan (Nachvak et al. 2018). Insulin secretion changed during the 24-hour circadian rhythm. Blood insulin concentration decreases during the evening and at midnight, then increases after 6 am until early afternoon (Boden et al. 1996). Another reason for the elevation in FBI in Ramadan is the fact that people consume a large meal at midnight and insulin secretion increases in response to food intake. Finally, during Ramadan, carbohydrate consumption was significantly increased, and protein, fat and total energy intake were significantly decreased (Nachvak et al. 2018).

There are several possible explanations for the elevated FBG at the end of Ramadan in our study. One potential explanation may be the significant decline in muscle volume. One study highlighted an association between elevated glucose and/or insulin concentrations and lower muscle mass (Kalyani et al. 2012). Also, Dirks *et al.* (2016) induced muscle atrophy after one week of bed rest, resulting in a significant decline in glucose disposal and a significant increase in insulin resistance. In addition, this study also demonstrated a trend toward significantly elevated blood glucose on day 7 of inactivity (Dirks et al. 2016). Moreover, disruption to the circadian clock during RF, as food intake is only allowed in the evening until midnight, could cause the elevation in FBG. *Aragon et al.* (2022) review have compared early TRE with delayed TRE studies and concluded that delayed TRE causes an adverse disturbance to the circadian clock and the development of IR (Aragon and Schoenfeld 2022).

Body dehydration could also cause elevated blood glucose concentrations (Roussel et al. 2011). However, increased plasma albumin is a sign of dehydration (Sirotkin, Korolev, and Silakova 2007) and there was no significant changes in plasma albumin in the present study.

Our findings were consistent with Carlson *et al.* (2007) and Stote *et al.* (2007), who published two articles from one dTRE study examined eight weeks of TRE with 20 hrs/day of fasting (with a 4-hour window to consume all the energy required to maintain body weight, equivalent to one large meal per day). The study design was a randomised cross-over study with an 11-week interval between TRE (1-meal) and normal (3-meal) diets. In the TRE stage, participants fasted from food, but calorie-free drinks were allowed. Total body water measured by BIA was higher in the TRE stage, which is expected as calorie-free fluids were consumed all day. Despite that, researchers intended to maintain body weight by keeping the same amount of energy, macronutrients and physical activity in each stage of this study. They reported a significant reduction in body weight, increased FBG level, and impaired oral glucose tolerance with no significant changes in HOMA-IR and plasma insulin after TRE intervention (Carlson et al. 2007). There was a significant reduction of fat mass with no changes in fat-free mass (muscle) and a significant elevation of total cholesterol LDL and HDL (Stote et al. 2007). The authors proposed different explanations for the increased blood glucose level under this fasting condition; firstly, the consumption of a large meal in the late evening caused glucose absorption to be continued until morning or consuming one high-energy meal at once could affect insulin sensitivity (Stote et al. 2007; Carlson et al. 2007). In Ramadan, Muslims consume a large meal in the late evening. However, in our study, the FBG level was not changed after the first week of fasting. Both FBG increased, and muscle volume decreased significantly at the end of Ramadan. In humans, blood glucose concentrations are reduced after 12 to 24hrs of fasting (Longo and Mattson 2014). However, in the current experiment, fasting blood was taken 8-12 hours after the last meal, and the absorption of the late

midnight meal may be still occurring (Carlson et al. 2007), which could be one explanation for the recorded high FBG.

In the present study, the observed metabolic changes may have occurred due to the prolonged fasting period that reached semi-starvation at the end of Ramadan (Nachvak et al. 2018)**.** The human body adapts to starvation by activating a gluconeogenesis process. Excessive hepatic glycogenolysis (breakdown of stored glycogen into glucose) due to prolonged fasting or starvation leads to the depletion of glycogen stores in the liver, then hepatic gluconeogenesis is initiated to produce endogenous glucose from amino acids, lactate and glycerol (Rigby and Schwarz 2001). Fasting also promotes lipolysis in adipose tissue to produce FFAs which are converted into ketone bodies in the liver (Rui 2014). This process could explain the reduction in AVF and ASF volumes at the end of RF, leading to the increased net flux of free fatty acids (Stote et al. 2007). There was a significant increase in LDL in our study, which is a risk factor for cardiovascular disease. Two Ramadan studies (N. Khan et al. 2017; Nachvak et al. 2018) and four TRE studies (Stote et al. 2007; McAllister et al. 2020; Martens et al. 2020; Jamshed et al. 2019) reported elevated LDL **(Chapter 1, Table 1.9, Table 1.10** and they linked this to different causes; some subjects may omit the late meal (suhur) before fasting, which enhances lipolysis. During fasting, lipolysis increases the level of fatty acids in the body. This increase in FFA can affect circulating lipid levels, including LDL. Studies have shown that a 24-hour fast consisting only of water causes an acute increase in total serum cholesterol by raising both LDL and HDL (Keirns et al. 2021). The other reasons may be consuming unhealthy fat SFA (saturated fatty acid) during Ramadan, (Adlouni et al. 1997; Nachvak et al. 2018; Stote et al. 2007), or there was increased reliance on fat oxidation (Jamshed et al. 2019). In the current study, there was a significant elevation

in plasma acetoacetate in Ramadan in the female group (*P*=0.048), indicating the ketogenesis mechanisms. Thus, it is suggested that a shifting of fuel utilisation from glucose to fat and ketone bodies occurs in response to long days of fasting or starvation (Longo and Mattson 2014).

In a healthy human, starvation causes a significant decline in insulin sensitivity and glucose uptake by the muscle (Tsintzas et al. 2006). According to two reviews focused on TRE and the effects of Ramadan on many metabolic factors, including FBG, BMI, and lipid profile, the results were heterogeneous (Kul et al. 2014; Rothschild et al. 2014). The discrepancy in the results may be due to many confounding factors: fasting duration per day, numbers of days fasting, ethnicity, age, sex, climate, geographic location, personal diet, lifestyle and more importantly the circadian clock effect (Ongsara et al. 2017; Soliman 2022; Regmi and Heilbronn 2020; Nachvak et al. 2018).

In the present study, one month after the end of Ramadan was set as a follow-up period. A comparison between pre-Ramadan and one month after Ramadan ends reveals that all biological markers returned to pre-Ramadan status after a month of normal habitual energy intake. However, BMI and muscle volume were not fully recovered with a trend of lowered BMI and muscle volume in both sexes (*P*=0.06, interaction; *P*=0.1 and *P*=0.08, interaction; *P*=0.9 respectively). There was also a trend toward elevated plasma acetoacetate one month post Ramadan (*P*=0.075, interaction; *P*=0.2), which could be a residual sign of gluconeogenesis and ketogenesis (Longo and Mattson 2014).

It is suggested that the Ramadan month with fasting of more than 16 hrs/day may alter fuel utility from glucose to fat and protein, resulting in an increase in endogenous glucose production (gluconeogenesis) in the human body and net fatty acid flux

(lipolysis). Ramadan fasting could induce beneficial metabolic changes, i.e., decreased BMI and fat in some fat deposits (AVF and ASF). However, an unfavourable elevation of FBG level and reduction in muscle volume were recorded. During fasting, insulin secretion decreases, and glucagon is released. This adaptive response to energy homeostasis increases lipolysis and glycogenolysis, causing a reduction in muscle protein synthesis and lipogenesis (Nachvak et al. 2018). The Ramadan month of fasting is well tolerated by healthy people, even on long days (e.g., in the UK during the spring/summer, as in the present study), as the increases in FBG and LDL recovered one month after Ramadan. Awareness of a healthy balanced diet is recommended, as it is recognised that protein intake was reduced during Ramadan. Also, those taking part in Ramadan could consider resistance exercise and higher protein intake during and after Ramadan to compensate for lost muscle volume. The female group did not fast for the whole month, as they stopped fasting in the range of (0-10 days). However, the metabolic changes appeared quite similar in both sexes, except that, males showed a significant reduction in visceral fat volume compared to females.

Limitations

Data collection was completed over two separate years, 2019 and 2021, with a one-year gap, due to the consequences of the COVID-19 pandemic. MR images were from different scanners and sequences each year, with geometric differences between sequences and the area covered and number of slices were different which may cause slight differences in sensitivity of detecting volume changes. Most participants had no experience in completing nutritional diaries. There were some missing hours on

activity watches; on some occasions, subjects removed the watch for taking a shower or prayer ablution and forgot to wear it for some hours, so missing hours were accounted as sedentary hours. Fasting insulin and lipids were analysed either from plasma or serum alternatively in 2019 and 2021, and we have used different analytical methods which may affect the results.

Chapter 5

The effect of Ramadan fasting on infiltrated muscle and liver fat, continuous glucose and body hydration

5.1 Introduction

Ramadan fasting (RF) is one common form of delay time-restricted eating (dTRE). It is considered an interesting model to study the biological changes when people abstain from eating and drinking for many hours per day (Antoni et al. 2017). In chapter 4, it was found that RF for 18 hours resulted in elevated fasting blood glucose (FBG) and LDL, and reduced BMI, muscle volume, and abdominal visceral and subcutaneous fats. These occurred in conjunction with reduced protein intake during RF. However, all these changes returned to baseline after a month of normal habitual dietary intake, although BMI and muscle volume were lower than baseline levels. Elevated FBG at the end of RF is not combined with increased FBI or HOMA-IR. The liver is the main organ regulating glucose and lipid metabolism. Liver insulin resistance is the key reason for fasting hyperglycaemia (Bock et al. 2007). During fasting, the blood insulin level decreases and the liver releases glucose (Santoleri and Titchenell 2019). FFAs released from adipose tissues are used as an energy source by lean tissues (e.g., liver and muscle). This may alter glucose homeostasis. An increase in fatty acid oxidation in the liver stimulates gluconeogenesis, and in the muscle increased IMCL level, which may reduce hepatic insulin sensitivity and impair glucose disposal in the muscle (Browning et al. 2012). The muscular system is responsible for over 80% of postprandial glucose uptake during insulin clamps (Merz and Thurmond 2020). Ectopic lipids refer to the accumulation of triglycerides and other lipids intermediates in non-adipose tissue, e.g., intrahepatocellular lipids (IHCL) in liver and intramyocellular lipids (IMCL) in muscle (Lettner and Roden 2008). Insulin resistance is positively correlated with increased ectopic lipids as a consequence of increase plasma lipid profile and lipid flux towards these targeted tissues, (Trouwborst et al. 2018). A study done by *Johnson et al. (2006)* compared short term (67hrs) water only

starvation to a very low carb/high fat and a control mixed diet found that insulin sensitivity was impaired and IMCL was significantly higher in starvation and low carb/high fat diets. These responses are due to increases in plasma free fatty acids (FFAs), endogenous from starvation due to lipolysis, and exogenous from a low carb/high fat diet (Johnson et al. 2006).

Several *in vitro* studies reported beneficial effects of TRE over *ad libitum,* such as maintaining body weight, reduced liver fat accumulation, improved glucose tolerance and normal insulin level despite a high fat diet (Hatori et al. 2012; de Cabo and Mattson 2019). However, to the best of our knowledge, few studies focus on the effect of RF on ectopic lipids. One recent RF study estimated liver fat fraction (FF%), using an MRI Dixon sequence, in subjects with no chronic health problems and found no significant change in FF% after 29 days of RF (Dündar and Yavuz 2021). No previous research has studied the effect of RF or TRE on ectopic muscle lipids. Interestingly, IMCL increased due to starvation and during high-fat diet conditions, which indicates the complexity of interpreting IMCL results (Johnson et al. 2006). This can be demonstrated in a study that compared three diet regimes; normal carbohydrate mixed diet, 67 hrs starvation (water only allowed), and a very low-carbohydrate / high-fat diet. It was found that the latter two interventions both resulted in decreased insulin sensitivity and increased IMCL. Although starvation and a high-fat diet are completely different dietary models, they lead to a similar result of increased circulated free fatty acid (FFA).

The IDEAL-DIXON and MRS quantification of ectopic lipids deposition have been applied in clinical and pre-clinical research fields for liver and skeletal muscle and also in other organs such as the heart and pancreas (Reeder et al. 2005; Grimm et al.

2018; Bray et al. 2018). These two MRI quantification methods can be used repeatedly as they are safe and can be rapidly processed. However, this study focused on the muscle and liver as they are the main sites for glucose and liver homeostasis (Tamura et al. 2005).

RF represents a dramatic shift in meal timing and content that could alter glycaemic markers (Lessan et al. 2015). Continuous glucose monitoring (CGM) is a beneficial tool for assessing real-time glycaemic status changes. A study done by *Lessan et al. (2015)* had three groups; one with type 1 diabetes mellitus (T1DM) (*n*=6, 23.3±7 years), one with type 2 diabetes mellitus (T2DM) (*n*= 50, 47.3±10.6years) and control with healthy subjects (*n*=7, 36.2±13.4 years) that underwent fasting during Ramadan. CGM was used to monitor the hypo and hyper glycaemic events and mean interstitial glucose (IG) level. In all groups, there were a rapid increase in IG after iftar (breaking of the fast at sunset) with no significant change in mean IG (Lessan et al. 2015). Time in range (TIR) is the total time spent within the normal glucose range (3.9-10 mmol/L) during 24h and is a predictor of vascular disease and neuropathies in T2DM. A study on 85 T2DM patients investigated the effect of body compositions measured by BIA on time in range (TIR). Reported that, during 3 days of continuous insulin infusion therapy, body fat percentage was negatively and strongly related to TIR. They concluded that high body fat affects glycaemic control unfavourably and decreasing body fat improves glycaemic control. They also mention that not using MRI to estimate body composition was one of the study limits (Y. Ruan et al. 2021). Non-diabetic hyperglycaemia is related to subclinical CVD (Echouffo-Tcheugui et al. 2019). Excessive ectopic lipids accumulation and body fat percentage affect glycaemic control and are a greater predictor of T2DM than BMI. Liver fat accumulation is a

strong predictor of IR and is associated with increased blood glucose as measured by CGM, especially during the nocturnal period (Bian et al. 2011).

5.2 Study aims

The aim is to study the effect of RF on ectopic lipids in liver, muscle and the muscle adjacent adipose fat deposits, which are thigh subcutaneous adipose tissue (SAT) and intramuscular adipose tissue (IMAT), using MRS and MRI techniques.

The second aim is to understand, in depth, the causes that may contribute to elevated fasting blood glucose (FBG) at the end of Ramadan fasting, which we recognised in our results, see **chapter 4, section 4.4.5.** Our hypothesis is that RF increases CGM readings due to hepatic insulin resistance as a consequence of lipolysis which reduces adipose tissues and increases IHCL and IMCL levels. Also, it is possible that body dehydration is occurring and affecting blood glucose concentrations.

5.3 Methods

5.3.1 Participants

Twenty-two healthy (11 females, 11 males) with age range 20- 35 years Muslims in the UK participated in this study. The participants were recruited in 2021 and they were part of the study described in Chapter 4. The inclusion-exclusion criteria explained in chapter 2, section 2. The enrolled participants intended to fast for the Ramadan month in the UK. One female was excluded because she could only fast for fifteen days due to hormonal imbalance and a long menstrual period. The non-fasting days for the other females for the same reason were (7±2 days), in the range of 5-10 days. Only two men broke fast due to travelling, one for one day and another for six separated days. Participant characteristics are shown in **Table 5.3.1**. The study was done during Ramadan 2021 and was approved by the Sport and Health Sciences ethics committee, University of Exeter (Ref No: 200325/A/04). The Ramadan month in 2021 was 30 days, starting on April 13 and ending on May 12 with the fasting hours were between 17-18 hours.

Table 5.3.1. Participant Characteristics.

Sex	**Females (*n*=10)**	**Males (*n*=11)**
Age(y)	30±4	29±5
Body mass (**Kg)**	63.2±14.7	80.1±18.4
Height (cm)	159.6±7.0	172±6.4
BMI (kg.m^{-2})	24.6±4.6	27±5.8

Values are represented as mean±Stdv, total sample number (n=21, females n=10, males n=11). BMI = body mass index

5.3.2 Experimental Protocol

Participants attended the Mireille Gilling's Neuroimaging Centre, University of Exeter, four times and the Nutritional Physiology Research Unit (NPRU), St. Luke's Campus, University of Exeter, at least two times. The study was designed into four main phases, and each phase took 45 minutes: Phase1 (Pre-Ramadan), Phase2 (one week after commencing Fasting), Phase 3 (3.5 weeks after commencing Fasting) and Phase 4 (one month after end of Fasting). Two short visits (10 mins) to the NPRU were completed in order to insert or remove a Dexcom continuous glucose monitoring device (CGM). Each non-fasting phase (1 and 4) was completed within four days, and the schedule started at 8:15 am until 12:00 pm. Each Ramadan phase (2 and 3) was completed within two days to allow just one-day fasting variation. The schedule started at 9:30 am until 5:15 pm to set a period of 8-12 h for blood fasting samples. Muslims eat an overnight meal (suhur) around (1-2 am) hence early morning testing was not viable. An overview of the experimental protocol is presented in **Figure 5.3.2.**

Phases	Phase 1	Phase 2	Phase 3	Phase 4
Ramadan Fasting		O	O	
Height	O			
Weight	O	O	O	O
MRI	O	O	O	O
FBS	O	O	O	O
CGM			O	O

Figure 5.3.2. Illustration of the experimental protocol. The study involved four phases, and in all of them, body mass, MRI scan and FBG were taken for the participants. Height was only taken in the first phase, and CGM devices were placed on the participants' upper arms during the last two weeks of Ramadan and one month after the end of Ramadan. Subjects wore the devices for one week in each period. FBS: fasting blood sample, CGM: continuous glucose monitor.

5.3.3 Image acquisition

After recording body mass, MRI scans of the abdomen and bilateral thighs were performed. A body 32 array coil for both anatomical regions was used, and axial images were obtained for mid-bilateral thighs and abdomen. An MRI 3 Tesla (Siemens scanner, MAGNETOM Prisma, Erlangen, Germany) was used in this study. Three MR sequences were used; firstly, 3 point-Dixon, 3D Proton density fat fraction Spoiled Gradient echo (3D-PDFF -SGE) for bilateral thighs imaging. For detailed parameters, see Chapter 2, section 2.8. Two measurements were taken from this sequence: 1. thigh muscle total fat volume, 2. IMAT PDFF%. Secondly, MR-Spectroscopy (^{1}H MRS) with Point RESolved single-voxel Spectroscopy (PRESS-SVS) (TE=30, TR= 3000, Acquisitions= 64, spectra position=-3.6 ppm) for measuring IMCL concentration. The voxel was carefully placed over the vastus medialis of the left thigh, avoiding vascular structures and contamination by gross adipose tissue or EMCL peaks (White et al. 2003; Chris Boesch 2007). as shown in **Figure 5.3.2**. Optimization of the B0 magnetic external was achieved via a shimming procedure until the full width half maximum (FWHM) of the spectral peak was below 30Hz. MRS was completed twice in each visit, one with and one without water signal suppression. From these sequences, a value for the IMCL: Water ratio was estimated with the unsuppressed water signal acting as an internal standard (Stannard et al. 2002), as the water concentration varies only slightly in muscular tissue (Chris Boesch et al. 2006).

The third sequence was a Siemens designed Liver lab package that included; 3 point-Dixon, proton density fat fraction (PDFF%), and HISTO (a voxel-based spectroscopic method, as shown in see **Figure 5.3.3**, (Imaging time <20s, breath-hold, Field of view (FOV)= 450mm, constant repetition time (TR)= 9ms, with 12 different echo times TEs =1/ 2/ 3/ 4/ 5/ 6/ 1.05/ 2.46/ 3.69/ 4,92/ 6.15/ 7.38. Flip angle= 4°, Slice thickness=

3.5mm, Slice spacing= 20% of slice thickness, Number of slices= 64, Number of averages= 1) for abdominal liver fat quantification.

5.3.4 Image Post Processing

Right thigh total fat volume was measured for each participant using 3D-slicer software, version 4.11. The muscle ROI PDFF%, which estimated IMAT automatically, was estimated by defining a region of interest (ROI) over the left thigh vastus medialis muscle for Dixon PD FF% analysis. Numerical values were gathered from the Siemens MRI workstation. This technique analyses the percentage fat signal contribution in each voxel with parametric maps of fat and water being subtracted, allowing to be obtained. PDFF% comprises a contribution from three fat pools IMAT, EMCL and IMCL (Grimm et al., 2018). The muscle MRS IMCL/ water ratio was determined from peak amplitude post-processed using the jMRUI.v5.2. Software package.

Two MR numerical data values from the Siemens Liver lab package were generated. One is called HISTO (voxel-based MRS) evaluation, and the other is ROI PDFF% (image-based), with these quantifications acquired automatically as part of the Siemens Liver Lab and taken directly from the Siemens workstation.

A

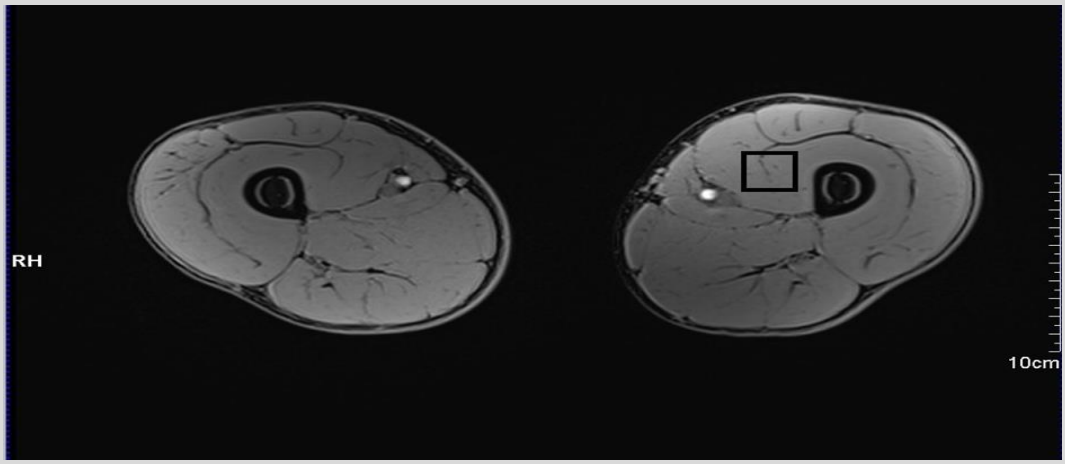

B

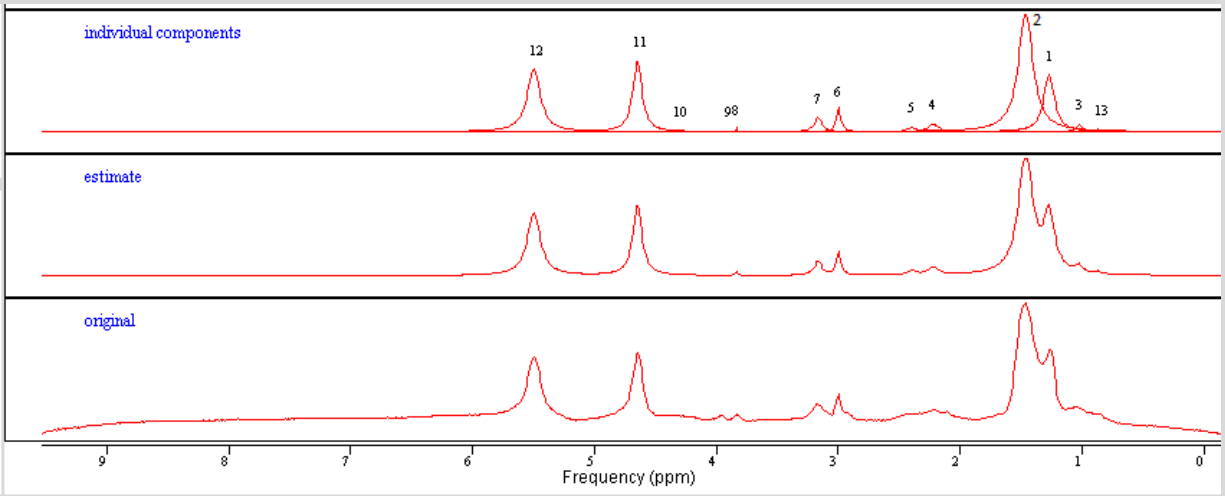

Figure 5.3.2. MRS single voxel positioning on m.vastus medialis, this region of interest was chose for MRS and Dixon FF% analysis (A). Quantification of (1) IMCL at 1.3 ppm, (2) EMCL at 1.5 ppm, and (11) water, although water signal was suppressed, there was a residual content of water at 4.7 ppm(B). A sample of 1H-MRS water unsaturated spectrum was markedly large compared to other spectra(C).

C

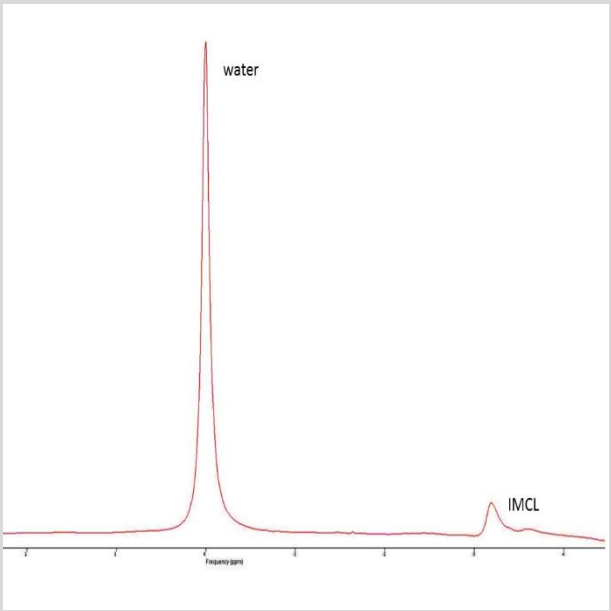

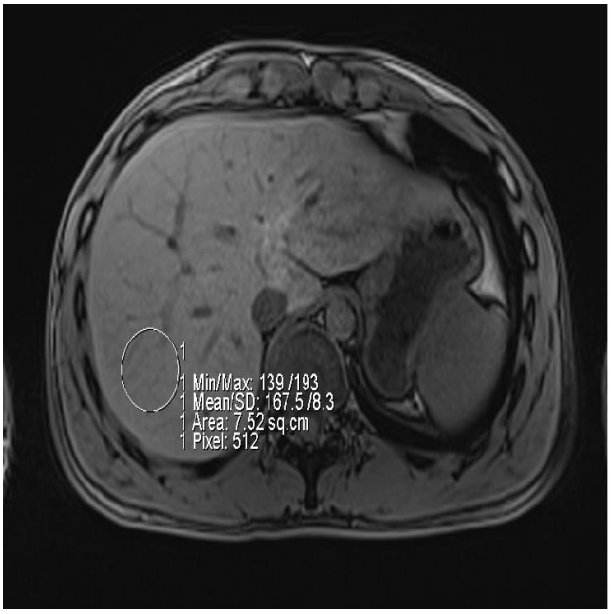

Figure 5.3.3. MRS-HISTO liver ROI for measuring IHCL. Area was carefully selected to avoid any large vessels.

5.3.5 Thigh muscle fat volume

Thigh fat volume was measured from right mid-thigh using the 3D-PDFF-SGE Dixon fat only image (FOI). The number of slices= 104. Thigh total fat volume was estimated from subcutaneous adipose tissue (SAT) and intramuscular adipose tissue (IMAT) **(Figure5.3.4)**.

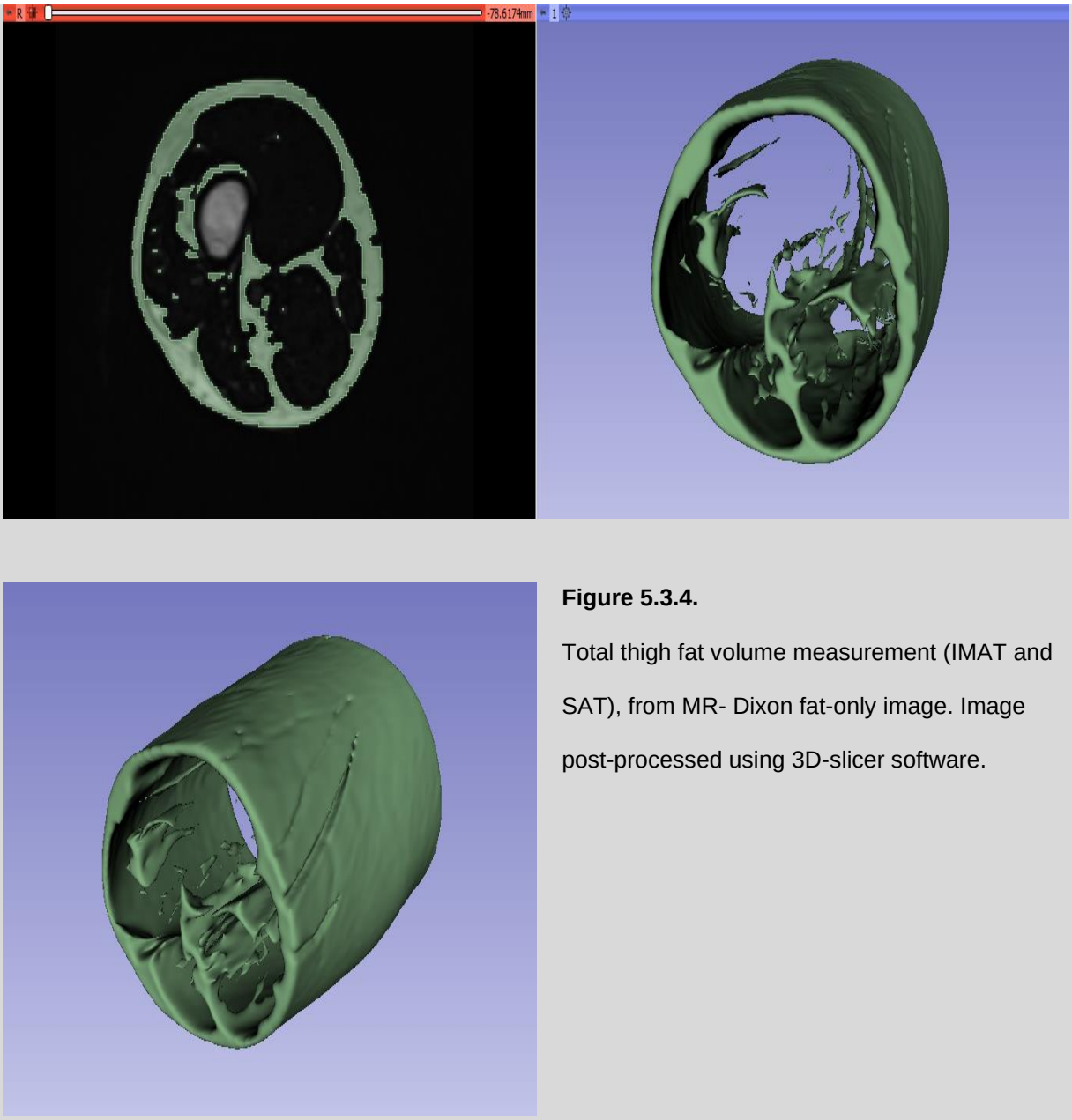

Figure 5.3.4.

Total thigh fat volume measurement (IMAT and SAT), from MR- Dixon fat-only image. Image post-processed using 3D-slicer software.

5.3.6 Body hydration

Two methods were used to assess body hydration during Ramadan and one month after the end of Ramadan. The first method estimated hydration from serum calcium concentration. The detailed blood sample collection and store methods are presented in section 2.6. Serum calcium concentrations were analysed automatically by (Roche/Hitachi Cobas c 701/702) system (Roche, Basel, Switzerland), using a Roche calcium Gen.2 kit (Roche Diagnostics GmbH, Mannheim, Germany). The Roche Calcium Gen.2 reagent was compared with those determined using the corresponding reagent on a Roche/Hitachi Cobas c 501analyzer (x). Dehydration can cause an increase in the calcium concentration in blood as calcium is a component of blood solutes (Parameswaran Rajeev 2022; Barley, Chapman, and Abbiss 2020) The second method estimated hydration from participants' records of water consumption. Participants were asked to measure and estimate the amount of water they consumed within two periods; during Ramadan fasting and one month after Ramadan ended. A digital kitchen scale was given to each participant with a recording diary to record in (ml) the consumed liquid for 3-days in each period. This method was validated against another method previously described.

5.3.7 Continuous glucose monitoring

Time in range (TIR) and mean continuous glucose level were estimated via Dexcom G6 a continuous glucose monitor (CGM) system (Dexcom G6, Inc., San Diego, CA, USA) for two study periods. The first one was during Ramadan fasting, and the second started one month after the end of Ramadan. There were only eleven transmitters so, during Ramadan, subjects were separated into two groups; the first group wore the CGM after two weeks (day 17-22) and the second group after three weeks (day 23-

30) of fasting. This process was repeated during the second period. Dexcom CGM contains a sensor placed on the participant's upper arm by an auto-applicator, then a small transmitter connected to the sensor. The transmitter was connected to the participant's mobile phone via Bluetooth, and the participants installed the Dexcom G6 app. 2 hrs after placing and connecting the transmitter to the mobile, interstitial fluid glucose concentration was recorded every 5-mins. The readings were stored in the Dexcom iCloud, and the operator could monitor the data and the analytical results from the Dexcom clarity healthcare professional's website account. CGM data were collected from eight males (two males did not have mobile phones compatible with the Dexcom G6 App, and one male could not attend the last visit) and ten females (one excluded from the study, see participant characteristics). Some signals were missed due to Bluetooth cut-off, so only the days with complete signals were included. The complete CGM readings from a minimum of one day and a maximum of three days were compiled into an individual average for each subject with an equal number of days in each period analysed for each subject. According to Dexcom CLARITY, **Table 5.3.7.** classifies the glucose concentration levels from an international consensus (Dexcom Clarity).

Table 5.3.7. An international consensus of interstitial fluid glucose concentration levels in (mmol/L).

Very high	>13.9
High	10.0 - 13.9
Normal	3.9 - 10.0
low	3.0 - 3.9
Very low	< 3.0

5.3.8 Statistical analyses

A Two-factor analysis of variance (2-way ANOVA) was used to analyse time X sex differences. A mixed-effects model was used instead of two-way ANOVA when some data were missing. One factor was matching/repeated measures (time), and another factor was not (sex). The analyses were performed twice: firstly, between Phases 1,2 and 3 to study the changes from baseline (pre-RF) to one week and 3.5 weeks of RF, then between Phases 1 and 4 to elicit any residual effects one month after the end of RF on the following: liver Dixon ROI PDFF%, liver HISTO-MRS FF%, muscle Dixon ROI PDFF%, muscle MRS, and serum calcium. Firstly, Phase1 (pre-Ramadan) compared to Phase 2 and 3 (after commencing one week and 3.5 weeks of Fasting), then Phase 1 (pre-Ramadan) compared to Phase 4 (one month after the end of Ramadan). CGM and hydration data were analysed once using 2-way ANOVA to compare participants hydration status during the Ramadan fasting period on week 2-3.5 and the non-fasting period started at Phase 4. Šídák's multiple comparisons test was used when time or interaction effects were significant in a Two-way ANOVA or mixed-effect tests. Pearson’s correlation test was used to assess if there was a correlation between the changes in FBG and IMCL or FBG and IHCL. All statistical analyses were conducted using GraphPad Prism 9.3.1 (GraphPad Software, San Diego, California, USA). $P<0.05$ was considered statistically significant, with all data in text and tables expressed as mean±Stdv and in figures expressed as mean±SEM.

5.4 Results

5.4.1 Body mass index

Body mass index (BMI) significantly decreased at the end of Ramadan month in both groups (*P*<0.001, interaction; *P*=0.4). There was no difference between pre-Ramadan BMI and one month after Ramadan ended (*P*=0.2, interaction; *P*=0.2) (**Figure 5.4.1**).

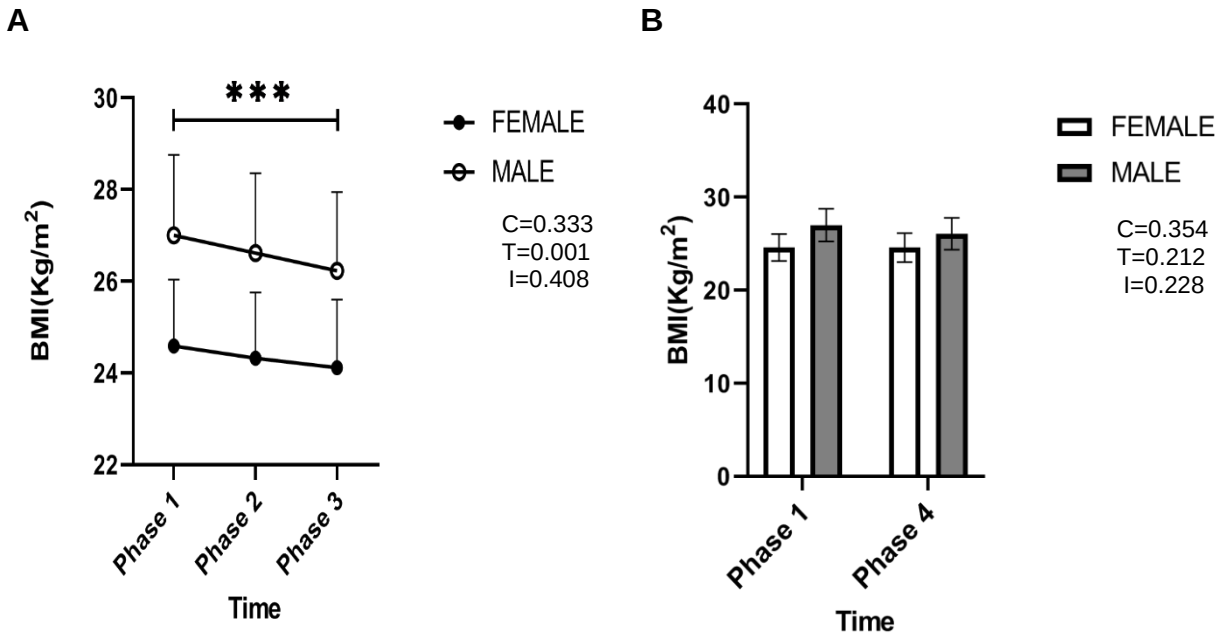

Figure 5.4.1. Comparisons of Body mass index (BMI). Phase1(Pre-Ramadan) compared to Phase2(one week after commencing Ramadan fasting) and Phase3 (3.5 weeks after commencing Ramadan fasting) to show Ramadan fasting effect (A). Phase1 (Pre-Ramadan) and Phase4 (one month after end of Ramadan fasting) (B) to explore if the impact of Ramadan fasting is continuous one month later. Data are presented as means with error bars representing standard error (SEM) (n=10 females, n=11 males). Statistical analysis was performed with Two-way ANOVA (A) and Mixed-effects model (B). (*) represent the significant difference between time points, three symbols (*P*<0.001).

5.4.2 Thigh muscle IMCL

IMCL/ Water ratio significantly increased during RF in both sexes (*P*<0.004, interaction; *P*=0.95) the increase was sharp after one week of Fasting, then plateaued after 3.5 weeks of fasting in both sexes. The IMCL level a month after the end of Ramadan was still higher than the pre-Ramadan fasting level in both sexes (*P*<0.03, interaction; *P*<0.2), and the high IMCL level was significant in males only (*post hoc* *P*=0.024), see (Figure 5.4.2).

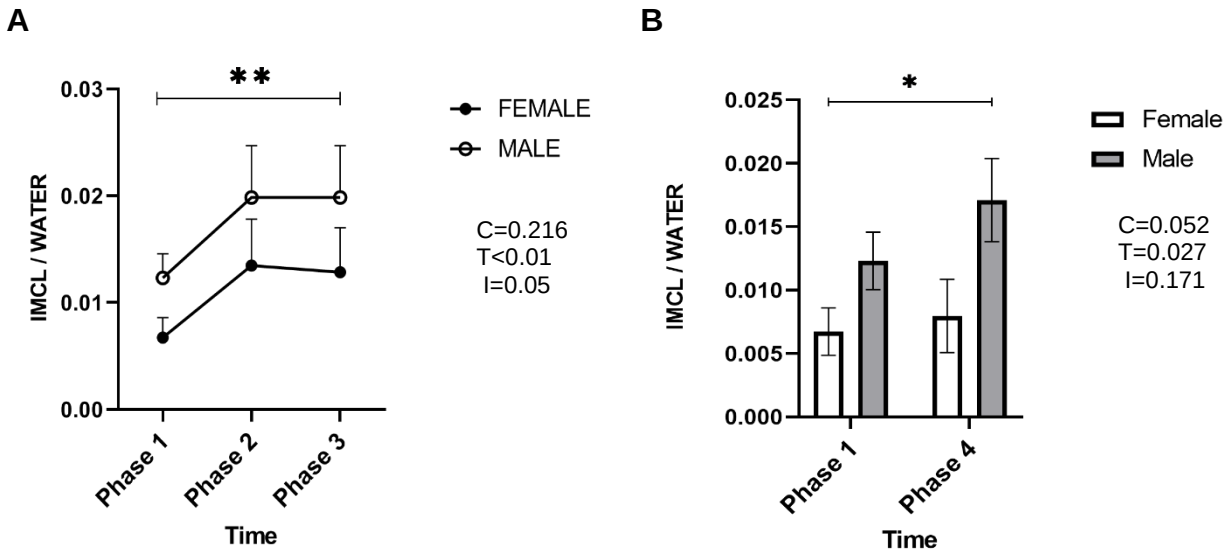

Figure 5.4.2. Comparisons of IMCL / Water ratio. Phase1 (pre-Ramadan) compared to Phase2 (one week after commencing Ramadan fasting) and Phase3 (3.5 weeks after commencing Ramadan fasting) shows the effect of Ramadan fasting (A). A comparison between Phase1 (pre-Ramadan) and Phase4 (one month after end of Ramadan fasting) to elicit if the significant impact of Ramadan month fasting persists one month later (B). Data are presented as means with error bars representing standard error (SEM) (n=10 females, n=11 males). Statistical analysis was performed with Two-way ANOVA (A) and Mixed-effects model (B). (*) represent the significant difference between time points, one symbol (*P*<0.05), two symbols *P*<0.01.

5.4.3 Thigh muscle Proton density fat fraction (PDFF%)

There was a significant change and interaction between sexes in PDFF% due to RF (*P*<0.05, interaction; *P*<0.01). In females PDFF% did not change significantly due to RF (*P*>0.05) when comparing pre-Ramadan phase with Ramadan phases (2 and 3) and when comparing Ramadan phases against each other. In contrast to males, PDFF% fluctuated as there was no significant decrease after one week of commencing fasting (phase 1 vs phase 2, mean difference -0.2%, *P*=0.6), and a significant increase when comparing phase 2 vs phase 3, mean difference= 2.4% (*P*<0.05). There is a trend toward increased PDFF% when comparing phase 1 vs phase 3, mean difference= 1.4% (*P*=0.07) **(Figure.5.4.3. A)**. No significant differences between phase 1 and phase 4 was found for either sex (*P*=0.1, interaction; *P*=0.5) **(Figure.5.4.3. B)**.

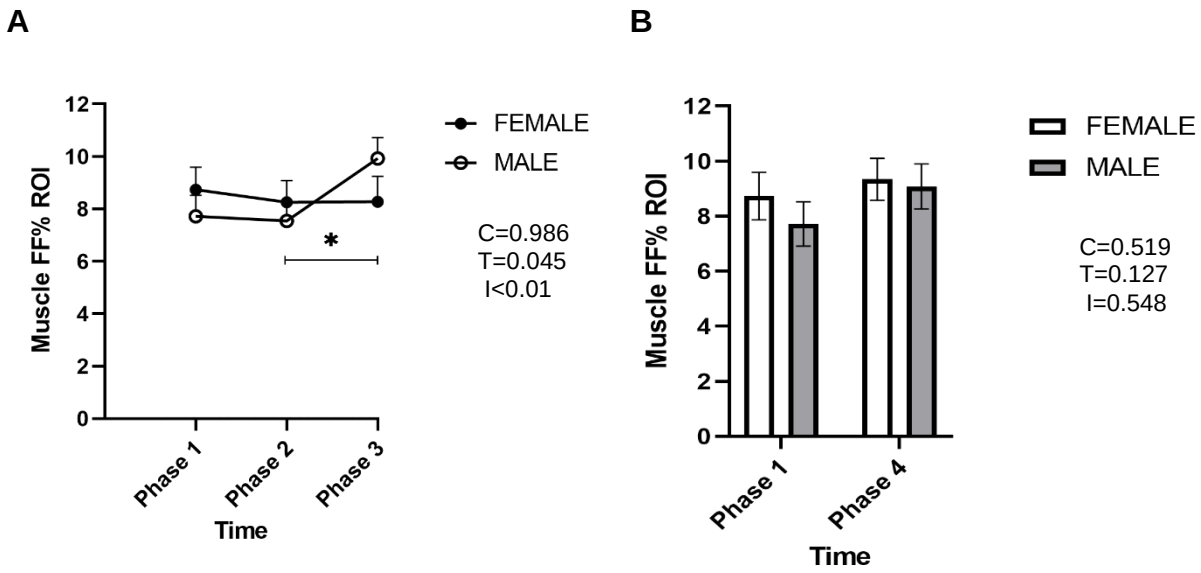

Figure 5.4.3. Phase1 (pre-Ramadan) compared to Phase2 (one week after commencing Ramadan fasting) and Phase3 (3.5 weeks after commencing Ramadan fasting) shows the effect of Ramadan fasting (A). A comparison between Phase1 (pre-Ramadan) and Phase4 (one month after end of Ramadan fasting) to elicit if the significant impact of Ramadan month fasting persists one month later (B). Data are presented as means with error bars representing standard error (SEM) (n=10 females, n=11 males). Statistical analysis was performed with Two-way ANOVA (A) and Mixed-effects model (B). (*) represent the significant difference between time points, one symbol (P<0.05).

5.4.4 Total thigh fat volume (SAT and IMAT)

No significant changes were detected after one week or 3.5 weeks in thigh total fat (IMAT and SAT) volume (*P*=0.3, interaction; *P*=0.7). Also, no differences between pre-Ramadan and one month after Ramadan ended were found (*P*=0.9, interaction; *P*=0.6) **(Figure 5.4.4).** Also, females tend to have higher thigh fat volume than males, but the results were not statistically not significant (P=0.76).

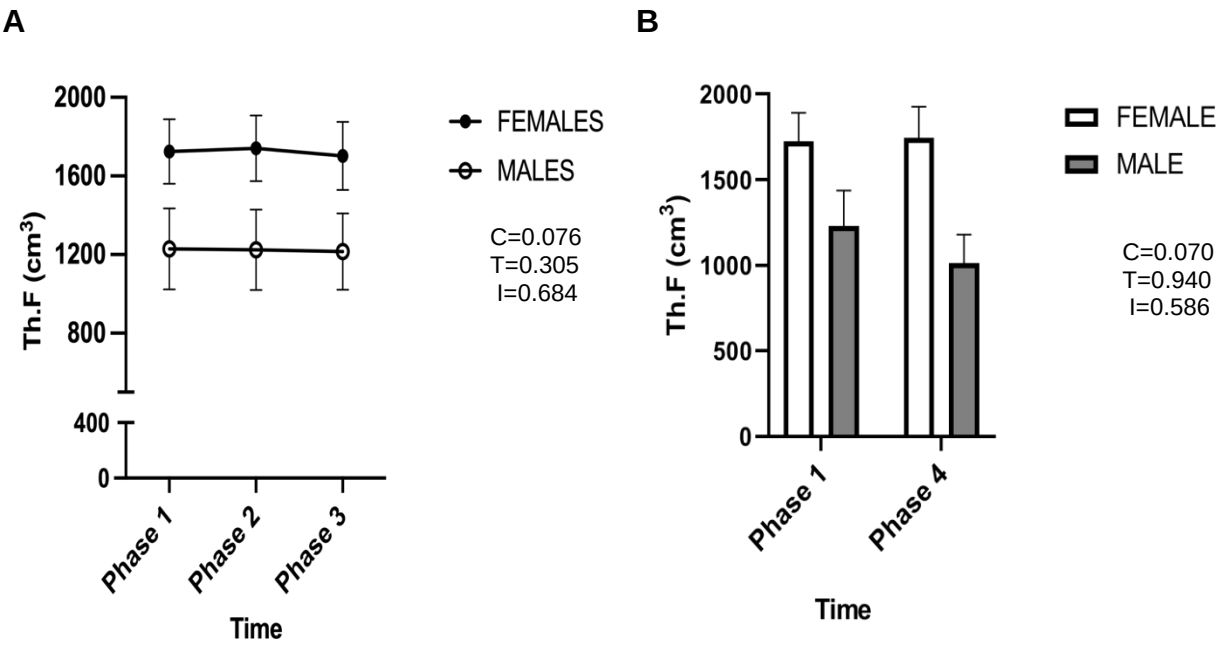

Figure 5.4.4. Comparisons of right thigh fat volume (Th. F). Phase 1 (pre-Ramadan) compared to Phase 2 (one week after commencing Ramadan fasting) and Phase 3 (3.5 weeks after commencing Ramadan fasting) shows the effect of Ramadan fasting (A). A comparison between Phase 1 (pre-Ramadan) and Phase 4 (one month after end of Ramadan fasting) to elicit if the significant impact of Ramadan month fasting persists one month later (B). MR Dixon-fat images of right thigh fat volume measured automatically via thresholding technique using 3D slicer software. Data are presented as means with error bars representing standard error (SEM) (n=10 females, n=11 males). Statistical analysis was performed with mixed effect models.

5.4.5 Liver fat deposition

There were no significant differences in liver fat over time in both sexes for Dixon% (*P*=0.4, interaction; *P*=0.8) or IHCL-MRS% (*P*=0.3, interaction; *P*=1.0) for the three phases comparison (pre-Ramadan, one week and 3.5 weeks after commencing Ramadan fasting). Likewise, no significant differences were found for Dixon PDFF

ROI% (*P*=0.2, interaction; *P*=1.0), HISTO-MRS% (*P*=0.8, interaction; *P*=0.9) for the two phases comparison (Pre-Ramadan and one month after the end of Ramadan) (**Figure 5.4.5**).

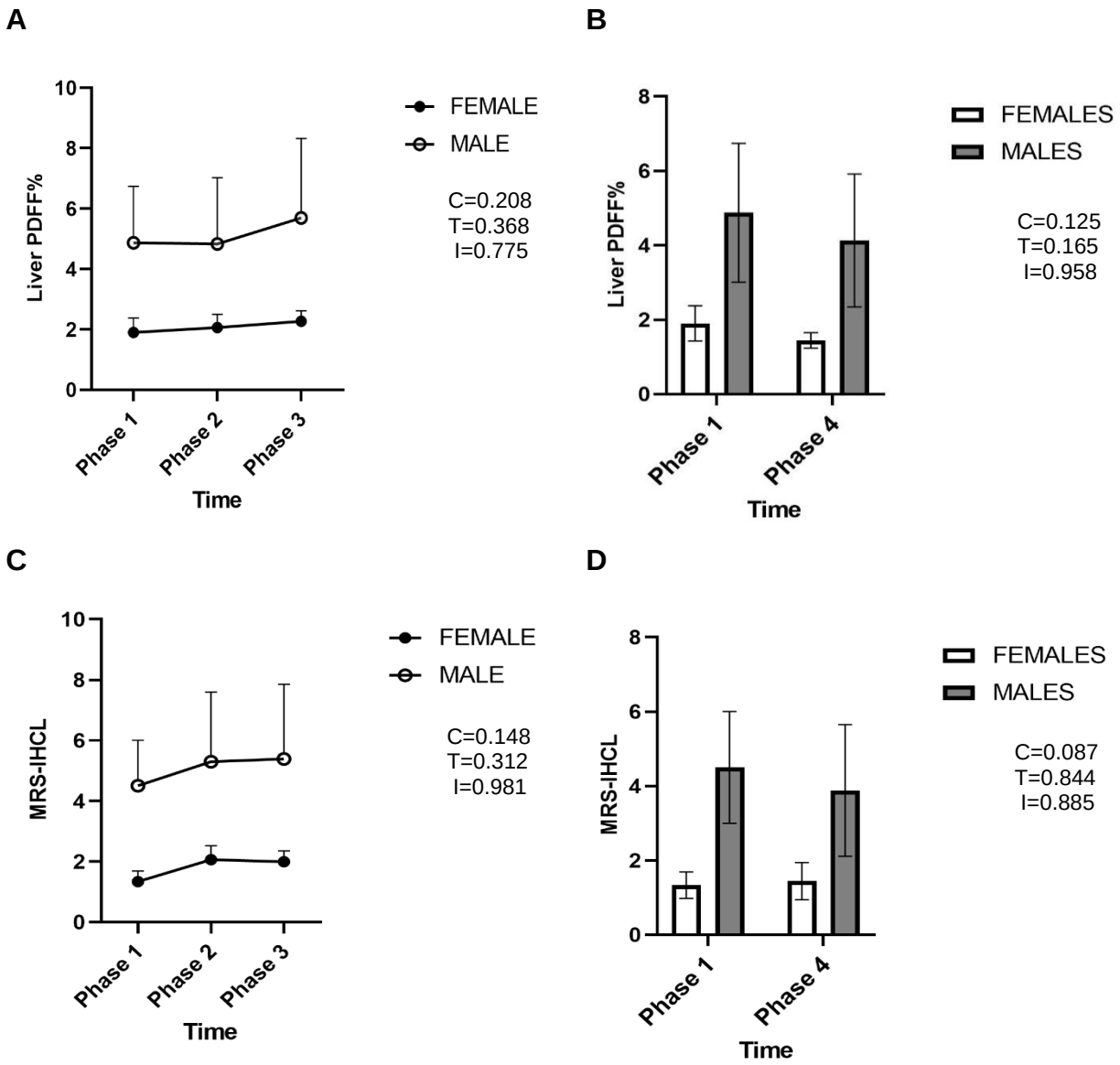

Figure 5.4.5 Estimation of liver fat deposition. (A&B) Dixon- PDFF sequences quantify %FF. (C, D) HISTO-MRS-STEAM quantify IHCL. (A&C) comparisons between; Phase1 (pre-Ramadan), Phase2 (one week after commencing Ramadan fasting) and Phase3 (3.5 weeks after commencing Ramadan fasting) show the temporal effect of Ramadan fasting. (B&D) Comparisons between Phase1 (pre-Ramadan) and Phase4 (one month after end of Ramadan fasting) to elicit if there are any significant changes one month after the end of Ramadan fasting. Data are presented as means with error bars representing standard error (SEM) (n=10 females, n=11 males). Statistical analysis was performed with mixed effect models.

5.4.6 Body hydration

Serum Calcium

There were no differences in serum calcium concentrations (mmol/L) over time for Pre-Ramadan compared to one week (7±1day) or 3.5 weeks (26±1) after commencing Fasting. There were also no differences between sexes (*P*=0.8, interaction; *P*=0.2). Furthermore, there were no differences between pre and one month after the end of Ramadan (*P*=0.7, interaction; *P*=0.3) (**Figure 5.4.6**).

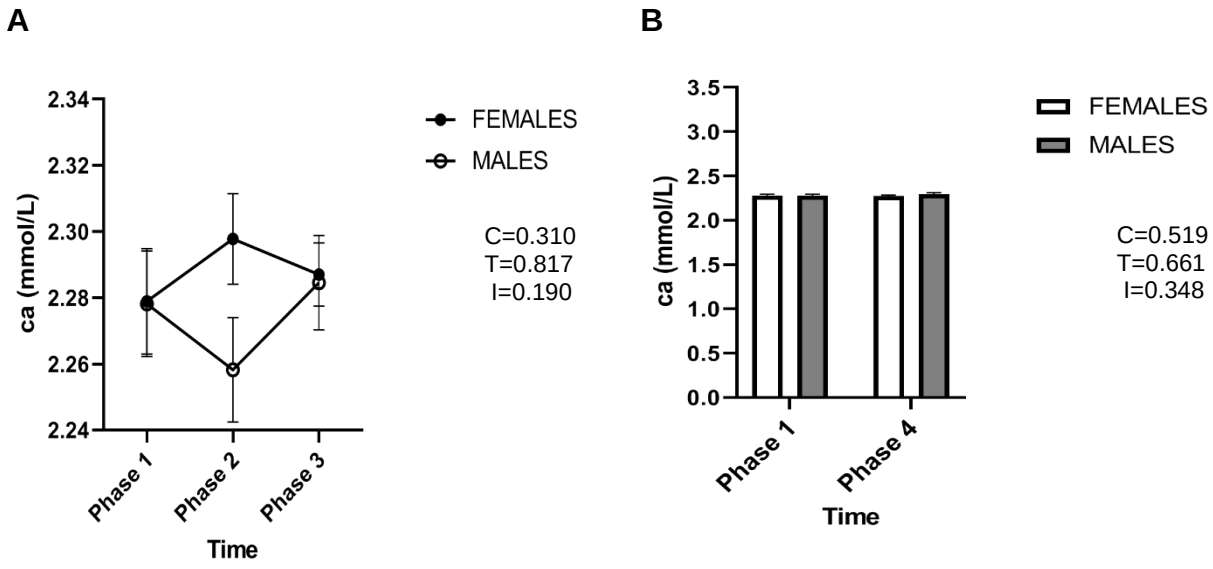

Figure 5.4.6. serum calcium concentrations. A comparison between baseline (Pre-Ramadan) and Phase2 (one week after commencing Ramadan fasting) and Phase3 (3.5 weeks after commencing Ramadan fasting) to show Ramadan fasting effects (A). A comparison between Phase1 (Pre-Ramadan) and Phase4(one month after end of Ramadan fasting) shows no significant difference (B). Data are presented as means with error bars representing standard error (SEM) (n=10 females, n=11 males). Statistical analysis was performed with mixed effect models.

Water consumption

There were no significant differences in the amount of water consumed during Ramadan fasting and one month after Ramadan ended (*P*=0.1, interaction; *P*=0.9) (**Figure 5.4.7**) with 1904±533 ml consumed by females in Ramadan compared to

2190±877 ml one month after Ramadan ended, and 2283±944 ml for males in Ramadan compared to 2627±1131ml one month after Ramadan ended.

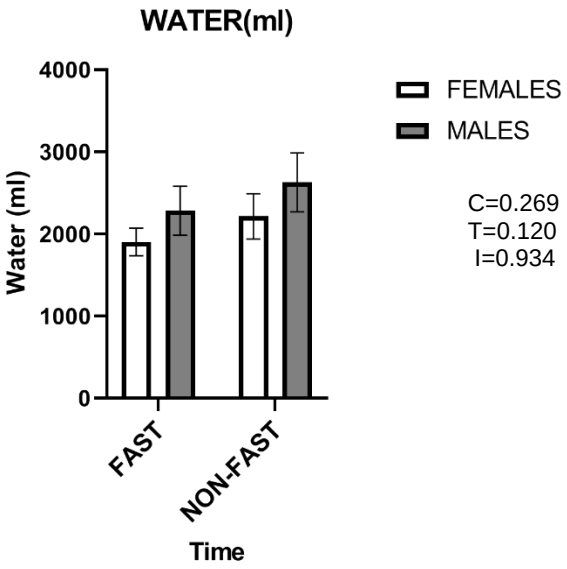

Figure 5.4.7. A comparison of the mean of 3-days water consumption during Ramadan fasting and one month after the end of Ramadan. Data are presented as means with error bars representing standard error (SEM) (n=10 females, n=11 males). Statistical analysis was performed with mixed effect models. Water amount recorded by participants in food diaries.

5.4.7 Continuous glucose monitor

There was no significant difference in the average glucose concentrations (GCs) between Ramadan and the non-fasting period (one month after the end of Ramadan) in both sexes (*P*>0.2, interaction; *P*>0.2). The average GCs in Ramadan for females and males were 6.18±0.73 and 6.06±0.66 mmol/L, respectively, and in the non-fasting period, 5.7±0.5 and 6.0±0.8 mmol/L, respectively. There was no significant difference in the percentage average of TIR during Ramadan against a month after the end of Ramadan (non-fasting period) in both sexes. In Ramadan, the females average TIR was 98.7±2.0%; only 2 out of 10 females recorded high GCs, and this only occurred for 0.5% and 4% of the time and 3 recorded low GCs for 1, 2, and 6% of the time. In

the non-fasting period, the average TIR for females was 98.6±1.3%, only one female recorded high GCs for 1% of the time, and 7 females recorded low GCs (in a range of 1- 3 % of the time). For males, the average TIR during Ramadan was 97.6±3.7%; 3 out of the 8 males recorded high GCs, with two males being in that high range for 1% of the time and one male for 3% of the time. Two males recorded very low GCs for 1% and 8% of the time and one recorded low GCs for 1% of the time. In the non-fasting period, the GCs were within TIR for 98.0±2.5% of the time; 2 males recorded high GCs for 6% and1% of the time, and 3 recorded low GCs for 0.2%, 5%, and 1% of the time (**Figure 5.4.7**).

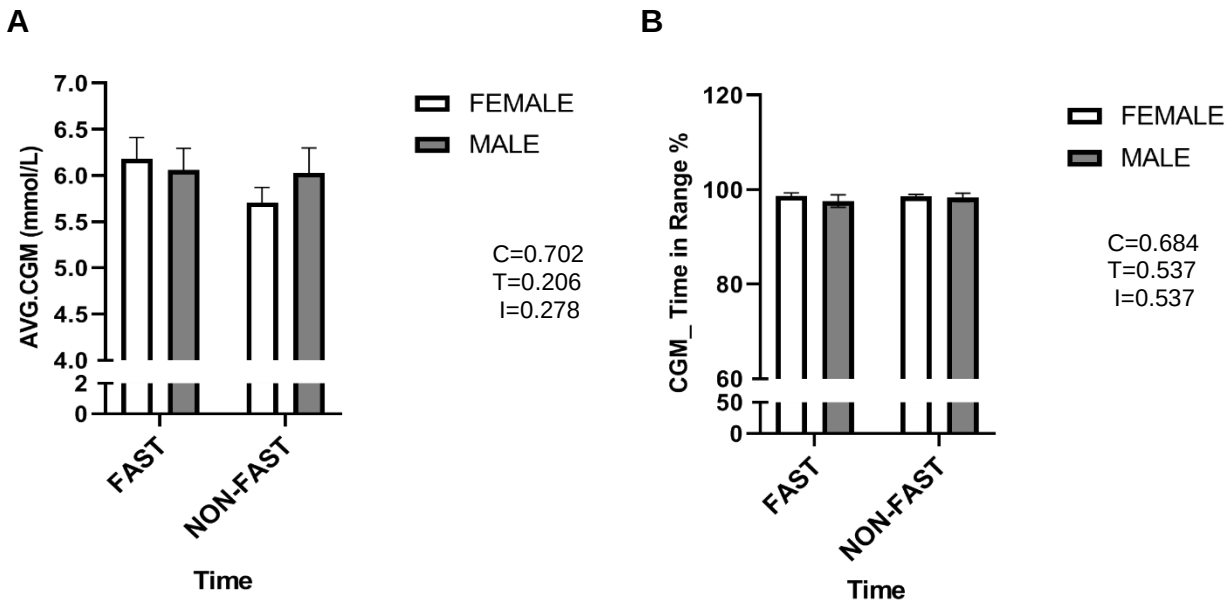

Figure 5.4.7. Continuous interstitial fluid glucose concentration. A comparison between Ramadan fasting and one month after the end of Ramadan fasting periods. (A) average glucose concentrations. (B) the average percentage of glucose concentration readings in the normal range. Data are presented as means with error bars representing standard error (SEM) (*n*=10 females, *n*=8 males). Statistical analysis was performed with Two-way ANOVA.

5.4.8 Correlations between fasting blood glucose and intrahepatocellular lipid, and between fasting glucose and intramyocellular lipid

There was no correlation between FBG and IHCL changes (Phase3 - Phase1); (r^2=0.0.093; *P*=0.391), (r^2=0.159; *P*=0.224) females and males respectively. Also, no correlation between FBG and IMCL changes (Phase3 – Phase1), **Figure 5.4.8.1.** Also, no correlation between FBG and IMCL changes (Phase3 - Phase1); (r^2=0.085; *P*=0.415), (r^2=0.0184; *P*=0.691), females and males respectively, **Figure 5.4.8.2.**

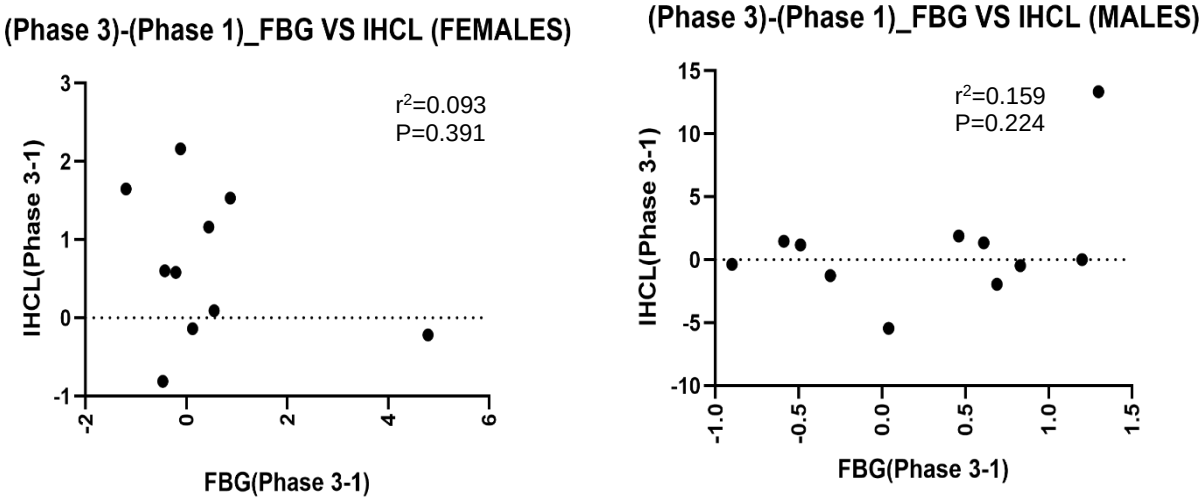

Figure 5.4.8.1. Relationship between the changes in changes fasting blood glucose (FBG) and intrahepatocellular lipid (IHCL), (Phase 3) - (Phase 1). Left females (n=10) and right males (n=11). Statistical analysis was performed with Pearson's correlation test.

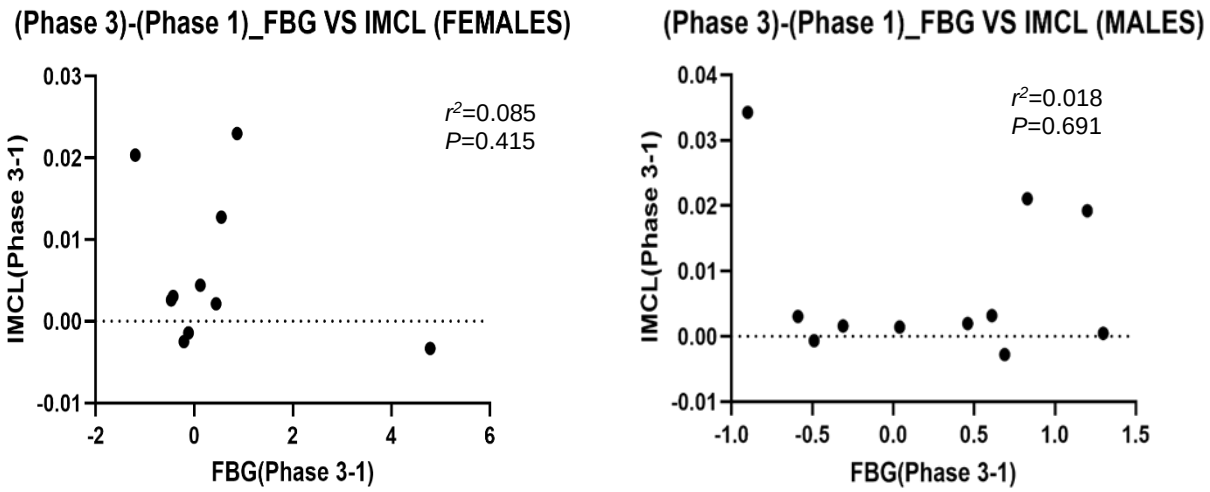

Figure 5.4.8.2 Relationship between the changes in changes fasting blood glucose (FBG) and intramyocellular lipid (IMCL), (Phase 3) - (Phase 1). Left females (n=10) and right males(n=11). Statistical analysis was performed with Pearson's correlation test.

5.5 Discussion

Ramadan month involving fasting for 18 hr/day, caused some metabolic changes that reflect the gluconeogenesis and to a lesser extent ketogenesis processes as discussed in chapter 4. The novelty of the current study was investigating the changes in ectopic lipids in order to understand the temporal effect of the long days of RF on human body metabolism.

5.5.1 Body mass, thigh muscle total fat volume (SAT and IMAT)

In the present study, a gradual and significant decline in BMI after 1 week and 3.5 weeks of RF were seen in line with most other RF and TRE studies which report a decline in body weight **(Chapter 1, Table 1.9)**. Total thigh muscle fat (SAT and IMAT) volume was not significantly decreased despite there being a decline in muscle volume. In muscle disuse studies, the decrease in muscle volume is usually

associated with an increase in IMAT, indicating muscle deconditioning (Pagano et al. 2018). Our results contrast with another study that reported that SAT is the main pool of releasing FFA in non-obese males, as they recorded a significant decrease in the leg and abdominal SATs and an increase in IMCL following extended Fasting for 28hrs (Thankamony et al. 2018). In chapter 4, we recorded a significant decline in AVF, which is suggested to be the main pool of FFA efflux.

5.5.2 Muscle ectopic IMCL level and fat fraction (FF%)

After one week of RF, a sharp significant increase in the IMCL: water ratio was recorded which plateaued at the end of RF and did not return back to baseline after one month from the end of RF (Phase 4). It was also recorded that acetoacetate (a sign of ketone body) in Phase 4 was trending higher than baseline**.** It is well-known that elevated FFA in fasting leads to increased IMCL concentration (C Boesch et al. 2006), and it is suggested that increased IMCL levels alone do not affect insulin sensitivity. An increased IMCL level is a sign of a fuel shift in skeletal muscle from glucose to lipids as an adaption to the fasting for one month. When the fasting condition ended (Phase 4), the FBG returned to normal status. However, IMCL remained higher than Pre-RF level, potentially related to the decline in muscle metabolic flexibility after fasting (Hoeks et al. 2010).

The IMCL: water ratio estimation method was based on the determination of the IMCL methylene (CH2) peak, which occurs at 1.3 ppm. This is a common method to estimate IMCL levels that has been proposed in other studies (C Boesch et al. 2006; Torriani et al. 2007; Johannsen et al. 2012). IMCL is determined by the rate of fatty acid availability and oxidation rather than circulating insulin levels (45). A study of control

subjects reported an accumulation of IMCL after prolonged fasting, concomitant with elevated blood FFA, triglyceride and 3-hydroxybutyrate signs of ketogenesis. After prolonged fasting for 28hrs, an increase of the methylene CH2 peak (at 1.3 ppm, a marker of both concentration and composition, relative to the increase of the methyl CH3 peak (at 0.9 ppm, a marker of concentration alone) was seen, leading to a significant decrease in the CH3:CH2 ratio (a compositional marker of IMCL). This implies a selective efflux of unsaturated FA from the IMCL pool during fasting (Thankamony et al. 2018). Recently, the importance of studying IMCL composition and concentration, has been proposed. The effects of different fatty acid types are varied and thus, for example, saturated fatty acids (SFAs) decrease insulin sensitivity, while mono-unsaturated (MUFA) and poly-unsaturated fatty acids (PUFA) improve insulin sensitivity (Lindeboom and de Graaf 2018).

In the current study a direct measurement of the triglyceride IMCL-CH2 1.3 ppm resonance peak relative to water was determined. However, we did not differentiate between SFA and UFA or estimate the saturation index (CH2:CH3 ratio of IMCL), as the spectra did not have a sufficient signal: noise to allow accurate peak discrimination of the IMCL-CH3 peak at 0.9 ppm given the overlapping nature of the peaks within the spectra. (Thankamony et al. 2018).

Recently, the compositional saturation index method of IMCL has been validated from ^{1}H MRS that was acquired from 3T systems and standard PRESS sequences (Savage et al. 2019). The most important additional tool is a transmitter-receiver local volume MR coils e.g peripheral Angio or knee coil, that provides strong and homogeneous rf pulses that overcome the inhomogeneity limitation of the receiver surface Phased array coil that was used in the current study (Savage et al. 2019; Thankamony et al. 2018; Krššák et al. 2021). The athlete's paradox is a widely observed and discussed

phenomenon that refers to an increase in muscle lipid accumulation in insulin sensitive endurance-trained_athletes (Loher et al. 2016; Thankamony et al. 2018; Morales, Bucarey, and Espinosa 2017; Savage et al. 2019). This phenomenon confirms that increasing IMCL triglycerides concentration per se is not responsible for insulin resistance. Saturated fat is involved in many metabolic diseases, such as insulin resistance, cardiovascular and liver diseases (Savage et al. 2019; Briggs, Petersen, and Kris-Etherton 2017; Luukkonen et al. 2018). Our study recorded increases in IMCL during and after Ramadan, but that did not coincide with an increase in insulin resistance, as HOMA-IR remained unchanged. The rise in FBG is likely due hepatic insulin resistance and lipolysis, or decreased blood glucose disposal in skeletal muscle and adipose tissue.

5.5.3 Liver fat deposition

Few studies have investigated the effect of TRE on humans' liver fat deposition in terms of PDFF% or MRS Intrahepatic lipid (IHL) levels, as most studies have been conducted in mice. One study examined two groups of mice fed a high-fat diet for 32 weeks after weaning: group one fasted for 24 hrs, and group two continued *ad libitum*. The fasted group significantly lost 3.3 g of weight and had 63 % higher hepatic fat fraction; however, this increase was not significant (P=0.18) (Narayan et al. 2015). *Hatori et al. (2012)* compared two mice groups, ad libitum and TRE. Both groups consumed high-fat diets and the same energy content from foods. However, the TRE group who had restricted food access for 8hrs/day over 17 weeks did not show an increase in body weight or levels of microscopic hepatic intracellular lipid droplets (HILDs), compared to the *ad libitum* group who, showed a 28% increase in body weight and large HILDs. The TRE group also had 70% less fat deposition (measured by MRI) compared to the ad libitum group (Hatori et al. 2012).

However, in the current study, no significant increase in liver fat deposition due to RF was found, and this result was consistent a recent Ramadan study of healthy obese NAFLD subjects, liver FF% was measured after 29 days of 16 hrs RF with no significant increase of FF% reported (mean FF% changes from 2.92±.7.99% to 3.44±8.11 (Dündar and Yavuz 2021).

5.5.4 Body hydration

There were no changes in hydration status as indicated by no changes in calcium level due to RF. There were also no differences in the amount of water consumption recorded by the participants during RF and non-RF periods. Although we speculated a change in hydration status due to RF in summer with long fasting days could affect FBG concentration and muscle volume, we did not record any significant changes in hydration status.

5.4.5 Continuous glucose monitoring (CGM)

Average and percentage time in range CGM were not significantly different during RF compared to one month after the end of RF. These may be due to the small sample size (18 subjects), whereas the G-Power test for sample size indicated 24 subjects. The CGM system measures interstitial glucose and is a useful tool to monitor 24 hrs glucose levels in the body and indicate hypo and hyper glucose events, however, it is not as sensitive as blood glucose results (Boyne et al. 2003). A Ramadan study on participants with type one and two diabetes mellitus, and a control group with healthy subjects, used CGM and found no significant change in mean CGM during fasting compared to the non-fasting period and no major hypoglycaemic events in all groups. In that study, sudden hyperglycaemic events after iftar (the first meal after fasting)

were recorded in all groups; however, it was higher in participants with diabetes than in the control group (Lessan et al. 2015).

Limitations

The main limitation of this study is the small sample size, and also, we could not control the visiting times to fit with the female menstrual period. This resulted in some females completing one of the Ramadan visits while they were non fasting. In addition, we did not use the most recent method IMCL saturation ratio (Savage et al. 2019) which may add more knowledge to our understanding to the effect of RF on the ectopic lipids intermediates or saturated lipids, which strongly relates to lipids toxicity and insulin resistance. Some difficulties were faced in recording CGM data, as the sensors connected to the participants' mobile through Dexcom G6 app and some mobiles were not compatible with the Dexcom G6 App and some others eventually disconnected for several hours, which caused loss of many CGM readings.

Conclusion

The important findings in the current study were that RF significantly elevated ectopic IMCL. However, other fat sites did not decrease in level (SAT and IMAT). Interestingly, after a month of normal habitual diet, IMCL continues to be significantly higher than the pre-Ramadan level. The saturated ratio method of IMCL (Savage et al. 2019) is recommended in future studies to confirm whether the elevation of IMCL is beneficial or not especially as the FBG returned to baseline after a month from the end of RF. Also, in this sample BMI decreased significantly at the end of Ramadan but returned to pre-Ramadan status after a month of normal habitual diet. No other changes in hydration signs or in average and percentage TIR of CGM were detected.

Chapter 6

General Discussion

6.1 Overview

This thesis is concerned with extensively studying the effect of Ramadan fasting on human body metabolites and how people change their activities and nutritional habits during Ramadan. We aimed to measure various physiological changes due to Ramadan fasting with minimal invasiveness when taking blood samples and using the advances in medical imaging technology to measure the changes in skeletal muscle volume and various body lipids pools. We extensively studied the effect of 18 hrs RF on metabolic markers, including: BMI, skeletal muscle and fat volumes, FBG, FBI, AVF and ASF deposits, blood lipids profile, ectopic lipids fat fractions (FF%) in skeletal muscle and liver, also specific lipid droplets (IMCL, IHCL). Moreover, we compared the habitual diet and physical activity, as well as continuous interstitial glucose concentration (CGCs) and its time in range (TIR) during RF and one month later. Furthermore, we have linked the physiological and anatomical changes to interpret how the human body adapts to TRE. RF is Islamic religious practice; however, it is proposed as a lifestyle change to improve metabolic health by reducing body weight and fat. Also, it could induce beneficial metabolic changes and act as a strategy to prevent metabolic syndrome. However, mild adverse reactions (increased FGB and LDL) were observed at the end of RF.

In terms of medical imaging, we used Magnetic resonance imaging, a versatile diagnostic technology with unique properties of providing quantitative and qualitative anatomical and physiological information. It is widely acceptable in research due to its safety, reproducibility, and repeatability. We have proposed an automated MR image segmentation that conveniently measures skeletal muscle and fat volume changes that benefits our RF study and can be utilized in other musculoskeletal studies.

6.2 Validating and optimising automated segmentation and volume measurement of MRI images

The aims of chapter 3 were to validate the automated segmentation method and optimise the measurements of muscle and fat volumes. These were achieved by comparing automated with a gold standard manual method. The automated method was conducted by practically testing many MR sequences and choosing the most appropriate sequences for automated volume measurement. The automated measurement is advantageous compared to the manual one because it allows muscle volume, adipose fat volume (SAT and IMAT) and abdominal fat deposits (AVF and ASF) measurements within a shorter time. The test of reproducibility. The coefficient of variation (CV%) for the two methods was comparable, CV%=1.60% in the automated method and CV%= 1.07% in the manual method. There was strong agreement between the two methods in detecting temporal muscle volume changes due to immobilisation when both were applied using the same MR sequence (T1-TSE). The bias and 95% limits between the two methods after 2 and 7 days were 0.3±1.7%, [-3.63, 2.96] and 0.02±1.7%, [-3.30, 3.26], respectively. Both methods detected temporal changes in muscle volume resulting from immobilisation with no significant interaction ($P<0.001$, interaction; $P=0.9$)**.**

T1-TSE is a routinely used sequence presenting anatomical structures (Westbrook, Roth, and Talbot 2011). However, 3D T1-WATS is more compatible for use with threshold segmentation and automated measurement method due to its properties of providing higher SNR and CNR (Grande et al. 2014). For optimising the automated method, it was hypothesised that 3D T1-WATS sequence sensitivity in detecting muscle volume changes would be comparable to or more sensitive than the routine 2D T1-TSE sequence. A CV% test of the two sequences were similar, with CV%=2.7%

for T1-WATS and CV=2.3% for T1-TSE. Also, there was strong agreement between the two sequences in detecting temporal muscle volume changes in the damaged immobilised unilateral thigh model when they were segmented by the automated method. The bias and 95% limits of the agreement after 2-days and 7-days of damage and immobilisation were -0.3±2.2 %, [-4.7, 4.1] and -0.9±1.1%, [-3.1, 1.2] respectively. Moreover, both sequences detected the temporal changes significantly without interaction (P=0.003, interaction; P=0.48). However, T1-WATS showed more sensitivity in detecting muscle volume changes.

We could not confirm the agreement between the automated and the manual methods in direct volume measurement for several reasons. Firstly, the manual measurements were completed by one operator, and the automated measurements were completed by another one. Secondly, in the manual method, the operator outlined each muscle in the slice separately and excluded any vessels or connective tissue between muscle groups. In contrast, the automated method included them. Finally, there was no direct measurement in the manual method for each slice. The measurement done on every third slice means that most slices were estimated and not measured directly. The thigh muscle cross-sectional area enlarged, moving from distal to proximal, and the automated method directly measures all the given slices.

Furthermore, we could not confirm the agreement between the T1-WATS and T1-TSE MR sequences in direct volume measurement because they have different geometric parameters. T1-WATS (10mm thickness,5mm gap, 29 slices) compared to T-TSE (5mm thickness,10 mm gap,14 slices). Due to these differences, we could not cover exactly the same thigh volumes, and there were around 0.5mm height differences, see **Figure 3.3.2.1, A, B**. It is recommended in future work to use similar geometric parameters when comparing volume measurements of two or more sequences.

Finally, we found that fat volume measurements were possible using the T1-FATS GRE sequence, which has a higher CNR than T1-TSE. However, there were some difficulties due to the small size of IMAT (thin white lines dispersed between muscle groups) in healthy subjects, so any small differences in signal intensity due to slight heterogeneity of magnetic field that are experienced in the peripheral slices will affect the threshold segmentation accuracy of the fat pool (MR-TIP.com n.d.). In order to accurately measures thigh total fat, we selected only 5 central slices where the MR field is most homogeneous.

6.3 Metabolic changes due to Ramadan month fasting 18 hrs/day (time-restricted eating model)

In chapter 4, we observed many metabolic changes due to RF. BMI significantly reduced after one week ($P<0.05$) and reached a nadir at the end of RF ($P<0.001$). The BMI reduction was combined with muscle volume reduction ($P=0.01$) and FBG elevation ($P<0.003$), and both changes were gradual and reached significant values at the end of RF in both sexes. Also, at the end of RF, AVF reduced significantly in males ($P<0.01$), and there was a trend of ASF reduction in both sexes ($P=0.08$). Blood LDL was significantly raised at the end of RF in both sexes ($P<0.05$). However, acetoacetate increased significantly in females after one week ($P<0.05$) and then decreased to reach the pre-RF level. Both sexes showed a trend towards an increase in acetoacetate after a month from the end of RF ($P=0.08$). There was a significant decline in protein consumption during RF in both sexes ($P<0.01$), however, there were no significant changes in total energy, carbohydrate, or fat intake ($P>0.05$). Also, there

were no significant differences in physical activity between RF and non-RF periods (P>0.05).

In chapter 5, we detected the following metabolic changes, a sharp increase in IMCL level after one week of RF (*P*<0.004), then it was steady at the end of RF. IMCL was also significantly higher than the pre-RF level after a month from the end of RF in both sexes (*P*<0.03). However, the thigh muscle FF% response was not similar among the sexes, with no significant changes in females, while in males, it decreased a little after one week and then recorded a significant increase when comparing Phase 2 vs Phase 3 (*P*<0.05).

The beneficial effects of RF were the significant reduction in BMI and adipose fat (AVF and ASF). On the other hand, there were significant increases in FBG, LDL and IMCL and muscle volume decline in both sexes, in addition to elevated muscular FF% in males only. These responses are not regarded as beneficial; they were higher pre-RF but still within a “normal range” as the subjects were healthy and young. The adverse reactions could be explained as a physiological reaction to semi-starvation or prolonged fasting. In this condition, there was a sign of insulin resistance (indicated by the rise in FBG in the current study) to save glucose for brain nutrition which does not require insulin for its uptake. Also, elevated LDL and IMCL reflect increases in circulated FFA fat oxidation. Since muscles can use lipids as an alternative to glucose as a fuel source (Hoeks et al. 2010; Johnson et al. 2006). Although we did not estimate plasma FFA, other prolonged fasting studies reported a direct correlation between IMCL and FFA, as shown in **Table 1.5.3**.

As mentioned, earlier in the findings, there was a significant increase in FBG only. *Salgado et al. (2010)* completed a study in participants with NAFLD (116 men) and a

normal group without NAFLD (88 men) to determine the cut-off value of HOMA-IR to predict IR, which was 2.5- 3 (Salgado et al. 2010). In the current study, the mean of HOMA-IR was within the normal range during all study phases. Still, in the males, there were individuals with elevations in HOMA-IR more than the normal range (2.5-3) at the end of RF. This may be due to higher ectopic lipids infiltration and AVF deposition compared to females. Thus, the little elevation in FBG at the end of RF in our study and other RF and TRE-studies, see Table 1.9 and 1.10 was not combined with hyperinsulinemia.

Most of the significant changes that occurred during RF returned to pre-RF levels a month after the end of RF. Although the average protein consumption was higher a month after the end of RF (non-fasting period), BMI and muscle volume showed a trend towards a reduction. In contrast, IMCL during and a month after RF was significantly higher than pre-RF with a trend of increased blood acetoacetate concentration (a sign of increased fat oxidation) due to liver gluconeogenesis and ketogenesis, combined with reduced muscle glucose oxidation. No RF studies measured IMCL changes, while some prolonged fasting studies (e.g., fasting for 28, 60, 67 hrs) reported increased IMCL due to prolonged fasting, see Table1.5.3. One 5:2 IER study on health females showed a significant increase in βHB ketone body levels due to fasting, which was remarkable at the end of 24 hrs fasting (Cerniuc et al. 2019). It can be speculated from the previous literature and this current study that muscles continued to use fat rather than glucose despite a month of normal habitual diet and restored insulin sensitivity (decreased FBG to the normal pre-RF level).

The question that emerged is why IMCL did not return to the normal level after a month of normal habitual diet and restored insulin sensitivity. In 60 hrs prolonged fasting, after a glucose clamp, fat oxidation was higher in the fasting condition than in control

(non-fasting) condition (Hoeks et al. 2010). Also, after induced insulin, carbohydrate oxidation was lower in the fasting state. The authors also found that prolonged exposure to elevated FFA levels reduced mitochondrial oxidative capacity and flexibility (i.e., the ability to switch from fat to glucose oxidation) after 60 hrs fasting (Hoeks et al. 2010). However, high IMCL with normal insulin sensitivity is a well-known condition usually seen in the physically fit cohort (athletic paradox), which suggests that the change in IMCL is a normal adaption to food availability or activity status, not a pathological response. In the case of food restriction, fatty acids move from adipose tissue to skeletal muscle to provide alternative energy for muscle contraction (Johnson et al. 2006). The interpretation of the increases in ectopic lipids (e.g., IMCL, IHCL, ICCL) should, therefore, carefully consider the medical situation, habitual diet, or activity change. A study of healthy non-obese subjects with 3-days of a very low-calorie diet showed a significant increase in plasma fatty acids and ICCL, which would mimic diabetes and obesity conditions; however, IHCL decreased (van der Meer et al. 2007). On the other hand, in 36h fasted healthy young non-obese males, FFA and IHCL markedly increased (Moller et al. 2008). Also, in Ramadan with 14 hrs fasting, there was a non-significant increase in hepatic FF% in subjects with obesity, steatosis, and impaired lipids profile (Dündar and Yavuz 2021).

The novelty of the current study is that this is the first Ramadan fasting study which investigated metabolic changes comprehensively. Several studies have investigated this topic; however, no study used MRI to measure muscle volume changes or IMCL, see **Chapter 1, Table 1.9, Table1.10** and **Table 1.5.3.** Also, the strength of our study was to analyse the effect of RF with regard to sex differences. We recognised that males inherently have higher ectopic and visceral fat deposits than females, and females have higher subcutaneous fat, while BMI, FBG and FBI were similar among

sexes in the study sample. IHCL-MRS levels greater than 5.5% indicate hepatic steatosis. However, the median value varies among ethnicity and sexes (Browning et al. 2004). In the current study, the mean basal IHL for males was 4.5%, which increased to 5.4% at the end of RF, while the mean basal IHL for females was 1.33%, which increased to 2% at the end of RF. A small increase in IHL is reported to be associated with IR and an unfavourable lipid profile (Bian et al. 2011; Dündar and Yavuz 2021). However, especially in males, IHCL became lower after a month from the end of RF compared to baseline (Phase 4 =3.9% vs Phase 1= 4.5%), whereas the change was negligible in females (Phase 4= 1.4% vs Phase 1= 1.3%).

In the current study, we recorded but did not control the habitual diet during RF, to investigate the ordinary habitual changes during Ramadan month. Protein intake was lower during RF, and this is a confounder when interpreting the effects of RF. It is unclear whether the increase in FBG at the end of Ramadan is due to liver IR or muscle IR. Liver IR appears to be the key reason of increased FBG at the end of RF. Disruption to the circadian clock and change in meal timings may also contribute to the elevated FBG (Nachvak et al. 2018). Moreover, during fasting, the liver decreases the rate of glucose consumption and shifts to gluconeogenesis (Santoleri and Titchenell 2019). Although the decline in protein intake was not lower than the recommended guideline (0.75-0.80g/kg/day) (EFSA 2017), females consumed 58g/day, and males consumed 90g/day in Ramadan. It has been reported that IF strategies could lower daily muscle protein synthesis. An increased protein consumption of up to 2.4g/kg has been recommended (Aragon and Schoenfeld 2022). A 20hrs dTRE study that involved consuming one meal versus 3 meals with similar macronutrient, saturated/ unsaturated fat and energy intake lean mass was maintained and the decline in body mass and fat in the TRE group was concomitant

with increased FBG, LDL and TC (Stote et al. 2007). Also, another RF 12 hrs fasting/day study analysed the effect of RF in conjunction with detailed dietary intake information and found that the quality of food intake (e.g. increased protein, mono/polyunsaturated fat, decreased saturated fat) has beneficial impacts on cardiovascular markers when combined with fasting (Adlouni et al. 1997), see **Chapter 1, Table 1.9**.

Fasting has been proposed as a therapeutic intervention to improve metabolic syndrome and obesity, combined with a specific diet and/or physical activity (Wilhelmi De Toledo et al. 2013; Chaix et al. 2014). However, RF studies with less than 16 hrs fasting per day or more than 16 hrs for only one week with no intention to change habitual diet or activity also reported beneficial effects on the metabolic index e.g., BMI, WC, adipose fats (Hutchison et al. 2019; Wilkinson et al. 2020). These effects aligned with the current study when BMI was reduced while no other significant changes were recorded after one week.

TRE, IF, and RF have been investigated as therapeutic interventions or metabolic shift models. TRE and RF for long durations (more than 16hrs/day) could induce a metabolic shift toward increased fat oxidation and decreased carbohydrate oxidation, as seen in prolonged fasting studies. This leads to increased lipolysis, hepatic gluconeogenesis and ketogenesis that lead to temporary insulin resistance. This can also lead to an increase in blood lipid profile components due to increased FFAs in blood circulation as they move from adipose tissue to muscle and the liver to be used as an alternative fuel source, and this could be seen as elevated ectopic lipids However, other eTRE studies reported no change or decrease in FBG, see Chapter 1, Table 1.10. Emerging evidence shows that dTRE can cause adverse disruptions in the circadian rhythm. When comparing these two TRE models, the former shows

improvement in IS (Aragon and Schoenfeld 2022; Jamshed et al. 2019). Moreover, LDL increased in some IF studies and this is consistent with our results. Such a finding could be due to the circadian rhythm disruption, or a month of 18hrs of daily fasting period leading to increased fat oxidation (Jamshed et al. 2019). Healthy people and well-controlled diabetic patients could tolerate RF for up to 18hrs. However, diabetic patients and people with metabolic syndrome (e.g., steatosis, high lipid profile, pre-diabetic) should be aware of the transient insulin resistance and the sudden sharp hyperglycaemia after Iftar (the first meal on the evening after a day fasting), that is frequently reported. Also, they are more likely to experience hypoglycaemia and dehydration (Lessan et al. 2015; Hanif et al. 2020). Moreover, the increases in blood lipids due to increased circulating FFAs on long Ramadan days (more than 16hrs) should be considered in patients with metabolic diseases (Dündar and Yavuz 2021). It is important to highlight the beneficial weight management and the improvement of metabolic index due to TRE in obese individuals (Peeke et al. 2021) and patients with Mets (Wilkinson et al. 2020).Finally, several studies focused on the effect of protein intake on insulin sensitivity, for example, a study on 12 mild untreated diabetic subjects (mean age 61 y, mean BMI 31 kg/m^2). Followed a high protein diet (166g of protein), (protein: carbohydrate: fat ratio 30:40:30) for 5 weeks versus a control diet containing 84g of protein) (protein: carbohydrate: fat ratio 15:55:30). The study concluded that with no change in body weight, a high protein/low carbohydrate diet beneficially reduces postprandial blood glucose and glycated haemoglobin (Gannon et al. 2003). The current recommendation on daily protein intake is in the range of 0.75-0.80 g/kg/day (McCarthy and Berg 2021) and the recommended amount of activity is 150-300 minutes of moderate or 75-150 minutes of vigorous activity in combination with minimum 2-days/week strengthening activity (Piercy et al. 2018). Although, there were

no significant differences in total calorie intake in our sample, protein intake significantly lowered during Ramadan. Also, they were under the recommended level of physical activity, and it declined further during Ramadan. The recommendations to the people practising Ramadan fasting are increasing protein and physical activity levels, especially during Ramadan.

6.4 Limitations and future work

In our RF study, we took blood samples in the basal state (within 8-12 hrs of fasting). In contrast, other RF- and IF studies took samples in the basal state and at the end of intervention. In metabolic studies investigating Ramadan fasting (more than 16 hrs), blood samples were taken after 12 or 14 hours of fasting (Nachvak et al. 2018; Mohammadzade et al. 2017). The differences in the blood sample time could be one cause of the confounding results in Ramadan studies. In future studies of RF, it is recommended to take blood samples at the basal status and one or two hours before breaking the fast (before Iftar) and two hours after Iftar to see the peak of all metabolic changes. Also, for the CGM results in the current study, the sample size was small (8 males and 10 females).

In several prolonged fasting studies, fasting blood glucose and insulin did not increase. However, there were significant increases in peripheral IR (i.e., reduced glucose uptake by muscle) (7,154) that was estimated by the gold standard method for assessing insulin sensitivity, the hyperinsulinemic-euglycemic clamp. The disadvantage of this method is the complexity, invasiveness, and time burden (over 3 hours per subject) (Salgado et al. 2010). Also, it is not applicable during Ramadan month during the day because it is forbidden to induce any nutritional substance orally

or intravenously during fasting time. Fasting insulin, glucose, and HOMA-IR have been used alternatively as an indirect measure of insulin sensitivity (Vaccaro et al. 2004).

Fasting can markedly alter rates of muscle protein synthesis (MPS), which was not measured directly in this study. This can be measured using stable isotope techniques. Previous studies have reported a significant decline in protein synthesis upon fasting for 15 hrs with no changes in protein breakdown (Rennie et al. 1982). The gluconeogenesis process, initiated by a prolonged fasting period of more than 16 hrs, induces muscle protein breakdown (MPB), and it has been suggested that resistance exercise could help preserve muscle mass during prolonged fasting (Williamson and Moore 2021). A combination of resistance exercise and the use of stable isotopes to investigate the effect of RF on MPS and MPB is recommended for future work.

Ketone bodies results were from only 8 males and 8 females while a larger sample could yield significant changes. Studying RF in the older population and in menopausal women who can fast for the whole month without interruption due to the menstrual cycle would allow for more rigid results, especially since ageing is more related to metabolic syndrome. Although there are many Ramadan studies worldwide, there is a lack of research in the Middle East, the region with the maximum Muslim population and a high prevalence of metabolic syndrome (Demangel et al. 2017). Studying RF with additional interventions such as exercise or a control diet is a research area worth considering. Finally, estimating IMCL using the new MRS compositional saturation index method (CH2:CH3 ratio) is recommended for future studies to add more knowledge about the IMCL composition and because the saturation index is suggested to be more related to IR than only measuring the IMCL concentration (Kim et al. 2017).

6.5 Conclusion

Metabolic syndrome (MetS) is a worldwide epidemic disease, and its prevalence is expected to increase further in the next decade. MetS populations are at a higher risk of coronary heart disease (CHD) and cardiovascular disease (CVD) (Trouwborst et al. 2018; Al-Rubeaan et al. 2018). Regions with the highest Muslim population who annually practice Ramadan fasting reported high MetS prevalence (Al-Rubeaan et al. 2018). Although BMI and WC are common predictor tools for MetS, in line with FBG and blood lipid profile, they do not reflect the internal fat distribution and infiltration. Also, not all obese subjects are at risk of MetS (Thomas et al. 2012). Visceral adiposity, muscle and liver ectopic lipids infiltration are all linked to MetS. However, there is no consensus on which form of adiposity is most strongly related to MetS. There is also a link between these lipids' deposits and other biological markers such as muscle quality or muscle mass, level of activity, nutrition quality and quantity and MetS (Williamson and Moore 2021; Pieńkowska et al. 2020; Lang et al. 2015; Thomas et al. 2012).

IF includes IER and TRE forms of fasting or abstaining from food for a period of time. Ramadan fasting is a kind of TRE practised annually for religious purposes and has been studied for the last decade. Recently IF has gained interest as a non-pharmaceutical intervention suggested to improve metabolic health and body composition via reducing energy consumption and increasing lipolysis and fat oxidation (Williamson and Moore 2021).

MRI is the most reliable and sensitive tool to detect muscle and fat changes. It is nominated as a biomarker in clinical and research fields due to its safety, sensitivity, and imaging technique variety (Carlier et al. 2016). Skeletal muscle volume and lipids depositions are important factors in monitoring the physiological changes related to

metabolic disorders. The studies presented in this thesis have established that water-only and fat-only MR images can be effectively used with automated volume measurements to estimate muscle-only and fat-only volumes. This thesis has also demonstrated that long days of Ramadan month fasting (more than 16 hrs per day) cause liver insulin resistance which is a normal body reaction to semi-starvation status that leads the skeletal muscle to shift energy utilisation from carbohydrates to lipids causing an increase in circulated free fatty acids “lipolysis process” and synthesis of endogenous glucose from non-carbohydrate substrates, e.g. lactate, amino acids and glycerol “gluconeogenesis process”. All these processes work to save glucose nutrition to the central nervous system.

Finally, we observed the following metabolic changes: deceased BMI and abdominal adipose fat combined with muscle volume decline, high FBG and LDL at the end of 18 hrs/day RF in normal healthy females and males. Increasing protein intake and resistance exercise are recommended to avoid muscle loss and improve the metabolic index.

References

Addeman, Bryan T., Shelby Kutty, Thomas G. Perkins, Abraam S. Soliman, Curtis N. Wiens, Colin M. McCurdy, Melanie D. Beaton, Robert A. Hegele, and Charles A. McKenzie. 2015. 'Validation of Volumetric and Single-Slice MRI Adipose Analysis Using a Novel Fully Automated Segmentation Method'. *Journal of Magnetic Resonance Imaging* 41 (1): 233–41. https://doi.org/10.1002/jmri.24526.

Adlouni, Ahmed, Noreddine Ghalim, Abdellah Benslimane, Jean Michel Lecerf, and Rachid Saíle. 1997. 'Fasting during Ramadan Induces a Marked Increase in High-Density Lipoprotein Cholesterol and Decrease in Low-Density Lipoprotein Cholesterol'. *Annals of Nutrition and Metabolism* 41 (4): 242–49. https://doi.org/10.1159/000177999.

Akhmedov, Dmitry, and Rebecca Berdeaux. 2013. 'The Effects of Obesity on Skeletal Muscle Regeneration'. *Frontiers in Physiology* 4 DEC (December): 1–12. https://doi.org/10.3389/fphys.2013.00371.

Akhtar, Perveen, Amir Kazmi, Tarun Sharma, and Aradhna Sharma. 2020. 'Effects of Ramadan Fasting on Serum Lipid Profile'. *Journal of Family Medicine and Primary Care* 9 (5): 2337. https://doi.org/10.4103/jfmpc.jfmpc_550_19.

Al-Rubeaan, Khalid, Nahla Bawazeer, Yousuf al Farsi, Amira M. Youssef, Abdulrahman A. Al-Yahya, Hamid AlQumaidi, Basim M. Al-Malki, Khalid A. Naji, Khalid Al-Shehri, and Fahd I. al Rumaih. 2018. 'Prevalence of Metabolic Syndrome in Saudi Arabia - a Cross Sectional Study'. *BMC Endocrine Disorders 2018 18:1* 18 (1): 1–9. https://doi.org/10.1186/S12902-018-0244-4.

Anton, Stephen, Armin Ezzati, Danielle Witt, Christian McLaren, and Patricia Vial. 2021. ‘The Effects of Intermittent Fasting Regimens in Middle-Age and Older Adults: Current State of Evidence’. *Experimental Gerontology* 156 (December). https://doi.org/10.1016/J.EXGER.2021.111617.

Antoni, Rona, Kelly L. Johnston, Adam L. Collins, and M. Denise Robertson. 2017. ‘Effects of Intermittent Fasting on Glucose and Lipid Metabolism’. *Proceedings of the Nutrition Society* 76 (3): 361–68. https://doi.org/10.1017/S0029665116002986.

Aragon, Alan A., and Brad J. Schoenfeld. 2022. ‘Does Timing Matter? A Narrative Review of Intermittent Fasting Variants and Their Effects on Bodyweight and Body Composition’. *Nutrients*. MDPI. https://doi.org/10.3390/nu14235022.

Bakker, Leontine E.H., Linda D. van Schinkel, Bruno Guigas, Trea C.M. Streefland, Jacqueline T. Jonker, Jan B. van Klinken, Gerard C.M. van der Zon, et al. 2014. ‘A 5-Day High-Fat, High-Calorie Diet Impairs Insulin Sensitivity in Healthy, Young South Asian Men but Not in Caucasian Men’. *Diabetes* 63 (1): 248–58. https://doi.org/10.2337/db13-0696.

Barley, Oliver R., Dale W. Chapman, and Chris R. Abbiss. 2020. ‘Reviewing the Current Methods of Assessing Hydration in Athletes’. *Journal of the International Society of Sports Nutrition* 17 (1): 1–13. https://doi.org/10.1186/S12970-020-00381-6/FIGURES/1.

Bass, Joseph, and Joseph S. Takahashi. 2010. ‘Circadian Integration of Metabolism and Energetics’. *Science (New York, N.Y.)* 330 (6009): 1349–54. https://doi.org/10.1126/SCIENCE.1195027.

Berg, Hans E, Daniel Truong, Elisabeth Skoglund, Thomas Gustafsson, and Tommy R Lundberg. 2020. ‘Threshold-automated CT-measurements of Muscle Size and Radiological Attenuation in Multiple Lower-extremity Muscles of Older Individuals’. *Clinical Physiology and Functional Imaging*, 0–2. https://doi.org/10.1111/cpf.12618.

Bergens, Oscar, Jort Veen, Diego Montiel-Rojas, Peter Edholm, Fawzi Kadi, and Andreas Nilsson. 2020. ‘Impact of Healthy Diet and Physical Activity on Metabolic Health in Men and Women’. *Medicine* 99 (16): e19584. https://doi.org/10.1097/md.0000000000019584.

Bian, Hua, Hongmei Yan, Mengsu Zeng, Shengxiang Rao, Xiuzhong Yao, Jian Zhou, Weiping Jia, and Xin Gao. 2011. ‘Increased Liver Fat Content and Unfavorable Glucose Profiles in Subjects without Diabetes’. *Diabetes Technology and Therapeutics* 13 (2): 149–55. https://doi.org/10.1089/dia.2010.0101.

‘Biosen Lactate and Glucose Analyzer | EKF Diagnostics’. n.d. Accessed 6 June 2023. https://www.ekfdiagnostics.com/biosen-analyzer.html.

Bley, Thorsten A., Oliver Wieben, Christopher J. François, Jean H. Brittain, and Scott B. Reeder. 2010. ‘Fat and Water Magnetic Resonance Imaging’. *Journal of Magnetic Resonance Imaging* 31 (1): 4–18. https://doi.org/10.1002/JMRI.21895.

Bock, Gerlies, Elizabeth Chittilapilly, Rita Basu, Gianna Toffolo, Claudio Cobelli, Visvanathan Chandramouli, Bernard R. Landau, and Robert A. Rizza. 2007. ‘Contribution of Hepatic and Extrahepatic Insulin Resistance to the Pathogenesis of Impaired Fasting Glucose: Role of Increased Rates of

Gluconeogenesis'. *Diabetes* 56 (6): 1703–11. https://doi.org/10.2337/db06-1776.

Boden, Guenther, Jose Ruiz, Jean-luc Urbain, Xinhua Chen, and Jean-Luc Urbain. 1996. 'Evidence for a Circadian Rhythm of Insulin Secretion'.

Boesch, C, J Decombaz, J Slotboom, and R Kreis. 2006. 'Observation of Intramyocellular Lipids by Means of 1H Magnetic Resonance Spectroscopy'. *Annals of the New York Academy of Sciences The Sciences* 58 (4): 25–31. https://doi.org/10.1111/j.1749-6632.2000.tb06417.x.

Boesch, Chris. 2007. 'Musculoskeletal Spectroscopy'. *Journal of Magnetic Resonance Imaging* 25 (2): 321–38. https://doi.org/10.1002/jmri.20806.

Boesch, Chris, Juergen Machann, Peter Vermathen, and Fritz Schick. 2006. '14)Role of Proton MR for the Study of Muscle Lipid Metabolism'. *NMR in Biomedicine* 19 (7): 968–88. https://doi.org/10.1002/nbm.1096.

Borga, Magnus, Janne West, Jimmy D. Bell, Nicholas C. Harvey, Thobias Romu, Steven B. Heymsfield, and Olof Dahlqvist Leinhard. 2018. 'Advanced Body Composition Assessment: From Body Mass Index to Body Composition Profiling'. *Journal of Investigative Medicine* 66 (5): 1–9. https://doi.org/10.1136/JIM-2018-000722.

Boyne, Michael S., David M. Silver, Joy Kaplan, and Christopher D. Saudek. 2003. 'Timing of Changes in Interstitial and Venous Blood Glucose Measured With a Continuous Subcutaneous Glucose Sensor'. *Diabetes* 52 (11): 2790–94. https://doi.org/10.2337/DIABETES.52.11.2790.

Bray, Timothy J.P., Manil D. Chouhan, Shonit Punwani, Alanbain Bridge, and Margaret A. Hall-Craggs. 2018. ‘Fat Fraction Mapping Using Magnetic Resonance Imaging: Insight into Pathophysiology’. *British Journal of Radiology* 91 (1089). https://doi.org/10.1259/BJR.20170344/FORMAT/EPUB.

Briggs, Michelle A., Kristina S. Petersen, and Penny M. Kris-Etherton. 2017. ‘Saturated Fatty Acids and Cardiovascular Disease: Replacements for Saturated Fat to Reduce Cardiovascular Risk’. *Healthcare (Switzerland)*. Multidisciplinary Digital Publishing Institute (MDPI). https://doi.org/10.3390/healthcare5020029.

Browning, Jeffrey D., Jeannie Baxter, Santhosh Satapati, and Shawn C. Burgess. 2012. ‘The Effect of Short-Term Fasting on Liver and Skeletal Muscle Lipid, Glucose, and Energy Metabolism in Healthy Women and Men’. *Journal of Lipid Research* 53 (3): 577–86. https://doi.org/10.1194/JLR.P020867.

Browning, Jeffrey D., Lidia S. Szczepaniak, Robert Dobbins, Pamela Nuremberg, Jay D. Horton, Jonathan C. Cohen, Scott M. Grundy, and Helen H. Hobbs. 2004. ‘Prevalence of Hepatic Steatosis in an Urban Population in the United States: Impact of Ethnicity’. *Hepatology (Baltimore, Md.)* 40 (6): 1387–95. https://doi.org/10.1002/HEP.20466.

Burakiewicz, Jedrzej, Christopher D.J. Sinclair, Dirk Fischer, Glenn A. Walter, Hermien E. Kan, and Kieren G. Hollingsworth. 2017. ‘Quantifying Fat Replacement of Muscle by Quantitative MRI in Muscular Dystrophy’. *Journal of Neurology* 264 (10): 2053–67. https://doi.org/10.1007/s00415-017-8547-3.

Cabo, Rafael de, and Mark P. Mattson. 2019. ‘Effects of Intermittent Fasting on Health, Aging, and Disease’. *New England Journal of Medicine* 381 (26): 2541–51. https://doi.org/10.1056/nejmra1905136.

Carlier, Pierre G., Benjamin Marty, Olivier Scheidegger, Paulo Loureiro De Sousa, Pierre Yves Baudin, Eduard Snezhko, and Dmitry Vlodavets. 2016. 'Skeletal Muscle Quantitative Nuclear Magnetic Resonance Imaging and Spectroscopy as an Outcome Measure for Clinical Trials'. *Journal of Neuromuscular Diseases* 3 (1): 1–28. https://doi.org/10.3233/JND-160145.

Carlson, Olga, Bronwen Martin, Kim S. Stote, Erin Golden, Stuart Maudsley, Samer S. Najjar, Luigi Ferrucci, et al. 2007. 'Impact of Reduced Meal Frequency without Caloric Restriction on Glucose Regulation in Healthy, Normal-Weight Middle-Aged Men and Women'. *Metabolism: Clinical and Experimental* 56 (12): 1729–34. https://doi.org/10.1016/j.metabol.2007.07.018.

Cerniuc, Christin, Tobias Fisher, Anna Baumeister, and Ur Bordewick-Dell. 2019. 'Impact of Intermittent Fasting (5:2) on Ketone Body Production in Healthy Female Subjects Development of New Dietetic Therapies for SLO View Project Improvement of Ketogenic Nutrition Therapy View Project Impact of Intermittent Fasting (5:2) on Ketone Body Production in Healthy Female Subjects'. *Ernahrugs Umschau* 66 (1): 2–9. https://doi.org/10.4455/eu.2019.002.

Chaix, Amandine, Amir Zarrinpar, Phuong Miu, and Satchidananda Panda. 2014. 'Time-Restricted Feeding Is a Preventative and Therapeutic Intervention against Diverse Nutritional Challenges'. *Cell Metabolism* 20 (6): 991–1005. https://doi.org/10.1016/j.cmet.2014.11.001.

Chee, Carolyn, Chris E. Shannon, Aisling Burns, Anna L. Selby, Daniel Wilkinson, Kenneth Smith, Paul L. Greenhaff, and Francis B. Stephens. 2016. 'Relative Contribution of Intramyocellular Lipid to Whole-Body Fat Oxidation Is Reduced With Age but Subsarcolemmal Lipid Accumulation and Insulin Resistance Are

Only Associated With Overweight Individuals'. *Diabetes* 65 (4): 840–50. https://doi.org/10.2337/DB15-1383.

Cioffi, Iolanda, Andrea Evangelista, Valentina Ponzo, Giovannino Ciccone, Laura Soldati, Lidia Santarpia, Franco Contaldo, Fabrizio Pasanisi, Ezio Ghigo, and Simona Bo. 2018. 'Intermittent versus Continuous Energy Restriction on Weight Loss and Cardiometabolic Outcomes: A Systematic Review and Meta-Analysis of Randomized Controlled Trials'. *Journal of Translational Medicine* 16 (1): 1–15. https://doi.org/10.1186/s12967-018-1748-4.

Clarke, Callisia N., Haesun Choi, Ping Hou, Catherine H. Davis, Jingfei Ma, Asif Rashid, Jean Nicolas Vauthey, and Thomas A. Aloia. 2017. 'Using MRI to Non-Invasively and Accurately Quantify Preoperative Hepatic Steatosis'. *HPB* 19 (8): 706–12. https://doi.org/10.1016/j.hpb.2017.04.009.

Culvenor, Adam G., David T. Felson, Jingbo Niu, Wolfgang Wirth, Martina Sattler, Torben Dannhauer, and Felix Eckstein. 2017. 'Thigh Muscle Specific-Strength and the Risk of Incident Knee Osteoarthritis: The Influence of Sex and Greater Body Mass Index'. *Arthritis Care and Research* 69 (8): 1266–70. https://doi.org/10.1002/acr.23182.

Demangel, Rémi, Loïc Treffel, Guillaume Py, Thomas Brioche, Allan F. Pagano, Marie Pierre Bareille, Arnaud Beck, et al. 2017. 'Early Structural and Functional Signature of 3-Day Human Skeletal Muscle Disuse Using the Dry Immersion Model'. *Journal of Physiology* 595 (13): 4301–15. https://doi.org/10.1113/JP273895.

Demerath, Ellen W., Derek Reed, Nikki Rogers, Shumei S. Sun, Miryoung Lee, Audrey C. Choh, William Couch, et al. 2008. 'Visceral Adiposity and Its

Anatomical Distribution as Predictors of the Metabolic Syndrome and Cardiometabolic Risk Factor Levels'. *The American Journal of Clinical Nutrition* 88 (5): 1263. https://doi.org/10.3945/ajcn.2008.26546.

Dexcom Clarity. n.d. 'Dexcom CLARITY ® User Guide'. Accessed 4 July 2022. https://productstore.clarity.dexcom.eu/Documentation/en/Dexcom_Clarity_User_Guide_Home_User.pdf.

Dirks, Marlou L., Benjamin T. Wall, Bas van de Valk, Tanya M. Holloway, Graham P. Holloway, Adrian Chabowski, Gijs H. Goossens, and Luc J. van Loon. 2016. 'One Week of Bed Rest Leads to Substantial Muscle Atrophy and Induces Whole-Body Insulin Resistance in the Absence of Skeletal Muscle Lipid Accumulation'. *Diabetes* 65 (10): 2862–75. https://doi.org/10.2337/db15-1661.

Dong, Tiffany A., Pratik B. Sandesara, Devinder S. Dhindsa, Anurag Mehta, Laura C. Arneson, Allen L. Dollar, Pam R. Taub, and Laurence S. Sperling. 2020. 'Intermittent Fasting: A Heart Healthy Dietary Pattern?' *American Journal of Medicine*. Elsevier Inc. https://doi.org/10.1016/j.amjmed.2020.03.030.

Drinda, Stefan, Franziska Grundler, Thomas Neumann, Thomas Lehmann, Nico Steckhan, Andreas Michalsen, and Francoise Wilhelmi De Toledo. 2019. 'Effects of Periodic Fasting on Fatty Liver Index-A Prospective Observational Study'. https://doi.org/10.3390/nu11112601.

Dündar, İ, and A Yavuz. 2021. 'Effects of Ramadan Fasting on Hepatic Steatosis and Liver Volume in Individuals without Chronic Liver Conditions'. *J Nutr Fast Health* 9 (3): 221–28. https://doi.org/10.22038/jnfh.2021.54384.1312.

Echouffo-Tcheugui, Justin B., Haiying Chen, Rita R. Kalyani, Mario Sims, Sean Simpson, Valery S. Effoe, Adolfo Correa, Alain G. Bertoni, and Sherita H.

Golden. 2019. ‘Glycemic Markers and Subclinical Cardiovascular Disease: The Jackson Heart Study’. *Circulation: Cardiovascular Imaging* 12 (3): 8641. https://doi.org/10.1161/CIRCIMAGING.118.008641.

EFSA. 2017. ‘Dietary Reference Values for Nutrients Summary Report’. *EFSA Supporting Publications* 14 (12). https://doi.org/10.2903/sp.efsa.2017.e15121.

Elortegui Pascual, Paloma, Maryann R. Rolands, Alison L. Eldridge, Amira Kassis, Fabio Mainardi, L. Kim-Anne, Leonidas G. Karagounis, Philipp Gut, and Krista A. Varady. 2023. ‘A Meta-Analysis Comparing the Effectiveness of Alternate Day Fasting, the 5:2 Diet, and Time-Restricted Eating for Weight Loss’. *Obesity* 31 (S1): 9–21. https://doi.org/10.1002/OBY.23568.

Fakhrzadeh, H., B. Larijani, M. Sanjari, R. Baradar-Jalili, and M. R. Amini. 2003. ‘Effect of Ramadan Fasting on Clinical and Biochemical Parameters in Healthy Adults’. *Annals of Saudi Medicine* 23 (3–4): 223–26. https://doi.org/10.5144/0256-4947.2003.223.

Faris, Mo’ez Al Islam, Haitham Jahrami, Ahmed BaHammam, Zaina Kalaji, Mohammed Madkour, and Mohamed Hassanein. 2020. ‘A Systematic Review, Meta-Analysis, and Meta-Regression of the Impact of Diurnal Intermittent Fasting during Ramadan on Glucometabolic Markers in Healthy Subjects’. *Diabetes Research and Clinical Practice* 165: 108226. https://doi.org/10.1016/j.diabres.2020.108226.

‘Fat-Water Chemical Shift - Questions and Answers in MRI’. 2021. 2021. https://www.mriquestions.com/f-w-chemical-shift.html.

Fedorov, Andriy, Reinhard Beichel, Jayashree Kalpathy-Cramer, Julien Finet, Jean-Christophe Fillion-Robin, Sonia Pujol, Christian Bauer, et al. 2012. ‘3D Slicer as

an Image Computing Platform for the Quantitative Imaging Network'. *Magn Reson Imaging* 30 (9): 1323–41. https://doi.org/10.1016/j.mri.2012.05.001.

Fernando, Hamish A., Jessica Zibellini, Rebecca A. Harris, Radhika v. Seimon, and Amanda Sainsbury. 2019. 'Effect of Ramadan Fasting on Weight and Body Composition in Healthy Non-Athlete Adults: A Systematic Review and Meta-Analysis'. *Nutrients* 11 (2): 1–24. https://doi.org/10.3390/nu11020478.

Fischmann, Arne, Selina Kaspar, Julia Reinhardt, Monika Gloor, Christoph Stippich, and Dirk Fischer. 2012. 'Exercise Might Bias Skeletal-Muscle Fat Fraction Calculation from Dixon Images'. *Neuromuscular Disorders* 22 (SUPPL. 2): S107–10. https://doi.org/10.1016/j.nmd.2012.05.014.

Franchi, M. v., S. Longo, J. Mallinson, J. I. Quinlan, T. Taylor, P. L. Greenhaff, and M. v. Narici. 2018. 'Muscle Thickness Correlates to Muscle Cross-Sectional Area in the Assessment of Strength Training-Induced Hypertrophy'. *Scandinavian Journal of Medicine & Science in Sports* 28 (3): 846–53. https://doi.org/10.1111/sms.12961.

Frittoli, Barbara, Martina Bertuletti, Valentina Angelini, Luigi Grazioli, and " Federico. 2020. 'Case Series: Clinical Application in Liver Fat and Iron Quantification Using LiverLab'. *Siemens*, no. 76.

Gannon, Mary C., Frank Q. Nuttall, Asad Saeed, Kelly Jordan, and Heidi Hoover. 2003. 'An Increase in Dietary Protein Improves the Blood Glucose Response in Persons with Type 2 Diabetes'. *American Journal of Clinical Nutrition* 78 (4): 734–41. https://doi.org/10.1093/ajcn/78.4.734.

Gao, Yangfan, Kostas Tsintzas, Ian A. Macdonald, Sally M. Cordon, and Moira A. Taylor. 2022. 'Effects of Intermittent (5:2) or Continuous Energy Restriction on

Basal and Postprandial Metabolism: A Randomised Study in Normal-Weight, Young Participants'. *European Journal of Clinical Nutrition* 76 (1): 65–73. https://doi.org/10.1038/S41430-021-00909-2.

Gemmink, Anne, Madeleen Bosma, Helma J.H. Kuijpers, Joris Hoeks, Gert Schaart, Marc A.M.J. van Zandvoort, Patrick Schrauwen, and Matthijs K.C. Hesselink. 2016. 'Decoration of Intramyocellular Lipid Droplets with PLIN5 Modulates Fasting-Induced Insulin Resistance and Lipotoxicity in Humans'. *Diabetologia* 59 (5): 1040–48. https://doi.org/10.1007/s00125-016-3865-z.

Gibson, A. A., R. V. Seimon, C. M.Y. Lee, J. Ayre, J. Franklin, T. P. Markovic, I. D. Caterson, and A. Sainsbury. 2015. 'Do Ketogenic Diets Really Suppress Appetite? A Systematic Review and Meta-Analysis'. *Obesity Reviews : An Official Journal of the International Association for the Study of Obesity* 16 (1): 64–76. https://doi.org/10.1111/OBR.12230.

Gloor, Monika, Susanne Fasler, Tanja Haas, Oliver Bieri, Klaus Scheffler, and Dirk Fischer. 2010. 'Quantification of Fat Infiltration in Thigh and Calf Muscles in Oculopharyngeal Muscular Dystrophy : Comparison of Three MRI Methods'. *Proc Intl Soc Magn Reson Med* 18: 2010.

Goodpaster, Bret H., F. Leland Thaete, and David E. Kelley. 2000. 'Thigh Adipose Tissue Distribution Is Associated with Insulin Resistance in Obesity and in Type 2 Diabetes Mellitus'. *The American Journal of Clinical Nutrition* 71 (4): 885–92. https://doi.org/10.1093/AJCN/71.4.885.

Graessner, Joachim. 2013. 'Bandwidth in MRI? MAGNETOM Flash'. *Siemens Healthcare*, 3–8. www.siemens.com/magnetom-world.

Grande, Filippo del, Francesco Santini, Daniel A. Herzka, Michael R. Aro, Cooper W. Dean, Garry E. Gold, and John A. Carrino. 2014. 'Fat-Suppression Techniques for 3-T MR Imaging of the Musculoskeletal System'. *Radiographics : A Review Publication of the Radiological Society of North America, Inc* 34 (1): 217–33. https://doi.org/10.1148/RG.341135130.

Grimm, Alexandra, Heiko Meyer, Marcel D. Nickel, Mathias Nittka, Esther Raithel, Oliver Chaudry, Andreas Friedberger, et al. 2018. 'Evaluation of 2-Point, 3-Point, and 6-Point Dixon Magnetic Resonance Imaging with Flexible Echo Timing for Muscle Fat Quantification'. *European Journal of Radiology* 103 (March): 57–64. https://doi.org/10.1016/j.ejrad.2018.04.011.

Guerini, Henri, Patrick Omoumi, François Guichoux, Valérie Vuillemin, Gérard Morvan, Marc Zins, Fabrice Thevenin, and Jean Luc Drape. 2015. 'Fat Suppression with Dixon Techniques in Musculoskeletal Magnetic Resonance Imaging: A Pictorial Review'. *Seminars in Musculoskeletal Radiology* 19 (4): 335–47. https://doi.org/10.1055/s-0035-1565913.

Hamrick, Mark W., Meghan E. McGee-Lawrence, and Danielle M. Frechette. 2016. 'Fatty Infiltration of Skeletal Muscle: Mechanisms and Comparisons with Bone Marrow Adiposity'. *Frontiers in Endocrinology* 7 (June): 1–7. https://doi.org/10.3389/fendo.2016.00069.

Hanif, S., S. N. Ali, M. Hassanein, K. Khunti, and W. Hanif. 2020. 'Managing People with Diabetes Fasting for Ramadan During the COVID-19 Pandemic: A South Asian Health Foundation Update'. *Diabetic Medicine* 37 (7): 1094–1102. https://doi.org/10.1111/DME.14312.

Hatori, Megumi, Christopher Vollmers, Amir Zarrinpar, Luciano DiTacchio, Eric A. Bushong, Shubhroz Gill, Mathias Leblanc, et al. 2012. 'Time-Restricted Feeding without Reducing Caloric Intake Prevents Metabolic Diseases in Mice Fed a High-Fat Diet'. *Cell Metabolism* 15 (6): 848–60. https://doi.org/10.1016/j.cmet.2012.04.019.

Hoeks, Joris, Noud A. van Herpen, Marco Mensink, Esther Moonen-Kornips, Denis van Beurden, Matthijs K.C. Hesselink, and Patrick Schrauwen. 2010. 'Prolonged Fasting Identifies Skeletal Muscle Mitochondrial Dysfunction as Consequence Rather Than Cause of Human Insulin Resistance'. *Diabetes* 59 (9): 2117–25. https://doi.org/10.2337/DB10-0519.

Hogrel, Jean Yves, Yoann Barnouin, Noura Azzabou, Gillian Butler-Browne, Thomas Voit, Amélie Moraux, Gaëlle Leroux, Anthony Behin, Jamie S. McPhee, and Pierre G. Carlier. 2015. 'NMR Imaging Estimates of Muscle Volume and Intramuscular Fat Infiltration in the Thigh: Variations with Muscle, Gender, and Age'. *Age* 37 (3): 1–11. https://doi.org/10.1007/s11357-015-9798-5.

Howald, Hans, Chris Boesch, Roland Kreis, Sibylle Matter, Rudolf Billeter, Birgitta Essen-Gustavsson, and Hans Hoppeler. 2002. 'Content of Intramyocellular Lipids Derived by Electron Microscopy, Biochemical Assays, and (1)H-MR Spectroscopy.' *Journal of Applied Physiology (Bethesda, Md. : 1985)* 92 (6): 2264–72. https://doi.org/10.1152/japplphysiol.01174.2001.

Hu, H. H., and H. E. Kan. 2013. 'Quantitative Proton MR Techniques for Measuring Fat'. *NMR in Biomedicine* 26 (12): 1609–29. https://doi.org/10.1002/nbm.3025.

Hutchison, Amy T., Prashant Regmi, Emily N.C. Manoogian, Jason G. Fleischer, Gary A. Wittert, Satchidananda Panda, and Leonie K. Heilbronn. 2019. 'Time-

Restricted Feeding Improves Glucose Tolerance in Men at Risk for Type 2 Diabetes: A Randomized Crossover Trial'. *Obesity (Silver Spring, Md.)* 27 (5): 724–32. https://doi.org/10.1002/OBY.22449.

Hwang, Jong Hee, Daniel T. Stein, Nir Barzilai, Min Hui Cui, Julia Tonelli, Preeti Kishore, and Meredith Hawkins. 2007. 'Increased Intrahepatic Triglyceride Is Associated with Peripheral Insulin Resistance: In Vivo MR Imaging and Spectroscopy Studies'. *American Journal of Physiology. Endocrinology and Metabolism* 293 (6). https://doi.org/10.1152/AJPENDO.00590.2006.

Ikemoto-Uezumi, Madoka, Yasumoto Matsui, Masaki Hasegawa, Remi Fujita, Yasuhide Kanayama, Akiyoshi Uezumi, Tsuyoshi Watanabe, Atsushi Harada, A. Robin Poole, and Naohiro Hashimoto. 2017. 'Disuse Atrophy Accompanied by Intramuscular Ectopic Adipogenesis in Vastus Medialis Muscle of Advanced Osteoarthritis Patients'. *The American Journal of Pathology* 187 (12): 2674–85. https://doi.org/10.1016/J.AJPATH.2017.08.009.

Jameson, Tom S.O., Sean P. Kilroe, Jonathan Fulford, Doaa R. Abdelrahman, Andrew J. Murton, Marlou L. Dirks, Francis B. Stephens, and Benjamin T. Wall. 2021. 'Muscle Damaging Eccentric Exercise Attenuates Disuse-Induced Declines in Daily Myofibrillar Protein Synthesis and Transiently Prevents Muscle Atrophy in Healthy Men'. *American Journal of Physiology - Endocrinology and Metabolism* 321 (5): E674–88. https://doi.org/10.1152/ajpendo.00294.2021.

Jamshed, Humaira, Robbie A. Beyl, Deborah L.Della Manna, Eddy S. Yang, Eric Ravussin, and Courtney M. Peterson. 2019. 'Early Time-Restricted Feeding Improves 24-Hour Glucose Levels and Affects Markers of the Circadian Clock,

Aging, and Autophagy in Humans'. *Nutrients 2019, Vol. 11, Page 1234* 11 (6): 1234. https://doi.org/10.3390/NU11061234.

Johannsen, Darcy L., Kevin E. Conley, Sudip Bajpeyi, Mark Punyanitya, Dympna Gallagher, Zhengyu Zhang, Jeffrey Covington, Steven R. Smith, and Eric Ravussin. 2012. 'Ectopic Lipid Accumulation and Reduced Glucose Tolerance in Elderly Adults Are Accompanied by Altered Skeletal Muscle Mitochondrial Activity'. *Journal of Clinical Endocrinology and Metabolism* 97 (1): 242–50. https://doi.org/10.1210/jc.2011-1798.

Johnson, Nathan A., Stephen R. Stannard, David S. Rowlands, Phillip G. Chapman, Campbell H. Thompson, Helen O'Connor, Toos Sachinwalla, and Martin W. Thompson. 2006. 'Effect of Short-Term Starvation versus High-Fat Diet on Intramyocellular Triglyceride Accumulation and Insulin Resistance in Physically Fit Men'. *Experimental Physiology* 91 (4): 693–703. https://doi.org/10.1113/EXPPHYSIOL.2006.033399.

Kalyani, Rita R., E. Jeffrey Metter, Ramona Ramachandran, Chee W. Chia, Christopher D. Saudek, and Luigi Ferrucci. 2012. 'Glucose and Insulin Measurements From the Oral Glucose Tolerance Test and Relationship to Muscle Mass'. *The Journals of Gerontology Series A: Biological Sciences and Medical Sciences* 67A (1): 74–81. https://doi.org/10.1093/gerona/glr022.

Karlsson, Anette, Johannes Rosander, Thobias Romu, Joakim Tallberg, Anders Grönqvist, Magnus Borga, and Olof Dahlqvist Leinhard. 2015. 'Automatic and Quantitative Assessment of Regional Muscle Volume by Multi-Atlas Segmentation Using Whole-Body Water-Fat MRI'. *Journal of Magnetic Resonance Imaging* 41 (6): 1558–69. https://doi.org/10.1002/jmri.24726.

Keirns, Bryant H., Christina M. Sciarrillo, Nicholas A. Koemel, and Sam R. Emerson. 2021. ‘Fasting, Non-Fasting and Postprandial Triglycerides for Screening Cardiometabolic Risk’. *Journal of Nutritional Science* 10 (September): 1–14. https://doi.org/10.1017/JNS.2021.73.

Khan, Alam, and M Muzaffar Ali Khan Khattak. 2002. ‘Islamic Fasting: An Effective Strategy for Prevention and Control of Obesity’. *Pakistan Journal of Nutrition* 1 (4): 185–87.

Khan, Nazeer, Abdur Rasheed, Hassaan Ahmed, Faiza Aslam, and Fatima Kanwal. 2017. ‘Effect of Ramadan Fasting on Glucose Level, Lipid Profile, HbA1c and Uric Acid among Medical Students in Karachi, Pakistan’. *Eastern Mediterranean Health Journal* 23 (4): 274–79. https://doi.org/10.26719/2017.23.4.274.

Kilroe, Sean P., Jonathan Fulford, Sarah R. Jackman, Luc J.C. Van Loon, and Benjamin T. Wall. 2020. ‘Temporal Muscle-Specific Disuse Atrophy during One Week of Leg Immobilization’. *Medicine and Science in Sports and Exercise* 52 (4): 944–54. https://doi.org/10.1249/MSS.0000000000002200.

Kim, Jung Eun, Keagan Dunville, Junjie Li, Ji Xin Cheng, Travis B. Conley, Cortni S. Couture, and Wayne W. Campbell. 2017. ‘Intermuscular Adipose Tissue Content and Intramyocellular Lipid Fatty Acid Saturation Are Associated with Glucose Homeostasis in Middle-Aged and Older Adults’. *Endocrinology and Metabolism* 32 (2): 257–64. https://doi.org/10.3803/EnM.2017.32.2.257.

Komolka, Katrin, Elke Albrecht, Klaus Wimmers, Jennifer J. Michal, and Steffen Maak. 2014. ‘Molecular Heterogeneities of Adipose Depots - Potential Effects on Adipose-Muscle Cross-Talk in Humans, Mice and Farm Animals’. *Journal of Genomics* 2: 31–44. https://doi.org/10.7150/jgen.5260.

Kovanlikaya, Arzu, Steven D. Mittelman, Andrette Ward, Mitchell E. Geffner, Frederick Dorey, and Vicente Gilsanz. 2005. 'Obesity and Fat Quantification in Lean Tissues Using Three-Point Dixon MR Imaging'. *Pediatric Radiology* 35 (6): 601–7. https://doi.org/10.1007/s00247-005-1413-y.

Krššák, Martin, Lucas Lindeboom, Vera Schrauwen-Hinderling, Lidia S Szczepaniak, Wim Derave, Jesper Lundbom, Douglas Befroy, et al. 2021. 'Proton Magnetic Resonance Spectroscopy in Skeletal Muscle: Experts' Consensus Recommendations'. *NMR in Biomedicine* 34 (5). https://doi.org/10.1002/nbm.4266.

Kul, Seval, Esen Savaş, Zeynel Abidin Öztürk, and Gülendam Karadağ. 2014. 'Does Ramadan Fasting Alter Body Weight and Blood Lipids and Fasting Blood Glucose in a Healthy Population? A Meta-Analysis'. *Journal of Religion and Health* 53 (3): 929–42. https://doi.org/10.1007/s10943-013-9687-0.

Lang, Pierre Olivier, Christophe Trivalle, Thomas Vogel, Jacques Proust, and Jean Pierre Papazian. 2015. 'Markers of Metabolic and Cardiovascular Health in Adults: Comparative Analysis of DEXA-Based Body Composition Components and BMI Categories'. *Journal of Cardiology* 65 (1): 42–49. https://doi.org/10.1016/J.JJCC.2014.03.010.

Larijani, B, F Zahedi, M Sanjari, M R Amini, R B Jalili, H Adibi, and A R Vassigh. 2003. 'The Effect of Ramadan Fasting on Fasting Serum Glucose in Healthy Adults'. *Med J Malaysia* 58 (5): 678–80.

Lessan, N., Z. Hannoun, H. Hasan, and M. T. Barakat. 2015. 'Glucose Excursions and Glycaemic Control during Ramadan Fasting in Diabetic Patients: Insights

from Continuous Glucose Monitoring (CGM)'. *Diabetes & Metabolism* 41 (1): 28–36. https://doi.org/10.1016/J.DIABET.2014.11.004.

Lettner, Angelika, and Michael Roden. 2008. 'Ectopic Fat and Insulin Resistance'. *Current Diabetes Reports 2008 8:3* 8 (3): 185–91. https://doi.org/10.1007/S11892-008-0032-Z.

Lindeboom, Lucas, and Robin A. de Graaf. 2018. 'Measurement of Lipid Composition in Human Skeletal Muscle and Adipose Tissue with 1 H-MRS Homonuclear Spectral Editing'. *Magnetic Resonance in Medicine* 79 (2): 619–27. https://doi.org/10.1002/MRM.26740.

Lloyd-Jones, Graham. 2017. 'MRI Interpretation - T1 v T2 Images'. Salisbury NHS Foundation Trust UK. 2017. https://www.radiologymasterclass.co.uk/tutorials/mri/t1_and_t2_images.

Loher, Hannah, Roland Kreis, Chris Boesch, and Emanuel Christ. 2016. 'The Flexibility of Ectopic Lipids'. *International Journal of Molecular Sciences* 17 (12): 1554. https://doi.org/10.3390/ijms17091554.

Longo, Valter D., and Mark P. Mattson. 2014. 'Fasting: Molecular Mechanisms and Clinical Applications'. *Cell Metabolism* 19 (2): 181–92. https://doi.org/10.1016/j.cmet.2013.12.008.

Lowe, Dylan A., Nancy Wu, Linnea Rohdin-Bibby, A. Holliston Moore, Nisa Kelly, Yong En Liu, Errol Philip, et al. 2020. 'Effects of Time-Restricted Eating on Weight Loss and Other Metabolic Parameters in Women and Men with Overweight and Obesity: The TREAT Randomized Clinical Trial'. *JAMA Internal Medicine* 180 (11): 1491–99. https://doi.org/10.1001/jamainternmed.2020.4153.

Luukkonen, Panu K., Sanja Sädevirta, You Zhou, Brandon Kayser, Ashfaq Ali, Linda Ahonen, Susanna Lallukka, et al. 2018. 'Saturated Fat Is More Metabolically Harmful for the Human Liver Than Unsaturated Fat or Simple Sugars'. *Diabetes Care* 41 (8): 1732–39. https://doi.org/10.2337/DC18-0071.

Manini, Todd M, Brian C Clark, Michael A Nalls, Bret H Goodpaster, Lori L Ploutz-Snyder, and Tamara B Harris. 2007. 'Reduced Physical Activity Increases Intermuscular Adipose Tissue in Healthy Young Adults'. *The American Journal of Clinical Nutrition* 85 (2): 377–84. https://doi.org/10.1093/ajcn/85.2.377.

Marcus, R. L., O. Addison, J. P. Kidde, L. E. Dibble, and P. C. Lastayo. 2010. 'SKELETAL MUSCLE FAT INFILTRATION: IMPACT OF AGE, INACTIVITY, AND EXERCISE'. *The Journal of Nutrition, Health & Aging* 14 (5): 362. https://doi.org/10.1007/S12603-010-0081-2.

Marra, Marco A., Linda Heskamp, Karlien Mul, Saskia Lassche, Baziel G.M. van Engelen, Arend Heerschap, and Nico Verdonschot. 2018. 'Specific Muscle Strength Is Reduced in Facioscapulohumeral Dystrophy: An MRI Based Musculoskeletal Analysis'. *Neuromuscular Disorders* 28 (3): 238–45. https://doi.org/10.1016/j.nmd.2017.11.017.

Martens, Christopher R., Matthew J. Rossman, Melissa R. Mazzo, Lindsey R. Jankowski, Erzsebet E. Nagy, Blair A. Denman, James J. Richey, et al. 2020. 'Short-Term Time-Restricted Feeding Is Safe and Feasible in Non-Obese Healthy Midlife and Older Adults'. *GeroScience* 42 (2): 667–86. https://doi.org/10.1007/S11357-020-00156-6/METRICS.

Matsumura, Noboru, Sota Oguro, Shigeo Okuda, Masahiro Jinzaki, Morio Matsumoto, Masaya Nakamura, and Takeo Nagura. 2017. 'Quantitative

Assessment of Fatty Infiltration and Muscle Volume of the Rotator Cuff Muscles Using 3-Dimensional 2-Point Dixon Magnetic Resonance Imaging'. *Journal of Shoulder and Elbow Surgery* 26 (10): e309–18. https://doi.org/10.1016/J.JSE.2017.03.019.

Matthews, D. R., J. P. Hosker, A. S. Rudenski, B. A. Naylor, D. F. Treacher, and R. C. Turner. 1985. 'Homeostasis Model Assessment: Insulin Resistance and β-Cell Function from Fasting Plasma Glucose and Insulin Concentrations in Man'. *Diabetologia* 28 (7): 412–19. https://doi.org/10.1007/BF00280883.

McAllister, Matthew J., Brandon L. Pigg, Liliana I. Renteria, and Hunter S. Waldman. 2020. 'Time-Restricted Feeding Improves Markers of Cardiometabolic Health in Physically Active College-Age Men: A 4-Week Randomized Pre-Post Pilot Study'. *Nutrition Research* 75 (March): 32–43. https://doi.org/10.1016/J.NUTRES.2019.12.001.

McCarthy, David, and Aloys Berg. 2021. 'Weight Loss Strategies and the Risk of Skeletal Muscle Mass Loss'. *Nutrients 2021, Vol. 13, Page 2473* 13 (7): 2473. https://doi.org/10.3390/NU13072473.

Mccurdy, Colin M. 2014. 'Fully Automated Segmentation and Quantification of Abdominal Adipose Tissue Compartments in Mouse MRI', no. September.

McHale, Matthew J., Zaheer U. Sarwar, Damon P. Cardenas, Laurel Porter, Anna S. Salinas, Joel E. Michalek, Linda M. McManus, and Paula K. Shireman. 2012. 'Increased Fat Deposition in Injured Skeletal Muscle Is Regulated by Sex-Specific Hormones'. *American Journal of Physiology - Regulatory Integrative and Comparative Physiology* 302 (3): 331–39. https://doi.org/10.1152/AJPREGU.00427.2011.

McMahon, Katie L., Gary Cowin, and Graham Galloway. 2011. ‘Magnetic Resonance Imaging: The Underlying Principles’. *Journal of Orthopaedic and Sports Physical Therapy* 41 (11): 806–19. https://doi.org/10.2519/jospt.2011.3576.

Meer, Rutger W. van der, Sebastiaan Hammer, Johannes W.A. Smit, Marijke Frölich, Jeroen J. Bax, Michaela Diamant, Luuk J. Rijzewijk, Albert de Roos, Johannes A. Romijn, and Hildo J. Lamb. 2007. ‘Short-Term Caloric Restriction Induces Accumulation of Myocardial Triglycerides and Decreases Left Ventricular Diastolic Function in Healthy Subjects’. *Diabetes* 56 (12): 2849–53. https://doi.org/10.2337/db07-0768.

Merz, Karla E., and Debbie C. Thurmond. 2020. ‘Role of Skeletal Muscle in Insulin Resistance and Glucose Uptake’. *Comprehensive Physiology* 10 (3): 785–809. https://doi.org/10.1002/CPHY.C190029.

Mindikoglu, Ayse L., Mustafa M. Abdulsada, Antrix Jain, Jong Min Choi, Prasun K. Jalal, Sridevi Devaraj, Melissa P. Mezzari, Joseph F. Petrosino, Antone R. Opekun, and Sung Yun Jung. 2020. ‘Intermittent Fasting from Dawn to Sunset for 30 Consecutive Days Is Associated with Anticancer Proteomic Signature and Upregulates Key Regulatory Proteins of Glucose and Lipid Metabolism, Circadian Clock, DNA Repair, Cytoskeleton Remodeling, Immune System’. *Journal of Proteomics* 217 (April). https://doi.org/10.1016/j.jprot.2020.103645.

Mindikoglu, Ayse L., Antone R. Opekun, Sood K. Gagan, and Sridevi Devaraj. 2017. ‘Impact of Time-Restricted Feeding and Dawn-to-Sunset Fasting on Circadian Rhythm, Obesity, Metabolic Syndrome, and Nonalcoholic Fatty Liver Disease’. *Gastroenterology Research and Practice* 2017: 1–13. https://doi.org/10.1155/2017/3932491.

Mohammadzade, Fatemeh, Mohammad Ali Vakili, Alireza Seyediniaki, Saeed Amirkhanloo, Mehran Farajolahi, Hamideh Akbari, and Samira Eshghinia. 2017. 'Effect of Prolonged Intermittent Fasting in Ramadan on Biochemical and Inflammatory Parameters of Healthy Men'. *Journal of Clinical and Basic Research* 1 (1): 38–46. https://doi.org/10.18869/acadpub.jcbr.1.1.38.

Moller, Louise, Hans Stodkilde-Jorgensen, Finn T. Jensen, and Jens O.L. Jorgensen. 2008. 'Fasting in Healthy Subjects Is Associated with Intrahepatic Accumulation of Lipids as Assessed by 1H-Magnetic Resonance Spectroscopy'. *Clinical Science* 114 (8): 547–52. https://doi.org/10.1042/CS20070217.

Morales, Pablo Esteban, Jose Luis Bucarey, and Alejandra Espinosa. 2017. 'Muscle Lipid Metabolism: Role of Lipid Droplets and Perilipins'. *Journal of Diabetes Research* 2017. https://doi.org/10.1155/2017/1789395.

Moser, Ewald, Andreas Stadlbauer, Christian Windischberger, Harald H Quick, and Mark E Ladd. 2009. 'Magnetic Resonance Imaging Methodology'. *European Journal of Nuclear Medicine and Molecular Imaging* 36 (SUPPL. 1): 30–41. https://doi.org/10.1007/s00259-008-0938-3.

MR-TIP.com. n.d. 'MRI Artifacts - Field Inhomogeneity Artifact - MR-TIP.Com'. SoftWays' Medical Imaging Group. Accessed 9 August 2022. https://www.mr-tip.com/serv1.php?type=art&sub=Field Inhomogeneity Artifact.

Muhaimin, Muhaimin, Sensusiati A.D, Kartikasari A, Muqmiroh L, and Latifah R. 2019. 'Pulse Sequence 3D WATS for Evaluation Of The Anterior Cruciate Ligament (ACL) Nd Posterior Cruciate Ligament (PCL) on MRI Knee'. In , 469–74. Scitepress. https://doi.org/10.5220/0007545204690474.

Müller, M. J., M. Lagerpusch, J. Enderle, B. Schautz, M. Heller, and A. Bosy-Westphal. 2012. 'Beyond the Body Mass Index: Tracking Body Composition in the Pathogenesis of Obesity and the Metabolic Syndrome'. *Obesity Reviews* 13 (SUPPL.2): 6–13. https://doi.org/10.1111/J.1467-789X.2012.01033.X.

Nachvak, Seyed Mostafa, Yahya Pasdar, Sondos Pirsaheb, Mitra Darbandi, Parisa Niazi, Roghayeh Mostafai, and John R. Speakman. 2018. 'Effects of Ramadan on Food Intake, Glucose Homeostasis, Lipid Profiles and Body Composition Composition'. *European Journal of Clinical Nutrition* 73 (4): 594–600. https://doi.org/10.1038/s41430-018-0189-8.

Narayan, Sreenath, Chris A. Flask, Satish C. Kalhan, and David L. Wilson. 2015. 'Hepatic Fat during Fasting and Refeeding by MRI Fat Quantification'. *Journal of Magnetic Resonance Imaging* 41 (2): 347–53. https://doi.org/10.1002/jmri.24616.

Norouzy, A., M. Salehi, E. Philippou, H. Arabi, F. Shiva, S. Mehrnoosh, S. M.R. Mohajeri, S. A.Reza Mohajeri, A. Motaghedi Larijani, and M. Nematy. 2013. 'Effect of Fasting in Ramadan on Body Composition and Nutritional Intake: A Prospective Study'. *Journal of Human Nutrition and Dietetics* 26 (SUPPL.1): 97–104. https://doi.org/10.1111/jhn.12042.

Oh, Minsuk, Sue Kim, Ki Yong An, Jihee Min, Hyuk In Yang, Junga Lee, Mi Kyung Lee, et al. 2018. 'Effects of Alternate Day Calorie Restriction and Exercise on Cardio-Metabolic Risk Factors in Overweight and Obese Adults: An Exploratory Randomized Controlled Study'. *BMC Public Health* 18 (1). https://doi.org/10.1186/S12889-018-6009-1.

Ongsara, Sara, Sakulrat Boonpol, Nussaree Prompalad, and Nutjaree Jeenduang. 2017. ‘The Effect of Ramadan Fasting on Biochemical Parameters in Healthy Thai Subjects’. *Journal of Clinical and Diagnostic Research* 11 (9): BC14–18. https://doi.org/10.7860/JCDR/2017/27294.10634.

Pagano, Allan F., Thomas Brioche, Coralie Arc-Chagnaud, Rémi Demangel, Angèle Chopard, and Guillaume Py. 2018. ‘Short-Term Disuse Promotes Fatty Acid Infiltration into Skeletal Muscle’. *Journal of Cachexia, Sarcopenia and Muscle* 9 (2): 335–47. https://doi.org/10.1002/jcsm.12259.

Parameswaran Rajeev. 2022. ‘Assessment of Hypercalcaemia - Differential Diagnosis of Symptoms | BMJ Best Practice’. 7 June 2022. https://bestpractice.bmj.com/topics/en-gb/159.

Pavey, Toby G., Sjaan R. Gomersall, Bronwyn K. Clark, and Wendy J. Brown. 2016. ‘The Validity of the GENEActiv Wrist-Worn Accelerometer for Measuring Adult Sedentary Time in Free Living’. *Journal of Science and Medicine in Sport* 19 (5): 395–99. https://doi.org/10.1016/J.JSAMS.2015.04.007.

Peeke, Pamela M., Frank L. Greenway, Sonja K. Billes, Dachuan Zhang, and Ken Fujioka. 2021. ‘Effect of Time Restricted Eating on Body Weight and Fasting Glucose in Participants with Obesity: Results of a Randomized, Controlled, Virtual Clinical Trial’. *Nutrition and Diabetes* 11 (1). https://doi.org/10.1038/s41387-021-00149-0.

Pieńkowska, Joanna, Beata Brzeska, Mariusz Kaszubowski, Oliwia Kozak, Anna Jankowska, and Edyta Szurowska. 2020. ‘The Correlation between the MRI-Evaluated Ectopic Fat Accumulation and the Incidence of Diabetes Mellitus and Hypertension Depends on Body Mass Index and Waist Circumference Ratio’.

PLOS ONE 15 (1): e0226889. https://doi.org/10.1371/JOURNAL.PONE.0226889.

Piercy, Katrina L., Richard P. Troiano, Rachel M. Ballard, Susan A. Carlson, Janet E. Fulton, Deborah A. Galuska, Stephanie M. George, and Richard D. Olson. 2018. 'The Physical Activity Guidelines for Americans'. *JAMA* 320 (19): 2020–28. https://doi.org/10.1001/JAMA.2018.14854.

Pola, Arunima, Suresh Anand Sadananthan, Jadegoud Yaligar, Vijayasarathi Nagarajan, Weiping Han, Philip W. Kuchel, and S. Sendhil Velan. 2012. 'Skeletal Muscle Lipid Metabolism Studied by Advanced Magnetic Resonance Spectroscopy'. *Progress in Nuclear Magnetic Resonance Spectroscopy* 65: 66–76. https://doi.org/10.1016/j.pnmrs.2012.02.002.

Pons, Christelle, Bhushan Borotikar, Marc Garetier, Valérie Burdin, Douraied Ben Salem, Mathieu Lempereur, and Sylvain Brochard. 2018. 'Quantifying Skeletal Muscle Volume and Shape in Humans Using MRI: A Systematic Review of Validity and Reliability'. *PLoS ONE* 13 (11). https://doi.org/10.1371/journal.pone.0207847.

Preim, Bernhard, and Charl Botha. 2014. 'Image Analysis for Medical Visualization'. In *Visual Computing for Medicine*, 111–75. Morgan Kaufmann. https://doi.org/10.1016/b978-0-12-415873-3.00004-3.

Reeder, Scott B., Angel R. Pineda, Zhifei Wen, Ann Shimakawa, Huanzhou Yu, Jean H. Brittain, Garry E. Gold, Christopher H. Beaulieu, and Norbert T. Pelc. 2005. 'Iterative Decomposition of Water and Fat with Echo Asymmetry and Least-Squares Estimation (IDEAL): Application with Fast Spin-Echo Imaging'.

Magnetic Resonance in Medicine 54 (3): 636–44. https://doi.org/10.1002/MRM.20624.

Regmi, Prashant, and Leonie K. Heilbronn. 2020. 'Time-Restricted Eating: Benefits, Mechanisms, and Challenges in Translation'. *IScience* 23 (6): 101161. https://doi.org/10.1016/J.ISCI.2020.101161.

Rennie, M. J., R. H.T. Edwards, D. Halliday, D. E. Matthews, S. L. Wolman, and D. J. Millward. 1982. 'Muscle Protein Synthesis Measured by Stable Isotope Techniques in Man: The Effects of Feeding and Fasting'. *Clinical Science* 63 (6): 519–23. https://doi.org/10.1042/CS0630519.

Rigby, Sarah H., and Kathleen B. Schwarz. 2001. 'Nutrition and Liver Disease'. In *Nutrition in the Prevention and Treatment of Disease*, edited by ELAINE R. MONSEN ANN M. COULSTON, CHERYL L. ROCK, 601–13. Elsevier. https://doi.org/10.1016/B978-012193155-1/50041-6.

Röder, Pia v., Bingbing Wu, Yixian Liu, and Weiping Han. 2016. 'Pancreatic Regulation of Glucose Homeostasis'. *Experimental & Molecular Medicine* 48 (November 2015): e219. https://doi.org/10.1038/emm.2016.6.

Rothschild, Jeff, Kristin K. Hoddy, Pera Jambazian, and Krista A. Varady. 2014. 'Time-Restricted Feeding and Risk of Metabolic Disease: A Review of Human and Animal Studies'. *Nutrition Reviews* 72 (5): 308–18. https://doi.org/10.1111/nure.12104.

Roussel, Ronan, Léopold Fezeu, Nadine Bouby, Beverley Balkau, Olivier Lantieri, François Alhenc-Gelas, Michel Marre, and Lise Bankir. 2011. 'Low Water Intake and Risk for New-Onset Hyperglycemia'. *Diabetes Care* 34 (12): 2551–54. https://doi.org/10.2337/dc11-0652.

Ruan, Xiang Yan, Dympna Gallagher, Tamara Harris, Jeanine Albu, Steven Heymsfield, Patrick Kuznia, and Stanley Heshka. 2007. 'Estimating Whole Body Intermuscular Adipose Tissue from Single Cross-Sectional Magnetic Resonance Images'. *NIH* 102 (2): 748–54. https://doi.org/10.1152/japplphysiol.00304.2006.

Ruan, Yuting, Jiana Zhong, Rongping Chen, Zhen Zhang, Dixing Liu, Jia Sun, and Hong Chen. 2021. 'Association of Body Fat Percentage with Time in Range Generated by Continuous Glucose Monitoring during Continuous Subcutaneous Insulin Infusion Therapy in Type 2 Diabetes'. *Journal of Diabetes Research* 2021. https://doi.org/10.1155/2021/5551216.

Rui, Liangyou. 2014. 'Energy Metabolism in the Liver'. *Comprehensive Physiology* 4 (1): 177. https://doi.org/10.1002/CPHY.C130024.

Ruschke, Stefan, Hermine Kienberger, Thomas Baum, Hendrik Kooijman, Marcus Settles, Axel Haase, Michael Rychlik, Ernst J. Rummeny, and Dimitrios C. Karampinos. 2016. 'Diffusion-Weighted Stimulated Echo Acquisition Mode (DW-STEAM) MR Spectroscopy to Measure Fat Unsaturation in Regions with Low Proton-Density Fat Fraction'. *Magnetic Resonance in Medicine* 75 (1): 32–41. https://doi.org/10.1002/mrm.25578.

Ryan, Donna, and Martica Heaner. 2014. 'Preface to the Full Report'. *Obesity* 22 (S2): S1–3. https://doi.org/10.1002/OBY.20819.

Sadiya, Amena, Ahmed, Siddieg, Joy, and Carlsson. 2011. 'Effect of Ramadan Fasting on Metabolic Markers, Body Composition, and Dietary Intake in Emiratis of Ajman (UAE) with Metabolic Syndrome'. *Diabetes, Metabolic Syndrome and Obesity: Targets and Therapy*, December, 409. https://doi.org/10.2147/DMSO.S24221.

Saleh, Salhamoud Abdelfatah, Salah Anies Elsharouni, Boby Cherian, and M. Mourou. 2005. ‘Effects of Ramadan Fasting on Waist Circumference, Blood Pressure, Lipid Profile, and Blood Sugar on a Sample of Healthy Kuwaiti Men and Women’. *Malaysian Journal of Nutrition* 11 (2): 143–50. https://www.sid.ir/en/journal/ViewPaper.aspx?ID=232513.

Salgado, Ana Lúcia Farias De Azevedo, Luciana de Carvalho, Ana Claudia Oliveira, Virgínia Nascimento dos Santos, Jose Gilberto Vieira, and Edison Roberto Parise. 2010. ‘Insulin Resistance Index (HOMA-IR) in the Differentiation of Patients with Non-Alcoholic Fatty Liver Disease and Healthy Individuals’. *Arquivos de Gastroenterologia* 47 (2): 165–69. https://doi.org/10.1590/S0004-28032010000200009.

Santoleri, Dominic, and Paul M. Titchenell. 2019. ‘Resolving the Paradox of Hepatic Insulin Resistance’. *Cellular and Molecular Gastroenterology and Hepatology* 7 (2): 447–56. https://doi.org/10.1016/J.JCMGH.2018.10.016.

Santos, Heitor O., and Rodrigo C.O. Macedo. 2018. ‘Impact of Intermittent Fasting on the Lipid Profile: Assessment Associated with Diet and Weight Loss’. *Clinical Nutrition ESPEN* 24: 14–21. https://doi.org/10.1016/j.clnesp.2018.01.002.

Savage, David B., Laura Watson, Katie Carr, Claire Adams, Soren Brage, Krishna K. Chatterjee, Leanne Hodson, Chris Boesch, Graham J. Kemp, and Alison Sleigh. 2019. ‘Accumulation of Saturated Intramyocellular Lipid Is Associated with Insulin Resistance’. *Journal of Lipid Research* 60 (7): 1323–32. https://doi.org/10.1194/jlr.M091942.

Scheer, Frank A.J.L., Michael F. Hilton, Christos S. Mantzoros, and Steven A. Shea. 2009. ‘Adverse Metabolic and Cardiovascular Consequences of Circadian

Misalignment'. *Proceedings of the National Academy of Sciences of the United States of America* 106 (11): 4453–58. https://doi.org/10.1073/PNAS.0808180106.

Shetty, Anup S., Adam L. Sipe, Maria Zulfiqar, Richard Tsai, Demetrios A. Raptis, Constantine A. Raptis, and Sanjeev Bhalla. 2019. 'In-Phase and Opposed-Phase Imaging: Applications of Chemical Shift and Magnetic Susceptibility in the Chest and Abdomen'. *Radiographics* 39 (1): 115–35. https://doi.org/10.1148/rg.2019180043.

Sirirat, Rawiwan, Celine Heskey, Christine Wilson, Edward Bitok, Julie Jones, Abigail Clarke, and Joan Sabaté. 2020. 'A Comparison of Body Composition Measurements Between Bioelectrical Impedance Analysis (InBody 570) and Air Displacement Plethysmography (BOD POD®)'. *Current Developments in Nutrition* 4 (Suppl 2): 1689. https://doi.org/10.1093/CDN/NZAA063_087.

Sirotkin, V. A., D. v. Korolev, and A. E. Silakova. 2007. 'Hydration-Dehydration of Human Serum Albumin Studied by Isothermal Calorimetry and IR Spectroscopy'. *Russian Journal of Physical Chemistry A* 81 (8): 1341–45. https://doi.org/10.1134/S0036024407080298.

Snijder, M. B., M. Visser, J. M. Dekker, B. H. Goodpaster, T. B. Harris, S. B. Kritchevsky, N. De Rekeneire, et al. 2005. 'Low Subcutaneous Thigh Fat Is a Risk Factor for Unfavourable Glucose and Lipid Levels, Independently of High Abdominal Fat. The Health ABC Study'. *Diabetologia* 48 (2): 301–8. https://doi.org/10.1007/S00125-004-1637-7.

Soininen, Pasi, Antti J. Kangas, Peter Würtz, Teemu Suna, and Mika Ala-Korpela. 2015. 'Quantitative Serum Nuclear Magnetic Resonance Metabolomics in

Cardiovascular Epidemiology and Genetics'. *Circulation. Cardiovascular Genetics* 8 (1): 192–206. https://doi.org/10.1161/CIRCGENETICS.114.000216.

Soliman, Ghada A. 2022. 'Intermittent Fasting and Time-Restricted Eating Role in Dietary Interventions and Precision Nutrition'. *Frontiers in Public Health* 10 (May). https://doi.org/10.3389/FPUBH.2022.1017254.

Stannard, S. R., M. W. Thompson, K. Fairbairn, B. Huard, T. Sachinwalla, and C. H. Thompson. 2002. 'Fasting for 72 h Increases Intramyocellular Lipid Content in Nondiabetic, Physically Fit Men'. *American Journal of Physiology - Endocrinology and Metabolism* 283 (6 46-6): 1185–91. https://doi.org/10.1152/AJPENDO.00108.2002/ASSET/IMAGES/LARGE/H11221063005.JPEG.

Stephens, Francis B., Carolyn Chee, Benjamin T. Wall, Andrew J. Murton, Chris E. Shannon, Luc J.C. van Loon, and Kostas Tsintzas. 2015. 'Lipid-Induced Insulin Resistance Is Associated with an Impaired Skeletal Muscle Protein Synthetic Response to Amino Acid Ingestion in Healthy Young Men'. *Diabetes* 64 (5): 1615–20. https://doi.org/10.2337/db14-0961.

Stote, Kim S., David J. Baer, Karen Spears, David R. Paul, G. Keith Harris, William V. Rumpler, Pilar Strycula, et al. 2007. 'A Controlled Trial of Reduced Meal Frequency without Caloric Restriction in Healthy, Normal-Weight, Middle-Aged Adults'. *American Journal of Clinical Nutrition* 85 (4): 981–88. https://doi.org/10.1093/ajcn/85.4.981.

Stovall, Glenda. 2013. 'Muscle System Diagram Not Labeled : Biological Science Picture Directory – Pulpbits.Net'. PULPBITS. 2013. https://pulpbits.net/3-

breakdown-of-skeletal-muscle-tissue/skeletal-muscle-breakdown-what-are-muscles/.

Stump, Craig S., Erik J. Henriksen, Yongzhong Wei, and James R. Sowers. 2009. 'The Metabolic Syndrome: Role of Skeletal Muscle Metabolism'. *Https://Doi.Org/10.1080/07853890600888413* 38 (6): 389–402. https://doi.org/10.1080/07853890600888413.

Sujji, G Evelin, Y V S Lakshmi, and G Wiselin Jiji. 2013. 'MRI Brain Image Segmentation Based on Thresholding'. *International Journal of Advanced Computer Research* 3 (8): 1–5. http://wiselinjiji.com/journals/8.pdf.

Tamura, Yoshifumi, Yasushi Tanaka, Fumihiko Sato, Bock Choi Jong, Hirotaka Watada, Masataka Niwa, Junichiro Kinoshita, et al. 2005. 'Effects of Diet and Exercise on Muscle and Liver Intracellular Lipid Contents and Insulin Sensitivity in Type 2 Diabetic Patients'. *The Journal of Clinical Endocrinology & Metabolism* 90 (6): 3191–96. https://doi.org/10.1210/JC.2004-1959.

Thankamony, Ajay, Graham J. Kemp, Albert Koulman, Vlada Bokii, David B. Savage, Chris Boesch, Leanne Hodson, David B. Dunger, and Alison Sleigh. 2018. 'Compositional Marker in Vivo Reveals Intramyocellular Lipid Turnover during Fasting-Induced Lipolysis'. *Scientific Reports 2018 8:1* 8 (1): 1–8. https://doi.org/10.1038/s41598-018-21170-x.

Thomas, E. Louise, James R. Parkinson, Gary S. Frost, Anthony P. Goldstone, Caroline J. Doré, John P. McCarthy, Adam L. Collins, et al. 2012. 'The Missing Risk: MRI and MRS Phenotyping of Abdominal Adiposity and Ectopic Fat'. *Obesity (Silver Spring, Md.)* 20 (1): 76–87. https://doi.org/10.1038/OBY.2011.142.

Thomas, E. Louise, Nadeem Saeed, Joseph V. Hajnal, Audrey Brynes, Anthony P. Goldstone, Gary Frost, and Jimmy D. Bell. 1998. 'Magnetic Resonance Imaging of Total Body Fat'. *Journal of Applied Physiology* 85 (5): 1778–85. https://doi.org/10.1152/JAPPL.1998.85.5.1778/ASSET/IMAGES/LARGE/JAPP06139006BX.JPEG.

Torriani, Martin, Bijoy J. Thomas, Miriam A. Bredella, and Hugue Ouellette. 2007. 'INTRAMYOCELLULAR LIPID QUANTIFICATION: COMPARISON BETWEEN 3.0- AND 1.5-TESLA 1H MR SPECTROSCOPY'. *Magnetic Resonance Imaging* 25 (7): 1105. https://doi.org/10.1016/J.MRI.2006.12.003.

Troter, Arnaud le, Alexandre Fouré, Maxime Guye, Sylviane Confort-Gouny, Jean Pierre Mattei, Julien Gondin, Emmanuelle Salort-Campana, and David Bendahan. 2016. 'Volume Measurements of Individual Muscles in Human Quadriceps Femoris Using Atlas-Based Segmentation Approaches'. *Magnetic Resonance Materials in Physics, Biology and Medicine* 29 (2): 245–57. https://doi.org/10.1007/s10334-016-0535-6.

Trouwborst, Inez, Suzanne M. Bowser, Gijs H. Goossens, and Ellen E. Blaak. 2018. 'Ectopic Fat Accumulation in Distinct Insulin Resistant Phenotypes; Targets for Personalized Nutritional Interventions'. *Frontiers in Nutrition* 5 (September): 77. https://doi.org/10.3389/fnut.2018.00077.

Tsintzas, Kostas, Kirsty Jewell, Mo Kamran, David Laithwaite, Tantip Boonsong, Julie Littlewood, Ian Macdonald, and Andrew Bennett. 2006. 'Differential Regulation of Metabolic Genes in Skeletal Muscle during Starvation and Refeeding in Humans'. *Journal of Physiology* 575 (1): 291–303. https://doi.org/10.1113/jphysiol.2006.109892.

Vaccaro, Olga, Maria Masulli, Vincenzo Cuomo, Angela Albarosa Rivellese, Matti Uusitupa, Bengt Vessby, Kjeld Hermansen, Linda Tapsell, and Gabriele Riccardi. 2004. 'Comparative Evaluation of Simple Indices of Insulin Resistance'. *Metabolism: Clinical and Experimental* 53 (12): 1522–26. https://doi.org/10.1016/j.metabol.2004.05.017.

Varady, Krista A., Sofia Cienfuegos, Mark Ezpeleta, and Kelsey Gabel. 2022. 'Clinical Application of Intermittent Fasting for Weight Loss: Progress and Future Directions'. *Nature Reviews Endocrinology 2022 18:5* 18 (5): 309–21. https://doi.org/10.1038/s41574-022-00638-x.

Vasim, Izzah, Chaudry N. Majeed, and Mark D. DeBoer. 2022. 'Intermittent Fasting and Metabolic Health'. *Nutrients* 14 (3). https://doi.org/10.3390/NU14030631.

Wallace, Tara M., Jonathan C. Levy, and David R. Matthews. 2004. 'Use and Abuse of HOMA Modeling'. *Diabetes Care* 27 (6): 1487–95. https://doi.org/10.2337/diacare.27.6.1487.

Welton, Stephanie, Robert Minty, Teresa O'Driscoll, Hannah Willms, Denise Poirier, Sharen Madden, and Len Kelly. 2020. 'Intermittent Fasting and Weight Loss: Systematic Review'. *Canadian Family Physician* 66 (2): 117. /pmc/articles/PMC7021351/.

Westbrook, Catherine., Carolyn Kaut. Roth, and John (Writer on magnetic resonance imaging) Talbot. 2011. *MRI in Practice*. Wiley-Blackwell. https://www.wiley.com/en-us/MRI+in+Practice%2C+4th+Edition-p-9781444337433.

White, Lesley J, Robert A Robergs, Wilmer L Sibbitt, Michael A Ferguson, Sean Mccoy, and William M Brooks. 2003. 'Effects of Intermittent Cycle Exercise on Intramyocellular Lipid Use and Recovery'. *Lipids* 38 (1).

WHO. 2020. 'Healthy Diet'. World Health Organization. 29 April 2020. https://www.who.int/news-room/fact-sheets/detail/healthy-diet.

Wilhelmi De Toledo, Françoise, Andreas Buchinger, Hilmar Burggrabe, Gunter Hölz, Christian Kuhn, Eva Lischka, Norbert Lischka, et al. 2013. 'Fasting Therapy - an Expert Panel Update of the 2002 Consensus Guidelines'. *Forschende Komplementarmedizin (2006)* 20 (6): 434–43. https://doi.org/10.1159/000357602.

Wilkinson, Michael J., Emily N.C. Manoogian, Adena Zadourian, Hannah Lo, Savannah Fakhouri, Azarin Shoghi, Xinran Wang, et al. 2020. 'Ten-Hour Time-Restricted Eating Reduces Weight, Blood Pressure, and Atherogenic Lipids in Patients with Metabolic Syndrome'. *Cell Metabolism* 31 (1): 92-104.e5. https://doi.org/10.1016/j.cmet.2019.11.004.

Williamson, Eric, and Daniel R. Moore. 2021. 'A Muscle-Centric Perspective on Intermittent Fasting: A Suboptimal Dietary Strategy for Supporting Muscle Protein Remodeling and Muscle Mass?' *Frontiers in Nutrition* 8 (June). https://doi.org/10.3389/fnut.2021.640621.

Wokke, B. H., J. C. van den Bergen, M. J. Versluis, E. H. Niks, J. Milles, A. G. Webb, E. W. van Zwet, A. Aartsma-Rus, J. J. Verschuuren, and H. E. Kan. 2014. 'Quantitative MRI and Strength Measurements in the Assessment of Muscle Quality in Duchenne Muscular Dystrophy'. *Neuromuscular Disorders* 24 (5): 409–16. https://doi.org/10.1016/j.nmd.2014.01.015.

World Medical Association. 2013. ‘WMA Declaration of Helsinki – Ethical Principles for Medical Research Involving Human Subjects – WMA – The World Medical Association’. 2013. https://www.wma.net/policies-post/wma-declaration-of-helsinki-ethical-principles-for-medical-research-involving-human-subjects/.

Wroblewski, Andrew P., Francesca Amati, Mark A. Smiley, Bret Goodpaster, and Vonda Wright. 2011. ‘Chronic Exercise Preserves Lean Muscle Mass in Masters Athletes’. *The Physician and Sportsmedicine* 39 (3): 172–78. https://doi.org/10.3810/PSM.2011.09.1933.

Yang, Yoon Jung, Mi Kyung Kim, Se Hee Hwang, Younjhin Ahn, Jae Eun Shim, and Dong Hyun Kim. 2010. ‘Relative Validities of 3-Day Food Records and the Food Frequency Questionnaire’. *Nutrition Research and Practice* 4 (2): 142. https://doi.org/10.4162/NRP.2010.4.2.142.

Yim, J. E., S. Heshka, J. Albu, S. Heymsfield, P. Kuznia, T. Harris, and D. Gallagher. 2007. ‘Intermuscular Adipose Tissue Rivals Visceral Adipose Tissue in Independent Associations with Cardiovascular Risk’. *International Journal of Obesity (2005)* 31 (9): 1400. https://doi.org/10.1038/SJ.IJO.0803621.

Zeb, Falak, Xiaoyue Wu, Lijun Chen, Sadia Fatima, Ijaz Ul Haq, Aochang Chen, Min Li, and Qing Feng. 2020. ‘Effect of Time-Restricted Feeding on Metabolic Risk and Circadian Rhythm Associated with Gut Microbiome in Healthy Males’. *British Journal of Nutrition* 123 (11): 1216–26. https://doi.org/10.1017/S0007114519003428.

Zhao, Yu Zhen, Jian Li Zhou, Jia Qi Liu, Da Ming Bai, Shao Ming Zhou, Yun Gen Gan, Wei Guo Cao, Shu Mei Cheng, Meng Zhu Wang, and Fang Qin Gao. 2019. ‘Accuracy of Multi-Echo Dixon Sequence in Quantification of Hepatic

Steatosis in Chinese Children and Adolescents'. *World Journal of Gastroenterology* 25 (12): 1513. https://doi.org/10.3748/WJG.V25.I12.1513.